

**CRANFIELD UNIVERSITY**

**SCHOOL OF ENGINEERING**

**PHD THESIS**

**DEVAIAH K NALIANDA**

**IMPACT OF ENVIRONMENTAL TAXATION POLICIES ON CIVIL AVIATION-  
A TECHNO-ECONOMIC ENVIRONMENTAL RISK ASSESSMENT**

**SUPERVISORS: DR.VISHAL SETHI  
PROF. RITI SINGH**

**SEPTEMBER 2012**

This thesis is submitted in partial fulfilment of the requirements for the degree  
**Doctor of Philosophy**

© Cranfield University 2012. All rights reserved. No part of this publication may  
be reproduced without the written permission of the copyright owner.



## EXECUTIVE SUMMARY

Sustainability of the aviation industry, as any other industry, depends on the elasticity of demand for the product and profitability through minimising operating costs and hence assessing and understanding the interdependency and effects of environmentally optimised solutions and emission mitigation policies, is paramount.

The contribution to knowledge, from this research, is the development and application of assessment methodologies to better understand the effects that future potential environmental taxation may have on the adaptation of optimised “greener” operations and novel technologies. These studies are undertaken using a Techno-economic Environmental Risk Assessment approach (TERA).

The first methodology introduced to assess optimised operation methods (based on operating cost analysis), demonstrated that carbon taxation has limited effect if applied in isolation. Increasing it to extreme levels, apart from resulting in an increase in operational costs and raising governmental revenues, may not necessarily result in influencing an airline operator’s operational strategy to move to greener solutions. Instead, an application of a taxation level, commensurate to global standards, coupled with an improved air traffic management system, would allow aircraft to fly closer to their design efficiency and hence aid in reducing the environmental impact.

The second methodology introduced (based on an operating and investment cost analysis) allows the assessment of the economic viability of a new technology in comparison to a conventional technology, when considered in terms of relative increase in acquisition price and maintenance costs, for various emission taxation and fuel price scenarios. A study undertaken as a ‘proof of concept’, comparing a Counter Rotating Open Rotor (CROR) aircraft with a conventional aircraft, indicates that at a current fuel price and no carbon taxation, despite being demonstrated as a highly fuel efficient technology, a relative increase in acquisition price and maintenance costs in comparison to the conventional aircraft, could render the CROR technology, economically unviable. The work further demonstrates that for the CROR technology to be economically beneficial, a simultaneous introduction of emission taxes may be required.

The study shows that in order to achieve lower environmental impact, the implementation of taxation with the introduction of greener technologies will evidently increase the cost of civil aviation operation. This research subsequently identifies the following questions, more of a ‘political and socio-economic nature’, to consider as part of further work.

- If taxes above the global industry standards are introduced for the aviation industry, and they are higher in comparison to those applied on some other carbon intensive sectors, will it raise questions on equity of treatment?
- If taxation is introduced, airline operators and the ticket price paying passengers being amongst the key stakeholders in the aviation industry, will such high pricing as demonstrated be practical for long term sustenance?
- Will policies be driven by the fact that they will be aimed as a trade-off between achieving global sustenance of the industry and achieving environmental gain?
- Will high taxation as demonstrated, have global acceptance or will it have to be compromised, based on the growth potential or GDP of a country/ region?



## ACKNOWLEDGEMENTS

It would not have been possible to write this doctoral thesis without the help and support of the kind people around me, to only some of whom it is possible to give particular mention here.

Above all, I would like to thank my wife Priyanka, who helped me believe I could achieve the 'impossible dream', for her unrelenting support and endless patience through these years and most importantly being an integral part of all my adventures. My mere expression of thanks, likewise, does not suffice to my parents Jimmy and Rathie, and sister Anu, who have given me their unequivocal support throughout my academic endeavours, and for the highest level of confidence, they have always had in me.

This thesis would not have been possible without the help, support and patience of my PhD advisor Prof. Riti Singh. I will forever remain indebted and grateful to him for this opportunity, advice and guidance, through his unsurpassed knowledge in this field. I would also like to thank Prof. Pericles Pilidis, for his support, invaluable advice along the way and funding for this PhD.

I very gratefully acknowledge the excellent advice, support and friendship of my supervisor, Dr. Vishal Sethi, which has been invaluable on both an academic and a personal level.

I would like to thank my very clever friends Mr.Hugo Pervier, Mr.Panos Giannakakis and Ms.Alice Stitt for their support, friendship and for the most scintillating discussions, which made the arduous journey so much more enjoyable and a lot easier.

Finally, and not the least, I would like to thank Mrs. Gillian Hargreaves, Mrs. Nicola Datt, Mrs. Maria Negus Mrs. Sheila Holroyd and Mr. Josh Redmond for the administrative support extended and most importantly, their kindness and patience in sorting all our issues out, through the course of this PhD.



## TABLE OF CONTENTS

EXECUTIVE SUMMARY .....	3
ACKNOWLEDGEMENTS .....	5
TABLE OF CONTENTS.....	7
GLOSSARY .....	12
NOMENCLATURE AND SYMBOLS.....	15
1. INTRODUCTION .....	17
2. LITERATURE REVIEW.....	19
2.1 INTRODUCTION .....	19
2.2 CIVIL AVIATION AND TECHNOLOGY .....	19
2.3 INTERNATIONAL CIVIL AVIATION ORGANISATION AND ITS POLICIES .....	22
2.4 GLOBAL STATISTICS AND RESEARCH .....	23
2.5 KEY ENVIRONMENTAL POLLUTANTS UNDER FOCUS .....	26
2.6 CURRENTLY IMPLEMENTED INTERNATIONAL EMISSION AND NOISE TAXES .....	29
2.7 GLOBAL AVIATION ENVIRONMENTAL PROGRAMS AND INITIATIVES .....	31
2.8 INDUSTRY RESEARCH ORIENTATION.....	32
2.8.1 AIRCRAFT AND POWER PLANT TECHNOLOGY .....	32
2.8.2 OPERATIONAL IMPROVEMENTS .....	34
2.8.3 ECONOMIC INSTRUMENTS .....	35
2.8.4 ALTERNATIVE FUELS .....	35
2.9 RESEARCH ON TERA .....	36
2.10 SCOPE OF WORK.....	41
3. THE OPTIMISATION FRAMEWORK AND THE MODELS .....	44

3.1	INTRODUCTION .....	44
3.2	FRAMEWORK .....	44
3.2.1	AIRCRAFT PERFORMANCE MODEL .....	45
3.2.2	ENGINE PERFORMANCE MODEL.....	55
3.2.3	MISSION APPLICATIONS OF INTEGRATED AIRCRAFT MODEL .....	59
3.3	EMISSION PREDICTION MODEL – NO <sub>x</sub> .....	62
3.4	EMISSION PREDICTION MODEL – CO <sub>2</sub> AND H <sub>2</sub> O.....	65
3.5	CONTRAIL PREDICTION MODEL .....	65
3.6	OPERATING COST MODEL .....	66
3.6.1	IMPLEMENTATION OF THE OPERATING COST MODEL.....	71
3.7	THE OPTIMISER.....	75
3.7.1	NUMERICAL METHODS FOR TRAJECTORY OPTIMISATION.....	76
3.7.2	TRAJECTORY OPTIMISATION TECHNIQUE SELECTION.....	79
3.8	CONCLUSION.....	80
4.	TRAJECTORY OPTIMISATION .....	81
4.1	INTRODUCTION .....	81
4.2	DEFINITION OF FLIGHT PHASES .....	82
4.2.1	DEPARTURE .....	82
4.2.2	CLIMB .....	83
4.2.3	CRUISE .....	83
4.2.4	DESCENT .....	84
4.2.5	APPROACH AND LANDING.....	85
4.3	AIRCRAFT TRAJECTORY DEFINITION .....	86

4.4	CASE STUDIES .....	88
4.4.1	CASE 1: SHORT-MEDIUM RANGE (815 NM) .....	91
4.4.2	CASE 2: MEDIUM RANGE (1614 NM) .....	109
4.4.3	CASE 3: SHORT RANGE (227 NM) .....	121
4.5	CONCLUSIONS .....	125
5.	POLICY ASSESSMENTS - OPTIMISED OPERATIONS .....	129
5.1	INTRODUCTION .....	129
5.2	THE POLICY MODULE .....	130
5.2.1	THE CONTOUR PLOT .....	131
5.2.2	THE LINE PLOT .....	131
5.3	CASE STUDIES .....	131
5.3.1	CASE STUDY: SHORT-MEDIUM RANGE (815 NM) .....	132
5.3.2	CASE STUDY: SHORT RANGE (227 NM) .....	141
5.3.3	CASE STUDY: MEDIUM RANGE (1614 NM) .....	146
5.4	CONCLUSION .....	150
6	POLICY ASSESSMENTS - TECHNOLOGY .....	152
6.1	INTRODUCTION .....	152
6.2	TECHNICAL APPROACH .....	153
6.3	CASE STUDY .....	155
6.4	CROR AIRCRAFT/ENGINE MODELLING .....	157
6.4.1	ENGINE MODELLING .....	158
6.4.2	AIRCRAFT MODELLING .....	166
6.5	PAYOUT RANGE PERFORMANCE AND ENERGY EFFICIENCY .....	168

6.6	OPERATING COST ANALYSIS .....	169
6.7	INVESTMENT COST ANALYSIS APPROACH .....	175
6.7.1	INTRODUCTION TO THE APPROACH.....	175
6.7.2	APPLICATION OF THE APPROACH.....	178
6.8	CONCLUSIONS.....	187
7	DISCUSSION AND CONCLUSION.....	190
7.1	BACKGROUND .....	190
7.2	SUMMARY OF WORK AND DISCUSSION ON FINDINGS .....	191
7.2.1	POLICY ASSESSMENTS – OPTIMISED OPERATIONS.....	191
7.2.2	POLICY ASSESSMENTS – TECHNOLOGY.....	195
7.3	CONCLUSION .....	197
7.4	RECOMMENDATIONS FOR FUTURE WORK.....	199
	REFERENCES .....	202
	APPENDIX A: BENCHMARKING AND TESTING OF THE OPTIMISER.....	210
A1	INTRODUCTION .....	210
A2	GENETIC ALGORITHMS.....	210
A3	MULTI OBJECTIVE GENETIC ALGORITHM (MOGA) .....	211
A4	OBJECTIVES OF MULTI OBJECTIVE OPTIMISATION.....	212
A5	PERFORMANCE METRICS .....	212
A6	NON-DOMINATED SORTING GENETIC ALGORITHM II (NSGA II).....	214
A7	STRENGTH PARETO EVOLUTIONARY ALGORITHM II (SPEA II).....	215
A8	ADAPTATION OF NSGAIID FOR THE GATAC OPTIMISER- NSGA MO2 .....	216
A9	BENCHMARKING AND TESTING OF MULTI OBJECTIVE ALGORITHM .....	217

A9.1	PHASE 1: PERFORMANCE TESTING USING ZDT TEST PROBLEMS .....	217
A9.2	PHASE 2: PERFORMANCE TESTING FOR CONSTRAINT HANDLING .....	226
A9.3	PHASE 3: AIRCRAFT TRAJECTORY OPTIMISATION .....	229
	APPENDIX B: CONTRAIL MODEL: SPECIFICATION AND DESCRIPTION .....	235

## GLOSSARY

AAT	Aeronautics and Air Transport
ACARE	Advisory Council for Aviation Research in Europe
AIC	Aviation Induced Cloudiness
alt	Altitude
ATA	Air Transport Association
ATC	Air Traffic Control
ATM	Air Traffic Management
ATR	Avions de Transport Régional
BADA	Base of Aircraft Data
BAU	Business As Usual
BET	Baseline Emission Tax
BPR	Bypass Ratio
CAEE	Committee on Aircraft Engine Emission
CAEP	Committee on Aviation Environmental Protection
CAS	Calibrated Air Speed
CDA	Continuous Descent Approach
CDO	Continuous Descent Operations
CFD	Computational Fluid Dynamics
CI	Cost Index
CNG	Carbon Neutral Growth
CROR	Counter Rotating Open Rotor
DMC	Direct Maintenance Cost
DOC	Direct Operating Cost
DREAM	valiDation of Radical Engine Architecture systeMs
EEA	European Environment Agency
EI	Emission Index
EPN	Effective Perceived Noise
ETRW	Energy To Revenue Work
ETS	Emission Trading Scheme
EU	European Union
FAR	Fuel to Air Ratio
FC	Flight Cycle
FCM	Fuel Composition Method
FH	Flight Hour
FH/FC	Flight Hour to Flight Cycle ratio
FL	Flight Level
FP	Framework Programme
FPA	Flight Path angle
GA	Genetic Algorithm
GDP	Gross Domestic Product
GIACC	Group on International Aviation and Climate Change

gl	Ground Level
HC	Hydrocarbon
HEA	High Environmental Awareness
HFP	High Fuel Price
HPC	High Pressure Compressor
IATA	International Air Transport Association
ICAO	International Civil Aviation Organization
IOC	Indirect Operating Cost
IPCC	Intergovernmental Panel on Climate Change
IRR	Internal Rate of Return
ISA	International Standard Atmosphere
ITD	Integrated Technology Demonstrator
JTI	Joint Technology Initiative
LAQ	Local Air Quality
LCV	Lower Calorific Value
LOSU	Level Of Scientific Understanding
LPC	Low Pressure Compressor
LRC	Long Range Cruise
LTO	Landing and Takeoff (cycle)
MAE	Management of Aircraft Energy
MCT	Maximum Climb Thrust
MLW	Maximum Landing Weight
MRC	Maximum Range Cruise
MTM	Management of Trajectory and Mission
MTOW	Maximum Take Off Weight
MZFW	Maximum Zero Fuel Weight
NACRE	New Aircraft Concepts REsearch
NEWAC	New Aero engine Concepts
NPV	Net Present Value
NSGA	Non-dominated Sorting Genetic Algorithm
OEW	Operating Empty Weight
OPD	Optimised Profile Descents
OPR	Overall Pressure Ratio
PBN	Performance Based Navigation
PEA	Progressive Environmental Awareness
PFEE	Payload Fuel Energy Efficiency
QC	Quota Count
RF	Radiative Forcing
ROC	Rate Of Climb
ROD	Rate Of Descent
RPK	Revenue Passenger Kilometre
RPM	Revenue Passenger Mile
RTK	Revenue Ton Kilometre
RVSM	Reduced Vertical Separation Minima

SAE	Society of Automotive Engineers
SESAR	Single European Sky ATM Research
SFC	Specific Fuel Consumption
SGO	Systems for Green Operation
SID	Standard Instrument Departure
STAR	Standard Terminal arrival Route
TAS	True Air Speed
TERA	Techno-economic Environmental Assessments
TET	Turbine Entry Temperature
TOC	Top of Climb
TOD	Top of Descent
Trns	Transition (altitude)
UDF	Un-Ducted Fan
WACC	Weighted Average Cost of Capital

## NOMENCLATURE AND SYMBOLS

$c$	Specific fuel consumption (mg/Ns)
$C_D$	Drag coefficient
$C_{D0}$	Parasitic drag coefficient
$C_{D2}$	Induced drag coefficient
$CH_4$	Methane
$C_L$	Lift coefficient
$C_{L\_MAX}$	Maximum lift coefficient
$CO_2$	Carbon di Oxide
$D$	Aerodynamic drag (N)
$dB$	Decibels
$EPNdB$	Effective Perceived Noise in Decibels
$EPNL/L_{EPN}$	Effective Perceived Noise Level
$g_0$	Gravitational acceleration ( $9.80665\text{ m/s}^2$ )
$h$	Altitude above mean sea level (m)
$h_e$	Energy height(m, ft)
$h_t$	Height at transition(m, ft)
$k$	Adiabatic index of air
$K$	Kelvin
$K_A$	Calculated takeoff coefficient 2
$K_T$	Calculated takeoff coefficient 1
$kt$	Knots
$L$	Aerodynamic lift
$LAMAX/L_{Asmx}$	A-Weighted Maximum Sound E levels
$m$	Mass (kg)
$M$	Mach Number
$M_{31}$	Mass flow Inlet Temperature
$N$	Newton
$NO_x$	Oxides of Nitrogen
$O_3$	Ozone
$P_{31}$	Combustor Inlet Pressure
$PNLT M/ L_{PNTSsmx}$	Tone –Corrected Maximum Perceived Noise level
$P_{se}$	Specific excess power
$Q$	Mass of fuel per unit time(kg/s)
$r$	Radius of arc (m)
$R$	Universal gas constant ( $\text{J kg}^{-1}\text{ K}^{-1}$ )
$r_a$	Specific Air Range
$R_w$	Wheel reaction
$S$	Aircraft wing reference area ( $\text{m}^2$ )
$SEL/L_{AE}$	A-Weighted Sound Exposure levels
$S_g$	Distance for ground run (m)
$S_t$	Distance covered in transition(m)
$T_{31}$	Combustor Inlet Temperature

$T_{\text{amb}}$	Ambient Temperature
$T_{\text{HR}}$	Thrust (N)
$V_1$	Decision Speed
$V_2$	take off safety speed
$V_{2+10}$	take off safety speed plus 10 kt
$V_{\text{lof}}$	Lift off(the) ground speed(m/s, kt)
$V_r$	Speed of rotation(m/s, kt)
$V_s$	Stall speed(m/s, kt)
$V_{\text{TAS}}$	True Air Speed (m/s, kt)
$V_{\text{trans}}$	Transition speed (m/s, kt)
$W$	Weight (N)
$\text{Wm}^2$	Watts per square meter
$x$	Carbon coefficient in chemical formula for fuel (in moles)
$y$	Hydrogen coefficient in chemical formula for fuel (in moles)
$z$	Sulphur coefficient in chemical formula for fuel (in moles)
$\beta_{T,<}$	ISA temperature gradient below the tropopause
$\beta$	Drag to lift ratio
$\gamma$	Climb angle
$\rho$	Air density ( $\text{kg/m}^3$ )
$\emptyset$	Bank angle
$\mu$	Runway coefficient of friction

## 1. INTRODUCTION

The rapid growth of global economies and the corresponding sharp rise in the number of people now wanting to travel on business and for pleasure, has largely been responsible for the development of the aviation industry. However the significantly large increase in air passengers over the years has led to an increase in air traffic and a corresponding rise in fuel consumption, aviation emissions and noise.

Over the years, the industry has consistently invested in improving technology and infusing it into commercial application, with an aim to always remain profitable. With fuel expenses being a significant part of an airlines operating cost, the core focus of technology development has been to constantly improve fuel economy, whilst maintaining Landing and Takeoff (LTO) cycle noise and NO<sub>x</sub> within certification limits and improving safety and reliability. However with predictions of consistent future growth in air traffic, the aviation industry's probable impact on the environment has now become a cause for growing global concern.

Consequent to these environmental concerns, organisations like the ICAO have set up ambitious environmental goals to enable the industry to achieve a carbon neutral status by 2020 and further achieve a 50% reduction in CO<sub>2</sub> emissions by 2050 (relative to 2005). In line with these goals various research programs have been launched around the world, which aim to achieve these environmental targets by implementing improvements through every aspect of civil aviation and through the lifecycle of the civil aircraft.

These initiatives include improvements of current technology, operations and infrastructure, application of bio-fuels as a substitute to fossil fuels and introduction of economic policies/measures such as emission trading schemes and environmental taxation. However, in the process of achieving their stipulated environmental goals, these environmental initiatives will affect the operational cost of the aircraft operator.

To then maintain low operating costs and profitability, some of the key criteria for sustainability within the industry, will then necessitate adequate analysis of the interdependency/effects of introducing these environmental initiatives and emission mitigation policies.

This thesis therefore introduces methodologies to understand the effect of fuel prices and emission related taxation policies (emission trading, emission related charges/taxes) on selection of future technology and methods of operation. The framework built in this PhD, enables comparing optimal solutions with respect to certain objectives in a consistent manner and to ascertain their environmental suitability. As profitability is an important factor for sustainability in the aviation industry, the framework can be used to also understand the effect of taxation policies on the economic viability of these solutions, while being environmentally friendly.

Following the introduction, this report begins with a literature review (Chapter 2) to understand the past and current research on emissions and policies. This chapter by summarising related research and literature on the subject strives to then bring into perspective the context of the work in this PhD.

A description of Techno economic Environmental Risk Assessment (TERA) framework, the optimisation module and the various models follow in chapter 3. The chapter aims to explain in detail the structure of the optimisation framework and the models used within it which is then used to perform a series of operational, environmental and economic analysis, on short – medium range conventional aircraft. The chapter also describes various tests conducted on the models to validate the performance of the models and to further improve the confidence in the analysis.

Utilising the models described in chapter 3, and to progress towards optimising of operations, the next chapter (chapter 4) considers the concept of optimised trajectories. The chapter describes in detail the definition of trajectories and the critical objectives based on current research being undertaken in the field. It is then followed by a set of optimisation case studies, undertaken for a series of short to medium range routes, optimised for various environmental, operational and economic objectives.

Chapter 5 introduces the proposed methodology to assess optimised operations under various taxation scenarios. Essentially considering the optimised trajectories established in chapter 5, the methodology utilises a policy module to analyse the effect of taxation and assess the economic viability of the optimised trajectories. It is then and further used to deduce the taxation rate at which an airline may be driven towards more environmentally optimal solutions.

Chapter 6 then introduces a methodology to assess a novel technology for economic viability, when compared with conventional technology under varying taxation scenarios. The proof of concept is provided by analysing the Counter Rotating Open Rotor (CROR) / propfan aircraft.

The report on the research is then concluded with chapter 7, which includes a summary of all the work undertaken within the scope of this PhD, with a final conclusion of the key findings and recommendations for further work.

For the reader's reference, the thesis also includes a list of references and two appendices at the end. The appendices have been included to essentially provide the reader with a description of the bench marking and testing procedures used in validating the optimiser (Appendix A), followed by the specification of the contrail prediction model used in the framework (Appendix B). The work from this PhD has resulted in two conference publications and one journal publication. Reference to these publications may also be found in the list included. [1.1, 2.2, 3.23]

## 2. LITERATURE REVIEW

### 2.1 INTRODUCTION

A series of significant developments in the past decade have influenced the exponential growth and current direction of the aviation industry, thereby enabling millions of people to travel around the globe at the fastest speed possible and in the most convenient and efficient manner. On the positive side of the global equation, aviation has made tremendous contribution towards trade. This has happened by improving accessibility to more productive and geographically disparate markets; to skills and resources. This has led to encouraging globalisation, thus leading to greater investment; improved productivity, innovation and greater efficiency and encouraging man's quest to travel through tourism. Airbus in its Global Market Forecast has therefore stated that in economic terms alone, aviation is considered to have contributed more to world Gross Domestic Product (GDP) when compared to some G20 nations. [2.1]

This chapter by summarising related research and literature on the subject strives to then bring into perspective the context of the work in this PhD.

### 2.2 CIVIL AVIATION AND TECHNOLOGY

Over the years aviation and associated technology have improved vastly to become an extremely efficient and safe mode of transportation. Even though compared to fifty years ago, today's aircraft are known to create 75% less noise and utilize 80% lower fuel, yet carry twice as many passengers at much lower Direct Operating Costs (DOC) and with increased safety [2.2].

In the 1950s with the advent of the jet age, considered a revolutionary step in the field of transportation, aircraft were finally able to cover vast distances at higher speeds. The 1960's saw the industry transition from the turbojet to the more fuel efficient and significantly quieter bypass turbofan. Figure 2.1 shows the transition of towards more fuel efficient solutions.

The world experienced two major oil crises first in 1973 and then in the early 1980s. With the industry suffering catastrophic economic losses, solutions aimed towards higher fuel efficiency were actively pursued. Figure 2.2 shows a graphical representation of the fluctuation in fuel price over the years with the red bands indicating the years in which the CROR technology has been envisaged as a probable solution. Even though these programs reached fairly advanced levels of technology readiness, the radical efficiency improvements they promised in commercial aviation, are barely noticeable in today's industry. This clearly demonstrates that these technologies were and continue to be primarily driven by economic and market forces [2.4].

Therefore, since the introduction of the high bypass turbofan, progress in aviation has been a matter of evolution rather than revolution. The incremental benefits accrued from improvements in existing technology accompanied with lowered risk, were sufficient to keep the industry viable.

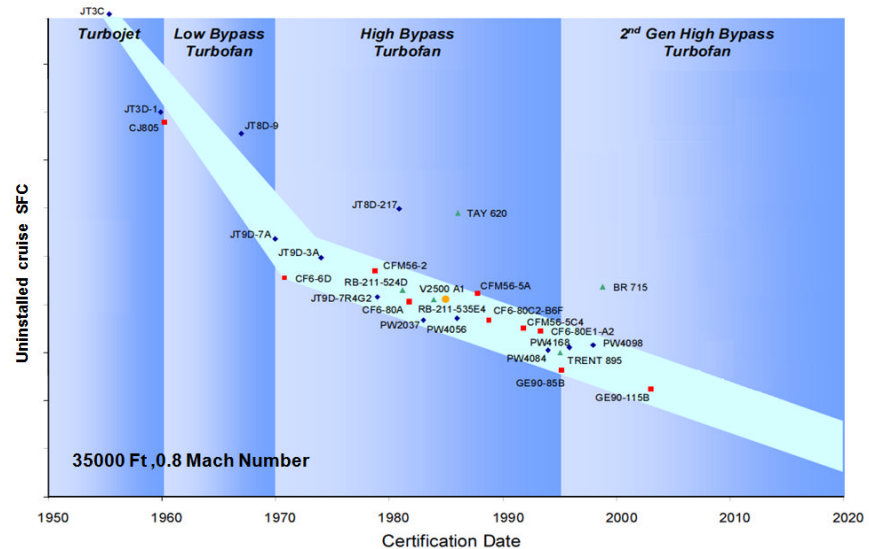


Fig 2.1 Schematic representation of the transition in engine technology towards higher efficiency

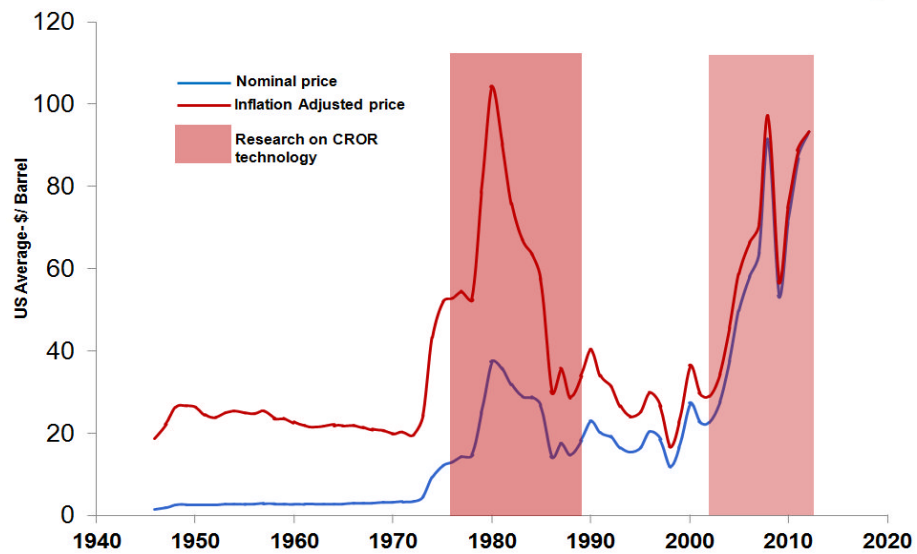


Fig 2.2 Historical fluctuation in oil price [2.3]

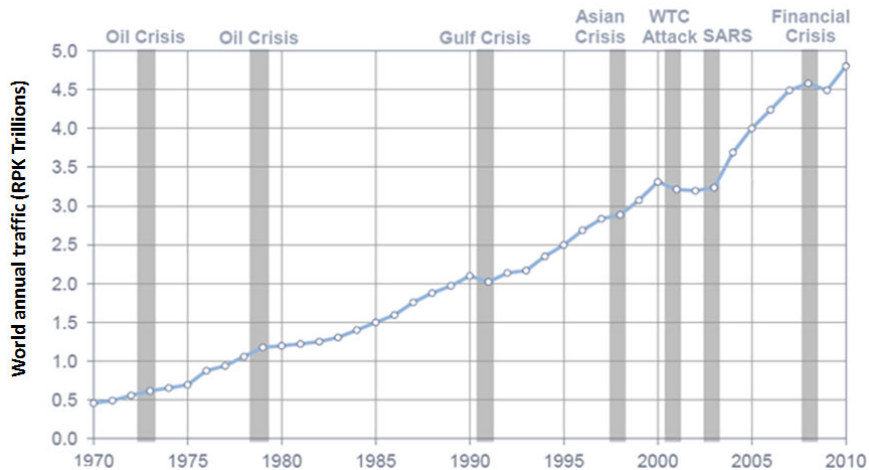


Fig 2.3 Increase in annual passenger traffic [2.1]

Passenger traffic has shown a significant rise over the past decades. Figure 2.3 shows a plot by Airbus which graphically represents the rise in passenger traffic over the past few decades. The world has experienced calamities and crisis through this time, but apart from a marginal dip after 9/11 attacks, growth in air traffic has been fairly consistent. ICAO's data shows that since 1979 the industry has averaged an annual growth of approximately 4.7% and industry estimates show that this growth rate will be sustained and lie between 4.8% and 5.5% per year till 2036 [2.1,2.4].

The increased air traffic has therefore brought into focus amongst others, two important aspects that will be critical in the future

- Fuel consumption by the aircraft needed to cater for the increased number of passengers
- Environmental emissions from aviation.

Fuel expenses form a significant part of an airliner's operating costs and vary from 28%-35% [2.5]. With the price of fuel rising to unprecedented levels in the last decade( as seen in figure 2.2 ) and global aircraft fuel consumption expected to increase at a rate of between 3% to 3.5% per annum, the industry has, yet again, begun pursuing technology solutions that will deliver a significant decrease in fuel consumption.

The concern of environmental emissions from civil aviation, till the late nineties, was restricted to concerns on Local Air Quality ( $\text{NO}_x$  emissions and noise) from the landing and takeoff (LTO) cycle, restricted primarily to the proximity of airports, as it is known to affect the health and well being of population inhabiting neighbouring areas.

The increased air traffic has however brought into focus the effects of various environmental pollutants which are being considered to have global warming potential and hence may be

attributed to climate change. These primarily include, amongst others, CO<sub>2</sub>, NO<sub>x</sub> at cruise altitude, and Contrails and Cirrus clouds formation.

## 2.3 INTERNATIONAL CIVIL AVIATION ORGANISATION AND ITS POLICIES

To monitor the aviation industry globally and ensure its structured development towards greener and safer aviation, the International Civil Aviation Organisation (ICAO), is a specialised agency of the United Nations which performs a critical role in setting targets for future safety and emission standards. It exists to codify the principles and techniques of international air navigation and fosters the planning and development of international air transport to ensure safe and orderly growth [2.6].

ICAO works to achieve its vision for safe, secure and sustainable development of civil aviation through cooperation amongst its member States. One of its key strategic objectives is Environmental Protection, which it strives to achieve by minimizing the adverse effects of global civil aviation on the environment [2.7]. As defined by its mandate the ICAO has three environmental goals for international aviation which aim to: 1) reduce the number of people exposed to significant aircraft noise; 2) reduce the impact of aviation emissions on local air quality; and 3) reduce the impact of aviation emissions on the global climate. [2.4]

The Committee on Aviation Environmental Protection (CAEP) is a technical committee of the ICAO Council. In support of ICAO's environmental goals and in its role as international aviation's leading environmental body, the CAEP is responsible for conducting studies and recommending measures to minimise and reduce aviation's impact on the environment, including setting certification standards for aircraft noise and aircraft engine emissions.

The CAEP has adopted a structured approach to developing and delivering solutions to the air transport sector—initially by quantifying related environmental impacts and then by establishing practical mitigation measures to address them.

These measures are enforced through a set of environmental certification standards which every aircraft in the world is required to adhere to before being inducted into service and during its operational life. These standards are specified as Annex 16 (Environmental Protection) to the *Convention on International Civil Aviation*

Annex 16 consists of two volumes: Volume I - Aircraft Noise and Volume II – Aircraft Engine Emissions. These certification Standards have been designed and are kept up to date in order to respond to concerns regarding the environmental impact of aviation on communities in the vicinity of airports, as well as society at large.

## 2.4 GLOBAL STATISTICS AND RESEARCH

The literature available on environmental impact of emissions is extensive on the public domain. A literature survey was undertaken to understand the impact of climate change on Civil Aviation as an Industry, with the main purpose of identifying its effect more from an economic and risk perspective, thus delving into possible scenarios that could result in the future and eventually their repercussions in terms of policies affecting the Civil Aviation Industry.

Aviation's effect on climate has been under scrutiny from the late 1960s and early 1970s and has therefore been of interest for many decades. The initial and most significant stir began over the proposed fleet of supersonic jets (Concorde and Tupolev-144) and their potential damage to Stratospheric Ozone ( $O_3$ ) (and the resulting depletion of it) and the excessively high Noise levels resulting in Sonic Booms.

Although  $CO_2$  is the only recognised 'Kyoto greenhouse gas' aviation emits, it has been established through scientific research, that apart from the highly documented effects of  $CO_2$ , non- CO emissions also have a perceivable effect on the climate at high altitudes. In the course of Literature survey, various studies were found which discussed certain key projects in 1997 (EU AERONOX and the US SASS projects) which primarily examined the potential of anthropogenic activities and effects from aviation. These studies were aimed at identifying a number of emissions (apart from  $CO_2$ ) which had potential to affect climate and included the emission of particles, contrails and other AIC (aviation-induced cloudiness). [2.8]

It was established through the course of these studies that aviation stood out primarily as the only sector, whose largest fraction of emissions are injected at aircraft cruise altitudes of 8–12 km. The emissions released at these altitudes were found to have increased effectiveness and hence were responsible for climate forcing due to relevant chemical and aerosol effects (e.g., cloud formation and  $O_3$  production). [2.8]

A European study was undertaken to assess the environmental effects/impacts of aviation in 1988 (Brasseur et al.,1998). This was followed in 1999 by the Intergovernmental Panel on Climate Change (IPCC) report '*Aviation and the Global Atmosphere*' which used the environmental metric 'RF' (*Radiative Forcing*) to make an assessment on Climate change. [2.8, 2.9]

Radiative Forcing (RF) as described in referenced literature[2.8] is "*a measure of the perturbation of the Earth-atmosphere energy budget since 1750 (by convention in IPCC usage) resulting from changes in trace gases and particles in the atmosphere and other effects such as changed albedo, and is measured in units of watts per square metre ( $W\ m^2$ ) at the top of the atmosphere.*" The resulting changes in RF, due to physical effects of these emissions and cloud formation, is to change the particle and micro-physical properties of the atmosphere above

cruise altitude. This is considered to be detrimental to climate, thus damaging the ecosystem. [2.8]

The RF components from aviation are known to arise from the following:

- CO<sub>2</sub> (+ RF)
- NO<sub>x</sub> (+RF) (sum of three component terms: production of tropospheric O<sub>3</sub> (+ RF); a longer-term reduction in ambient methane (CH<sub>4</sub>) (- RF), and a further longer-term small decrease in O<sub>3</sub> (-RF))
- H<sub>2</sub>O (+RF)
- Persistent linear contrails (+RF)
- AIC (+RF)
- Sulphate particles (-RF);
- Soot particles (+RF).

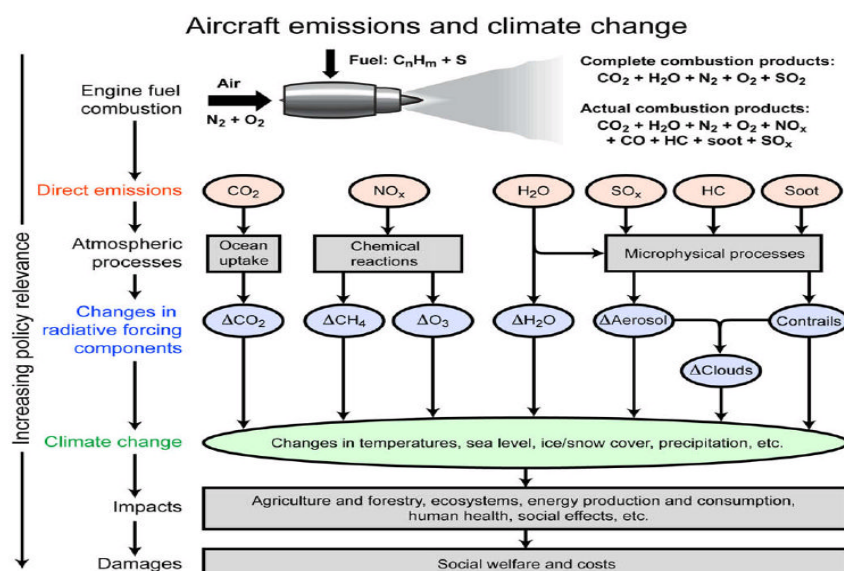


Fig 2.4 Principal emissions and the atmospheric processes that lead to changes in RF components [2.8]

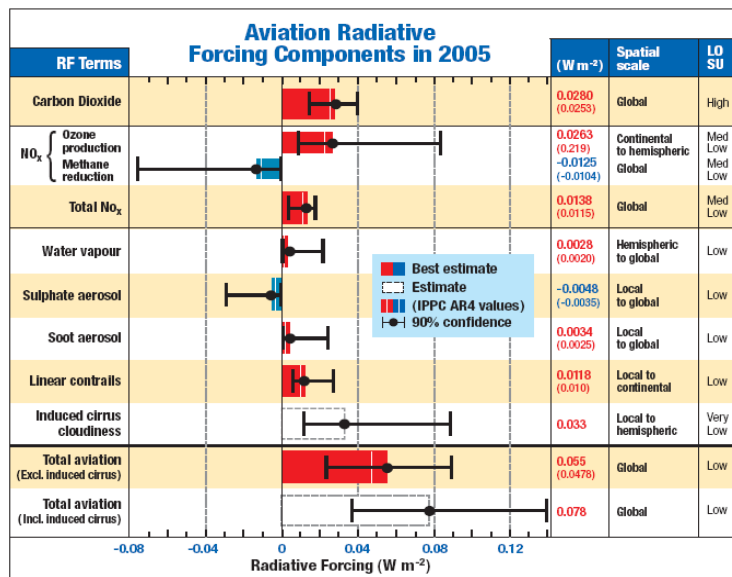


Fig 2.5 Aviation RF components 2005 [2.4]

The Intergovernmental Panel on Climatic Change (IPCC), while establishing in its report, concluded that aviation did cause a (small but) significant increase in global RF. The report was uncertain in the overall magnitude but estimated it to be about 3.5% (excluding AIC) of the total anthropogenic RF in 1992. An updated study by the same author [2.8] in 2005 (and widely accepted as reference by the ICAO) calculated that the CO<sub>2</sub> and non-CO<sub>2</sub> RF attributable to aviation in 2005 were 4.9% of the total RF, when best estimates for the effects of aviation induced cirrus cloud formation were included.[2.10]

The Group on International Aviation and Climate change (GIACC) of the ICAO, in May 2009 reviewed the IPCC 4<sup>th</sup> Assessment Report and reassessed aviation emissions based on civil aviation operational data till 2005. The report indicated that CO<sub>2</sub> emissions from civil aviation had reached an estimated 733 million tonnes a year and had increased by 45% from 1992 to 2005. It was also further estimated that between the year 2000 and 2007, aviation traffic had grown at an annual average rate of 5.3% leading to a 38% increase in passenger traffic. Further the European Environment Agency (EEA) estimated that the cumulative CO<sub>2</sub> emissions of the European Union from Civil aviation alone grew by 102% between 1990 and 2006. [2.10].

The GIACC in its report states [2.10] " Estimates that the total aviation RF (excluding cirrus) in 2050, using fuel usage growth factors of 2.7 to 3.9 over baseline year 2000, will result in an increase of upto 3 to 4 times greater than that observed in the year 2000. The IPCC (1999) also forecast that global aviation CO<sub>2</sub> emissions could reach 2,300 million tonnes annually (as a high estimate) by 2050 if left unmitigated. The earth's capacity to absorb anthropogenic CO<sub>2</sub>, and therefore the level to which emissions will have to be reduced in the long-term, is around 5,000 million tonnes annually – around twice the estimated level for 2050 aviation emissions if left unmitigated." [2.10]

## 2.5 KEY ENVIRONMENTAL POLLUTANTS UNDER FOCUS

A brief discussion on the key pollutants identified in the previous section and ICAO's regulations is found pertinent at this stage to bring into context their effects.

a. **CO<sub>2</sub> emissions:** Carbon dioxide is categorised as a dominant anthropogenic greenhouse emission, as it is retained in the atmosphere for over a hundred years. Globally Civil Aviation is estimated to account for approximately 2% of anthropogenic CO<sub>2</sub> emissions, compared with 16% from other forms of transport and over 30% from electricity and heat supply. Currently no definitive standard or global framework actually exists to manage CO<sub>2</sub> emissions (and aviation emissions in general). However, in 2009, under the leadership of ICAO, a "globally-harmonised agreement to address climate change from a specific sector" was agreed upon and consequently the ICAO is now in the process of developing a 'global carbon dioxide standard' by 2013 [2.11]. For CO<sub>2</sub> emissions, ICAO targets a 1.5-2% annual improvement in fuel efficiency globally until the year 2050 with 2005 as the base year. It has planned to achieve this by first attaining 'Carbon Neutral Growth' by 2020 through medium term goals and an absolute reduction of net CO<sub>2</sub> emissions by 50% in 2050, compared to 2005 levels (long term goals) [2.12]. Figure 2.6 shows the proposed CO<sub>2</sub> reduction measures over time.

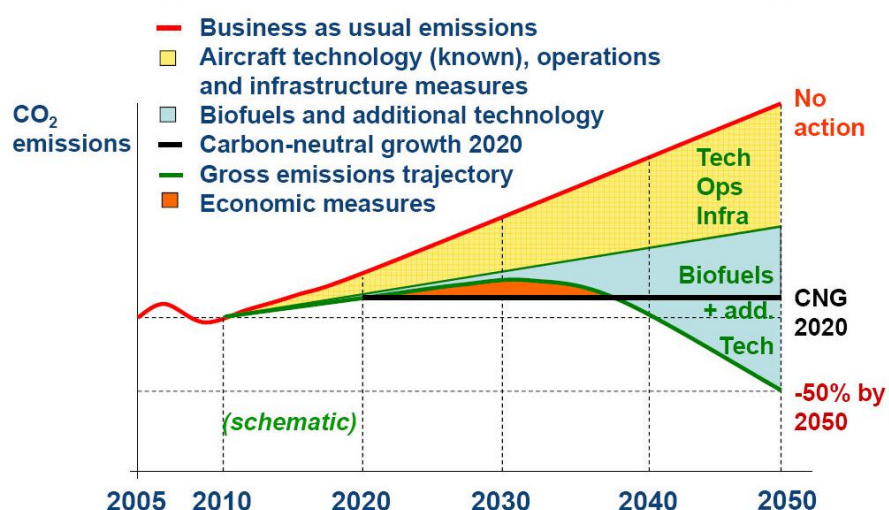


Fig 2.6 Future carbon reduction goals as proposed by the ICAO [2.4]

b. **NO<sub>x</sub> emissions:** NO<sub>x</sub> (nitrogen oxides) emissions for its effect from aviation are primarily considered during the LTO cycle and at cruise. As per available literature [2.8], research over the recent years has been focussed in providing scientific evidence to establish the affects of cruise NO<sub>x</sub> emissions on global warming from aviation. Scientific research indicates that through a process of photochemistry, aviation NO<sub>x</sub> emissions at cruise altitudes result in an enhancement of ozone (O<sub>3</sub>) (in the lower stratosphere and

upper troposphere, which results in climate warming) and a reduction of a small amount of ambient methane ( $\text{CH}_4$ ) (approx. 1-2% of overall concentration, which results in a cooling effect).

The effects of  $\text{NO}_x$  emissions on ground (specifically near airports) are also known to affect local air quality is considered fairly established. These emissions essentially contribute to various health/environmental problems whilst forming a main component of ground-level ozone [2.13]. Currently as per ICAO regulations and in order to improve Local Air Quality only LTO  $\text{NO}_x$  is currently prioritised. Figure 2.7 shows the transition of the LTO  $\text{NO}_x$  standards over the years. The current standard for  $\text{NO}_x$  is specified under CAEP/8 and is based on the overall pressure ratio. It stipulates a limit in g/kN for  $\text{NO}_x$  emissions [2.14]. The first standard set by ICAO for  $\text{NO}_x$  was in 1981 (indicated by CAEE in figure 2.7), since then it is now 50% more stringent. The CAEP/6 standard which is currently in force will be further improved upon, to more stringent levels (up to 15%) over the current limit for all engines certified after 31 December 2013, to form CAEP/8 [2.15].

The ICAO's stand on the effects of cruise  $\text{NO}_x$  may be considered currently non committal. Literature has indicated that there is a broad correlation between the amounts of  $\text{NO}_x$  produced in the LTO cycle, with the amounts produced at cruise. However as currently no standard or database exists, the ICAO is seeking further scientific advice on the relative importance of cruise  $\text{NO}_x$  before formulating any specific standard [2.4].

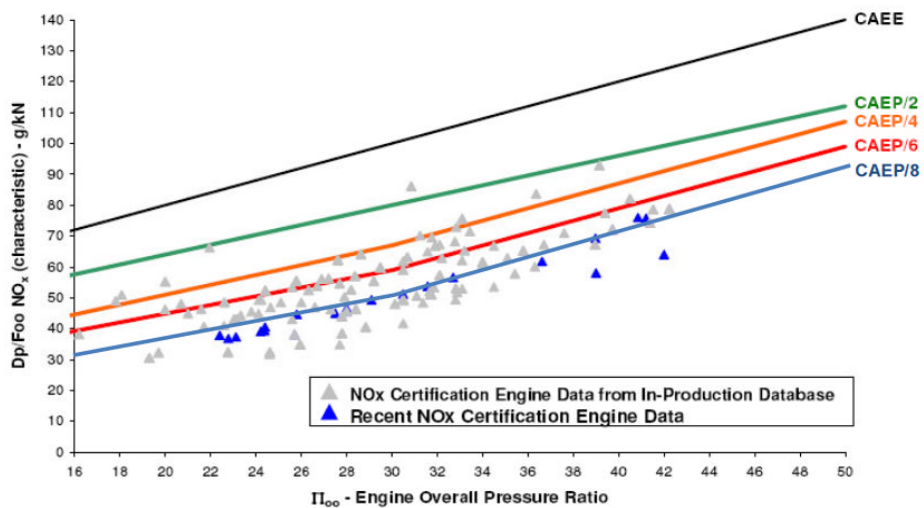


Fig 2.7  $\text{NO}_x$  emission standards for civil aviation by ICAO [2.14]

c. Contrails and Cirrus Cloud Formation: An aircraft gas turbine in the process of complete combustion of fuel emits water vapour as one of the by-products. At cruise altitude this water vapour can lead to the formation of condensation trails and are visible as line-shaped clouds (also known as Contrails). Depending on prevailing atmospheric conditions and humidity levels, these contrails are known to spread and

under certain conditions form cirrus clouds. Research in this field is continually ongoing but current literature has suggested that Contrails and induced cirrus clouds may result in climate warming as they tend to absorb and emit infrared terrestrial radiation and reflect visible radiation from the sun [2.13]. Apart from this, aircraft induced aerosols (soot and particles formed from sulphur oxides) indirectly affect natural cirrus-cloud formation by acting as ice nuclei long after emission and long distances away from the flight routes.[2.14]

Reference [2.4] states that even though significant scientific advances have been made over the last decade to better characterise aviation climate impacts, the level of scientific understanding, particularly for quantification of the climate impacts of contrails and induced cirrus clouds remains unchanged, and ranges between low and very low, respectively. Therefore as there still are many scientific uncertainties related to the duration, and their variability over time and location and consequently their effects, it currently does not include any standard on contrails and water vapour.

d. Aviation Noise: Literature [2.17] indicates that aircraft noise is acknowledged to be "one of the most objectionable impacts of airport development." Aircraft noise has been known to affect sleep patterns of population around airports, in turn affecting concentration and resulting in "fatigue, feelings of anger, frustration and powerlessness to control the noise". These factors adversely affect people's quality of life and therefore have resulted in the fact that all current international standards, with respect to aviation noise, are concerned with communities in the neighbourhood of airports.

Through technological advances today's aircraft are 75% quieter than they were 50 years ago. This has been primarily possible due to the stringent ICAO Noise regulation stipulated for civil aircraft. The current regulations are covered under Chapter 4 of Annex 16 to the Convention on Civil Aviation. It is applicable for all aircraft which entered into service after 2006 and is based on stipulated noise levels for a particular Maximum Takeoff Weight (MTOW) (Figure 2.8). [2.14]

It specifies maximum noise levels at each of three defined measuring points, which are to the sideline of the runway at Take off, under the flight path at Take off, and under the flight path on final approach. The commonly used Noise metrics are as follows [2.17, 2.18]:

- dBA: The A-weighted Decibel (dBA) is the most common unit used for measuring environmental sound levels. It adjusts, or weights, the frequency components of sound to conform to the normal response of the human ear at conversational levels.
- Decibel: The strength of a noise source is usually measured in decibels. Decibels are abbreviated as dB. They are logarithmic units, this is because sound powers and consequently intensities, typical different sources, cover a very wide range of values

- EPNdB: The Effective Perceived Noise Level (EPNdB) is a unit of measure of aircraft noise. It is based how people judge the annoyance of sounds they hear with corrections for the duration of the event and for pure tones.
- Intensity: The sound energy flow through a unit area in a unit time.
- L<sub>A</sub>max : Maximum A-weighted sound pressure level.
- L<sub>eq</sub>: The term L<sub>eq</sub> is shorthand for 'equivalent continuous noise level', which is a parameter that calculates a constant level of noise with the same energy content as the varying acoustic noise signal being measured.
- Quota Count System (QC): The Quota Count (QC) System is currently used for administering the night noise quotas at Heathrow, Gatwick and Stansted airports. The central feature of the system is that each aircraft given a quota count (QC) rating (e.g. QC/0.5, QC/1, QC/2, etc.) according to how much noise it makes. Aircraft are classified separately for landing and takeoff. The data used are the noise certification data: aircraft are required to possess a noise certificate demonstrating their compliance with the appropriate ICAO noise certification standards.

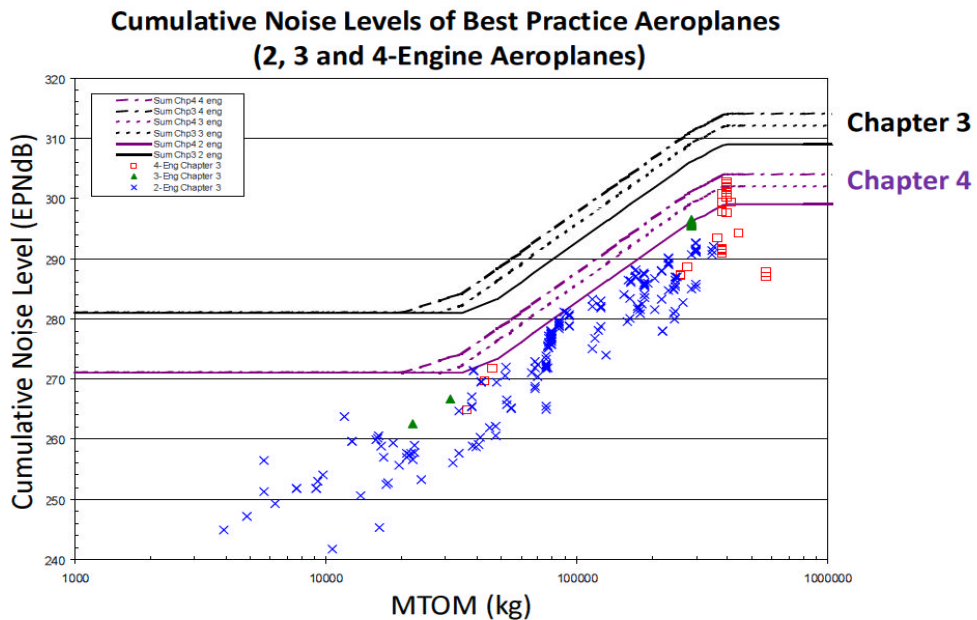


Fig 2.8 Noise standards for civil aviation by ICAO [2.14]

## 2.6 CURRENTLY IMPLEMENTED INTERNATIONAL EMISSION AND NOISE TAXES

With the effects of Global Warming having extensively been researched and documented as is evident in the literature review, various countries have taken voluntary initiatives to cap and reduce emissions with an aim to prevent a rapid increase in the future. Some of the key initiatives are discussed below:

CO<sub>2</sub>: European Union Emissions Trading Scheme (ETS) for CO<sub>2</sub> - As a part of the mandatory cap and trade policy (three phases) of the EU, the aviation sector is now included from 2012. Airlines operating within or to or from the EU are required to now monitor their fuel consumption and Revenue Tonne Kilometre (RTK) from January 2010. The total cap for annual CO<sub>2</sub> emissions produced by the aviation industry during 2012 will be 97% of average 2004-6 CO<sub>2</sub> emissions, falling to 95% in 2013-2020. The scheme run by The European Commission (EC), will use data on total fuel consumption and Revenue Passenger Kilometre (RPK) to allot each airline a share of the total aviation industry CO<sub>2</sub> emissions 'free allowance' (85% of an industry CO<sub>2</sub> emissions cap). Each airline's annual allowance will therefore depend on its volume of traffic and RTKs in the previous year, in comparison to the industry's total. The remaining 15% will be, as per requirement, made available to airlines via auction. [2.19, 2.20]

- New Zealand has planned a staged implementation of an ETS (2010-15) and plans to link its scheme to similar systems from other parts of the world.
- Switzerland will implement a system to voluntary cap and trade as an alternative to a CO<sub>2</sub> tax.
- Japan –will also begin voluntary cap and trade, to gather experience; however a proposal for a mandatory ETS is under consideration. [2.20]

NO<sub>x</sub> : At certain European airports (London, Stockholm, Zurich, Geneva and Mulhouse), airlines are currently charged a modular airport fees or tax, depending on the emissions levels (NO<sub>x</sub> and HC) of their aircraft. A high-performance aircraft pays a lower fee while an aircraft that performs less well in terms of NO<sub>x</sub> and HC will pay more sometimes. [2.21]

Noise: Most European Countries use internally defined taxation policies to levy charges on Noise. These taxation policies charge rates to be levied or discounted based on categories using aircraft noise measurement. Countries in Europe following this methodology include France, Netherlands, United Kingdom Switzerland and Germany. Italy and Austria use a taxation policy for noise which is only a function of aircraft weight. Literature has shown that the ICAO's (2004b) policy on economic instruments for noise taxation "does not explicitly mention efficiency as a goal, but rather recommends that the level of taxes be designed to recover no more than the costs applied to their alleviation or prevention". Research also indicates that the taxes collected for aviation noise by Australian and Dutch government are utilised in funding and implementing sound-proof modification programs for airport communities and are therefore aligned with the ICAO policy. [2.22]

## 2.7 GLOBAL AVIATION ENVIRONMENTAL PROGRAMS AND INITIATIVES

In line with ICAO's environmental objectives for the future, various research and development programs have been launched around the world, aimed specifically at generating technology solutions to achieve the stipulated environmental targets. Figure 2.9 shows some of the key international programs between 2001 and 2015.

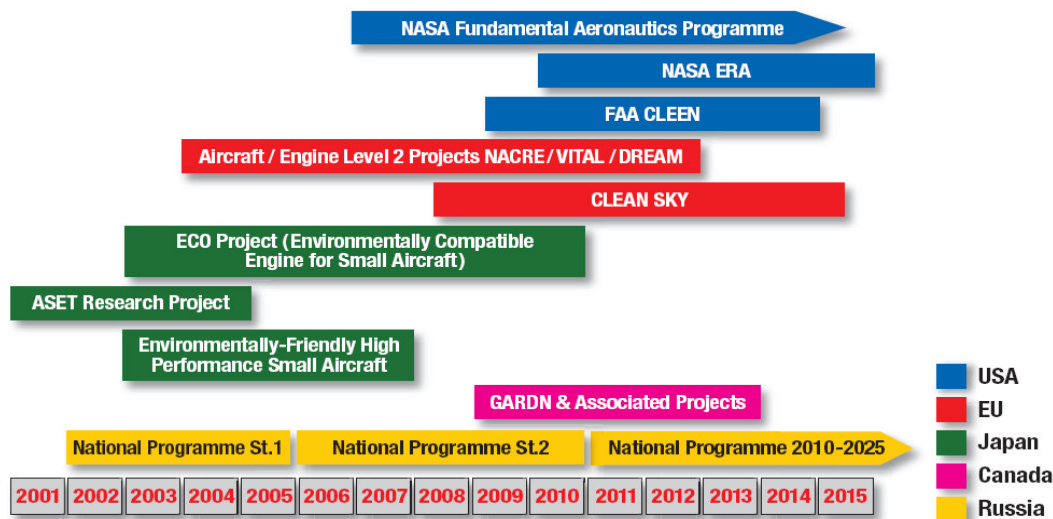


Fig 2.9 Programs aimed at reducing commercial aviation's impact on the environment [2.4]

Europe's initiative to remain at the forefront of the global aeronautics and air transport sector led to the formation of Advisory Council for Aeronautics Research (ACARE). ACARE is a council of at least 40 members from Europe, whose aim is to develop and maintain a Strategic Research Agenda (SRA) for aeronautics in Europe. The group has a clearly structured representation from the Member States and various fields of aviation which include the manufacturing industry, airlines, airports, service providers, regulators, the research establishments and academia. The organisation works under commonly agreed terms of reference, with a main focus to establish and carry forward a Strategic Research Agenda (SRA) that will influence all European stakeholders in the planning of national and EU research programmes, in line with the Vision 2020 and the goals it identifies [2.23]. In line with ICAO's environmental emission goals, ACARE has set up ambitious targets as its vision 2020 and aims to reduce environmental emissions from aviation by 2020 which include CO<sub>2</sub> by 50%, NO<sub>x</sub> by 80% and noise by half( compared to the year 2000 levels and standards).

One of the means by which the European Union supports scientific research and innovation is through Framework Programmes for Research and Technological Development. In the current Frame work Programme 7(FP7), Aeronautics and Air Transport (AAT) is part of the 'Transport' theme and is spread over 7 years with a budget for Collaborative Research [2.24]. Under this Framework and through JTI (Joint Technology Initiatives) the European Commission enables implementation of ambitious and complex projects.

In order to achieve these targets and to ensure that progress is made in relevant and conclusive research, the European commission orientated its work programmes in the AAT (FP7) on the recommendations of the ACARE Strategic Research Agenda. It focuses its efforts towards more environmentally friendly transport and 'Pioneering Air transport of the future', aiming to improve efficiency, time, cost safety and customer satisfaction. [2.24]

As a consequence of this, various programs have been initiated. Some of the key programs, launched as Joint Technology Initiatives (JTI) include- NEWAC, NACRE, VITAL, DREAM and Clean Sky.

The Clean Sky project was created in 2008 and focuses primarily on demonstration of Green Technologies capable of reducing the environmental impact of Aviation with a purpose of accelerating the integration in future European Aviation Transport. Clean Sky is structured into six Integrated Technology Demonstrators (ITDs) which are Smart Fixed Wing Aircraft, Green Regional Aircraft, Green Rotorcraft, Sustainable and Green Engines, Systems for Green Operations, and Eco-Design. As a part of receiving research funding from the Clean Sky project, a part of the research directly contributed (as a deliverable) to the Systems for Green Operation ITD (SGO ITD). This ITD focuses its efforts reducing the environmental impact ( $\text{NO}_x$ ,  $\text{CO}_2$  and noise) of aircraft in two areas- Management of Aircraft Energy which deals with an integrated approach towards a more electrical aircraft and Management of Trajectory and Mission to implement optimised operations [2.25]. A part of the work from this PhD entailed benchmarking and testing of the optimiser used for this purpose.

## 2.8 INDUSTRY RESEARCH ORIENTATION

In order to achieve ICAO's vision and consequently ACARE's extremely challenging environmental goals; various improvements are currently being researched into. The fact that optimisation of one objective may result in the deterioration of another objective in different phases of an aircrafts operation is in itself a significant challenge. Therefore achieving the environmental goals will require a synergised set of solutions which will necessitate the optimisation of every aspect of aviation in terms of aircraft technology and operations.

Research (and as seen in figure 2.6) has indicated achieving the 2050 targets for  $\text{CO}_2$  will require contributions from engine development (15% to 20%), airframes (20% to 25%) and improved air traffic management and operational efficiency (5% to 10%). Apart from this the use of alternative fuels and various policy and taxation measures will also be required to further augment the efforts in achieving the stipulated goals.

### 2.8.1 AIRCRAFT AND POWER PLANT TECHNOLOGY

The industry till date has achieved most of its gains in fuel efficiency from aircraft and power plant technology improvement. Aircraft technology improvements aimed at achieving future environmental goals are primarily focussed on the following three key areas:

1. *Improving overall specific performance of propulsion systems:* Optimisation of engines and thermodynamic cycles are aimed at reducing fuel burn per unit of delivered thrust. Research in this field is therefore aimed at improving the thermal propulsive and transmission efficiency of the engine. Thermal efficiencies are being improved through designs considering higher operating pressure ratios and engine cycle refinement. The major constraints include ensuring the optimal design has the least maintenance costs weight and size and consequently the drag whilst improving reliability and safety. Improvements in propulsive efficiency is being considered through adaptation of promising technologies like the geared turbo fans, CROR, hybrid configurations, advanced and ultra high bypass turbofans. Transmission efficiency is being improved through advanced architecture. [2.4]
2. *Improving the payload capability:* Current research is actively pursuing the reduction of the overall weight of an aircraft. Apart of improving the fuel burn characteristics of the aircraft it also reduces the carbon emissions whilst improving the payload capability and hence the economic efficiency of the aircraft. Aircraft weight is being reduced through application of advanced composites/ alloys and improvements in manufacturing process (through advanced welding technology, thus requiring no rivets and hence reducing weight and aerodynamic drag). Aircraft like the Boeing 787 and Airbus A350 will feature as much as 70% advanced materials and are slated to produce weight savings of as much as 15%. [2.4]
3. *Improving the aerodynamics of the aircraft:* The aerodynamic drag is primarily caused due to friction and lift dependant drag and results in higher fuel burn. Aerodynamic design optimisation of the aircraft results in reduced drag and consequently the required thrust. Research in reduction of lift dependant drag has led to the introduction of wing tip devices and is currently a well established fuel saving device of the industry. A significant part of the research however is aimed at the reduction of friction drag, which is known to have a huge potential in improving efficiency. This is being achieved through reduction of turbulent skin friction by attempting to maintain laminar flow through natural laminar flow and hybrid laminar flow control. This requires an optimised design to achieve minimum wetted areas, while minimising flow separation. The research in the field of laminar flow technology, even though being pursued for many years has not been commercially applied, but promises to provide significant efficiency benefits when applied in the future. Improvement in aerodynamics has also led to research in optimising air inlets and exhaust from devices and reducing external devices such as antennas. [2.4]

*Future revolutionary technology:* Certain future technologies which are also currently being actively researched and aimed at the distant future include electric propulsion, distributed

propulsion, pulse detonation engines and a move away from the conventional tube and wing concepts for aircraft, the blended wing body aircraft. [2.4]

## 2.8.2 OPERATIONAL IMPROVEMENTS

A study by Oxford University indicates that one of the most effective ways of minimising aviation emissions is to minimise the amount of fuel used in aircraft operations. Penner in his 1999 report for the IPCC indicated that globally due to inefficiencies in ATM systems the aviation industry loses up to 12% in fuel, which results in a financial loss of approximately US \$13.5 billion and 73 million tonnes of CO<sub>2</sub>[2.9,2.26]. With the increase in air traffic as predicted by the aviation industry in the future, this is set to continually rise. It is therefore imperative that operational procedures be optimised so as to ensure the efficiency of air traffic management is improved globally. While ICAO aims at an interoperable Global air traffic management system, various key ATM development programs around the world endorsing it are SESAR in Europe and NextGen in the US. The application of operational improvements through these programs, whilst not compromising on safety, considers the optimisation procedures of ground and in-flight procedures. These procedures do not require the introduction of new technology, but will still result in a radical change in which conventional aircraft will be operated and air traffic managed.

Currently due to safety requirements and high volume of traffic around commercial airports, all phases in flight for an aircraft are necessarily required to follow a certain set of rules and procedures. This restricts the aircraft from exploiting its full fuel saving potential. Currently through these projects discussed, research is being conducted into identifying the most optimal trajectories in terms of reduced fuel burn and lower environmental emissions. Some of the key initiatives are briefly discussed:

1. *Reduced Vertical Separation Minimum (RVSM)*: Aircraft currently are restricted to certain specific altitudes at cruise, due to safety considerations and air traffic management constraints. This leads to non optimal performance of aircraft at cruise, the longest segment of long range aircraft, and hence to reduced fuel economy. However Reduced Vertical Separation Minimum by more efficiently utilising airspace will allow aircraft to operate closer to their optimal altitude in terms of performance.
2. *Performance Based Navigation (PBN)*: This system is aimed to enable aircraft to fly more optimised 4D trajectories. It is also aimed at allowing more flexibility whilst ensuring safety predictability and efficiency in operations.
3. *Continuous Descent Operations (CDO)*: Currently aircraft during descent are not allowed to descend continually from the top of descent, thus leading to inefficiencies in terms of fuel burn performance. The Continuous Descent

Operations will allow the approach landing and arrival with a more energy efficient glide profile thus reducing the energy requirement.

4. *Trajectory Optimisation:* Optimised flight path for minimum fuel burn and lowered emissions in all phases of flight.

#### 2.8.3 ECONOMIC INSTRUMENTS

The ICAO's environment report [2.4] discusses various market based measures currently being considered, which form a significant part of the global environmental emission mitigation strategy. The various kinds of policy tools include emissions trading, emission related taxes or charges and emission offsetting. All these measures are aimed at achieving specific environmental goals with more flexibility than current control measures existing in various countries. In the context of this work, as it eventually examines emission taxation, it is found prudent to briefly discuss the various tools.

Under the Kyoto protocol, emission trading is recognised as a mechanism through which a developed country, to meet its emission limitation targets may choose to transfer emission units to/from another country. If followed, it ensures that the total emission allowances to all developed countries does not change, but allows inter country trading. A country may therefore buy any number of units, but is permitted to sell only a limited number based on the minimum number to be mandatorily held in its national registry. Emission levies on the other hand are charges or taxes designed to address emissions from international aviation. They are considered to be potentially advantageous in terms of simplicity in administration, implementation and low transaction costs. EU ETS in Europe is a typical example of emission trading scheme currently in use. [2.4]

#### 2.8.4 ALTERNATIVE FUELS

The reason the industry is actively pursuing alternative fuels is because irrespective of the aggressive drive towards more fuel efficient and environmentally friendly technology, as long as the industry uses conventional fuels they will be reliant on the global reserves of the fast depleting supplies of fossil fuels. Therefore in order to achieve sustainability, research is being conducted into various alternative fuels. These fuels currently do exist but are currently unavailable in required bulk quantities for commercial application. The fuels currently being researched include hybrid fuels, synthetic and biofuels as a near term solution and hydrogen fuel as long term goal.

## 2.9 RESEARCH ON TECHNO-ECONOMIC ENVIRONMENTAL RISK ASSESSMENTS

From the discussion this far it is evident that for a sustainable future, significant and continued improvements will need to be introduced in the field to balance the underlying growth within the aviation industry. It is also evident that technology changes essentially aimed at tackling emissions and to achieve steep environmental targets, will be subject to various regulations and policies in the future. Therefore, assessing and understanding the effects of emission mitigation policies on future technology / operations and further establishing their interdependency in finally achieving the desired goals of lowered environmental emission, is critical.

After basically understanding the prevailing scenario and the dynamic environment in the aviation industry in terms of future policies, a review of literature was undertaken, with an aim to establish the research conducted into understanding the applications and effects of environmental policies.

'Techno-economic & Environmental Risk Assessment' (TERA) is a concept developed at Cranfield University and essentially comprises a framework of mathematical models to simulate the performance of single or a set of technologies. The framework through its application allows an increased visibility of risks, whilst enabling the user to compare and rank competing schemes on a formal and consistent basis so that investment resources can be allocated efficiently.

The framework is modular in structure and consists of a set of core models which allow simulation of detailed power-plant systems and component mathematical models. The core models can be further coupled with a wide range of environment, economic and risk models. The assessments are conducted on a system and mission level and may be used to deliver a reasonably clear view of the relative risks and benefits of promising but uncertain concepts, at lower TRL levels of development. This method offers an independent and consistent evaluation procedure to allow comparative studies of complex systems, encompassing local and global conditions.

TERA has been used extensively in the past in various EU projects to conduct design space exploration and trade-off studies, parameter sensitivity analysis, asset management, multi - disciplinary optimisation and to assess the effects of environmental policies [2.28, 2.29].

A typical illustration of the framework for a civil aviation application is as shown in figure 2.10.

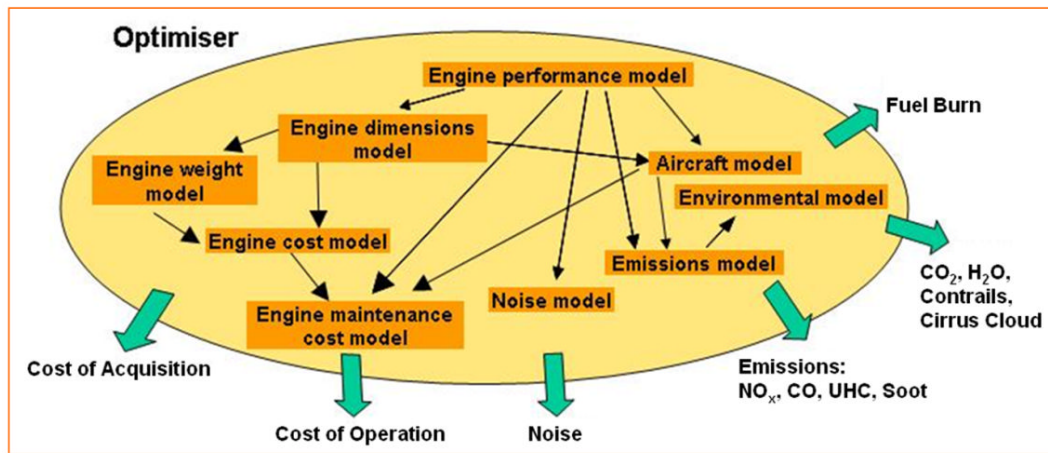


Fig 2.10 Typical TERA Framework for civil aviation [2.27]

Amongst the relevant research found some of the most notable are further discussed. A paper by Gabbrielli and Singh [2.30], exhaustively investigates the economics and scenario analysis of new gas turbine combined cycles, with no emissions of CO<sub>2</sub>. The work primarily considers industrial power generation systems using novel cycles. The aim of the work was to conduct an economic analysis to estimate the investment per unit electricity generated and the levelised discounted cost of electricity in comparison with a standard reference combined cycle power plant. Of particular interest in this study was the scenario analysis using the "2<sup>K</sup> Factorial design technique" which effectively permits the user to analyse the average effect of the variation of each input factor on the output variable. The scenario analysis in the research established the potential of the improved cycle power generation plant and the possible economic/ environmental policies that may be required to mitigate environmental pollution effects and encourage low emission applications.

The next relevant research found was undertaken by Maritato [2.31]. His research dealt with examining "Climate Energy prices and their likely impact on Civil Aviation and Power Generation". The main purpose of his work was to begin a study by undertaking an extensive literature review and further with the aid of a computing model and questionnaire, establish a possible set of future scenarios in the civil aviation and power generation sector. The aim of his work was to bring perspective to the effect of climate change and its actual implications on civil aviation and power generation on a global perspective.

Further literature research in this field was centred more towards civil aviation and led towards work undertaken by Pascovici [2.32]. Pascovici for his doctoral studies at Cranfield University investigated various future propulsion systems and novel cycles, with the aim of establishing an initial framework of optimised propulsion systems to achieve environmental targets as set by ACARE using the TERA approach. His work created a tool that provided a definitive approach to understanding the methodology of considering critical factors such as aircraft and engine performance, weight, noise emissions and direct operating cost (DOC)

when undertaking a Techno-economic Environmental and Risk Assessment (TERA) of a conceptual propulsion system.

Techer [2.33], basically continued Maritato's work (2008) further, but concentrated primarily on the civil aviation sector as a core part of the study. In order to forecast likely impacts of various recommendations made under a series of conditions, and assess aviation's medium and long term impacts on climate change and global warming, he utilised various statistical, numerical and computational tools in the course of his study. He considered three possible scenarios (Business as Usual, Progressive Environmental awareness and High Environmental Awareness) and the response to mitigating Climate Change. His assessment tool provides preliminary but relevant and relatively consistent results in terms of fuels consumption and induced emissions. It also throws light on RF and temperature rise results, taking into account the CO<sub>2</sub> and NO<sub>x</sub> emissions impact from civil air traffic.

The next step in the process of reviewing literature was to identify research that have used similar frameworks aimed to specifically establish the effect future policies aimed at reducing environmental emissions may have on induction and economic viability of future technology and optimised aircraft operations. Conversely, the potential of future technology and optimised aircraft operations may have in mitigating environmental emission and improve the profitability of an operator.

A significant insight into this area has been provided by Dray et al. [2.34, 2.35]. Based on the work for the Omega project, their comprehensive research assesses the effect mitigation policies and technology options may have on the potential of reducing emissions on a regional and global scale. One of the most relevant parts of this research investigates the effectiveness of various economic, emission and technology mitigation measures in reducing the total lifecycle CO<sub>2</sub> emissions of aviation fuels to below year 2005 levels, by 2050 for Europe. This work has resulted in numerous publications.

For economic measures it considers the introduction of emission trading through EU ETS. The technological strategies consider various options which include retrofits to conventional aircraft and airframes, changes to standard maintenance routines to improve operational and on wing performance, the introduction of revolutionary concepts in reducing fuel burn such as the propfan and adapting of environmental friendly biofuels. The operational strategies assume the fuel efficiency benefits in better air traffic management through SESAR. Apart from this it also considers alternatives to flying in order to reduce CO<sub>2</sub> emissions and hence looks at various interactions of multiple measures to produce the desired effect of reducing environmental emissions.

The effectiveness of a combination of these measures is examined under three socio economic conditions (high, medium and low) utilising forecasted values of GDP, fuel and CO<sub>2</sub> prices. Some of the key findings from this study show that of the measures considered, there exists no

single measure which will allow the emissions to reduce to below year-2005 levels by the 2050.

The study found mitigation will require the adoption of a combination of policies and is sensitive to the socio economic scenario prevailing. The combination of emissions trading and biofuels represents the most promising option, however compliance to SESAR, and introduction of CROR aircraft and high-speed rail networks may also be required to meet the emission reduction objectives. Each of these were however found sensitive to the scenarios and hence even though compliance to SESAR was adopted in all scenarios, bio-fuels was adopted only in the central and high scenarios while the open rotor technology was only adopted under the high GDP, oil and carbon price scenario.

The study effectively demonstrated the complexity of the system and the interaction between the various modules in understanding and quantifying the challenges of emission reduction on a geographical scale.

Kirby [2.37] in his work dealing with the forecasting and selecting future technologies proposes a methodology to select an ideal combination amongst a set of emerging technologies, to provide after induction, the maximum economic profitability and hence the maximum return on research and development investments.

The methodology demonstrated allows assessment of a set of technologies from a business strategy perspective. It quantitatively justifies the allocation of resources within an organisation by identifying high pay off technologies in the early phase of product design.

The approach begins by defining the problem through mapping customer requirements into quantitative evaluation criteria. The baseline configurations are then modelled to establish the baseline economic metrics such as acquisition and operating cost values. Any infusion of technology will result in the modification of the economic metrics as percent reduction of the baseline values established.

The method then goes on to establish the technology alternatives that may be infused to improve performance. This part of the process requires elaborate data on the technology selected such as the technology maturity/readiness level and depending on this, the author suggests, may have a level of uncertainty. It goes on to define an impact matrix which essentially produces estimated and theoretical upper limits on the impact each of the technology infusion may have on the aerodynamic and physical design of the aircraft. The compatibility matrix then establishes physical compatibility rules amongst the technologies. The next step of the process is to apply the selected technologies to the base line system and assess the impacts. The method then applies three techniques namely technology sensitivities using a full factorial evaluation , multi attribute decision making techniques in which multiple attributes are processed to arrive at a single choice for the best product and technology frontiers utilising an effectiveness parameter.

The reference further provides a proof of concept by applying the proposed methodology. Applied to conventional aircraft of 2001, it aimed to reduce the cost of air travel by 25% as a near term goal (by the year 2007) and by 50% as a long term goal (by the year 2022). Therefore in order to achieve the objective it defines the acquisition cost and direct operating cost as the system level metrics. It identifies a set of eleven technologies for infusion to choose from, to achieve the required objectives. The study concludes by identifying four of the eleven technologies most suitable for infusion into the technology, but was yet unable to achieve the affordability goals that were set and hence recommends pursuing more aggressive technologies to infuse.

Henderson [2.36] and Kroo [2.38] investigated the subject from a different approach. Their work essentially dealt with optimising engine conceptual design and aircraft operations, using genetic algorithms for minimum direct operating cost, mission fuel burn and NO<sub>x</sub>.

Henderson's [2.36] research, the most recent in this field, uses a multi disciplinary optimisation framework in an attempt to define requirements of an integrated design. The work effectively demonstrated optimised design aspects for an aircraft. The study indicated towards particular specificities such as, for an aircraft optimised for minimum fuel burn the, the design would require to have a high aspect ratio wing with lower induced drag , high bypass ratio engines and high core pressures/ temperatures for greater efficiency.

For low LTO NO<sub>x</sub> emissions the design required high aspect ratio wings with the largest wing area amongst the trade-off design studies. The engines had high bypass ratios and low core pressures and temperatures low thrust levels. This aircraft had high direct operating cost due to its low cruise speed, and high fuel burn due to poor engine efficiency.

The study also demonstrated the feasibility of using large aircraft for short ranges to reduce the environmental impact of aviation.

To summarise, the methods described use elaborate model integration frameworks and tools to provide interesting perspectives into the interdependencies of technology solutions and emission mitigation initiatives in unique ways. However, the work by Kirby and Henderson examine technology from an air framer or engine manufacturer's view point, thereby selecting the best technology for an investment given a particular scenario. Dray, on the other hand, purely assesses technology from a policy maker's viewpoint, thereby focussing on the global effectiveness of the technology or a policy, in reducing the impact on the environment.

However, one of the most important stake holders is the airline operator. No aircraft design can enter production without the firm support of orders from an airline operator. For the airline operator, sustainability within the aviation industry, as in any other industry, depends on the elasticity of demand for the product and profitability through minimising operating costs. Apart from other factors, this profitability is directly affected by any technology infusion

or change in operations, be it aimed towards any of the global objectives which include reducing fuel burn, environmental emissions or noise.

The case of the Counter Rotating Open Rotor (CROR) is the perfect example of this. The CROR introduced and well proven as a radical technology, promised to offer substantive reductions in fuel consumption in the 1980s. But a significant drop in the price of fuel in the 1980s was one of the primary reasons for it never being accepted for commercial use, as the industry just did not find the concept economically viable.

Therefore the literature review indicated that a requirement existed for creating a set of tools that would enable the airline operator, as an important stake holder to better understand the effect, various proposed environmental initiatives will have on their operational cost. This then forms the basis of the contribution to knowledge of this PhD research.

## 2.10 SCOPE OF WORK

Climate change and the aviation sector's contribution of to it have been a cause of concern for a while now. As the literature review has shown, in the recent past considerable amounts of resources in terms of capital and scientific research have been utilised to enable generate solutions to reduce its environmental impact. This chapter was aimed at firstly consolidating the vast amounts of information on the subject, and secondly to bring into perspective the existing regulations and policies in force today.

To briefly summarise, the earliest literature available on the concerns of the aviation sectors environmental impact dates to mid 1970's, but the more relevant research was observed to be from early 1990s and onwards and have been concentrated mostly on the effects of CO<sub>2</sub>. Numerous references were found in this discipline area and many others were also found on the effects of LTO cycle NO<sub>x</sub> and Noise, however to keep the review concise and precise, not all of these were included in the chapter.

The review indicated towards certain critical aspects. Most technological advancements have been focused towards reducing fuel consumption and consequentially CO<sub>2</sub> emissions. As discussed earlier most current regulations and emission trading schemes are currently aimed at addressing only CO<sub>2</sub>, due to the established fact that CO<sub>2</sub> has greater long term impact. NO<sub>x</sub> and Noise are taxed only at certain airports and in a limited capacity. Due to continuing scientific uncertainty and limited research of aviation's contribution towards contrails and cirrus cloud formation, no policies exist and hence they have not yet been taken into account in terms of taxation.

However literature indicates that with the strong and continued growth of aviation, the focus and research will gravitate towards-

- Reducing the uncertainties of aviation's non-CO<sub>2</sub> effects (specifically in the area of the environmental effects of cruise NO<sub>x</sub> and contrails).
- Development of technologies to firstly control and then mitigate commercial aviation's impact
- Implementation of regulations and policy measures to further encourage the aviation industry to transit towards optimal strategies in terms of technology and operation, thus striving to achieve stringent and steep environmental targets.

As indicated it is then imperative for an airline operator to understand the implications of the various environmental regulations and policies, and consequently be able to strategise accordingly. Therefore if a novel technology or change in operations needs to be introduced, then from a fleet planning and operations perspective, the following questions become necessarily pertinent:

- Can the introduction of a novel technology or optimised methods of operating current technology, actually translate the efficiency of reducing emissions to operating profits?
- In terms of operations, what kind of trajectories will be the most cost effective under potential taxation and fuel price scenario?
- For a novel technology, will these profits be sufficient to supersede what's already on the market and thus offset a higher acquisition price and complexity of technology?
- Given a higher acquisition price and maintenance cost of a new technology, what taxation or fuel price scenario will establish its viability and actually justify a technology shift from a conventional solution?
- Is the current level of taxation adequate to push the industry towards greener solutions?

Previous research reviewed does shed light on these aspects, but more from an airframe manufacturer's perspective. The aim of the work, and hence the contribution to knowledge from this PhD is to specifically answer the questions posed more from an operator's and policy maker's perspective and therefore through the insight it provides, the work in this PhD differs from those reviewed.

The entire work is based on a TERA framework described earlier. The first part of work approaches the subject from an operations perspective, wherein it establishes an environmental gain through application of concepts of optimised flight trajectories. A methodology, based on an operational cost analysis approach, is then introduced to examine the actual economic feasibility of the optimised trajectories under the current fuel price scenario. It then goes onto examine the effect future CO<sub>2</sub> taxation policies may have on the acceptance of trajectories. The method then further attempts to establish the taxation rate

required to force an operator to switch from a conventional trajectory to more environmentally friendly trajectories.

The second part of the study looks at the subject from the perspective of induction of novel technologies. It introduces another methodology which is based on set of specific assessments. These assessments essentially compare a novel technology with competing conventional solutions and establish its benefits in terms of performance and energy efficiency. These studies are undertaken for various emission taxation and fuel price scenarios to further establish if the observed efficiency may be translated to improvements in operating cost. The focus of the work is to then utilise these assessments and concepts of Net Present Value (NPV) and Internal Rate of Return (IRR) in an investment cost analysis approach.

The aim is to answer questions from a policymaker's or airline operator's perspective, on the issue of whether the technology can translate efficiency to operating profits, sufficient to supersede what's already on the market and thus offset a higher acquisition price and complexity of aircraft. Alternatively, what taxation or fuel price scenario will establish its viability and actually justify a technology shift from a conventional solution, given a particular acquisition and maintenance cost?

### 3. THE OPTIMISATION FRAMEWORK AND THE MODELS

#### 3.1 INTRODUCTION

As described in the previous chapter the Techno-economic & Environmental Risk Assessment (TERA) is a concept developed at Cranfield University and essentially comprises a framework of mathematical models to simulate the performance of single or a set of technologies. The framework is modular in structure and consists of a set of detailed mathematical models. Depending on the type of models used, the framework once integrated allows the simulation of a system and hence allows detailed analysis of the system from a component performance level to integrated system dynamics. The concept, proven in various EU projects, offers an independent and consistent evaluation procedure to allow comparative studies of complex systems, encompassing local and global conditions [2.28, 2.29].

Based on this concept and in order to accomplish the work in this PhD, a specific TERA framework was developed. This chapter aims to therefore give the reader an understanding of this framework and the associated models utilised for the work. The chapter begins with a description of the optimisation framework which was used to integrate the various models into a network and then goes on to describe in detail each model and its assumptions. In order to improve the confidence in the results from the models, certain validation and verification test were conducted and therefore a description of these test with an analysis of results is included wherever relevant.

The chapter finally concludes with a description of the genetic algorithm based optimiser used within the framework, which has been developed and benchmarked by the author in collaboration with Airbus France within the Systems for Green Operation Integrated Technology Demonstrator (SGOITD) in the Clean Sky Project.

#### 3.2 FRAMEWORK

The basic structure of the TERA framework used is as shown in figure 3.1. It basically shows the interlinking of models and the optimiser. The framework is essentially built using the Matlab software wherein each of the models exists as an executable. It may be noted based on the requirement of a case study the framework is customised, however the basic structure of the framework is as illustrated in figure 3.1.

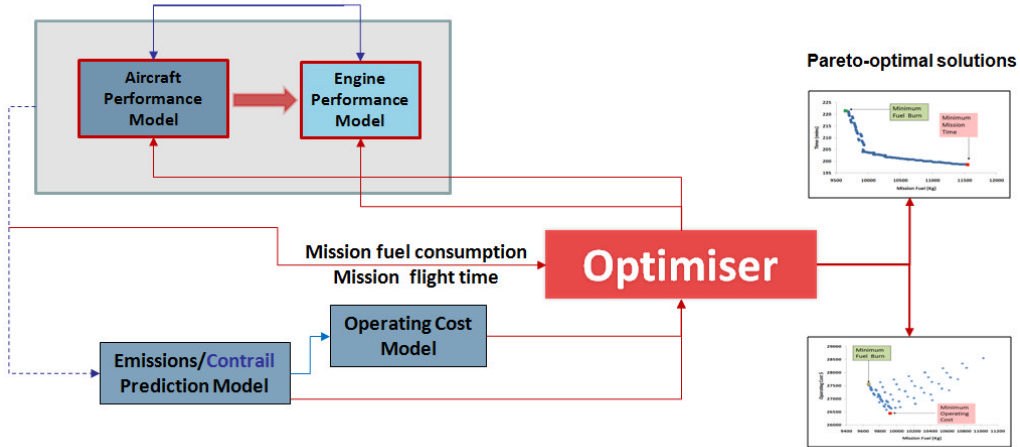


Fig 3.1 Interlinked models in the TERA framework

### 3.2.1 AIRCRAFT PERFORMANCE MODEL

The aircraft performance model is an essential part of the model setup. During the initial part of the research study, various aircraft performance models were considered for use. Cranfield University's in-house integrated engine and aircraft performance tool, *HERMES*, was initially used for preliminary analysis. Based on experience with this tool various additional requirements were identified and a new version of this tool was developed by the author.

The primary requirement of the generic aircraft model to be used in the framework is to be modular in structure and be easily interchangeable to simulate of various fixed wing civil aircraft. The model has been therefore been structured to enable the following:

1. Facilitate easy interchanging of aircraft type and engine using input text files and GUI
2. Input files to change mission requirements such as payloads, load factors
3. Detailed output files to enable the user to access various information such as gradient angles, ROC/D, speeds (airspeeds & mach numbers) etc.
4. Easy interfacing of other models such noise , emission, DOC and contrails
5. Analysis of individual flight segments (takeoff, climb, cruise, descent, approach and landing)
6. Analysis of a full mission
7. Facilitate engine cycle optimisation

Apart from the necessity to incorporate the above mentioned requirements, a secondary motivation was also to develop a code to understand better application and implementation of theories in aircraft performance modelling. The fundamental differences from the original version include the following:

- Unlike the previous version which utilises a database, this version interlinks the engine performance code (Turbomatch) directly with the aerodynamic model in order to process engine thermodynamic calculations.
- Modelling of some of the phases such as take off is more detailed
- The drag polar is adapted from the euro control database for aircraft (BADA) and hence switching of aircraft models is more convenient [3.1]

Utilising the generic aircraft model described in this chapter, specific models based on the characteristics of the conventionally used short/medium range single aisle aircraft (Boeing 737-800 equipped with two twin spool turbofan CFM56-7B27 engines) and a propfan aircraft (MD 90 equipped with two CROR engines) were modelled. It may however be noted that this chapter includes description and the validation/verification of only the Boeing 737-800 aircraft model. The description of the aircraft and engine model for the MD-90 equipped with two CROR engines will be taken up in the chapter 7, which discusses novel technologies.

### 3.2.1.1 Total Energy Model

The model is based on the Total Energy Model [3.1] which equates the rate of work done by forces acting on the aircraft to the rate of increase in potential and kinetic energy

$$(T_{HR} - D)V_{TAS} = mg_0 \frac{dh}{dt} + mV_{TAS} \frac{dV_{TAS}}{dt} \quad 3.1$$

$T_{HR}$ -Thrust acting parallel to the aircraft velocity vector (Newton)

D- Aerodynamic drag

m- Aircraft mass (Kilograms)

h- Geodetic altitude (m)

$g_0$ - Gravitational acceleration ( $9.80665 \text{ m/s}^2$ )

$V_{TAS}$ - True airspeed (m/s)

$d/dt$ - time derivative ( $\text{s}^{-1}$ )

### 3.2.1.2 Aerodynamic Drag

The lift coefficient  $C_L$  is determined using equation 3.2

$$C_L = \frac{2mg_0}{\rho V_{TAS}^2 S \cos \theta} \quad 3.2$$

$\cos \theta$  = bank angle

S = Aircraft wing reference area

$\rho$  = Air density (kg/m<sup>3</sup>)

Under nominal conditions the drag coefficient  $C_D$  is specified as a function of lift coefficient and  $C_{D0}$  and  $C_{D2}$  (being the parasitic drag coefficient and induced drag coefficient) [3.1], as described in the BADA model specification. These coefficients are specific to aircraft and flap setting and hence are varied through the trajectory as per aerodynamic surface requirements for a particular phase of flight.

$$C_D = C_{D0} + C_{D2} \times C_L^2 \quad 3.3$$

$$D = \frac{1}{2} \rho V_{TAS}^2 S C_D \quad 3.4$$

### 3.2.1.3 Take off

The primary objectives of the takeoff phase during engine cycle and mission optimisation analysis are field length, noise and LTO emissions. The takeoff segment therefore has been designed to calculate speeds distances and thrust variations through the phase. The calculations in the model during the takeoff phase assumes the standard procedure wherein the aircraft starting at rest, accelerates along a runway at a low angle of attack altitude and passes the stall speed  $V_s$ . After increasing the speed to  $V_r$  (speed of rotation) and an increased angle of attack the aircraft continues to move along the runway until the speed increases to  $V_{LOF}$ . The aircraft then lifts off the ground and begins to gain height until it reaches screen height (35 Ft/10.7m). At this point the aircraft reaches a speed  $V_2$ , a critical parameter in the estimation of takeoff performance it. [3.2, 3.3]

On resolving forces during ground roll (Figure 3.2)

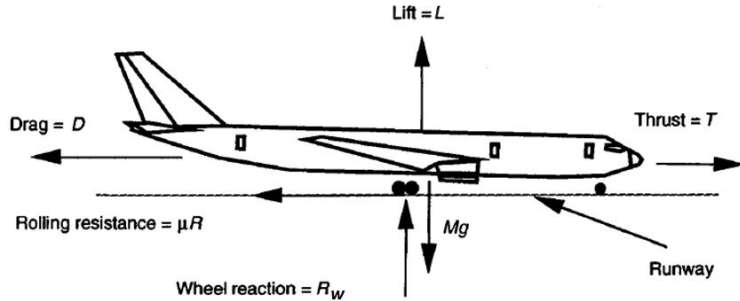


Fig 3.2 Aircraft at takeoff [3.2]

Resolving forces horizontally

$$T_{HR} = D + m \left( \frac{dV_{TAS}}{dt} \right) + \mu R_w \quad 3.5$$

$\mu$  = Runway Coefficient of friction (Paved Runway  $\mu=0.02$ )

Resolving forces vertically

$$R_w = mg_0 - L \quad 3.6$$

Combining

$$m \left( \frac{dV_{TAS}}{dt} \right) = T_{HR} - D - \mu(mg_0 - L) \quad 3.7$$

$$W = mg_0 \quad 3.8$$

$$L = \frac{1}{2} \rho V_{TAS}^2 S C_L \quad 3.9$$

$$(dV/dt) = [\left(\frac{T}{W} - \mu\right) + (\rho \left(\frac{2W}{S}\right))(-C_D - \mu C_L)V^2]g_0 \quad 3.10$$

The ground run  $S_g$  is then calculated using the integral

$$S_g = \int_0^{V_{LOF}} \frac{1}{2(dV/dt)} dV^2 \quad 3.11$$

The speeds are calculated as follows

$$V_{STALL} = \sqrt{\frac{2mg_0}{\rho S C_{Lmax}}} \quad 3.12$$

$$V_{LOF} = 1.1 \times V_{stall} \quad 3.13$$

Two constants  $K_T$  and  $K_A$  are defined as follows [3.2]

$$K_T = \left( \frac{T}{W} - \mu \right) \quad 3.14$$

$$K_A = \left( \rho \left( \frac{2W}{S} \right) \right) (-C_D - \mu C_L) g_0 \quad 3.15$$

Substituting equations

$$(dV/dt) = [K_T + K_A V_{lof}^2] g_0 \quad 3.16$$

Therefore the ground roll distance is

$$s_g = 1/(2gK_a) \ln [(K_T + K_A V_{lof}^2)/K_T] \quad 3.17$$

### Transition to Climb

During Transition the aircraft accelerates from  $V_{lof}$  to  $V_2$  the model uses a simplified method as recommended by reference [3.2](figure 3.3). The following assumptions are made:

- The aircraft is flying at  $0.9 C_{L_{max}}$
- The speeds  $V_{trans}$  and  $V_2$  are fractions of  $V_{stall}$
- The aircraft flies along an arc
- For small angles  $\cos\theta=1$

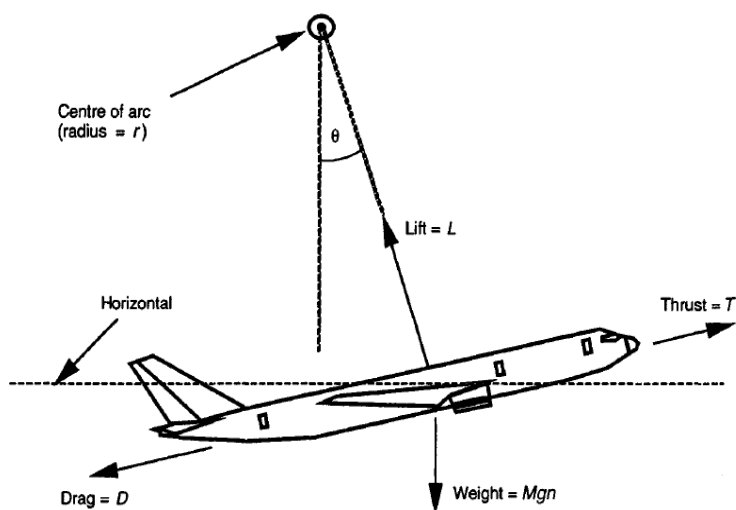


Fig 3.3 Aircraft in transition to climb [3.2]

$$V_{trans} = V_{stall} \times 1.15 \quad 3.18$$

$$V_2 = (V_{trans} \times 2) - V_{lof} \quad 3.19$$

Resolving the forces normal to the flight path

$$L = mg_0 \cos\theta + \frac{mv_{trans}^2}{r} \quad 3.20$$

r = radius of arc

$$\text{If } n = \frac{L}{mg_0} \text{ and } L = \frac{1}{2}\rho V_{trans}^2 S \times 0.9 C_{l,max} \quad 3.21$$

Substituting

$$n = 1 + \frac{V_{trans}^2}{rg_0} \quad 3.22$$

$$r = \frac{V_{trans}^2}{g_0(n-1)} \quad 3.23$$

Knowing the radius of the arc and the final gradient  $\gamma$  the ground distance  $S_t$  covered and height at the end of transition may be approximated by

$$S_t = \gamma r \quad 3.24$$

$$h_t = \frac{r\gamma^2}{2} \quad 3.25$$

As per regulations the height at the end of transition must exceed 35 ft. The take off segment is completed at 1500ft and aircraft is assumed to have reached a velocity of V2+10.

### 3.2.1.4 Climb

The climb phase of the trajectory begins at 1500ft and continues up to the cruise altitude. This phase is further divided into 4 sub segments:

- 1500 ft-3000 ft- The aircraft climbs at constant VCAS and speed V2+10.
- 3000 ft-10000 ft-the aircraft climbs at constant VCAS 250 kt
- 10000 ft-Transition altitude- The aircraft climbs at constant VCAS 310 kt till transition/ crossover altitude, which if airspeed and a mach number are specified, is defined as the (geo-potential pressure) altitude at which the VCAS and Mach number will represent the same TAS value.

- d. Transition altitude - cruise altitude: The aircraft climbs at constant mach number

The two main independent control inputs available for affecting the aircraft trajectory in the vertical plane include the throttle and the elevator. These inputs in turn allow three main variables to be controlled during climb namely the thrust, speed and rate of climb. The model essentially uses thrust and speed to control the rate of climb of the aircraft. The speed profile in the climb segment is defined as explained previously and the thrust is controlled by a variable power setting and maximum climb rating.

Climbing at constant equivalent/calibrated airspeed will result in a corresponding increase in true airspeed as altitude increases and climbing at constant Mach number below the tropopause implies a decrease in equivalent airspeed. Therefore the calculation of climb performance takes these effects into account.

Equation 3.1 is then rearranged to give

$$(T_{HR} - D)V_{TAS} = mg_0 \frac{dh}{dt} + mV_{TAS} \frac{dV_{TAS}}{dh} \frac{dh}{dt} \quad 3.1$$

$$\text{climb gradient} = \frac{(T_{HR}-D)}{mg_0} \quad 3.26$$

$$\frac{dh}{dt} = \frac{(T_{HR}-D)V_{TAS}}{mg_0} \left[ 1 + \left( \frac{V_{TAS}}{g_0} \right) \left( \frac{dV_{TAS}}{dh} \right) \right]^{-1} \quad 3.27$$

$dh/dt$  is the vertical speed or change of geodetic altitude with time.

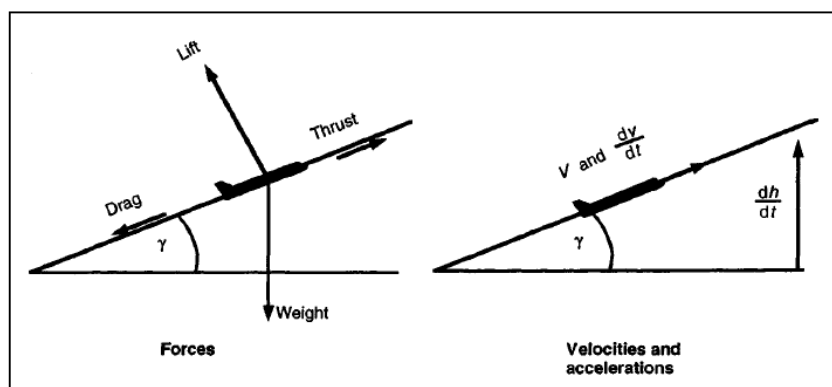


Fig 3.4 Aircraft in climb [3.2]

Assuming standard constant gravity field and hence identical geodetic and geo-potential altitudes, the ROC/D or variation of geo-potential pressure altitude Hp with time is given as

$$ROC = \frac{(T_{HR}-D)V_{TAS}}{mg_0} \left[ 1 + \left( \frac{V_{TAS}}{g_0} \right) \left( \frac{dV_{TAS}}{dh} \right) \right]^{-1} \quad 3.28$$

$$\text{If } f\{M\} = \left[ 1 + \left( \frac{V_{TAS}}{g_0} \right) \left( \frac{dV_{TAS}}{dh} \right) \right]^{-1} \quad 3.29$$

Then

$$ROC/D = \frac{(T_{HR}-D)V_{TAS}}{mg_0} f\{M\} \quad 3.30$$

where  $f\{M\}$  is defined as the acceleration factor or the energy share factor which essentially specifies the amount of power available to the aircraft to climb as opposed to acceleration while following a selected constant speed/ mach profile

$f\{M\}$  for particular flight conditions are defined as follows

- a. Constant Mach number in stratosphere  
 $f\{M\} = 1.0$  3.31
- b. Constant Mach number below tropopause

$$f\{M\} = \left[ 1 + \frac{kR\beta_{T,<\beta}}{2g_0} M^2 \frac{T - \Delta T}{T} \right]^{-1} \quad 3.32$$

$$R=287.05 \text{ J kg}^{-1}\text{K}^{-1}$$

$$g_0=9.81 \text{ m/s}^2$$

$$\beta_{T,<}=-0.0065 \text{ } ^\circ\text{K/m} (\text{ISA Temperature gradient below the tropopause})$$

M= Mach number

$k = 1.4$  (adiabatic index of air)

$\Delta$  = temperature deviation from ISA conditions

- c. Constant Calibrated Airspeed below tropopause 3.33

$$f\{M\} = \left[ 1 + \frac{kR\beta_{T,<\beta}}{2g_0} M^2 \frac{T - \Delta T}{T} + \left( 1 + \frac{k-1}{2} M^2 \right)^{\frac{-1}{k-1}} \left\{ \left( 1 + \frac{k-1}{2} M^2 \right)^{\frac{k}{k-1}} - 1 \right\} \right]^{-1}$$

- d. Constant Calibrated Airspeed above tropopause 3.34

$$f\{M\} = \left[ 1 + \left( 1 + \frac{k-1}{2} M^2 \right)^{\frac{-1}{k-1}} \left\{ \left( 1 + \frac{k-1}{2} M^2 \right)^{\frac{k}{k-1}} - 1 \right\} \right]^{-1}$$

### 3.2.1.5 Cruise

In cruise the aircraft is neither accelerating or climbing and will be assumed to fly at a constant Mach number and altitude

$$(T_{HR} - D)V_{TAS} = mg_0 \frac{dh}{dt} + mV_{TAS} \frac{dV_{TAS}}{dt} \quad 3.1$$

Hence from equation (3.1)

$$\frac{dh}{dt} = 0$$

$$\frac{dV_{TAS}}{dt} = 0$$

Therefore for the cruise segment

$$T_{HR} = D \quad 3.35$$

### 3.2.1.6 Descent

The descent phase is calculated similar to climb with the exception that in order to descend the thrust is less than the drag. However  $f\{M\}$  (deceleration factor in descent) is calculated similar to the climb phase.

$$ROD = \frac{(D-T_{HR})V_{TAS}}{mg_0} \left[ 1 + \left( \frac{V_{TAS}}{g_0} \right) \left( \frac{dV_{TAS}}{dh} \right) \right]^{-1} \quad 3.37$$

The descent phase of the trajectory begins at end of the Cruise segment and continues up to an altitude of 3000ft. This phase is further divided into 4 sub segments:

- a. Cruise altitude-Transition altitude: The aircraft descends at constant Mach number.
- b. Transition altitude – 10000 ft- The aircraft descends at constant VCAS 330 kt till an altitude of 10000 ft.
- c. 10000 ft-3000 ft- The aircraft descends at a constant VCAS 250 kt.

Similar to Climb phase the control inputs for this segment will include thrust (set by the flight idle rating), speed (as set through a speed schedule) or a fixed rate of descent (ROD). A key assumption in this phase is that the decent is continuous and speed changes between sub segments are assumed to be instantaneous. As per standard procedure, the ROD of descent is controlled so as to ensure that rate of descent in cabin does not exceed 300 ft/min.

### 3.2.1.7 Approach and landing

The approach phase for the aircraft is considered to begin at 3000 ft till 1500 ft and is currently calculated similar to the last sub-segment of descent (constant VCAS 200 kt). From 1500 ft the gradient angle is fixed at 3° to the horizontal with a speed of 1.3  $V_{stall}$ . The current version of the model does not calculate the ground run during landing. However the incorporation of the same is stipulated for future work.

### 3.2.1.8 Key assumptions

The BADA database[3.1], from where the calculations for this aircraft performance model originates, has drag coefficients available for over 60 different aircraft and hence converting the aircraft performance model to simulate different aircraft is convenient. References [3.2] and [3.3] have also been extensively used to formulate this model.

The speed profiles, power settings, segment altitudes and aircraft weight in terms of load factors may all be used as variables for trajectory optimisation. Some of the main assumptions in calculation of aircraft performance were:

- i. Change of speeds between sub segments are instantaneous as the implication on overall fuel consumption due to change in calibrated speeds and mach numbers in the speed profile is negligible.
- ii. Bank angles and wind effects have been neglected in all phases of flight
- iii.  $\cos \gamma = 1$
- iv. All segments (climb, cruise and descent ) are considered to be continuous and have no step segments
- v. Currently all calculations are done for the mission and do not account for block calculations. However the program calculates the ground idle and taxi thrusts and hence block calculations may be calculated if required
- vi. As the aerodynamic data for a modelled aircraft is adapted from the BADA database which is verified and validated [3.41], the model assumes the basic characteristics, dimensions and aircraft/ propulsion system limitation parameters remain unchanged and follow those as specified by the data sheets for an individual aircraft. These include the aircraft mass and balance (comprising maximum take-off weight (MTOW), maximum landing weight (MLW), maximum zero fuel weight (MZFW), operating empty weight (OEW), fuel capacity, max payload), number of passengers, mean centre of gravity position, maximum operational altitude, environmental envelope and aircraft dimensions (wing span, overall length, tail height, wing span, reference wing surface area).

### 3.2.2 ENGINE PERFORMANCE MODEL

The engine performance model to be used in conjunction with the aircraft performance model is built using Cranfield University's in-house gas turbine simulation and diagnostics software TURBOMATCH. As mentioned earlier, the engine model currently used with the aircraft performance model simulates the performance of a typical twin spool high bypass engine similar in design characteristics to a CFM 56-7B27 engine which is currently used by the industry to power a Boeing 737-800 aircraft.

The design point of the engine model was chosen at top of climb (i.e. Alt 10668 m, Mach speed 0.8, and the pressure recovery of 0.99) under International Standard Atmosphere (ISA) conditions. Several iterations were performed using the model at design and off-design point conditions to match the performance of the model with data obtained from the public domain for the engine on which the design was based. A summary of this data is presented in Table 3.1. [3.4, 3.5, 3.6]

The mass flow rate at the engine intake was estimated based on the measured intake area and assuming an average inlet Mach number of 0.55 – 0.65. The design point (top of climb) bypass ratio (BPR) and the turbine entry temperature (TET) were determined based on the overall pressure ratio and the net thrust at top of climb. The optimum fan pressure ratio corresponding to the calculated TET, overall pressure ratio (OPR) and bypass ratio (BPR) was also determined.

Additionally, values of component pressure ratios, component efficiencies, and compressor bleed for turbine cooling, and other parameters, were guessed and iterated to match the required engine performance at off design (maximum take off and cruise) conditions. It was observed that the discrepancies between the required and achieved values are minor and hence the engine performance model was deemed acceptable.

	As specified in public domain literature	Simulated model specification
Design Point Altitude (m)	10668	10668
Design flight mach no(-)	0.8	0.8
Top of climb thrust (N)	26511	26600
Top of climb SFC (mg/Ns)	-	16.21
Top of climb TET (K)	-	1510
Top of climb Mass Flow(kg/s)	-	140
Takeoff Thrust (N)	121400	121400
Takeoff Fuel flow (kg/s)	1.235	1.12
Takeoff TET(K)	-	1670
Takeoff BPR(-)	5.1	5.1
Takeoff Mass flow (kg/s)	358	350
Fan pressure ratio(-)	-	1.77
Booster pressure ratio(-)	-	1.881
HPC pressure ratio(-)	-	9.829
Overall pressure ratio(-)	32.8	32.7
Isentropic Compressor efficiencies	-	0.86
Isentropic Turbine efficiencies	-	0.91
Combustor efficiency	-	0.99

Table 3.1 Comparison of design and performance data of simulated engine with public domain literature

#### Off Design performance

Several off-design performance simulation calculations utilising the simulated engine model were performed. These simulations yielded off-design performance charts highlighting the effects of altitude, flight Mach number, ambient temperature and turbine entry temperature on net thrust and specific fuel consumption.

Figure 3.5 highlights the variation of net thrust ( $F_n$ ) as a function of altitude (Alt) and flight Mach number ( $M_{Nf}$ ) for a fixed value of turbine entry temperature (TET). The value of TET chosen was the design point i.e. top of climb (TET = 1340K).

Figure 3.6 highlights the variation of specific fuel consumption (SFC) as a function of altitude and flight Mach number for the same fixed value of TET. Figure 3.7 highlights, in turn, the variation of net thrust ( $F_n$ ) as a function of ambient temperature ( $T_{amb}$ ) and turbine entry temperature (TET) at Sea Level Static Conditions (Alt = 0m, mach = 0). Finally, figure 3.8 highlights the variation of specific fuel consumption (SFC) as a function of ambient temperature ( $T_{amb}$ ) and turbine entry temperature (TET) at Sea Level Static Conditions. It may be noted that for these analyses, the maximum TET considered was the TET corresponding to take-off conditions.

The three figures broadly follow the expected trend lines. Reference [3.42] provides detailed qualitative descriptions of the effects of altitude, flight Mach number, ambient conditions and turbine entry temperature on gas turbine performance.

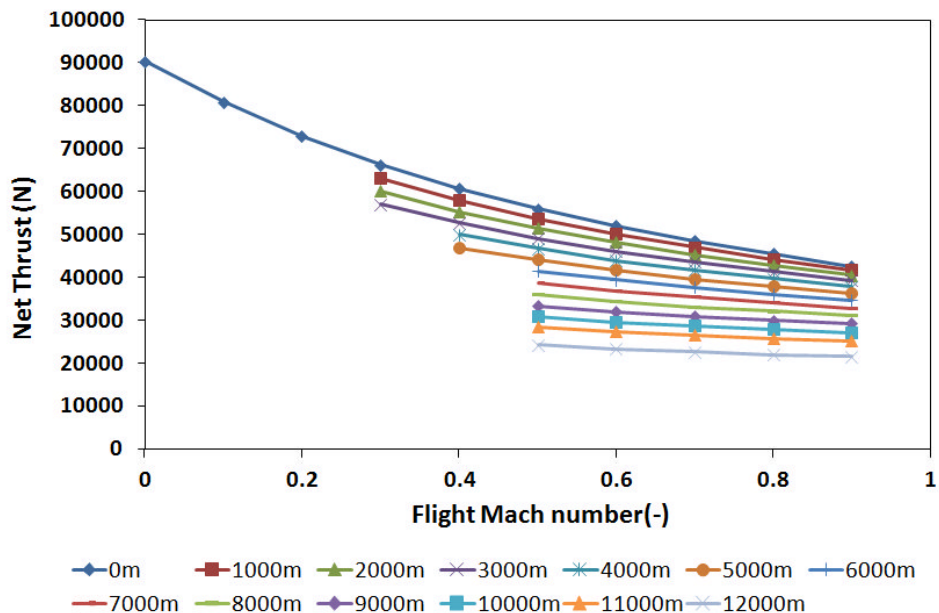


Fig 3.5 Variation of net thrust as a function of altitude and flight Mach number for the same fixed value of TET (DP TET:1510 K)

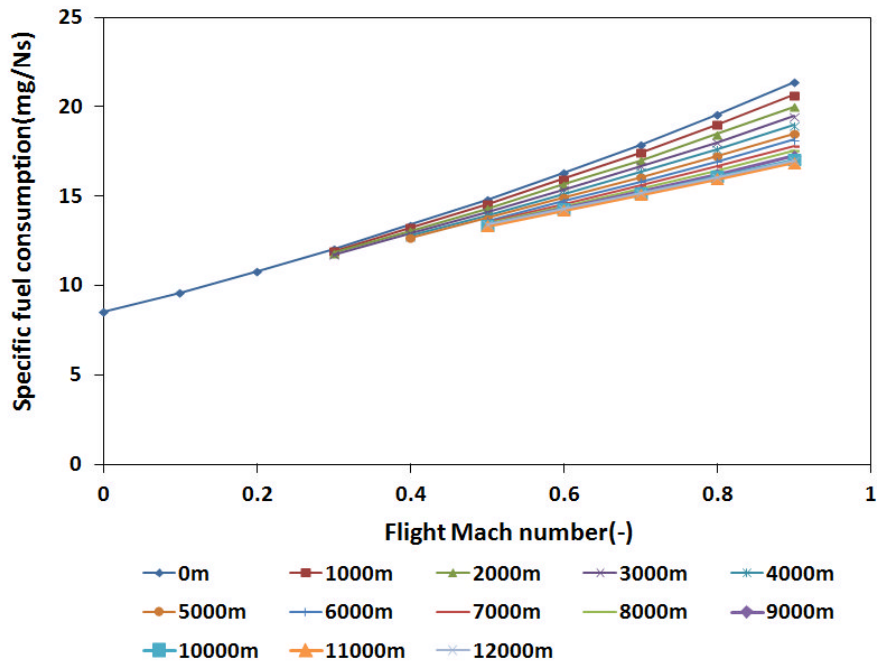


Fig 3.6 Variation of specific fuel consumption (SFC) as a function of altitude and flight Mach number for the same fixed value of TET(DP TET:1510 K)

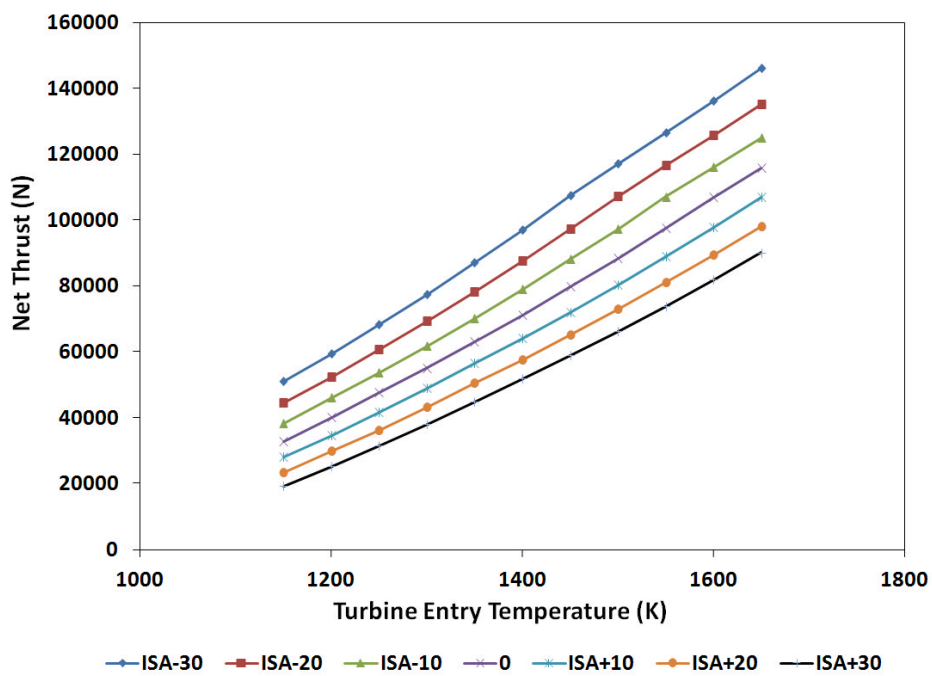


Fig 3.7 Variation of net thrust as a function of ambient temperature ( $T_{amb}$ ) and turbine entry temperature (TET) at Sea Level Static conditions

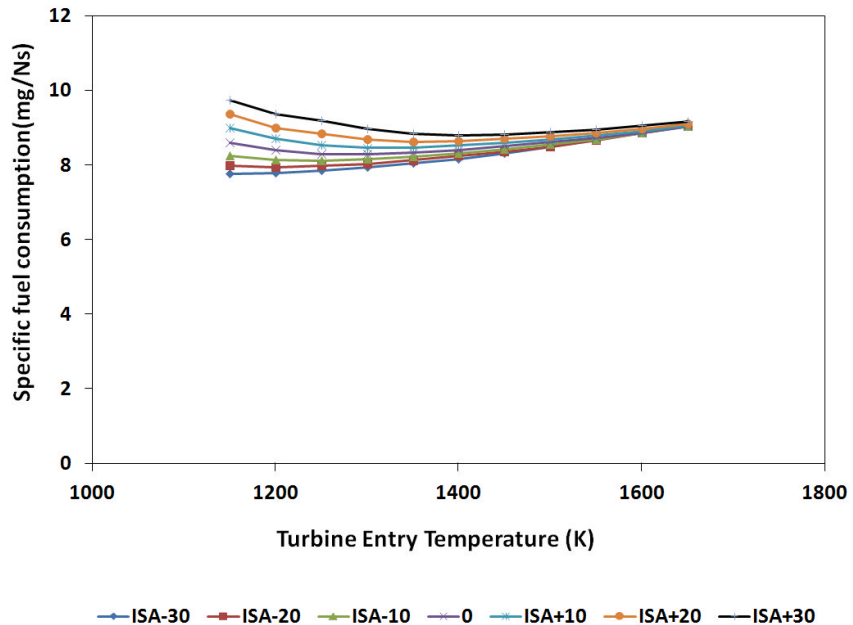


Fig 3.8 Specific fuel consumption (SFC) as a function of ambient temperature ( $T_{amb}$ ) and turbine entry temperature (TET) at Sea Level Static conditions

### 3.2.3 MISSION APPLICATIONS OF INTEGRATED AIRCRAFT MODEL

The aircraft and engine model were integrated and a series of validation tests were performed to validate/ verify the performance of the models.

*Performance assessment on the payload range chart:* The payload range (PR) chart is an important assessment tool for decision making, during an aircraft or fleet selection process. It depicts the maximum allowable revenue generating payload that may be carried by a particular aircraft. It also defines the combined mass of payload and fuel that may be allowed to achieve any particular range, within the aircrafts' performance ability. The payload range chart is usually accompanied by a specified flight profile wherein the performance calculation of each point is based on a set of International Flight Rules (standard assumptions on fuel reserves, diversion fuel and contingency fuel).

The PR chart has effectively four critical points (as shown in the figure 3.9). The point A shows the maximum volumetric payload carried by a particular aircraft, while keeping within its structural limitations. Line AB is essentially the line wherein the aircraft's range is increased by increasing the quantity of fuel on board. Point B is the maximum range flyable by the aircraft with maximum payload on board as it reaches its Maximum Take-off Weight (MTOW) limit. Line BC then depicts the range at which the aircraft will fly at MTOW, and therefore will result in reduction of payload with an increase in fuel on board. Point C is the range at which the fuel

on board is maximum and hence the payload is reduced to level at which the aircraft is still at its MTO weight. A further reduction in payload, with maximum fuel onboard, allows an increase in range along line CD, but only because the reduction of total weight increases the specific range  $r_a$ .

$$r_a = -\frac{dR_a}{dm} = \frac{V}{c\beta W} \quad 3.38$$

Where       $\beta$       =      drag to lift ratio  
                $W$       =      weight of aircraft  
                $c$       =      specific fuel consumption

One of the ways of assessing the performance of the simulated aircraft is to compare its performance on a payload range chart against that of the original aircraft on which it is modelled.

Figure 3.9 indicates the payload range capability of the simulated model compared with that of the aircraft it is based on (Boeing 737-800 with a CFM 56- 7B engine)[3.7] This is done for the three critical points (B, C and D) and as mentioned previously, for a specific flight profile assumed for all missions as discussed earlier. Therefore in establishing the payload range performance, similar to a standard flight profile found in BADA [3.41] the following flight profile was assumed:

- a. Take off - sea level, ISA conditions, max take off thrust, take off configuration, accelerate to 155 kt(V2+10)
- b. Initial climb - Constant CAS (155 kt), clean configuration, maximum climb thrust to altitude 1500 ft.
- c. Initial climb - CAS (193 kt), clean configuration, maximum climb thrust until altitude 3000 ft.
- d. Enroute climb - Constant CAS (250 kt), clean configuration, maximum climb thrust until altitude 10000 ft.
- e. Enroute climb - Constant CAS (300 kt), clean configuration, maximum climb thrust until crossover altitude 25756 ft.
- f. Enroute climb - Constant Mach (0.75), clean configuration, maximum climb thrust until cruising altitude 35000 ft.
- g. Cruise- Constant altitude and speed cruise (35000 ft and Mach 0.78), clean configuration. The cruise speed and altitude were based on long range cruise data for this aircraft and engine.
- h. Descent- Constant Mach (0.75), clean configuration, descent idle thrust until crossover altitude (25756 ft)
- i. Descent- Constant CAS (300 kt), clean configuration, descent idle thrust until altitude 10000 ft.

- j. Descent- Constant CAS (250 kt), clean configuration, descent idle thrust until altitude 3000 ft.
- k. Approach and landing – Constant path angle ( $3^\circ$ ), approach configuration, approach thrust until altitude 0 ft.

All missions were simulated with standard assumptions for hold, diversion and on board reserves fuel. Therefore at the end of the mission that the fuel onboard included the following:

- i. Fuel for 20 minute hold (760 Kg)
- ii. Fuel for 200 nm diversion route which includes a climb to 20000 ft, cruise at constant altitude and speed of 20000 ft and Mach 0.60 and descent (1633 kg).
- iii. Fuel for onboard reserves- 5% of trip fuel consumed.

Table 3.2 indicates the mission specific data for the three simulated points and figure 3.9 illustrates the PR performance of both aircraft. Given the various assumptions made in modelling, flight profile of the trajectories and numerical discretisation errors, discrepancies between the required and achieved ranges are observed. However, as this is an attempt to simulate the generic performance of a short to medium range aircraft, the errors are considered small and hence deemed acceptable.

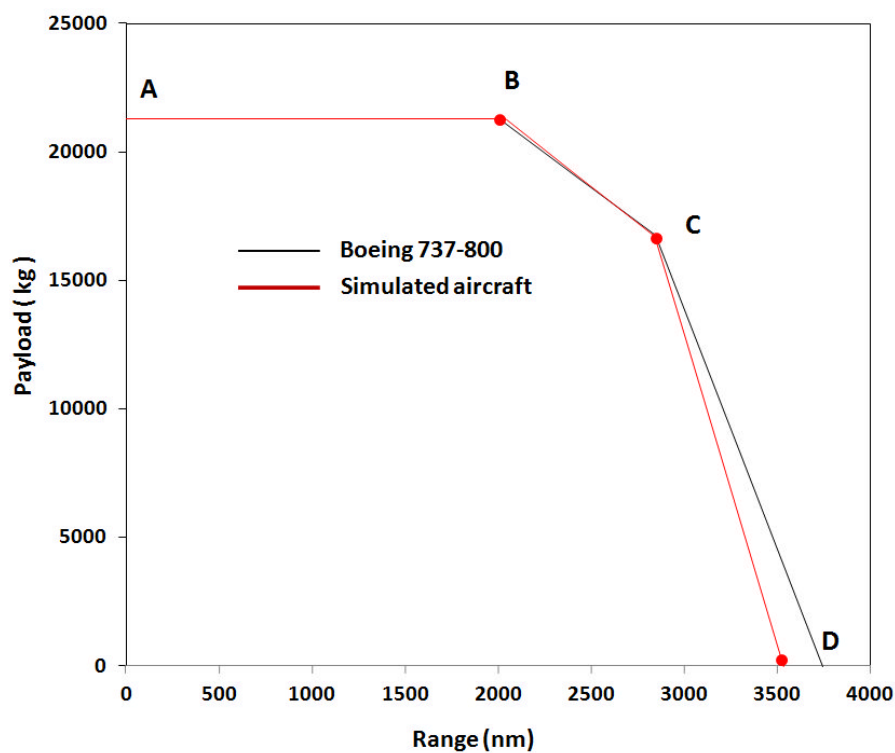


Fig 3.9 Payload range validation of aircraft/engine model

	Max payload range(B)	Max fuel range(C)	Max ferry range(D)
Cruise Flight Mach number(-)	0.78	0.78	0.78
Altitude at cruise (ft)	35000	35000	35000
Maximum takeoff weight (kg)	79016	79016	62307
Maximum payload(kg)	21319	16709	0
Operating empty weight(kg)	41413	41413	41413
Maximum fuel on board(kg)	16284	20894	20894
Hold (20 min) + diversion(200 nm) fuel (kg)	2394	2394	2394
5% contingency fuel (kg)	661	870	862
Fuel consumption -model (kg)	13219	17630	17638
Range _Boeing 737-800 (nm)	2000	2850	3750
Range _simulated aircraft (nm)	2033	2847	3531
Range Error% (in ref to B737 data)	1.6%	0.1%	5.8%

Table 3.2 Payload range validation of aircraft/engine model

### 3.3 EMISSION PREDICTION MODEL – NO<sub>x</sub>

NO<sub>x</sub> (nitrogen oxides) emissions for its effect from aviation are primarily considered during the Landing-Take Off Cycle (LTO) and in the cruise segment of the flight. As per literature, research has been focused in providing scientific evidence to establish the effects of NO<sub>x</sub> emissions on global warming, from aviation at cruise altitude. Through a process of photochemistry, NO<sub>x</sub> emissions from aircraft at cruise altitudes result in an enhancement of ozone (O<sub>3</sub>) (in the lower stratosphere and upper troposphere, which results in climate warming) and a reduction of a small amount of ambient methane (CH<sub>4</sub>)(approx. 1-2% of overall concentration, which results in a cooling effect). NO<sub>x</sub> emissions on ground (specifically near airports) are also known to affect Local Air Quality, which contributes to various health/environmental problems and also form a main component of ground-level ozone. [3.8]

In general there exist three methodologies to estimate the level of gaseous emissions produced by gas turbine combustors: stirred reactor models, numerical simulations involving CFD calculations and empirical correlations. Cranfield University's proprietary emission prediction tool Hephaestus utilises two of these, namely the stirred reactor based model and empirical correlations. [3.9]

Stirred reactor models are fairly elaborate emission prediction models, especially for prediction of NO<sub>x</sub> where the residence times are relatively short and the pollutant is not in

local chemical equilibrium. However this methodology is expensive in terms of computational time and is more suited in the study of combustion process in a more rapidly evolving design phase of the combustor as a component and for potential future combustor designs. [3.9]

For the purpose of the research work in this PhD, the combustor will be assumed to be of conventional design and will undergo no design change. The methodology used to calculate  $\text{NO}_x$  in this work uses the empirical correlation based 'P3T3 method of altitude  $\text{NO}_x$  prediction', where the combustion chemistry and internal flow are completely subsumed into global expressions, largely established from measurements for the landing and take-off cycle (LTO) [3.5, 3.10]. The flowchart of the process for calculation of  $\text{EINO}_x$  is shown in figure 3.10A.

$\text{EINO}_x$  measurements at ground level, basically adapted from the ICAO emissions database for a particular engine [3.5], are plotted against combustor inlet temperature. The altitude condition for which the  $\text{EINO}_x$  may have to be calculated, determines its combustor inlet conditions. The ground level  $\text{EINO}_x$  at the altitude inlet temperature is obtained from the  $\text{EINO}_x$  plot. This  $\text{EINO}_x$  is then corrected for the difference in combustor inlet pressure and FAR between ground level and altitude. The values for the pressure and FAR exponents resolve the severity of  $\text{EINO}_x$  correction. There is also a humidity correction required, as air above approximately 20,000 feet is virtually dry. [3.10]

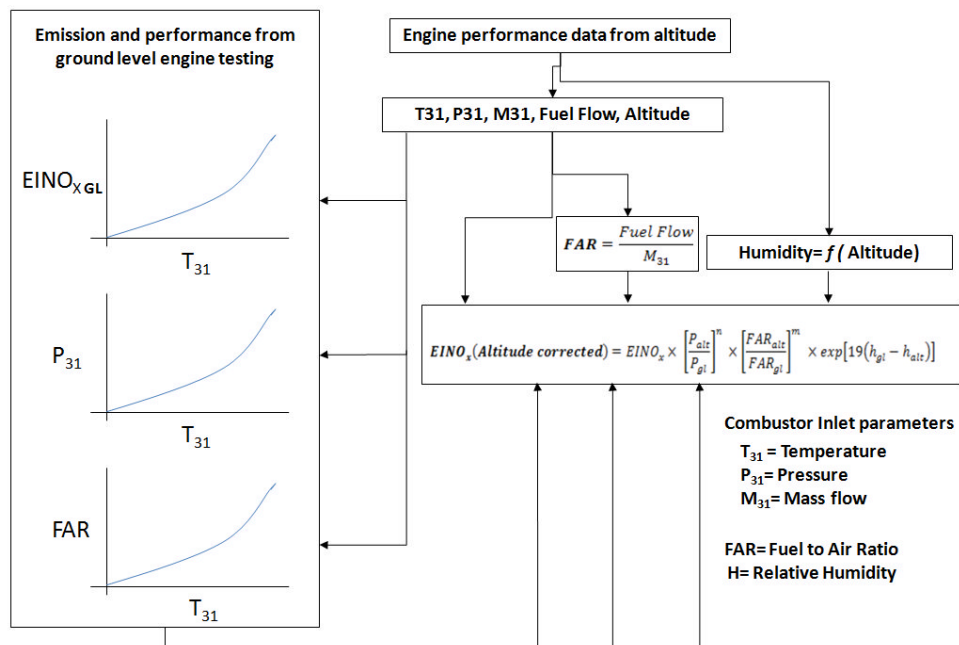


Fig 3.10A Flowchart for P3T3 methodology for  $\text{NO}_x$  prediction (with correction for altitude)  
[3.10]

As the altitude increases from sea level ISA, the air becomes drier and hence the humidity correction becomes larger. The reference suggests that at ground level EINO<sub>x</sub> (from the LTO cycle) is obtained at relatively high humidity, the EINO<sub>x</sub> for an equivalent high altitude condition will therefore increase by around 12 or 13% and the reference recommends 60% relative humidity to be used.

This method also requires the pressure and fuel to air ratio (FAR) corrections at a constant inlet temperature. The inlet pressure reduces by 35-45% at cruise inlet temperatures, from ground level to altitude. The reference includes recommended pressure correction exponent 'n', from data through rig and engine testing, by engine manufacturers. This study currently uses a pressure coefficient of 0.4, as it provides the best overall accuracy level for all civil engines, as suggested by the testing and validation report [3.10].

No correction is applied to FAR as the reference suggests that the engine manufacturer data shows that the FAR is typically 10% richer in cruise, relative to ground level for a constant combustor inlet temperature. However for rich burn combustors, where the primary zone is richer than stoichiometric at take off, the impact of this FAR change is known to be weak. Given the accuracy of the P3T3 method the FAR correction may be neglected, and hence the FAR correction exponent in this method is currently set at zero.

A more detailed description of the model, with a validation against experimental data and hence verified for accuracy may be found in referenced literature [3.10]. The model has been re-coded in MATLAB for easy integration into the framework. The values of EINO<sub>x</sub> at ground level for the four ICAO points are the reference points for calculation. The basic ICAO data sheet used for the model may be found from the ICAO emission databank [3.43]. It was tested for a standard full trajectory of mission length 1619 nm and the variation of EINO<sub>x</sub> with range for the segments is as shown in figure 3.10B.

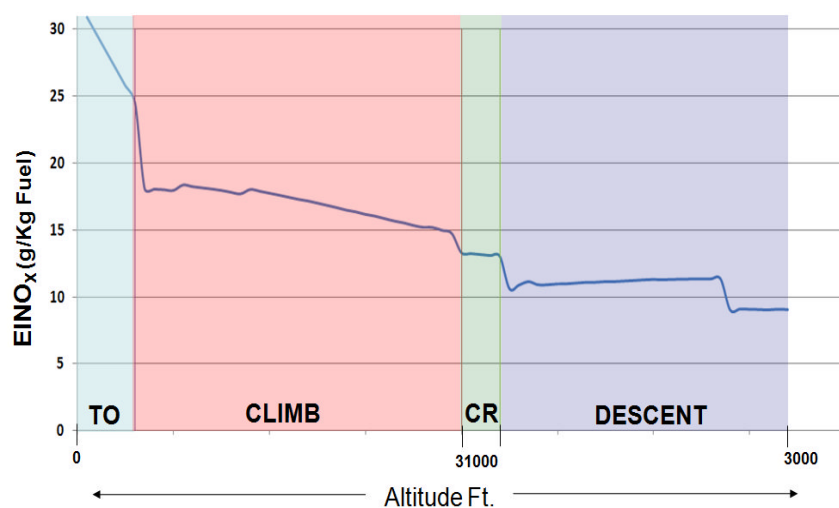


Fig 3.10B EINO<sub>x</sub> prediction using P3T3 methodology (with correction for altitude) for a full mission

### 3.4 EMISSION PREDICTION MODEL – CO<sub>2</sub> AND H<sub>2</sub>O

The calculation of CO<sub>2</sub> is an easier process than that of NO<sub>x</sub> as it is considered to be in equilibrium and can readily be calculated from equilibrium calculations. The model uses the Fuel Composition Method (FCM) to calculate the emissions of CO<sub>2</sub> and H<sub>2</sub>O. As these emissions are a product of combustion they are considered independent of operational parameters and modelled as proportional to fuel burn and fuel composition [3.9].

Assuming the combustion to be stoichiometric and the composition of fuel is represented as C<sub>x</sub>H<sub>y</sub>S<sub>z</sub>, the emission indices (EI) in terms of grams of pollutant per 1000 grams of fuel may be computed as follows:

$$x = \frac{X}{12.011} \quad 3.39$$

$$y = \frac{Y}{1.0079} \quad 3.40$$

$$z = \frac{Z}{32.06} \quad 3.41$$

$$EICO_2 = \frac{1000 \times x \times [12.011 + (2 \times 15.994)]}{(x \times 12.011) + (y \times 1.0079) + (z \times 32.06)} \quad 3.42$$

$$EIH_2O = \frac{1000 \times \frac{y}{2} \times [(2 \times 1.0079) + (15.994)]}{(x \times 12.011) + (y \times 1.0079) + (z \times 32.06)} \quad 3.43$$

Where

x= Carbon coefficient in chemical formula for fuel (in moles)

y= Hydrogen coefficient in chemical formula for fuel (in moles)

z= Sulphur coefficient in chemical formula for fuel (in moles)

### 3.5 CONTRAIL PREDICTION MODEL

Contrail formation is known to be primarily attributed to water vapour, formed as a by-product of combustion and the prevalent ambient conditions, essentially being temperature and relative humidity.

The design of an engine is responsible for the exhaust temperatures and hence for a same ambient air temperatures and relative humidity the formation of contrails will be strongly dependant on engine design. When the warm and moist exhaust air of the engine mixes colder

and less humid ambient air there will be an increase in relative humidity, and that is the primary cause of formation of 'condensation trails' or contrails. The contrail forms when liquid water is reaches or surpasses saturation in the exhaust trail of the engine.

As per current levels of scientific understanding (LOSU) on the RF effects of environmental pollutants, contrails are currently categorised between *low* and *very low*. However the contrail formation process is fairly well established and there exist a few prediction models currently available which are based on experimental data collected by various research organisations. The contrail prediction model for this work has been adapted from the Clean Sky project model suite [3.11]. An extract of the model specification is placed at appendix B for the reader's reference.

### 3.6 OPERATING COST MODEL

An airline as a business is most sensitive to profitability and safety, and every aspect of the business is looked at very carefully from these two perspectives. The operating cost and 'bottom lines' being critical parameters for sustainability in a dynamic financial environment such as today, leads to optimisation of all activities within the airline business to maximize profits. An important aspect therefore of this PhD is to understand the financial implications of various environmental taxation scenarios.

DOC for economic analysis is frequently used as the measure of merit to evaluate aircraft in design trade-off studies. Various literature have been consulted during the course of this PhD to establish the requirements and hence formulate a model to calculate operating cost.

Clark[3.12] like other references [3.2] classifies an airline operating cost into essentially two parts: Direct Operating Costs (DOC), being those costs which vary according to the aircraft type used and Indirect Operating Cost(IOC), which are those costs that are not affected by aircraft type. The work in this research essentially looks at optimised operations of conventional aircraft and hence considers only the direct operating cost aspect as it will be affected by a change in operational methodology.

A simple operating cost model has been built to enable the framework to feed the optimiser with operating cost as an input and hence use it as an objective. A general schematic of the DOC model used is as shown in figure 3.11.

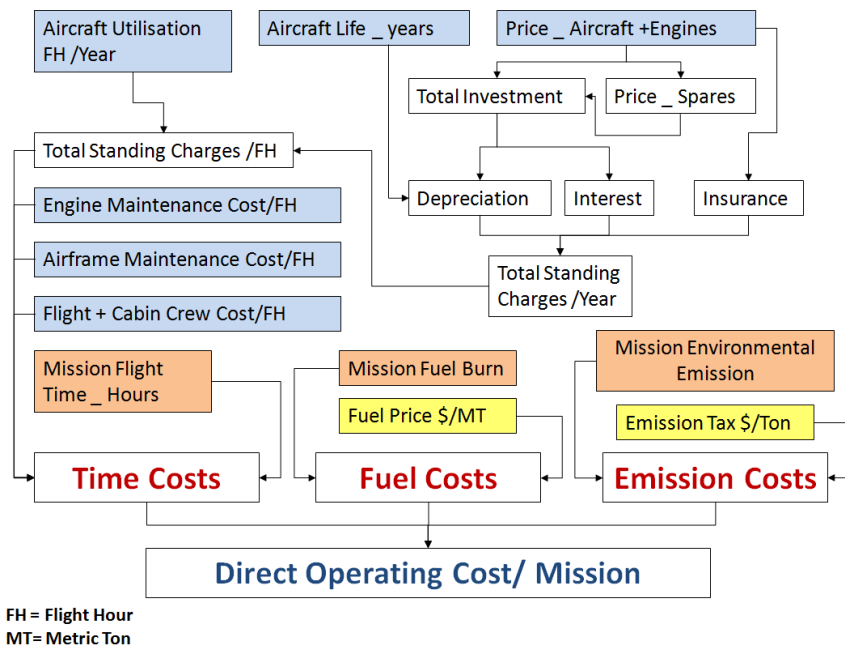


Fig 3.11 General schematic indicating the flow of costs in an operating model

The model is based on the approach as described by Jenkinson [3.2] and largely on the concept of Cost Index. The Cost Index method, essentially a trade-off between two key objectives – fuel consumed in a mission and time of the mission, and is one of the most prevalently used methods in the industry while optimising operations cost. [3.14, 3.15]

The cost index is essentially the ratio of the cost of fuel and the time related cost in an airline operation. The selected value of cost index reflects the relative value of the cost of fuel on cost of mission as compared to the time dependant direct operating cost.

The following section describes the key elements of a direct operating cost model which is then followed by the actual structure implemented with a justification of various assumptions made.

**Fuel costs:** The basic components of the fuel calculation usually comprise the price of fuel (expressed in US\$/ metric ton) the rate of consumption, the characteristics of fuel if different from standard fuel and the network the aircraft operates in. Fuel expenses, forms a 35% to 40% and hence a major component [3.5] of an airline's overall operating cost. Therefore every airline tries to reduce its fuel costs through improved efficiency in operations, investment in improved technology and fuel hedging.

- Aircraft fuel consumption is a function of the design of the aircraft and hence the overall operating cost diminishes when a fuel efficient aircraft is utilised. Literature [3.12] therefore recommends that economic analysis must decide if the fuel burn should reflect brand new aircraft or require an introduction of deterioration factor. The current study will be

examining a set of optimised trajectories of a single type of aircraft and hence be a comparative analysis. Therefore no deterioration factor has been introduced and the aircraft is assumed to fly at its design efficiency.

- Fuel characteristics and price: Standard aviation jet fuel and price of fuel as specified by IATA, have been assumed for the study [4.8].

*Maintenance costs:* In terms of aircraft fleet planning and costing analysis, literature indicates that these costs are considered to be one of the most difficult to account for by the industry. However broadly, these costs may be categorised in terms of direct and indirect maintenance cost. The direct maintenance costs essentially consider labour and material costs associated with the maintenance of airframe, components and engines. The indirect maintenance costs in turn consider aspects such as tooling, and administration. As the focus of this study is to only consider direct operating costs, therefore only the direct maintenance cost (DMC) will form a part of it [3.12, 3.2].

Literature indicates that one of the most frequently used analytical methods is based on the Air Transport Association Chapter System. This system is used to derive, for labour and material costs hourly and cyclic elements. There exist various data sources which enable modelling of maintenance costs and some of the key sources include data from manufacturers and IATA. This data is then adjusted for common assumptions to enable meaningful comparison to be made for similar conventional aircraft. [3.12, 3.2]

The main factors influencing maintenance cost include the following;

**Airline influence:** This essentially depends on the strategy followed by the respective airline based on whether the maintenance is subcontracted or is undertaken in-house thus resulting in differing costs based on the levels of investment on facilities and labour costs. This aspect is known to radically affect the aircraft selection process by an airline.

**Aircraft influence:** This influence is based on the aircraft type and is relevant when comparing two competing technologies.

**Geographical influence:** Aircraft operating in demanding conditions such as at higher altitudes and or in desert air strips will have higher maintenance costs and hence this influence is valid when comparing operations of aircraft at different geographic locations.

**Route network and operations:** The influence of route network and type of operations (depending on the average range of the aircraft, essentially short haul or long haul) is considered to be significant. Reference 3.12 indicates that it is not uncommon for a same aircraft type to incur double the DMC on a short haul compared to a long haul network. The average sector length that an aircraft is operated on is a critical factor as it decides the average flight hour to flight cycle ratio. This is due to the fact that certain cyclic effects such as acceleration and deceleration of engines, use of movable devices (landing gear and lift control devices) and pressurisation and depressurisation of the fuselage have fixed cyclical lives and

hence can be operated only for a set number of cycles as per allowed annual utilisation. Therefore higher average sector lengths and hence high flight hour to flight cycle ratios will necessitate the aircraft to perform fewer cycles annually. Figure 3.12 shows this relationship. This effect has been considered in the model and will be discussed with the assumptions.

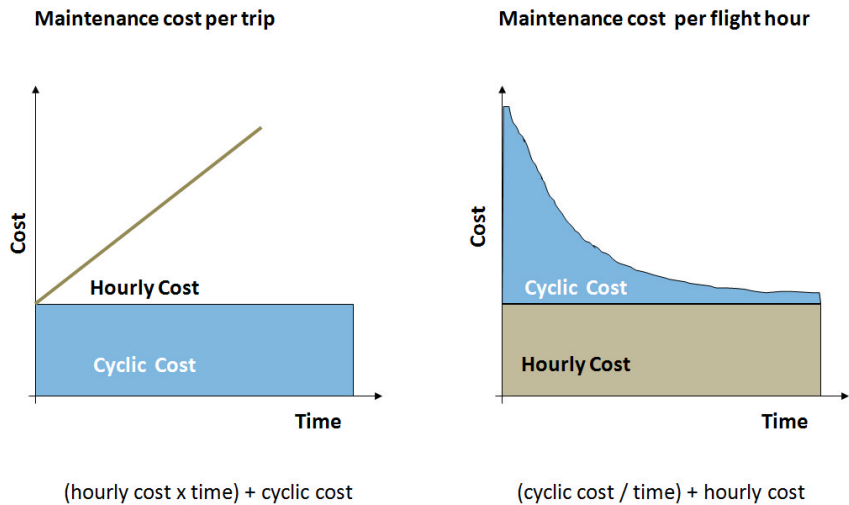


Fig 3.12 Maintenance costs- Influence of sector length

*Standing charges:* The standing / ownership charges are not directly linked to a specific mission of the aircraft, but depend on the type and annual utilisation of the aircraft. These charges are calculated by the operating cost model as a part of the direct operating cost when an aircraft is assumed to be procured through outright purchase, as opposed to being leased [3.12]. These charges are critical as they will apply even if the aircraft is not utilised as per its average annual utilisation and hence form a critical part of operating cost calculations for a mission. These charges include:

**Aircraft insurance:** The insurance costs of an aircraft depend on the probable risks involved and following and loss, the potential for an operator to make the claim. Due to very high safety standards within the airline industry and a categorisation of risks involved by various airworthiness authorities, technical risk are easily estimated. However based on geographical areas that the aircraft is being operated in, and based on a possibility of losing aircraft due to extraneous causes (such as terrorist strike and essentially non-technical occurrences), results in a varying rate of insurance fees in relation to the nature of the operation. For a generic study such as undertaken in this research, reference indicates that a rate of 1.5% is considered typical [3.2]

**Interest on capital employed:** The rate of interest on investment within the airline industry varies drastically and is very difficult to generalise. These charges are known to be influenced by the global economic scenario prevailing, local currency exchange rates, credit rating of the company making the investment and the export subsidies

given by a particular government of the operator. These costs may also be influenced by offset agreements. Due to this high variability these cost are sometimes ignored, but as recommended by references and for completeness it is usually necessary to include these costs in a general business plan.[3.2,3.12]

Depreciation of the capital investment: As per references [3.2, 3.12 ] depreciation is dependent on numerous factors including the capital involved, the airline purchasing policies, the accounting practices of the financial loan companies, the competition for capital and the overall world economic conditions at the time the aircraft is purchased. However in the model the depreciation in airline investments is calculated using a simple straight line method by initially deciding two key factors: depreciation period and residual value. This then allows the calculation of an hourly depreciation charge. Typically commercial aircraft are considered to have an operational/ useful life of 15-20 years and hence most airlines fix their depreciation period for their aircraft within this period. The model assumes the aircraft life to be 20 years.

In order to calculate the standing charges, the methodology suggested requires the following basic information for a particular type of aircraft

- Cost of the aircraft with engines(aircraft specific)
- Cost of the engines(aircraft specific)
- Cost of airframe spares as a percentage of airframe cost
- Cost of engine spares as a percentage of engine cost
- Aircraft utilisation in flying hours per year(aircraft specific)
- Aircraft operational life
- Cost depreciation of aircraft over operational life in percentage
- Interest on investment cost in percentage
- Insurance as a percentage of aircraft cost

Using the above information the following calculations are made

$$\text{Total investment cost} = \text{Cost of aircraft with engines} + \text{Cost of aircraft spare} + \text{Cost of engine spares} \quad 3.44$$

$$\begin{aligned} \text{Depreciation costs/year} &= \\ \text{Total investment cost} \times (\text{Cost of depreciation of aircraft over operational life \%}) / 100 & \quad 3.45 \end{aligned}$$

*Interest/year = Total investment cost x (Interest on investment cost % /100)*

3.46

*Insurance/year = Total investment cost x (Insurance as % of aircraft cost /100)*

3.47

*Total standing charges/year*

$$= \text{Depreciation costs/year} + \text{Interest/year} + \text{Insurance/year}$$

3.48

***Standing charge/ flight hour***

$$\begin{aligned} &= (\text{Total standing charges/year}) \\ &/ (\text{Aircraft utilisation in flying hours per year}) \end{aligned}$$

3.49

**Crew Costs:** This essentially includes the cost of salaries for the flight and cabin crew. The number of crew required per flight is dependent on airworthiness standards/ regulations and labour union agreements. However usually there is a requirement of two flight crew for smaller aircraft (single aisle narrow body) travelling shorter stages. The requirement of cabin staff is associated with the number of passengers with a mandatory regulation of at least one cabin attendant for 30-50 passengers per cabin attendant. The costs of crew wages are calculated on per block hour basis utilisation, but the rates differ between airlines and between aircraft type.

### 3.6.1 IMPLEMENTATION OF THE OPERATING COST MODEL

To enable the calculation of operating cost for the conventional aircraft (Boeing 737-800), data for the inputs as discussed, was adapted from public domain references which contained maintenance and operational data for the aircraft [3.16]. The assumptions for rates of interest, depreciation and insurance and aircraft age were made on recommendations by Jenkinson [3.2]

- a. *Time dependant costs:* In order to calculate the time dependant costs the basics assumptions for the various inputs discussed in the previous section include the following
  - i. *Price of the aircraft and propulsion unit :* The acquisition prices was set at US \$ million 80.8 and 8.4(per unit) for the aircraft and propulsion unit respectively [3.17]
  - ii. *Crew and salaries:* The crew salaries in the model are calculated on an hourly basis and assume the aircraft has 2 flight deck crew and 6 cabin crew. This is a standard

assumption for an aircraft of this type. The salaries have been set in the model for the flight deck crew and cabin crew at US\$ 140/hour and US\$ 50/hour, per individual respectively.[3.12, 3.18]

iii. *Standing charges*: the following assumptions were for the inputs required to calculate the standing charges as detailed earlier[3.2]:

1. Cost of airframe spares as a percentage of airframe cost: 10%
2. Cost of propulsion unit spares as a percentage of propulsion unit cost: 30%
3. Aircraft useful life : 20 years
4. Residual value of aircraft due to depreciation at end of life:10%
5. Interest on investment (Percentage of investment cost): 5.5%
6. Insurance on investment (Percentage of investment cost): 0.5%

iv. *Airframe and engine maintenance charges*: As discussed earlier the aircraft and engine model were based on a conventionally used single aisle narrow body, short/medium range aircraft - Boeing 737-800 with CFM 56 7B engines. As the aircraft has been in service since 1998, significant amount of information is available from literature[3.16].

While assessing the economic performance of an aircraft, every conventional aircraft is assumed to have a certain average annual utilisation in terms of number of flying hours, flight cycles and a ratio of flight hours to flight cycles (FH/FC). Based on the periodicity of the maintenance routines and the average number of annual flying hours a cost of maintenance per hour may be established. Table 3.3 lists the direct maintenance costs of the Boeing 737-800 which has been calculated for an average annual utilisation of 3300 flight hours and 1700 flight cycles thus resulting in an average flight hour to flight cycle ratio of 1.95.

As discussed earlier, literature indicates that the same aircraft type, when compared to its utilisation over a long haul route, may sometimes incur up to twice the direct maintenance cost when used for short ranges. Primarily attributed to cyclic costs, short range utilisation leads to higher number of cycles and hence higher cyclical costs and hence if the consolidated cost (cyclic costs + hourly costs) is considered on an hourly basis (as available in the data in table 3.3) , then as the time of the mission increases the hourly cost may be assumed to reduce.[3.2]

To simulate the effect of different route networks (in terms of range) and their corresponding effect on direct maintenance costs a certain number of assumptions are made in the model. Depending on the range of the mission, and consequently the time of the mission, the model recalculates the FH/FC ratio. If the FH/FC is less than that for which the maintenance cost data is provided (1.95), the cost per hour is recalculated assuming the annual cost remains the same and the aircraft does not exceed 1700 cycles per year. However if FH/FC ratio is greater than 1.95, the hourly cost maintenance cost is assumed to remain the same as shown in table 3.3. An illustrative example may be used to explain this assumption.

Annual Utilisation	
Flight hours(FH)/ year	3300
Flight cycles(FC)/year	1700
FH/FC ratio	1.95
Airframe maintenance	
Line and ramp checks (\$/FH)	110
A checks (\$/FH)	32
Base checks (\$/FH)	65-70
Stripping and repainting (\$/FH)	5
Interior refurbishment (\$/FH)	28
Heavy component (\$/FH)	130
	235-
LRU component support (\$/FH)	255
Total airframe and component maintenance (\$/FH)	617.5
Engine maintenance	
CFM56-7B27 (\$/FH)	222.5
Total maintenance cost (engine+ airframe) for FH/FC ratio (\$/FH)	1062.5

Table 3.3 Direct maintenance cost for Boeing 737-800 [3.16]

From the data (table 3.3) above, it is seen that for a FH/FC ratio of 1.95, the maintenance cost per hour is calculated to be US\$ 1062.5. Therefore for 3300 hours of operation the annual cost of maintenance for the airframe and engine (per unit) will be US\$ 2,037,750 and US\$ 734,250 respectively.

Consider an average mission of range 581 nm, for which the aircraft is assumed to have a flight time of 102 min [3.16]. Therefore for this flight the flight hour per flight cycle ratio is 1.7. If the annual cost of maintenance is then assumed to be the same as the data above for the model, then it is further assumed that either the flight cycles or the flight hours per year must be equal to the average stipulated utilisation, while not exceeding the other. Therefore in this case for an average maximum utilisation of 1700 cycles, the aircraft will be able fly up to 2890 flight hours annually, instead of 3300, thereby achieving an average utilisation of 4.65 flights per day (7.905 hours per day). This value is considered reasonable, as the utilisation per day for this particular aircraft on for average mission of range of 727nm is 4.67 flights per day (8.36 hours per day) [3.19]. If then, the total annual costs are assumed to remain the same, then the engine and airframe maintenance cost will increase to US\$ 254.06 and US\$ 705.10 respectively (averaging a consolidated cost of US\$ 1213.22 per hour). Further, based on this method

an equation was then generated to simulate the costs for missions of varying ranges (figure 3.13).

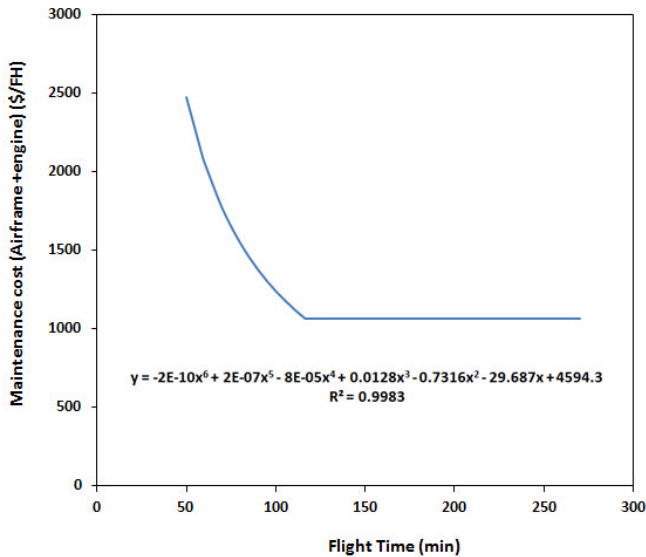


Fig 3.13 Maintenance costs with varying mission time

As the method utilises a derived correlation and significant assumptions, it is not of high accuracy in terms of actual maintenance cost calculations, but however given the wider scope of this study the trend observed is considered representative of what may be observed and hence was used in the model.

b. Fuel dependant costs: These costs essentially depend on the cost of the fuel used and the total amount of fuel consumed during the flight. Aviation Fuel price is available through IATA and the model may also use a fuel price based on future scenarios. For the first section of the study analysing operations, the fuel price has been assumed to be US\$1098/mt, while for the second section analysing technologies, the fuel price has been assumed to be US\$1062/mt. This difference has occurred because the studies have been carried out at different times during the course of the three year PhD, and hence as these models have been demonstrated at various forums to industrial partners, for illustration the prevailing prices at the time were assumed for analysis.

c. Emission dependant costs: The model currently calculates the emission costs for a flight based on the taxation scenario and the total amount of emissions (currently CO<sub>2</sub> and NO<sub>x</sub>) generated. As the framework calculates emissions per segment and also for a complete mission, emission taxation can be applied segment wise (such as a specific tax for cruise NO<sub>x</sub>) and also for a whole mission.

### 3.7 THE OPTIMISER

The optimisation module in this work utilises a genetic algorithm based multi objective optimiser. The optimiser was first developed as a requirement of the Clean Sky project for trajectory optimisation at Cranfield University, and is an implementation of the Non-dominated Sorting Genetic Algorithm (NSGAII) created by Deb [3.20, 3.21]. The work, in which the author has been an integral part of, was conducted as a collaborative effort between Cranfield University and Airbus France and is recognised as a key deliverable for the Sub-work Package 3.2- *Theoretical Transversal Optimisation and Trajectory Definition* in Work Package 3 - *Management of Trajectory and Mission (MTM)* area of the Systems for Green Operation Integrated Technology Demonstrator (SGOITD), in the Clean Sky project [3.22]. The author was responsible for the benchmarking and testing of the optimiser. For the reader's reference an extract of a report is placed at appendix A which describes the process of bench marking and testing, conducted as a part of the validation and verification process of the optimiser.

Whilst creating the optimiser, at the initial stages of this project and during the benchmarking and testing phase, a detailed literature review was conducted to identify suitable optimisation techniques. The literature review is now an integral part of WP3.2 deliverable documents on trajectory optimisation [3.40]. Also In collaboration with colleagues at Cranfield University and Airbus France, a part of the work on the benchmarking and testing resulted in publishing of papers in the International journal of aerospace and at the 2011 SAE conference [3.23].

For this report, in order to discuss the rationale behind the selection of genetic algorithms as the chosen optimisation technique for trajectory optimisation, this section is aimed at providing a summary of the literature review. [3.40].

Optimisation can be seen as the process of obtaining the best result or the best possible solution under any given set of circumstances. Thus, optimisation can be defined as the science of determining the best solutions to certain mathematically defined problems, which are often representations of physical reality [3.26]. There exists no single method available for efficiently solving all optimisation problems. Thus a number of optimisation methods have been developed in the past, many of which are customised for a specific problem. One particular group of optimisation methods is the optimum seeking methods, also known as mathematical programming techniques.

These techniques are particularly important because they determine the minimum of a function of several variables under a prescribed set of constraints [3.27]. In this section a particular emphasis is placed on some of the main mathematical programming techniques and their suitability to aircraft trajectory optimisation problems. In order to describe the different methods available for solving optimisation problems, a classification as per relevant criteria may be defined as follows:

- The presence of constraints (constrained and unconstrained; equality and inequality constraints)
- The nature of the design variables (parameter or static optimisation and trajectory or dynamic optimisation problems)
- The physical structure of the problem (optimal control and non-optimal control problems)
- The nature of the equations involved (linear, nonlinear, geometric, and quadratic programming problems; stationary and non-stationary problems)
- The permissible values of the design variables (integer and real-valued programming problems),
- The deterministic nature of the variables (deterministic and stochastic programming problems),
- The number of objective functions (single and multi-objective programming problems).

According to this classification of optimisation problems, the aircraft trajectory optimisation problem can be classified as constrained, dynamic, optimal control, nonlinear. As the optimiser and the framework will be developed to accept within the framework a model which is not specifically designed as an integral part of the system, the functions relating inputs/design variables and outputs/objective function of the particular model are unknown, but are presumed to be nonlinear, non-smooth, and non-differentiable – real-valued, deterministic, and multi-objective. In addition, the problem can also be classified as multimodal, as the space is unknown but it is assumed that there are several local minima (or maxima). It can also be classified as multi-dimensional since a number of parameters will be involved during the optimisation process.[3.40]

### 3.7.1 NUMERICAL METHODS FOR TRAJECTORY OPTIMISATION

In the course of establishing a suitable algorithm to perform optimisation an in-depth study was undertaken to investigate various established techniques and methods. The main methods as identified for aircraft trajectory optimisation problem according to Schwefel [3.28] and which are discussed here are – hill climbing methods, random search methods, and evolutionary methods. [3.40]

- a. Hill climbing methods - Hill climbing methods are most frequently applied in engineering design, and are characterised by their manner of searching for a maximum (optimum), which corresponds closely to the intuitive way a sightless climber might feel his way from a valley up to the highest peak of a

mountain [3.28]. These methods can be classified as: direct search methods (coordinate method, pattern search, Rosen rock method, simplex, and complex method, among others), gradient methods, and Newton methods.

- i. Direct search methods only use the values of the objective function during the optimisation process, i.e., they do not construct a model of the objective function; instead, the directions and to some extent the step lengths are fixed heuristically, or by other means, rather than in an optimal way [3.28]. The attraction of these techniques, which sometimes are called trial-and-error methods, lies in their simplicity and the fact that they have proved successful in practical applications. Examples of these methods, which are useful when the path followed to determine an optimum value is irrelevant, constitute the "hill climbing search" and simulated annealing search methods described by Russell and Norvig [3.29].
  - ii. Gradient methods such as the steepest descent and conjugate gradient, during the optimisation process, use not only the value of the objective function, but also its first partial derivative. They assume that the objective function is continuously differentiable. Thus all hill climbing techniques which use search directions based on the first partial derivatives of the objective function are called gradient methods [3.29].
  - iii. Newton methods, in addition, make use of the second partial derivatives of the objective function. These strategies exploit the fact that, if a function can be differentiated any number of times, its value at a given point can be represented by a Taylor series constructed at another point. The optimisation process is carried out in several steps involving the calculation of the function's first and second derivatives, and the inversion of the Hessian matrix. Newton methods can present convergence problems, as in the case in which the Hessian matrix is singular (non invertible), and the success (or failure) of finding the optimum value depends on the starting point, requiring a good knowledge of the objective function and the search space [3.28].
- b. Random search methods: According to Schwefel [3.28], random search methods are all those ones in which the parameters vary according to probabilistic, instead of deterministic, rules. Since these methods search for the optimum along random directions, which are not oriented with respect to the structure of the objective function, their use implies in general a higher cost because they do not take optimal single steps. However, the advantage is that these methods can be applied in every case [3.28]. These methods are utilized in situations in which many deterministic optimisation algorithms do not have the desired success. These situations include ones in which (i) the partial derivatives of the objective function are discontinuous, (ii) the finite step lengths are greater than a narrow valley, and (iii) the calculated or

measured values are subject to stochastic perturbation (e.g., rounding errors), among others. Owing to many deterministic optimisation methods, this process uses random decisions at some stage to avoid premature termination of the search for an optimum, random search methods will not be detailed here [3.28][3.29].

- c. Evolutionary methods: These methods are inspired by nature and rely on the replication of biological structures and processes that can be observed in natural environments with the object of solving technical problems. They are based on Darwin's principles of species evolution: the reproduction cycle, the natural selection, and the diversity by variation [3.30]. The most important evolutionary methods are:
  - I. Evolutionary programming: Since, by definition, different species do not exchange genetic material, evolutionary programming methods explicitly try to model organic evolution at the level of evolving species without making use of any kind of recombination [3.30].
  - II. Evolution strategies: Contain an element of recombination between solutions, in a similar manner to real numbered genetic algorithms.
  - III. Genetic programming: In genetic programming, the Darwinian principle of reproduction and survival of the fittest, and the genetic operation of recombination are utilised to create a new offspring population of individual computer programs from the initial population of programs [3.31].
  - IV. Genetic Algorithms (GAs) Similar to the other evolutionary techniques, GAs are based on the principles of natural genetics and natural selection. Thus, the basic elements of natural genetics – reproduction, crossover, and mutation – are used in the genetic search procedure.

Among all evolutionary techniques, GAs are probably the methods with the most widespread use, and they have had a significant impact on optimisation [3.29]. GAs differ from the traditional methods of optimisation, among others as follows [3.27]:

- GAs utilise a population of points to start the procedure instead of a single design point.
- GAs use only the values of the objective function, i.e., the derivatives are not used in the search procedure.
- In GAs the design variables are represented as strings of binary (or real) variables that correspond to the chromosomes in natural genetics.
- The objective function value corresponding to a design vector plays the role of fitness in natural genetics.
- In every new generation, a new set of strings is produced by using randomized parents selection and crossover from the old generation.

In general, of the evolutionary methods described, Genetic Algorithms are considered to be well suitable for problems in which the functions relating inputs to outputs are unknown and may have an unexpected behaviour. They also have been found to be effective where standard nonlinear programming techniques would be inefficient, computationally expensive, and in most cases, find a relative optimum that is the closest to the starting point [3.29]

### 3.7.2 TRAJECTORY OPTIMISATION TECHNIQUE SELECTION

Even though Betts [3.31] considers evolutionary methods – including GAs and other techniques involving some sort of stochastic process during the optimisation process – as not being appropriate for trajectory optimisation problems and as computationally inferior when compared to methods using gradient information, it has been found that evolutionary techniques, in particular GAs, are effective for solving the aircraft trajectory optimisation problem due to the following:

- Genetic Algorithms are problem independent and hence instead of using previously known domain-specific information to guide each step, they make random changes to their candidate solutions and then use the fitness function to determine whether those changes produce an improvement. This is an important aspect because, with multi-model integration, for aircraft trajectory optimisation, the functions relating inputs to outputs are unknown. Since GAs optimisation routines are both model and problem independent and allow the users to run different models (simultaneously if required) for simulating different disciplines (such as aircraft and engine performance, emissions formation etc.), they are found to be effective.
- Genetic Algorithms perform well in problems for which the fitness landscape is complex – discontinuous and multi-modal (many local optima), and in which a number of constraints and objectives (multi-objective) are involved.
- Genetic Algorithms use a parallel process of search for the optimum, which means that they can explore the solution space in multiple directions at once. Thus, if one path turns out to be a dead end, they can easily eliminate it and progress in more promising directions, thereby increasing the chance of finding the optimal solution. It is therefore found that Genetic Algorithms are well suited to solving problems where the space of all potential solutions is large – which is a particular characteristic of nonlinear problems.

From the four main evolutionary algorithms briefly described, Genetic Algorithms have been chosen because of their wide scale research and applications worldwide [3.32][3.33][3.34][3.35], including those ones described in the works developed by Gulati [3.36], Rogero [3.37], Sampath [3.38], and Whellens [3.39].

However, it is important to highlight that the hybridisation of Genetic Algorithms with other optimisation techniques has to be found more effective. This is attributed to the fact that although Genetic Algorithms are an efficient optimisation technique, they however are not the most efficient for the entire search phases [3.37]. Thus for future versions of this work, hybrid

optimisation methods will be considered as they have the potential to improve the performance in a given search phase. Examples of these techniques constitute of those associated with the use of both a random search phase during the beginning of the optimisation process (to increase the quality of the initial population) and a hill climbing phase at the end of the optimisation(to refine the quality of the optimum point once the global optimum region has been found)[3.40].

### 3.8 CONCLUSION

This chapter aimed to provide the reader with detailed information on the model integration framework, the basic models and the optimiser. Having explained and established the requirements, modelling physics and the assumptions of the next phase of the study involves the optimisation of trajectories using the integrated network of models and the genetic algorithm based optimiser.

## 4. TRAJECTORY OPTIMISATION

### 4.1 INTRODUCTION

With a primary goal of the aircraft decreasing its environmental impact, one of the key motivations of the Clean Sky project is to investigate optimised trajectories with a final aim of eventually implementing these ‘environmentally green’ yet flyable trajectories onto the Flight Management System (FMS). The key factor that makes altering trajectories an attractive option for environmental benefit, stems from the fact that operational measures do not require the introduction of new equipment or deployment of excessive technologies, instead they depend on more optimal and different ways of operating aircraft that are already in service.

These trajectories have a multitude of variables and constraints and hence as discussed in the previous section, Genetic Algorithms owing to their inherent characteristic of exhaustively screening the design search space, enable the system to effectively optimise for any given objective. However there exist limitations of time and computing resources onboard a conventional aircraft. As these are necessarily required for an optimisation purpose, it is therefore endeavoured, by the project, to conduct all simulations on ground, and eventually load the Flight Management System (FMS) at a later stage with all acquired applicable and suitable trajectories.

Currently owing to air traffic management constraints, a flight crew has a limited level of autonomy in altering a trajectory to suit a particular purpose unless done for safety reasons. Trajectories flown are strongly dependant on an airline operator’s policy, primarily planned for maximum profitability using the cost index method and on operational/technical procedures governing any civil controlled airspace.

The primary purpose of trajectory optimisation within the purview of Systems for Green Operation-Integrated Technology Demonstrator (SGO ITD) in the Clean Sky project is to therefore provide flyable trajectories with aims to reduce the traditional optimisation objectives such as noise with respect to levels perceived by the population surrounding airports, mission time, mission fuel, emissions ( $\text{CO}_2$   $\text{NO}_x$ , and Contrails on longer ranges) for all the phases of flight.

The work in this part of the PhD therefore aims to study the optimisation of trajectories from the perspective of traditional objectives and specific environmental objectives. The traditional objectives include mission fuel burn, mission time and operating cost, while the environmental objectives will include emissions produced over a mission and hence examine  $\text{CO}_2$  (as a consequence of fuel burn),  $\text{NO}_x$  and Contrails. The objective is to establish at a preliminary level how these optimised trajectories will differ in terms of operational parameters (speeds, altitude and throttle settings) in comparison to a baseline trajectory and further establish the

gain that may be accrued in terms of objectives. In the next chapter, it then further uses these optimised trajectories to analyse the effects of costs linked with CO<sub>2</sub> emissions and try and establish the taxation levels required to actually implement these trajectories.

In each of the cases considered in this study it is important to note, even though full trajectories have been analysed, as the aircraft spends a significant part of the mission in the climb and cruise phases of flight, and consequently at higher power settings, currently only these segments have been optimised.

This section therefore begins with a brief definition of flight phases and the current trajectory and ATM constraints based on operational/technical procedures governing any civil controlled airspace. This is then followed by the analysis of optimised trajectories for a series of short to medium range routes, with respect to the objectives discussed.

## 4.2 DEFINITION OF FLIGHT PHASES

### 4.2.1 DEPARTURE

The departure phase of a mission begins from the point at which the brakes are released on the runway till the point at which the aircraft is in clean configuration and essentially is constituted of two parts:

Take off: This phase is one of the most critical phases of flight and begins at brake release and ends at 35 ft above the runway which is the obstacle altitude. As per current levels of certification and safety requirements this phase is highly restricted, and hence it is opined by research within Clean Sky that it is difficult to gain any benefit through optimisation. Of relevance in this phase however are the strict ICAO limits on LTO phase (Landing and Take Off phase) NO<sub>x</sub> emissions and Noise restrictions. Therefore this phase is currently not optimised in this study.

Early/initial climb: This phase begins at 35 ft above the runway and ends when the aircraft is in clean configuration and has accelerated from V2+10 and reached the regulation speed (CAS) of 250 kt, with a max climb power setting. The optimisation objectives in this phase are noise (below 3000 ft) and hence this segment is usually flown using the ICAO defined NADP (Noise Abatement Departure Procedures 1 and 2) and SID (Standard Instrument Departure) procedures and is mostly optimised for reductions in noise levels. Other objectives include in this phase includes NO<sub>x</sub> emissions and fuel burn. The optimisation of this phase will need to consider a combination of thrust reduction with a trade-off between climb speeds.

#### 4.2.2 CLIMB

This phase begins soon after the initial climb phase and extends till the aircraft reaches the cruise altitude at the cruise speed. The procedure followed usually by an aircraft during climb is to initially follow ATC instructions which allows the flight to proceed "on-course" according to the route cleared in an initial flight. On reaching an en-route point, it is cleared to accelerate and gain altitude, climbing to the cruise altitude level. The climb is essentially divided into three parts, with the first part characterised by the aircraft's acceleration to cruise climb airspeed due to reduction of climb ratio with the power setting unchanged. The second part requires a climb at constant calibrated airspeed. The third phase is dependent on a crossover/ transition altitude, which is essentially the altitude at which the calibrated airspeed selected and the mach speed selected for transition to cruise represent the same true airspeed value.

The current operational constraints in this phase include the following:

- a. The aircraft must not operate beyond its absolute ceiling (operational flight envelope).
- b. The aircraft speed must not exceed the maximum operating limit speed (CAS).
- c. When reaching the top of climb (selected FL), the speed should be equal to optimal Mach cruise (no level-off acceleration).
- d. The speed should not be lower than the stall speed.
- e. The aircraft speed must not exceed the maximum operating limit Mach
- f. The operating aircraft speed must be greater than the minimum buffet speed.
- g. The aircraft speed in Mach number must not exceed the maximum operating limit Mach
- h. The steady gradient of climb may not be less than 1.2% for two-engine aircraft with one engine inoperative and the remaining engines at the available maximum continuous power or thrust.
- i. The engine rating should be lower than the maximum climb rating.

The key objectives in optimising this segment essentially include fuel ( $\text{CO}_2$  as a consequence of fuel burn) and time. As per clean sky requirements the optimal trajectory concept for climb is a continuous and unique phase obtainable through continuous variation of the throttle setting and airspeed. The variables in this phase include throttle setting altitude and speeds and hence the dynamic parameters in this phase include the aircraft mass, time, position (altitude and range), airspeed, flight path angle, and thrust, fuel flow and emission parameters ( $\text{CO}_2$ )

#### 4.2.3 CRUISE

The cruise phase of flight begins at the top of climb and is where the aircraft levels off. The aircraft is required to be the most fuel efficient in this phase as it will spend a significantly long duration of the flight in this phase. Current regulations usually require the aircraft to follow a particular heading at specific airspeed/ cost index and at constant altitude. The cruise phase

ends when an aircraft approaches top of descent, the point at which descent phase of flight starts.

Various fuel efficient concepts in the cruise phase can provide a substantial reduction in fuel consumption. These include continuous climb, optimal thrust setting by throttle control (and reduction of speed) and multiple steps climbs.

All these concepts under the current air traffic system is currently not practiced, primarily due to various physical and operational constraints. The physical constraints in this phase are similar to the climb segment and include

- a. The aircraft adhere to an absolute ceiling limit as defined by operational flight envelope.
- b. The aircraft must be flown at a constant flight level as cleared by air traffic control and continuously separated (longitudinal and vertical) from other flight levels.
- c. The aircraft speed must adhere to requisite operating speed limits which include CAS, Mach, between maximum and minimum buffet speed and above stall speed.
- d. When reaching the top of climb (selected FL), the speed should be equal to optimal Mach cruise (no level-off acceleration).
- e. A cruise segment is required to last at least 10 minutes or longer.

The key environmental issues in this phase of flight include CO<sub>2</sub>, and thus fuel burn, cruise NO<sub>x</sub> and its relation to ozone generation and contrails

#### 4.2.4 DESCENT

The point at which the descent is said to commence is called the Top of Descent (TOD), and is at which the aircraft power is lowered to descent idle and extends to 10000 ft above mean sea level and is the speed is then restricted to 250 kt CAS. Similar to the climb segment the initial part is flown at the cruise Mach number. As the altitude decreases and airspeed indications approach the desired initial descent airspeed the aircraft switches to a constant CAS speed until 10000 ft. Currently the descent phase can be controlled by the Aircraft Flight Management, which calculates a path based on a descent profile selected (essentially speed, geometry and range to TOD point) according to aircraft performance characteristics in the actual conditions. The airline operator depending on a cost index methodology, adjusts the economic profile and hence generates different enroute /descent TOD transition points, speed, descent profiles/slopes and therefore for a minimum time descent selects a late TOD and faster descent whereas for a minimum fuel burn descent a slower glided descent from an early TOD. However if a particular time slot is required to be adhered to this may be overridden. In an ideal situation with no ATC constraints an aircraft is able to glide to a final

approach with no thrust, however due to ATC constraints, descents are controlled and aircraft may require to execute constant altitude segments which requires the necessary use of thrust.

Optimal concepts suggest modification of ATM constraints to enable CDA (Continuous Descent Arrival) or OPD (Optimised Profile Descents) and hence reduce fuel burn through limited use of thrust. The current constraints on this segment include the following

- a. The aircraft speed must adhere to requisite operating speed limits which include CAS, Mach, between maximum and minimum buffet speed and above stall speed.
- b. The speed at the top of descent point should be equal to optimal cruise Mach (no level-off deceleration).
- c. The maximum speed at and below FL100 is 250 kt CAS.
- d. The engine rating should equal to or higher than the idle rating.

#### 4.2.5 APPROACH AND LANDING

The initial point for the approach phase is defined as the point when the aircraft reaches 10,000 ft above mean sea level and 250 kt CAS and ends when the aircraft is 50 ft above ground level. After this point the aircraft is required to execute the landing phase of the mission.

Currently the approach phase is function of STAR rules and ATC clearances. During the final approach phase, the aircraft is in approach configuration and utilises the flap extensions to produce the required deceleration to the final approach descent airspeed.

This airspeed and level flight are maintained until the descent landing gradient is intercepted. The landing sequences begins with the lowering of the landing gear and required flap settings, which results in slowing the aircraft further to landing airspeed. This phase ends when the aircraft touches down .The key constraints of this phase include the following

- a. During approach, the aircraft must not accelerate.
- b.  $\gamma(FPA)=5.2\% (3^\circ)$  Aircraft glide-slope at the final approach fixed point should correspond with the instrument landing system's glide-slope
- c. The engine rating should be higher than the idle rating.

At this point, the lowering of the landing gear and successive wing flaps extensions result in slowing of the aircraft and finally touching down. The environmental objectives in the approach and landing phase are the classical (i.e. fuel, time), the Engine emissions such as CO<sub>2</sub>, LTO NO<sub>x</sub> and most importantly aircraft noise.

## 4.3 AIRCRAFT TRAJECTORY DEFINITION

When optimising aircraft trajectories, the first step involves the definition of the aircraft trajectory to be optimised. As all the optimisation processes carried out here involved only vertical profiles basically three parameters have been used to define a given aircraft trajectory which include flight altitude ( $h$ ), aircraft speed (Calibrated Air Speed (CAS) or Mach number) and throttle setting.

**Take off:** This segment is the first segment calculated and as discussed earlier. The basic inputs of this phase includes the airport altitude, aircraft take-off weight, the thrust setting which is set at max take off thrust from the engine ratings calculated and the flap setting (takeoff configuration). The program calculates the speeds ( $V_{\text{stall}}, V_1, V_R$  and  $V_2$ ), range and time of flight in this phase. This segment is set to include a part of the initial climb and hence ends at 1500 ft above msl at which time the aircraft has reached  $V_{2+10}$ . This segment is not optimised.

**Climb:** This segment which includes a part of the initial climb and the en-route climb extends till the aircraft reaches cruising altitude, is optimised. Therefore in order to define the trajectory the segment has a set of 14 parameters of which 12 have been set as variables. The variables essentially include altitudes, speeds and throttle settings. The altitudes between two consecutive climb variables were computed by splitting the segment into it into 10 equal steps, maintaining a constant altitude increase at the same speed and throttle settings(as a percentage of rated maximum climb thrust). Table 4.1 and figure 4.1 indicate the various speeds altitudes selected for the variables. The speeds have all been selected within the design limits specified for the aircraft [3.1].

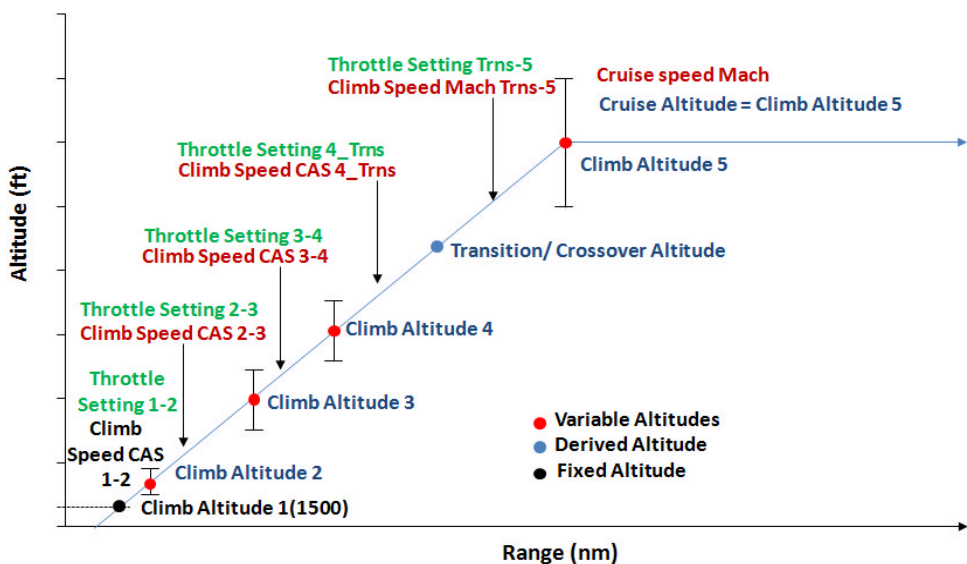


Fig 4.1 Variable parameters used to define climb and cruise phase

*Cruise:* This cruise segment simulated is done so at constant altitude and speed, and therefore to optimise is defined by 2 variables namely the cruise altitude and cruise speed (Mach) (as seen in the figure 4.1). In order to cater for change in weight of the aircraft due to consumption of fuel during the flight and hence for greater accuracy, the cruise phase is split into 5 equidistant segments. However in order to study the effects of contrail, cases with variable altitudes and speeds at cruise has also been demonstrated where in the optimiser has been allowed the flexibility of varying the altitudes at 5 equidistant points whilst changing the speeds between each consecutive point.

*Descent approach and landing:* This phase is not optimised and a constant descent approach is assumed. The aircraft follows the following profile

- a. Aircraft begins descent at Mach 0.7, thrust set at descent idle (25% of maximum thrust), clean configuration.
- b. After cross-over altitude, the aircraft maintains a constant CAS speed of 310 kt until 10000 ft, thrust set at descent idle (25% of maximum thrust), clean configuration.
- c. Below 10000 ft and until 3000 ft the aircraft maintains a constant CAS speed of 250 kt until 10000 ft, thrust set at descent idle (25% of maximum thrust), clean configuration.
- d. Below 3000 ft flight path angle set at  $3^\circ$ , thrust is set at approach rating (30% of maximum thrust), approach flaps configuration until 300 ft followed by landing flaps configuration till touchdown.

Mission parameter	Min	Max	Parameter-fixed/variable
Altitude1 (climb) (ft)	1500	1500	Fixed
Altitude2(climb) (ft)	2000	4000	Variable
Altitude3(climb) (ft)	8000	12000	Variable
Altitude4 (climb) (ft)	13000	17000	Variable
Altitude5 (climb) (ft)	25000	35000	Variable (set at cruise alt)
Climb speed CAS 1-2 (kt) (V2 +20)	193.7	193.7	Fixed
Climb speed CAS 2-3(kt)	200	275	Variable
Climb speed CAS 3-4 (kt)	250	300	Variable
Climb speed CAS 4-Trns(kt)	250	300	Variable
Climb speed Mach Trns-5	0.65	0.78	Variable
Throttle setting (climb)1-2	90% MCT	100% MCT	Variable
Throttle setting (climb)2-3	90% MCT	100% MCT	Variable
Throttle setting (climb)3-4	90% MCT	100% MCT	Variable
Throttle setting (climb)4-Trns	90% MCT	100% MCT	Variable
Throttle setting (climb)Trns-5	90% MCT	100% MCT	Variable
Cruise Altitude	25000	35000	Variable
Cruise speed Mach	0.65	0.82	Variable

Table 4.1 Parameter specification and bounds used to optimise climb and cruise phase

#### 4.4 CASE STUDIES

With the trajectory defined for an optimisation problem, in order to demonstrate the benefits accrued from optimised trajectories a set of three demonstrative cases were selected. The aircraft and engine model used for each of the cases is the short to medium range single aisle aircraft with twin spool turbofan engines as modelled and described in the chapter describing the models (similar to the Boeing 737-800 equipped with a CFM56-7B27 ).

Based on the typical utilisation information for this aircraft, available in reference [3.16], three routes based on the range capability of an aircraft of this type were selected. The ideology was to study a short range, short-medium range and medium range to enable a comparison of optimised trajectories and hence routes ranging 227nm, 815nm and 1614 nm were chosen. The case studies were begun by first simulating each of the routes to set up a baseline for comparison. The baselines trajectories were simulated following a set of pre defined

assumptions in terms of speeds altitudes and mach numbers and enumerated previously in section 3.2.3, to verify the performance of the aircraft against the actual payload range chart of the aircraft.

When the payload range chart is provided by the manufacturer it is done so to demonstrate the performance of the aircraft in ideal and specific conditions (such as absence of wind conditions and no hold time before landing). Therefore as the baseline cases have been simulated to match the performance of the aircraft on the payload range chart, they are assumed to be ideal. Further in order to bring perspective to the ranges selected, the typical city pairs represented by the ranges are as indicated in table 4.2. Finally apart from the trajectory assumptions as enumerated section 3.2.3, similar to a standard mission profile as followed by BADA [3.41], the baseline trajectories simulated have also been done so under the following basic assumptions:

- a. The range calculated is based on the great circle distance between the two cities.
- b. The simulated baseline trajectories were based on the typical mission rules and hence carried hold fuel for 20 minutes, diversion fuel to an airport 200 nm from destination and reserve fuel, as discussed in the model validation and verification section.
- c. The baseline trajectories have been calculated using standard profiles for takeoff, climb, descent approach and landing as described earlier.
- d. All routes have been calculated assuming a 100% load factor of 162 passengers (2 class configuration, accounting for 90.7 kg per passenger) onboard and hence at maximum passenger payload conditions resulting in a payload of 14696 kg on all routes.
- e. All optimised routes have been optimised in the cruise and climb segments but have been assessed for full mission performance in terms of required objectives and hence have similar takeoff, descent and approach/landing profiles
- f. The operating cost for all cases have been calculated for the fuel price set at US\$ 1098/ metric ton, nil CO<sub>2</sub> taxation and the basic assumptions as listed in section 3.6.1.[4.8]

Mission range nm (ESAD)	227	815	1614
Representative City pair	Paris(France) – Geneva (Switzerland)	Munich (Germany) – Athens(Greece)	Stockholm(Sweden)-Lisbon(Portugal)
Takeoff Weight (kg)	60167	63934	68602
Payload kg	14696	14696	14696
Mission Fuel Burn (kg)	2045	5319	9807
Time (min)	47	127	234
CO <sub>2</sub> emissions(tons)	6.4	16.7	30.95
NO <sub>x</sub> emissions (kg)	29.7	70.1	125.3
Operating cost (US\$/mission)	8867	15469	28558

Table 4.2 Baseline trajectories simulated for each of the routes selected

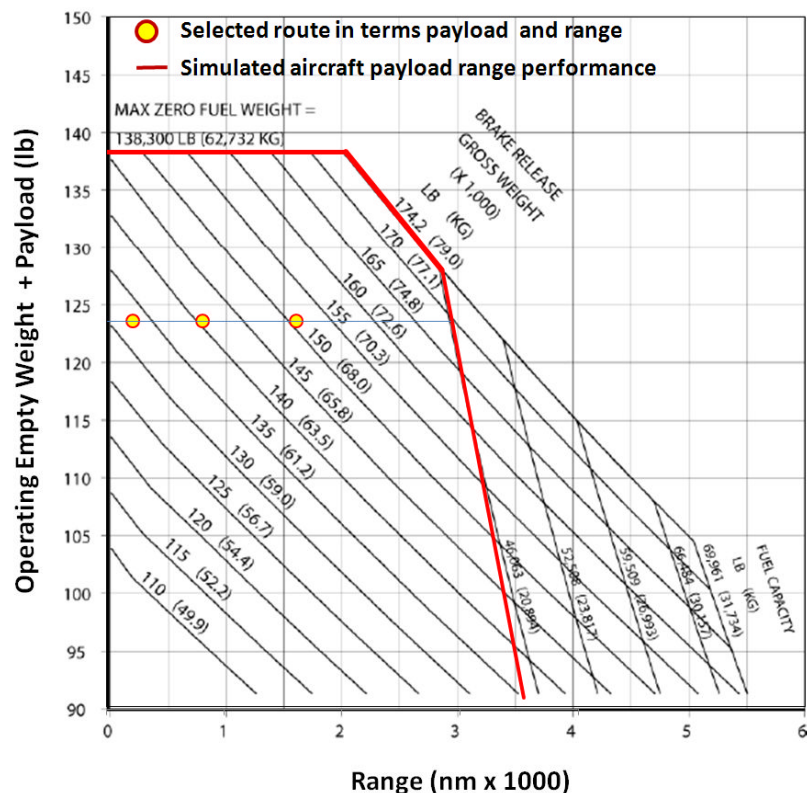


Fig 4.2 Selected routes on the payload range chart

#### 4.4.1 CASE 1: SHORT-MEDIUM RANGE (815 NM)

The first case study considered is the 815 nm (Munich to Athens) missions. The baseline trajectory was optimised for various objectives which included mission fuel, mission time, mission NO<sub>x</sub> and operating cost. The optimised climb /cruise segments and the parameters selected by the optimiser for each of the objectives are as indicated in table. All optimisations used fuel as one of the objectives, so as to have a consistent parameter to compare the results with.

The results may be summarised as follows:

- a. The baseline trajectory is seen to be close to the fuel time pareto-optimal front and is a trade-off between fuel and time. In comparison to a baseline trajectory, the fuel optimised trajectory will save 3.8 % fuel but will take 9.5 % more time, whereas the time optimised trajectory will consume 23.4% more fuel but will be 7.1% quicker in terms of time.
- b. The fuel optimised trajectory has an improvement of fuel consumption of 28.3% over the mission time optimised trajectory while it takes 18% longer in terms of time. The time optimised trajectory however has significantly higher CO<sub>2</sub> (corresponding to the fuel burn) the NO<sub>x</sub> emissions.
- c. The transition from the fuel optimised solution to the operating cost solution will lead to the increase in fuel burn by 4% and a decrease in operating cost by 5.18%. However the trajectory optimised for the best operating cost is very similar to the baseline case, as it is 2.38% lower in terms of mission time, 0.06% higher in mission fuel burn and hence better than the baseline by 1.3%. This again indicates that the baseline mission is a compromise between the best fuel and best time missions to optimise on operating cost.
- d. The transition from a fuel burn optimised trajectory to a NO<sub>x</sub> emission optimised trajectory will enable a reduction of 1.6 % NO<sub>x</sub> emissions in total. The NO<sub>x</sub> emission optimised trajectory is the highest in terms of operating cost, primarily attributed to a higher mission time. It however has a lower fuel burn, 0.5 % higher than fuel optimised solution whilst having a 2% longer mission time, thus resulting in a higher operating cost. When compared to the baseline trajectory the mission would cost 5.8% higher but be able to reduce the NO<sub>x</sub> emissions over the mission by 11.23%.

Mission parameter	Baseline mission	Mission fuel burn optimised trajectory	Mission time optimised trajectory	Mission Opn. cost optimised trajectory	Mission NO <sub>x</sub> optimised trajectory
Optimised variables					
Altitude2(climb) (ft)	3000	2002	2000	2000.2	2000
Altitude3(climb) (ft)	10000	11823	10878	10227	12000
Altitude4 (climb) (ft)	17000	17000	17000	17000	16999
Climb speed CAS 2-3(kt)	250	243	275	259.6	220.7
Climb speed CAS 3-4(kt)	300	250	266	250.3	250
Climb speed CAS 4-Trn(kt)	300	300	300	300	300
Climb speed Mach Trns-5	0.7	0.65	0.65	0.65	0.65
Throttle setting (climb) 1-2 (%)	100	100	100	100	90
Throttle setting (climb) 2-3 (%)	100	100	100	100	90
Throttle setting (climb) 3-4 (%)	100	100	100	100	90
Throttle setting (climb) 4-Trns (%)	100	100	100	100	100
Throttle setting (climb) Trn-5 (%)	100	100	100	100	90
Cruise altitude(ft)	35000	35000	25000	35000	35000
Cruise speed Mach	0.78	0.67	0.82	0.82	0.65
*Optimised objectives					
Mission fuel burn (kg)	5319	*5114	6565	5322	5141
Mission time (min)	127	138	*118	123	141
Mission operating cost(\$)	15469	16113	16145	*15202	16413
Mission NO <sub>x</sub> emission (kg)	70.1	63.48	101.23	70.8	*62.43

Table 4.3 Optimised climb and cruise segment parameters (815 nm)

#### 4.4.1.1 Optimisation objectives- fuel and time

The objectives fuel and time are currently the key objectives considered for optimising performance by the aviation industry. The fuel- time Pareto-optimal set of solutions is as shown in figure 4.3.

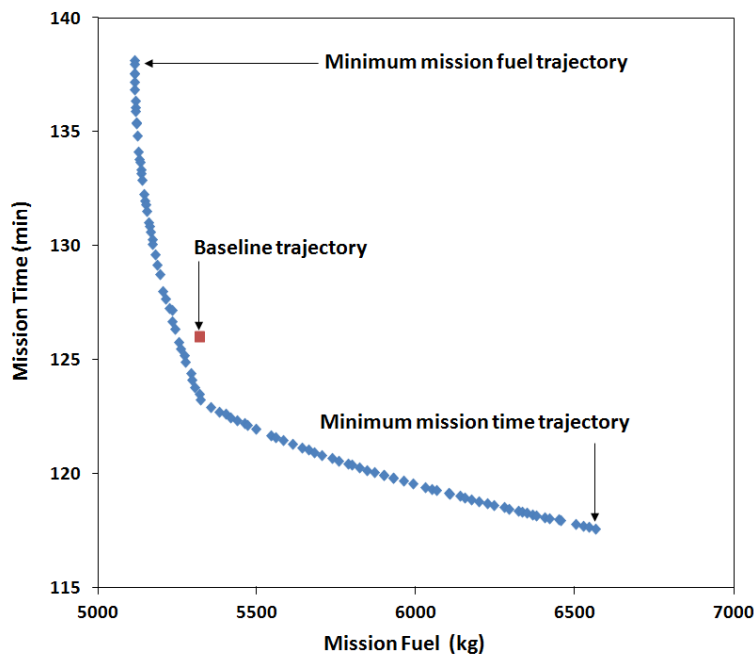


Fig 4.3 Objectives-mission fuel burn /mission time Pareto optimal front

#### Fuel optimised trajectory

As discussed earlier, the segments allowed to be varied by the optimiser included the climb and the cruise therefore 14 variables were allowed to be varied in order to optimise the trajectory for fuel burn. The trajectory consumed 5113 kg of fuel. Figure 4.4 shows the percentage of fuel consumed and the time per individual segment of the mission. It shows that when compared with the baseline the optimiser has tried to maximise the time (increased by 5%) spent at cruise whilst minimising time in the climb and descent.

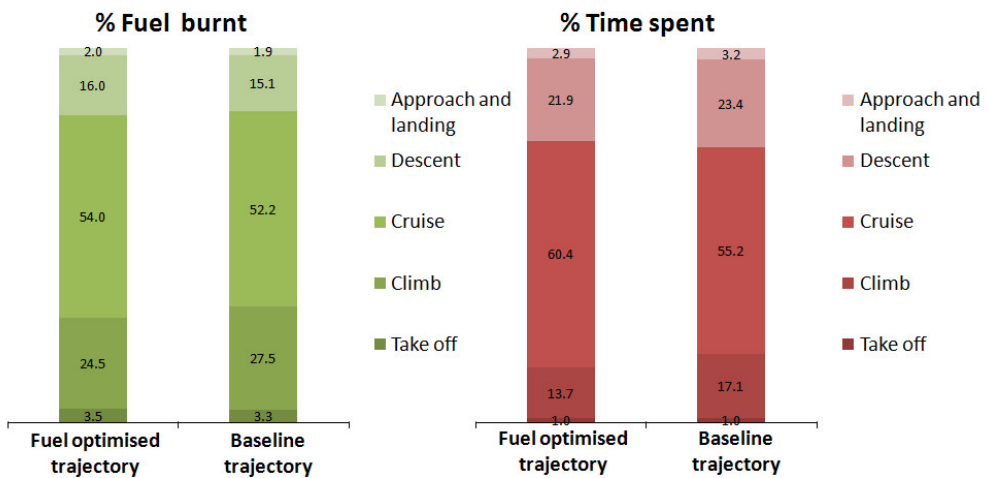


Fig 4.4 Percentage of fuel consumed and the time spent per individual segment of the mission

Considering now only the climb segment, it is observed that when directly compared with the baseline trajectory, the fuel optimised trajectory spends 10.5% less time covering 13.7% lesser range whilst spending 12.7% lesser fuel, and therefore gets to the top of climb more rapidly as mentioned. However when the cruise is compared the fuel consumed is 0.8% lesser than the baseline but for a range that is 3.2% longer and for 20% longer time.

#### Justification of selected variables for the fuel optimised trajectory

At the earliest allowed altitude 2000 ft (variable limits 2000 - 4000 ft) the aircraft switches to CAS speed 243 kt (variable limits 200 – 275 kt) and maintains this speed almost till the upper variable limit of this segment, 11823 ft (variable limits 8000 – 12000 ft). After this the aircraft maintains CAS 250 kt (variable limits (250 – 300 kt) till 17000 ft (variable limits 13000-17000). At this point the aircraft speeds changes to 300 kt, and then reaches transition/ cross over altitude of 19896 ft. From this altitude, the aircraft switches to constant mach speed of 0.65(variable limit 0.65- 0.78), till the top of climb.

#### Climb optimisation for fuel

When an aircraft executes a climb, it usually does so with a purpose of reaching a specified altitude, at a specific speed, either spending minimum time or consuming minimum fuel. Then in order to achieve the required objective, the speed of the aircraft is then required to be continually adjusted to an optimum value, at every stage of climb. This concept refers only to energy state of the vehicle, and not with the details of converting from one state to the other and was first introduced by Rutowski in 1953 [4.4, 3.3]. The method provides an explanation of how an optimal trajectory for fuel (or time) may be sought through the concept of the energy height.

As explained by Rutowski [4.4, 3.3] for an aircraft of mass  $m$  and at an altitude  $h$ , the total energy may be estimated as the sum of kinetic and potential energies

$$E = mgh + \frac{1}{2} mV^2 \quad 4.1$$

$$\text{Specific energy } e = \frac{E}{m} = gh + \frac{1}{2} V^2 \quad 4.2$$

The Energy Height  $h_e$  (in m if  $g=9.81 \text{ m/s}^2$ ) of the aircraft, is then defined as follows

$$h_e = \frac{E}{W} = \frac{e}{g} = h + \frac{1}{2} \frac{V^2}{g} \quad 4.3$$

This is the height at which the potential energy alone would be equal to  $E$ , the current total energy of the aircraft. If  $Q$  is the mass of fuel used per unit time, the mass of fuel used in an energy climb between two energy heights,  $h_{e1}$  and  $h_{e2}$  and  $P_{se}$  is specific excess power given by the following expression

$$P_{se} = \frac{V(F-D)}{W} \quad 4.4$$

Where

$V$ = Velocity of aircraft (m/s)

$F$ = Net Thrust of aircraft (N)

$D$ = Drag of aircraft (N)

$W= m \times g$  = Weight of aircraft (N)

Then

$$mf_{climb} = \int_{h_{e2}}^{h_{e1}} \frac{dm_f/dt}{dh_e/dt} dh_e = \int_{h_{e2}}^{h_{e1}} \frac{Q}{P_{se}} dh_e \quad 4.5$$

And hence for minimum  $mf$  or fuel burn, the speed should be chosen at each level of  $h_e$  so that  $\frac{P_{se}}{Q}$  has the maximum value at a constant  $h_e$ .

In order to compare the climb profile generated in the trajectory, the concept of energy height was implemented using a gradient based optimiser. The method is based on a procedure described in references [4.4-4.7].

The process essentially, for the set of altitudes and speeds used to generate the fuel optimised climb segment by the genetic algorithm based optimiser, first calculates the energy height  $h_e$ . The implemented method then for each of the particular energy heights, recalculates the

optimal altitude and speed for the aircraft by means of a "linear search", and thus solves for the location of the value of minimum  $dm_f/dh_e$  or maximum  $P_{se}/Q$ . Figure 4.5 shows the implementation of the procedure with a delta change in speeds and altitudes along the constant energy height contours.

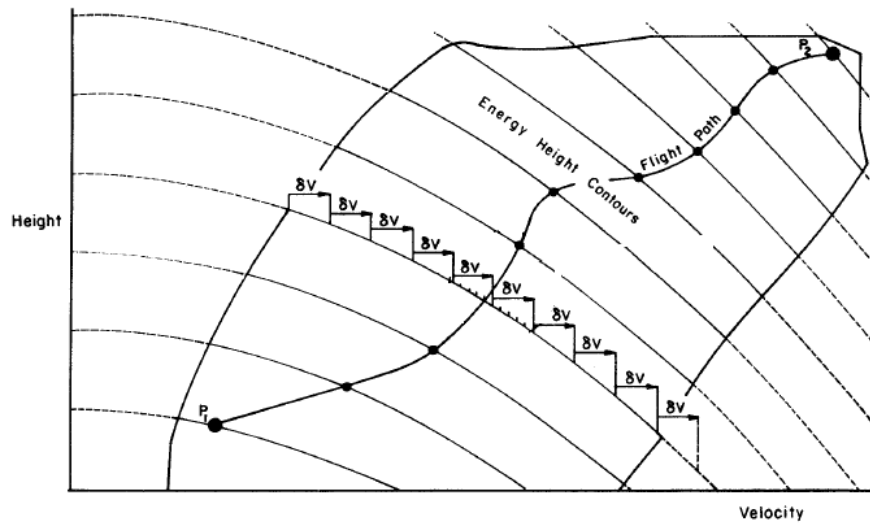


Fig 4.5 Calculation methodology at constant energy height [4.6]

To verify that the method has worked an illustrative example is now considered. From table it is observed that of the variables selected in the climb segment, the variables for altitude 2 and 3 were 2002 ft and 11823 ft respectively. The speed then selected for this segment (Climb speed CAS 2-3) was 243 kt. The altitude variables are separated by 9821 ft, therefore as per the segmentation set of 10 steps between the two variables, the next altitude and speed the aircraft reaches is 2984 ft and CAS 243 kt. Based on this speed and altitude, the energy height is 5837.19 ft (1779.17 m). The energy height model was then used to verify this speed and altitude at the particular energy height of 5837.19 ft.

As per the energy height concept, the optimal altitude and speed thus derived for (constant energy height of) 5837.19 ft, were 3094 ft and CAS 240.13 kt (TAS 129.03 m/s) respectively. As the error between the two sets of variables was marginal, it is opined that the optimiser had selected the correct mission variables. Figure 4.6 shows the graphical interpretation of the case just discussed.

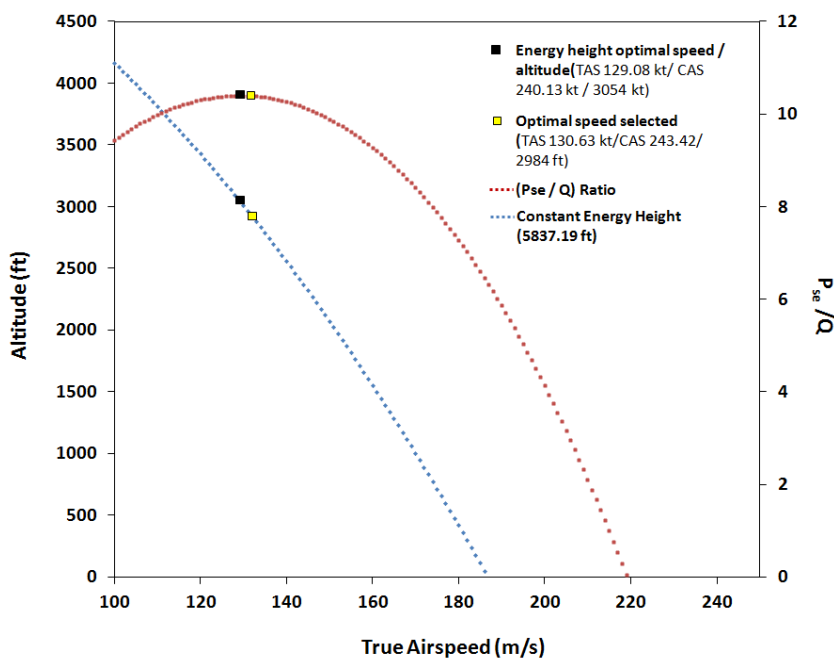


Fig 4.6 Verification of speed and altitude selected by the energy height method

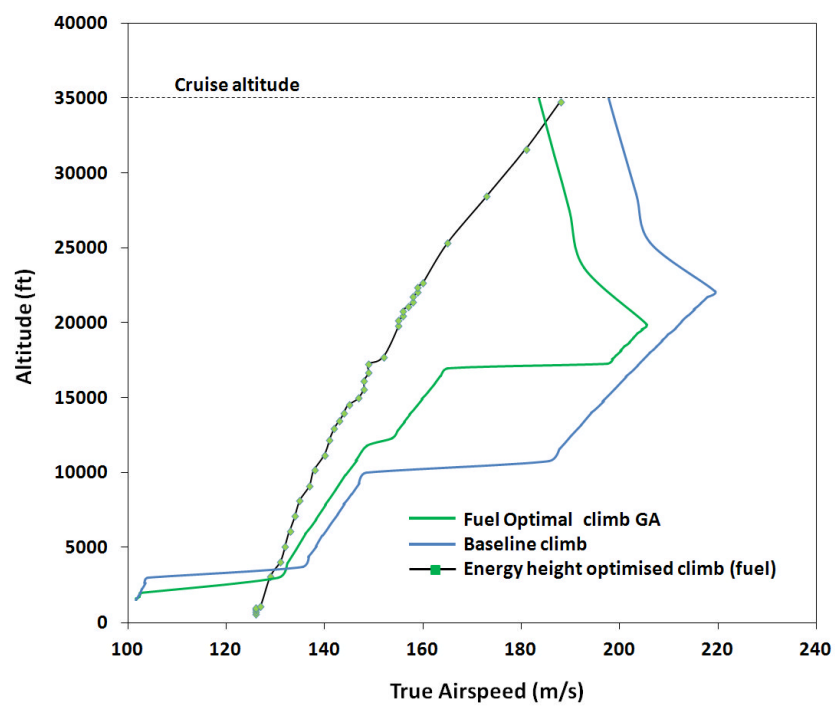


Fig 4.7 comparison of speed evolution (TAS) along the climb segment

Figure 4.7 shows the speed evolution and altitude variation for the fuel optimised trajectory, the baseline trajectory and the energy height optimised trajectory. In order to get the lowest fuel consumption the speed profile should be as close as possible to the energy height optimised climb profile.

Now considering the optimised climb trajectory, as discussed in the illustrative example, the speed and altitude selected between altitude 2 and 3 were found to be very close to the energy height optimal value. Altitude 2 was allowed to vary between 2000 and 4000 ft.

Below 2000 ft, the aircraft is flying essentially at a suboptimal speed, and hence it selected the earliest altitude at 2000 ft to change to the more optimal CAS speed of 243 kt. However as the altitude increases and as the speed between altitude 2 and 3 is fixed at 243 kt CAS, the true air speed in the figure 4.7 is observed to be moving away from the energy height optimised speed profile, in red. This speed however continues to 11823 ft, essentially the upper bound of the next altitude variable (altitude 3 set between 8000 and 12000 ft). The next speed variable (Climb speed CAS 3-4) is limited between 250 and 300 kt (CAS) and will be the speed of the aircraft between altitude variables 3 and 4. The variable selected for the speed is the lower limit of CAS 250 kt.

The optimiser essentially has picked 11823 ft for altitude 3 so as to remain at a CAS speed of 243 kt for the longest possible period. This is so that the aircraft is allowed to remain at a speed of 243 kt, which even though sub optimal, is more optimal than the next lowest allowable speed of 250 kt CAS. The next speed variable, climb speed 3-4, is therefore set at 250 kt and the aircraft remains at this speed between the selected altitude 3 (11823 ft) and altitude 4(17000 ft).

The aircraft is more fuel efficient at higher altitudes and lower speeds. The altitude at which the crossover from constant CAS to constant Mach transition occurs depends upon the two variables Climb speed CAS 4-Trns and Climb speed mach. As the minimum speed after transition/crossover altitude is 0.65, the aircraft therefore chooses a speed by which it can reach the slowest climb speed as quickly as possible. Selecting again the slowest speed Climb speed CAS 4-Trns of 250 kt would result in transition at 28657 ft, instead by selecting 300 kt for the next speed variable and 0.65 for the climb mach speed the crossover happens at 19896 ft, thus enabling a small fuel gain of 5kg. Apart from this, as the objective of optimisation is overall fuel consumed in the mission, the slow speed of 0.65 mach also results in higher rate of climb, thus enabling the aircraft to reach the cruise altitude where the maximum benefit in terms of fuel consumption is achieved for the whole trajectory.

The optimised climb segment using the genetic algorithm optimiser resulted in saving of 11% of fuel from takeoff. However the energy height optimised trajectory with a continuous speed evolution consumes approximately 1350 kg till top of climb and results in a saving of an approximate saving of 16.7% of fuel.

## Cruise optimisation

The cruise segment modelled is for a constant altitude and Mach speed and therefore was allowed variation of two variables. The altitude and Mach speed selected for a fuel optimised trajectory is the highest altitude allowable (variable range -25000 ft to 35000 ft) and 0.67 (variable range- 0.65 to 0.82).

For an aircraft powered by turbojet or turbofan engines the specific fuel consumption is defined by

$$c = \frac{Q}{F} \quad 4.6$$

Where Q is the mass of fuel used per unit time and F is the thrust

In level cruising flight thrust is assumed to be equal to the drag. If

$$\beta = \frac{\text{Drag}}{\text{Lift}} = \frac{c_d}{c_l} \quad 4.7$$

Then

$$F = D = \beta L = \beta W \quad 4.8$$

The mass of fuel used per unit distance may then be expressed as

$$\frac{cF}{V} = \frac{c\beta W}{V} \quad 4.9$$

As the aircraft travels a distance  $dR_a$  (in still air) its mass changes from  $m$  to  $(m+dm)$  where

$$dm = \frac{-c\beta W}{V} dR_a \quad 4.10$$

The specific range  $r_a$  is then defined as the distance travelled per unit mass of fuel used. Thus

$$r_a = \frac{-dR_a}{dm} = \frac{V}{c\beta W} \quad 4.11$$

A measure of the overall efficiency of an aircraft as a load carrier is

$$Wr_a = \frac{\text{Weight} \times \text{Distance}}{\text{mass of fuel used}} = \frac{V}{c\beta W} \quad 4.12$$

Therefore the overall efficiency of a load carrier is equal to the product of L/D and the ratio V/c, which is proportional to the overall efficiency of the engine and which increases with speed. Putting W=mg the total cruise range may be represented as

$$R_{ac} = - \int_{m_1}^{m_2} r_a dm = - \int_{m_1}^{m_2} \frac{V}{c\beta W} \frac{dm}{m} \quad 4.13$$

Where  $m_1$  and  $m_2$  are the masses of the aircraft at the beginning and at the end of cruise

For an aircraft flying at a constant height, if the SFC is not constant but varies with speed, the condition for maximum specific air range  $r_a$  is that  $\frac{c\beta W}{V}$  should be minimum. Therefore the highest altitude of 35000 ft will directly influence to minimise  $c$ ,  $\beta$  and  $v$ . The mach speed however was selected based on the optimal value for the maximum specific air range. Figure 4.8 shows a plot of the specific air range plotted against the increasing Mach number. The most optimal speed, as observed, for the maximum air range is the Mach speed selected 0.67. Air framers usually term this speed as the Maximum Range Cruise Mach number (MRC), while the higher speed of mach 0.78 typically used, is termed as the Long Range Cruise Mach number (LRC)

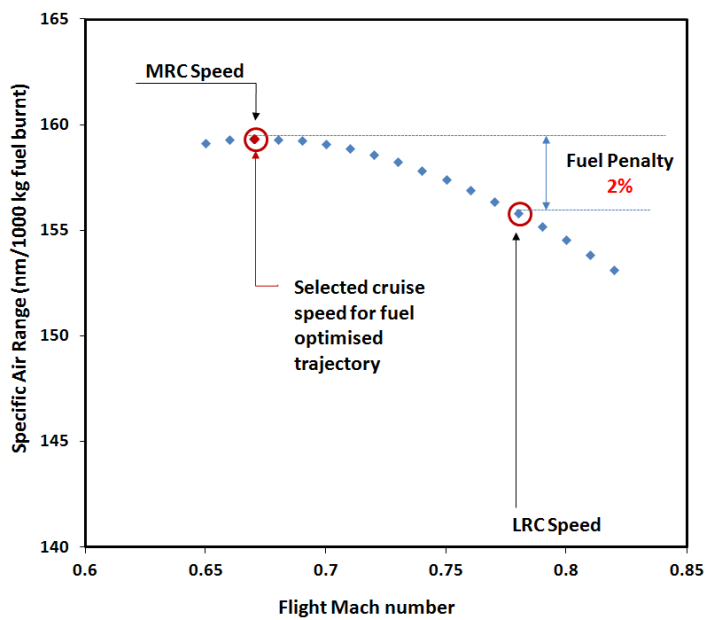


Fig 4.8 Optimal speed selection for maximum specific air range

Time optimised trajectory

Climb segment: An analysis of the climb segment in the time optimised trajectory may again be approached from an energy height perspective. As per the energy height concept, the time taken for an energy optimised climb flight, between two energy heights  $h_{e1}$  and  $h_{e2}$  is

$$t_{climb} = \int_{h_{e2}}^{h_{e1}} \frac{1}{dh_e/dt} dh_e = \int_{h_{e2}}^{h_{e1}} \frac{1}{P_{se}} dh_e \quad 4.14$$

And hence for minimum time the speed should be chosen at each level of  $h_e$  so that  $P_{se}$  has the maximum value at a constant  $h_e$ . The concept was implemented using a similar methodology, as described for minimum fuel. A comparison of the two energy height optimised speed evolution profiles (fuel and time) is as shown in figure 4.9.

When the time optimised solution produced by the genetic algorithm, a variance in expected values was observed. Based on the energy height solution optimised for time and maintaining the speeds and altitude bounds as established earlier, a solution that was (expected and) closest to the speed profile was set up. Table 4.3 provides a list of inputs used to create the expected profile and the relevant outputs (climb/cruise time and ranges) for comparison. Figure 4.10 shows the speed evolution plots of the three trajectories, while figure 4.11 shows the climb profiles of the expected trajectory and the time optimised trajectory by the GA.

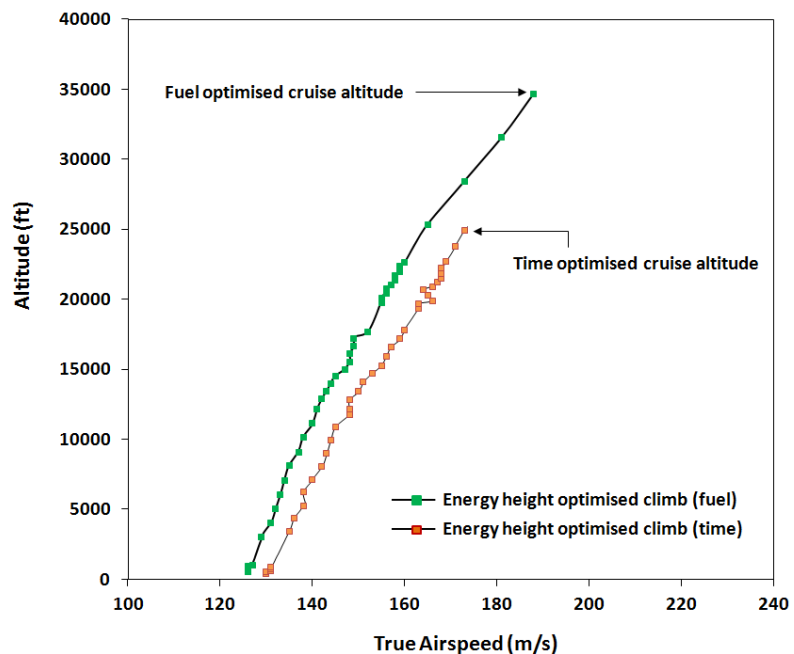


Fig 4.9 Speed evolution comparison for fuel and time by energy height method

Mission parameter	Mission time optimised trajectory GA	Expected trajectory based on EH method
Altitude2(climb) (ft)	2000	2000
Altitude3(climb) (ft)	10878	12000
Altitude4 (climb) (ft)	17000	17000
Climb speed CAS 2-3(kt)	275	250
Climb speed CAS 3-4(kt)	266	250
Climb speed CAS 4-Trns(kt)	300	250
Climb speed Mach Trns-5	0.65	0.65
Throttle setting (climb) 1-2 (%)	100	100
Throttle setting (climb) 2-3 (%)	100	100
Throttle setting (climb) 3-4 (%)	100	100
Throttle setting (climb) 4-Trns (%)	100	100
Throttle setting (climb) Trns-5 (%)	100	100
Cruise altitude(ft)	25000	25000
Cruise speed Mach	0.82	0.82
Climb segment time(min)	11.54	11.06
Climb segment range(nm)	60.4	50.5
Cruise segment time(min)	76.63	77.83
Cruise segment range(nm)	630.42	640.3
Mission time(min)	117.57	118.3

Table 4.4 Comparison between energy height optimised and GA optimised solution

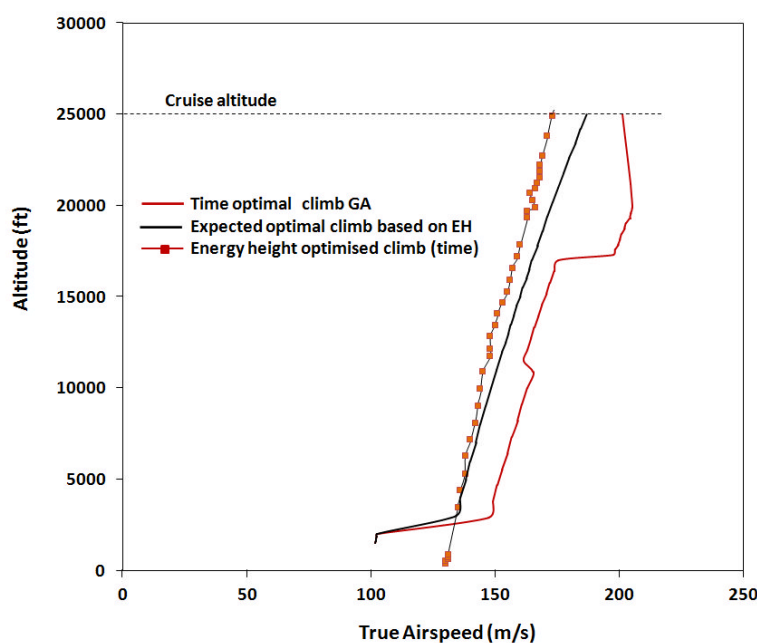


Fig 4.10 Speed evolution comparison for fuel and time by energy height method

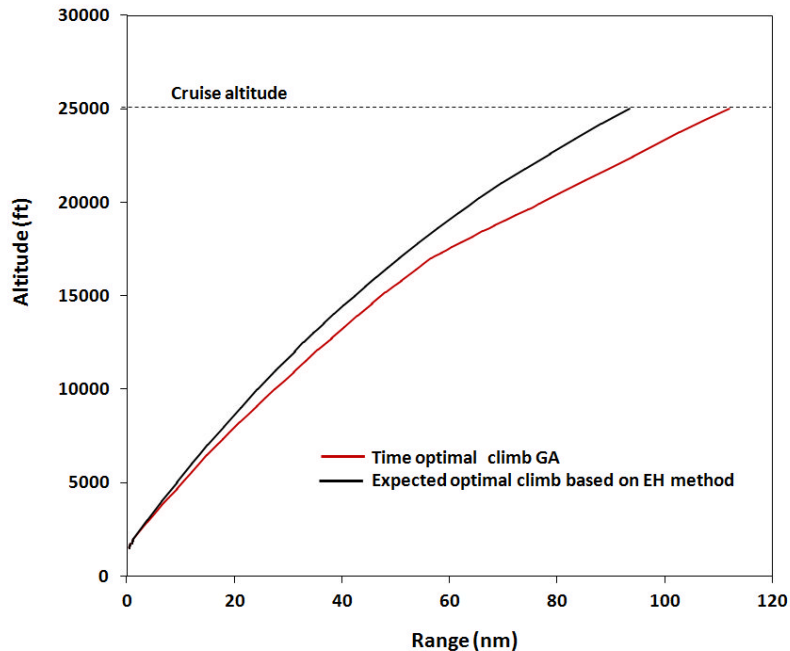


Fig 4.11 Climb profile comparison

The time optimal climb selected by GA uses predominantly higher speeds and hence is a shallower trajectory due to lower ROCs. However the climb segment based on EH method is set at lower speeds, resulting in higher ROCs, thus a steeper climb and hence a faster climb to reach the cruise altitude. As expected climb segment based on EH method is 28.8 sec (0.48 minutes as seen from the table 4.3) faster in terms of time to reach the cruise altitude, and hence is more optimal in terms of climb time. However, as for both the missions the aircraft is flown at the maximum cruise speed, it results in a longer time in the cruise segment (72 sec). Hence the benefit in time as gained in the climb segment diminishes in the cruise resulting in the total mission being longer by 43.8 sec or 0.62%. Even though the value seems insignificant GA optimisers are highly sensitive to such fine changes and hence the solution as demonstrated was selected.

This therefore leads to the conclusion that as the optimisation conducted, and as considered in this study, is based on the total mission and not an individual segment, the optimiser therefore selects variables such that an individual segment (as seen in the climb) may be suboptimal, with the global objective of optimising the whole mission.

Cruise segment: The variables selected for the cruise segment in a time optimised trajectory, have been done so in order to achieve the highest true airspeed possible, within the limits set for this segment. Therefore the mission is flown at 25000 ft (variable range 25000- 35000 ft) at the highest mach speed of 0.82.

## Discussion on the fuel time Pareto set

The fuel vs. time Pareto set of solutions is as indicated in figure 4.3. The plot demonstrates a distinct kink. An explanation to this observation may be provided by considering the variables used in arriving at the optimal solution. It has been proven in the past discussions that the cruise is a dominant segment of the complete trajectory. It was also demonstrated that the trajectory for minimum time is required to be flown at the lowest altitude (25000 ft) and highest speed (Mach 0.82), as per the variable bounds. However the minimum mission fuel trajectory required the cruise segment of the flight to be flown at the highest altitude (35000 ft) and at an optimal speed (Mach 0.67), based on the maximum specific air range, but closer to the lower bound for the allowable cruise speeds. Therefore a transition from the minimum time solution to the minimum fuel solution (as seen in the lower right corner and upper left corner respectively in figure 4.3) along the Pareto optimal front occurs by keeping the highest Mach speed constant while increasing the altitude for each corresponding solution. However once the highest altitude is reached as per the variable bounds, further improvement in mission fuel is then found by lowering the mach speed at this high altitude (35000 ft). The kink observed is attributed to this point at which the switchover occurs. This indicates that, as expected, increased altitude has greater effect in reducing fuel burn, while increase of speed has a similar on mission time.

### 4.4.1.2 Optimisation objectives- Operating cost and fuel

The next multi objective optimisation run was executed for minimisation of mission operating cost and mission fuel burn. The inputs for the operating cost model were as discussed in the earlier section describing the model setup. The Pareto optimal set of solutions derived from the optimisation run is as shown in figure 4.12.

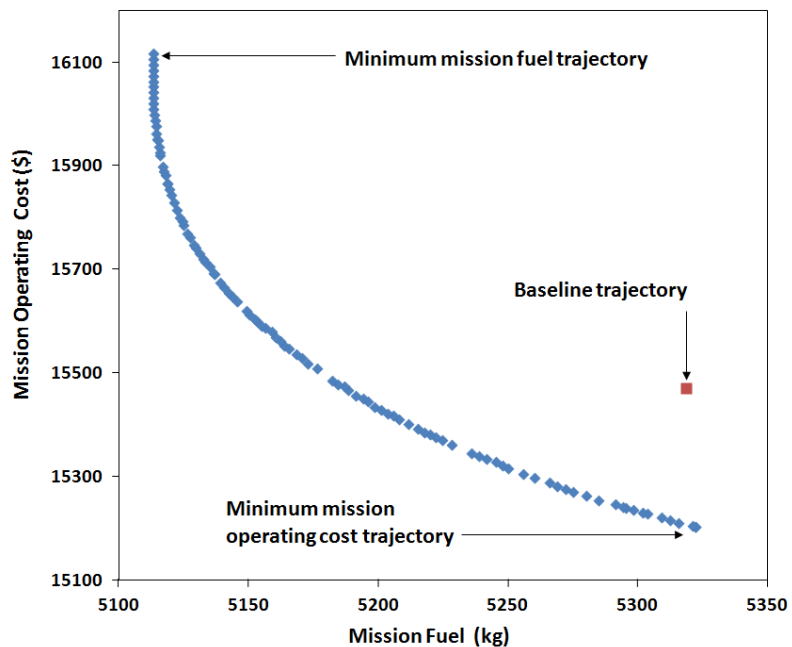


Fig 4.12 Objectives-mission fuel burn/mission operating cost Pareto optimal front

Climb segment: The variables of the climb segment of the trajectory optimised for operating cost (as seen in table 4.2) is a trade-off between the trajectory optimised for fuel and that for time. Figure 4.13 shows the speed evolution along the climb segment of the optimised trajectory and the intermediate speeds and altitudes selected is evident of the trade-off. However similar to other trajectories, with an aim of overall optimisation of the objective over the whole mission, the aircraft executes a similar profile wherein a low crossover altitude is selected to enable a low speed (Mach 0.65) and hence high ROC segment to cruise altitude.

Cruise segment: In the cruise segment the optimiser selects the highest altitude, for the lower fuel consumption benefit and the highest cruise speed (Mach 0.82) for reduction of flight time. This is again observed as a trade-off between the optimal fuel and time solutions discussed earlier.

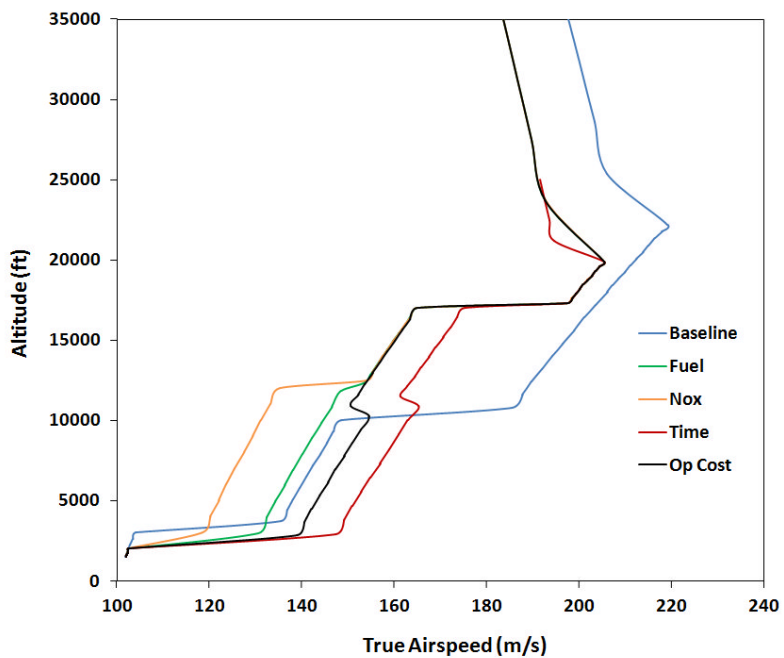


Fig 4.13 Speed evolution in climb segment of objective specific optimised trajectories

Key observations from the optimisation include the following

- In order to achieve a reduction of operating cost by 5.2%, there will be a necessary increase in overall mission fuel consumption by 4.1% but a reduction of mission time by 11%, in comparison with the optimal fuel burn trajectory.
- When compared with the time optimal solution, the operating cost optimal solution is more fuel efficient by 19% but takes 4.5% more time for the mission.
- The baseline trajectory is closer to the minimum operating cost trajectory when observed in reference to the Pareto optimal set, in figure 4.12.

The trajectory optimised for minimum operating cost is therefore opined to be a trade-off between the best fuel and time trajectories .It is therefore expected that, as the influence of either of these objectives increase( in terms of fuel(or emission) cost and/or cost of time of operation respectively), the actual optimal trajectory for minimal operating cost will vary.

#### 4.4.1.3 Optimisation objectives- NO<sub>x</sub> emission and fuel

The next objective to be optimised was the NO<sub>x</sub> emissions over the entire mission as a trade-off with mission fuel burn. Figure 4.14 and figure 4.15 shows the Pareto optimal set of trade off solutions between the optimal (low) NO<sub>x</sub> emission and mission fuel burn trajectories. The first noticeable aspect of the plot is that there the amount of NO<sub>x</sub> reduced by actually optimising the mission profile is significantly small (1.05 kg resulting in 1.6% saving).

Climb segment: NO<sub>x</sub> emissions being primarily attributed to high combustion temperatures the climb segment is predominantly flown at low throttle settings, as may be seen from table 4.2 (hence at 90%). However the segment between altitude 4 and crossover altitude of the climb is observed to be executed at 100% power and high speed. A mission was simulated by substituting the lowest throttle setting. It was found that by lowering the throttle setting by 10% (to 90% of maximum climb thrust) and maintaining the same speed, the ROC decreases by 32 to 34% thus taking a longer time of flight for the segment.

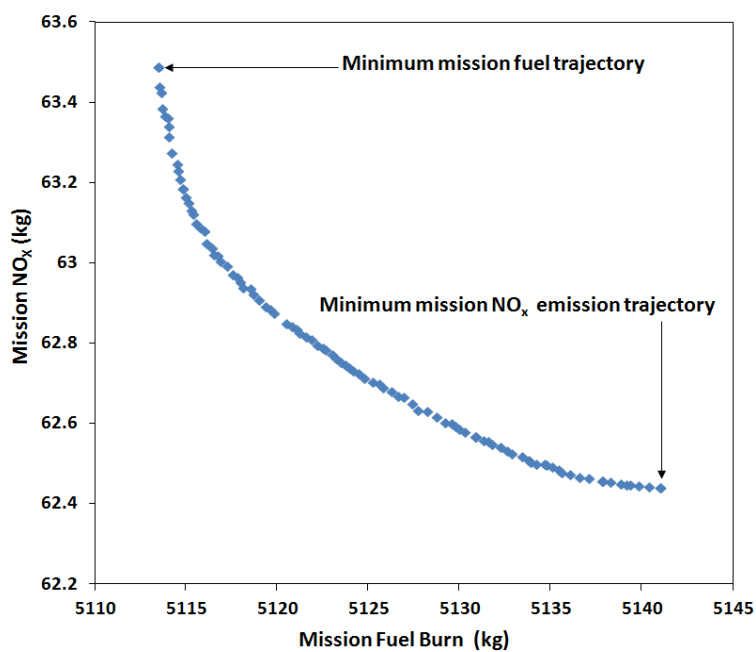


Fig 4.14 Objectives-mission fuel burn/mission NO<sub>x</sub> emission Pareto optimal front

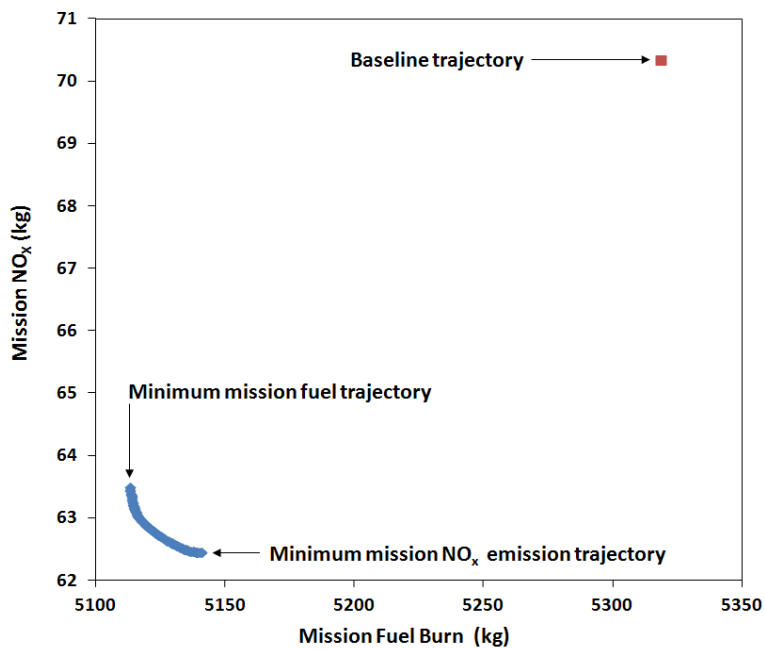


Fig 4.15 Mission fuel burn/mission NO<sub>x</sub> emission Pareto optimal front with baseline trajectory

A second effect noticed is that the SFC improves marginally (0.4-0.5%), and hence even though the EINO<sub>x</sub> decreases (by 11%), the overall effect is to decrease the NO<sub>x</sub> in the climb segment. A higher thrust in this segment also results in a shorter climb and hence longer cruise where the maximum benefit of the trajectory may be achieved. The overall effect results in an improvement of 0.3 %, it is therefore opined that as the optimiser strives to achieve a global optimum over the whole mission this result was selected.

Cruise segment: The altitude selected by the optimiser was the highest within the available range, while the mission was flown at the slowest speed (Mach 0.65). In cruise the thrust produced is assumed equal to the drag. As drag reduces the with an increase in altitude and reduction of speed the variables selected are considered to be accurately selected.

One notable observation from figure 4.15 is that the baseline solution produces a higher NO<sub>x</sub> emission, which may primarily attributed to the high speed required to economise the mission cost. The high speed results in a significantly higher drag, thus requiring higher thrusts and hence higher NO<sub>x</sub> emissions.

#### 4.4.2 CASE 2: MEDIUM RANGE (1614 NM)

The next case considered is a medium range route of 1614 nm (Stockholm to Lisbon). The route was selected, firstly to enable a comparison of the optimised trajectories with the previously discussed short-medium range case for the conventional objectives -mission fuel, mission time, mission operating cost and mission NO<sub>x</sub>, and secondly, this being a significantly longer mission provides an opportunity to study, as an environmental objective, optimised trajectories to avoid persistent contrails.

##### 4.4.2.1 ROUTE OPTIMISATION

The first part of this case considers only the conventional objectives and hence discusses the optimisation of mission fuel, mission time, mission operating cost and mission NO<sub>x</sub> over the route. Table 4.4 provides the values of the optimised objectives with a list of the selected mission parameters/ variables used by the optimiser, to arrive at the optimised solutions. Figures 4.16-4.19 indicate the Pareto optimal fronts for all the objectives investigated.

The key observation from the variables selected and the Pareto-optimal fronts are the following:

- a. The strategy used in optimising the climb and cruise was found to be the same as discussed for the previous case and hence a detailed justification of the optimised variables will not be undertaken.
- b. The fuel optimised trajectory when compared with the time optimised trajectory shows a reduction in fuel burn of 32.5%, however this is achieved at with a penalty in mission time of 17%. The cost of the mission is however is almost equal with the fuel optimised trajectory being cheaper by just 0.63%.
- c. The time optimised trajectory is evidently environmentally the worst trajectory as it produces significantly higher emissions than all other trajectories (32.5% higher CO<sub>2</sub> and up to 72% higher NO<sub>x</sub> than the fuel optimised trajectory)
- d. When the operating cost optimised trajectory is compared with the fuel optimised trajectory, it is observed the benefit in lower operating cost (6.8%) is achieved by burning 4.4% higher fuel. The lower operating cost is basically achieved by the trade-off of time and fuel (attributed to the high speed cruise) and hence an improvement of 13.1% in mission time. Environmentally it produces 4.4% higher CO<sub>2</sub> and 14% higher NO<sub>x</sub>.
- e. When compared with the rest of the trajectories, the NO<sub>x</sub> optimised trajectory may be considered to be the most environmentally beneficial. In comparison specifically to the fuel optimised solution, it 0.6% higher fuel burn it will produce 1.7% lower NO<sub>x</sub> emissions over the whole mission.

Mission parameter	Baseline mission	Mission fuel burn optimised trajectory	Mission time optimised trajectory	Mission Opn. cost optimised trajectory	Mission NO <sub>x</sub> optimised trajectory
Optimised variables					
Altitude2(climb) (ft)	3000	2000	2000	2000	2000
Altitude3(climb) (ft)	10000	11987	11106	11740	12000
Altitude4 (climb) (ft)	17000	16980	17000	17000	17000
Climb speed CAS 2-3(kt)	250	245	275	259	225
Climb speed CAS 3-4(kt)	300	251	269	254	250
Climb speed CAS 4-Trns(kt)	300	300	300	300	300
Climb speed Mach Trns-5	0.7	0.65	0.65	0.65	0.65
Throttle setting (climb) 1-2 (%)	100	100	100	100	90
Throttle setting (climb) 2-3 (%)	100	100	100	100	90
Throttle setting (climb) 3-4 (%)	100	100	100	100	90
Throttle setting (climb) 4-Trns (%)	100	100	100	100	100
Throttle setting (climb) Trns-5 (%)	100	100	100	100	90
Cruise altitude(ft)	35000	35000	25000	35000	35000
Cruise speed Mach	0.78	0.69	0.82	0.82	0.65
*Optimised objectives					
Mission fuel burn (kg)	9808	*9499	12586	9919	9559
Mission time (min)	234	259	*215	225	270
Mission operating cost(\$)	28558	30080	30191	*28025	31016
Mission NO <sub>x</sub> emission (kg)	125	114	196	130	*112

Table 4.5 Optimised variable climb and cruise segment parameters (1614 nm)

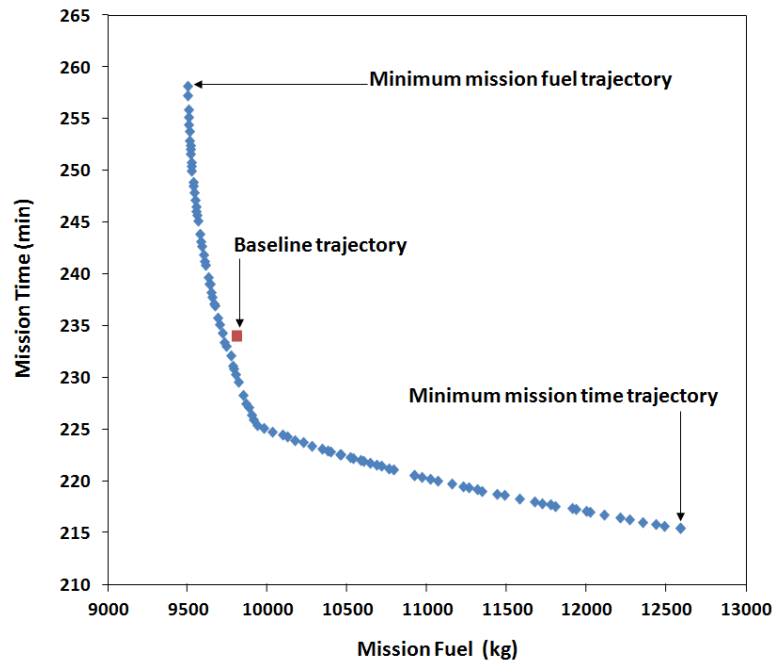


Fig 4.16 Objectives-mission fuel burn/mission time Pareto optimal front (1614 nm)

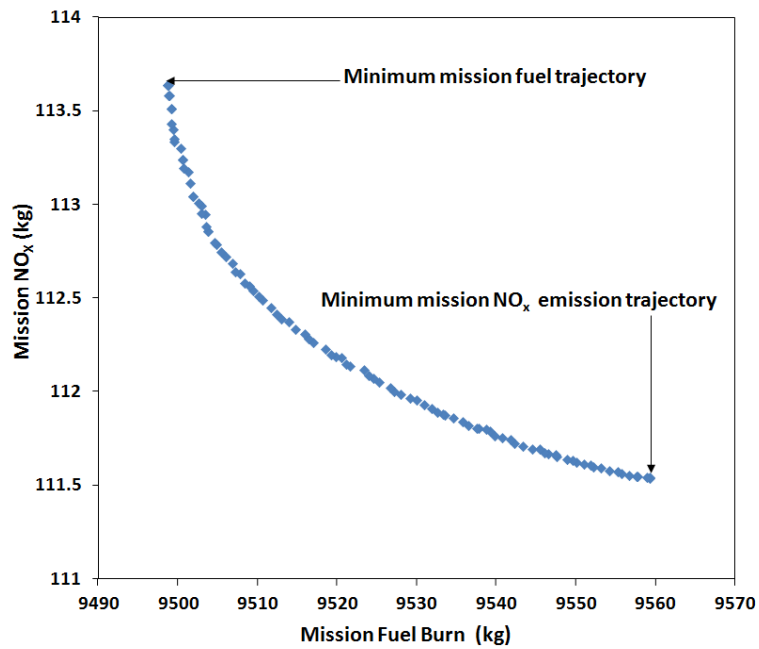


Fig 4.17 Objectives-mission fuel burn/mission  $\text{NO}_x$  emission Pareto optimal front (1614 nm)

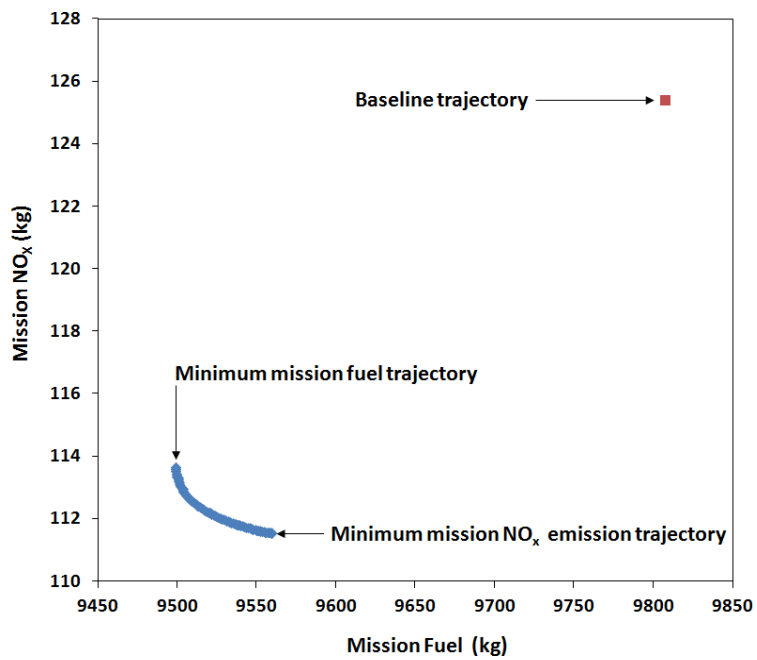


Fig 4.18 Mission fuel burn/mission  $\text{NO}_x$  emission Pareto optimal front with baseline trajectory (1614 nm)

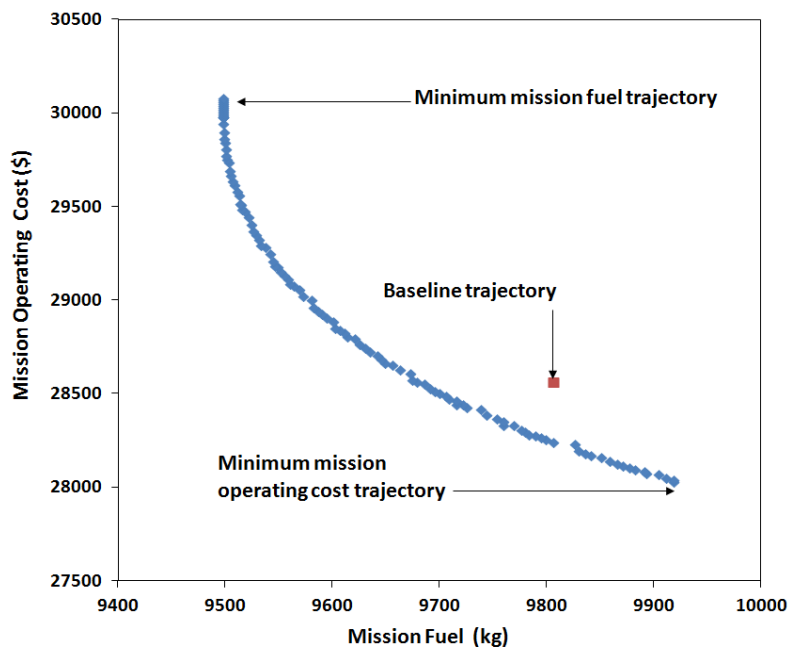


Fig 4.19 Objectives-mission fuel burn/mission operating cost emission Pareto optimal front (1614 nm)

#### 4.4.2.2 OPTIMISATION OBJECTIVES- PERSISTENT CONTRAILS AND FUEL BURN

As a preliminary step towards optimising aircraft trajectories to avoid forming contrails an analysis was undertaken within the scope of the research. The Contrail model used for the study has been essentially adapted from the Clean Sky project and the specifications of the same are as placed at Appendix B .The purpose of the study is primarily to enable preliminary estimation of the penalty in mission fuel burn and mission time that may be entailed by an aircraft trying to avoid contrail zones. This penalty once established is then used to further analyse the cost implications for various taxation policies and fuel price scenarios, which will follow in the next part of this study.

##### 4.4.2.2.1 Contrail Modelling

The contrail prediction model used is based on the methodology of Appleman and the Schumann definition of critical slope. The model requires a number of parameters which include the operational parameters of the engine and the atmospheric conditions (pressure, temperature and relative humidity). The model additionally also requires as an input the flight segment length, where contrails need to be predicted. [3.11]

As an output , for each of the segments considered, the model then predicts whether contrails will occur, if the contrails predicted are persistent or not and finally as a consolidated output the total length of persistent contrails produced in kilometres of persistent contrails. This output is then further used as an objective in a multidisciplinary optimisation framework.

For the purpose of the study and to introduce conditions for zone avoidance, the contrail model was set so that two separate contrails zones were formed, search zone lasting approximately 807 nm and hence each of the zones spread across one half of the entire mission. Depending on the engine exhaust conditions and operating parameters, the first zone forms contrails from 34000 ft and above, while the second zone starts forming contrails from a lower altitude of approximately 30000 ft. The reasoning for the set up was to study if the optimisation process was able to produce a trajectory with nil contrails formed by entirely avoiding the zones.

##### 4.4.2.2.2 Modification of the aircraft performance model

The previous trajectories for regular optimisation were all restricted to two variables - single cruise altitude and speed, with the cruise phase then being split into four equal segments. However in order to provide the optimiser with greater flexibility to modify the cruise segment of the trajectory to avoid contrails, the cruise module of the aircraft performance model was required to be restructured.

The final mission when setup, apart from the standard 12 variables in climb(as enumerated in table 4.1), enabled the optimiser to vary additionally nine variables in cruise, which essentially included 5 altitudes and fixed segment lengths and 4 speed (Mach) in between the altitudes. A schematic depicting the variables in the cruise segment of the trajectory is as shown in figure 4.20. The variable altitudes at cruise were allowed to vary between 35000 ft and 25000 ft, while the variable speeds were allowed to vary between Mach 0.65 and 0.82.

In the modified version of the model, in the cruise segment, when consecutive altitude variables are selected, depending on whether the next altitude is higher or lower than the previous one, the aircraft will be required to climb or descend accordingly. The climb and descent are done at the speed selected for the segment, however once the aircraft reaches the required altitude it cruises at that constant altitude till it reaches the next selected altitude in the cruise phase. Alternatively, if two consecutive altitudes happen to be at the same level then the aircraft executes a simple constant altitude cruise between them. This modification allows the aircraft to execute a stepped cruise when required.

Table 4.6 lists the variables selected for this optimisation, while figure 4.21 shows the Pareto optimal set of solutions depicting the trade-off between the mission fuel and the range of persistent contrail.

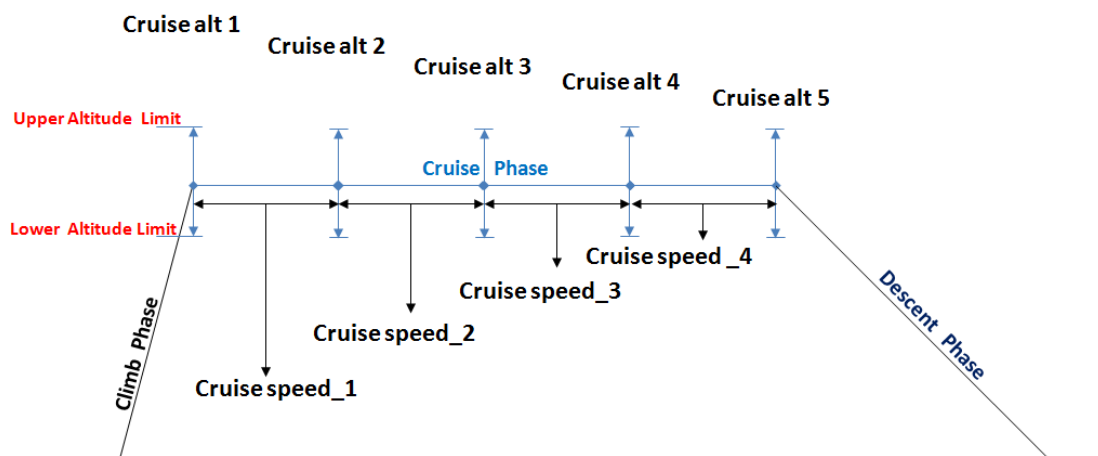


Fig 4.20 Schematic of modified cruise segment for minimum contrail optimisation

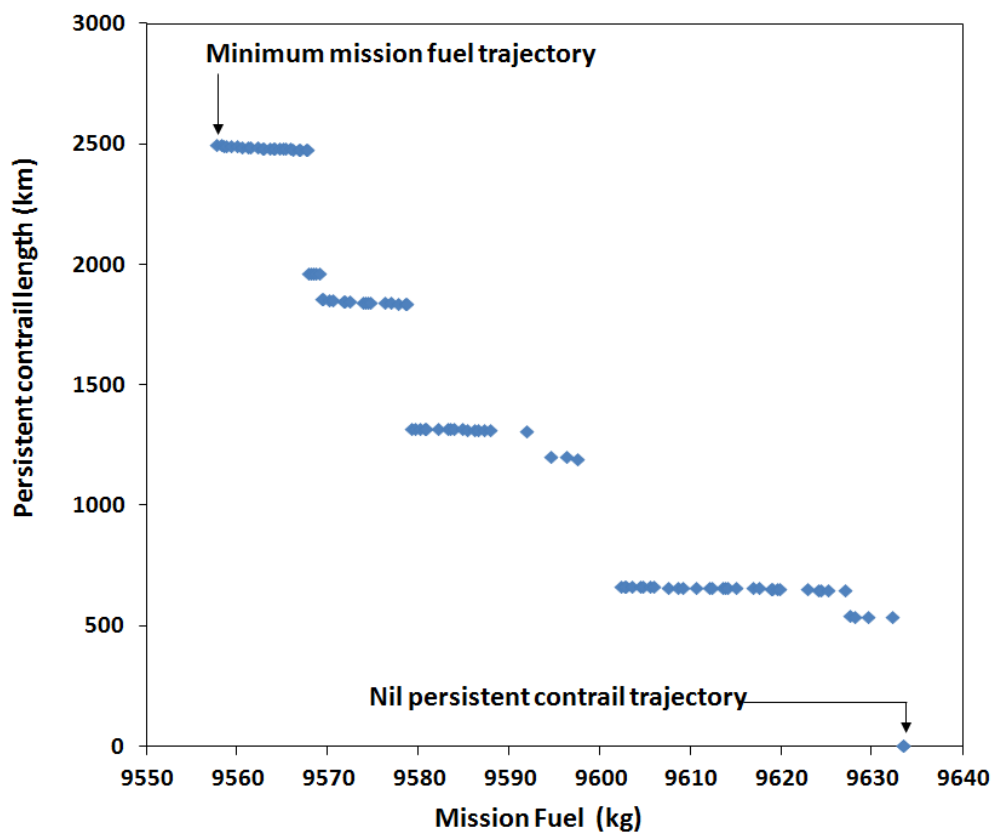


Fig 4.21 Objectives-mission fuel burn/range of persistent contrail Pareto optimal front  
(1614 nm)

Mission parameter	Minimum contrail optimised trajectory	Mission fuel burn optimised trajectory
<b>Optimised variables</b>		
Altitude2(climb) (ft)	2003	2000
Altitude3(climb) (ft)	16900	11987
Altitude4 (climb) (ft)	11380	16980
Climb speed CAS 2-3(kt)	245	249
Climb speed CAS 3-4(kt)	250	250
Climb speed CAS 4-Trns(kt)	250	250
Climb speed Mach Trns-5	0.65	0.65
Throttle setting (climb) 1-2 (%)	90	90
Throttle setting (climb) 2-3 (%)	100	100
Throttle setting (climb) 3-4 (%)	100	100
Throttle setting (climb) 4-Trns (%)	100	100
Throttle setting (climb) Trns-5 (%)	100	100
Cruise altitude 1(ft)	25002	25000
Cruise altitude 2(ft)	34420	34999
Cruise altitude 3(ft)	34419	35000
Cruise altitude 4(ft)	33644	35000
Cruise altitude 5(ft)	33625	35000
Cruise speed 1 -2(Mach)	0.69	0.71
Cruise speed 2-3(Mach)	0.68	0.69
Cruise speed 3-4 (Mach)	0.66	0.68
Cruise speed 4-5 (Mach)	0.65	0.67
<b>*Optimised objectives</b>		
Persistent contrail (nm)	*0	1347
Mission Fuel burn (kg)	9634	*9558

Table 4.6 Optimised variables for minimum fuel and contrail optimisation

#### **4.4.2.2.3      Optimal trajectory for minimum contrail generation**

Observation of the Pareto optimal set in figure 4.21 indicates a noticeably discontinued the front. However the optimiser has found a trajectory which produces no persistent contrail. The data when assessed indicated altitudes and the associated atmospheric conditions were primarily responsible for the production of contrails.

The discontinuity is attributed to the model of the cruise segment and the flexibility allowed in selecting the altitudes. Figures (4.22 and 4.23) show the two trajectories for minimum fuel burn and minimum contrails. It is seen that the minimum fuel burn trajectory has its cruise phase entirely in the persistent contrail formation zone, whereas the nil persistent contrail trajectory follows a stepped cruise allowing it to avoid the contrail formation zone entirely.

In order to explain the discontinuity figure 4.24 illustrates a magnified view of some of the intermediate trajectories selected from the Pareto optimal set (figure 4.23). When the altitudes selected for the trajectories are plotted(as seen in the fig 4.24) it is observed that depending on the altitudes selected, the aircraft is restricted to necessarily flying through one, two, three or four segments which may fall within the contrail zone. The higher the number of segments it flies through within the contrail zone, correspondingly higher will be the range of persistent contrails formed and hence the Pareto optimal front has distinct 4 sets of solution forming contrails with the fifth completely avoiding the zone and hence producing nil contrails.

#### **4.4.2.2.4      Optimal trajectory for minimum fuel burn**

The solution found for the minimum fuel burn trajectory in this case was found to be similar to the optimal fuel trajectory found earlier for the same mission, with a constant altitude and speed at cruise. However with the change in the problem setup for this optimisation, some of the key observations are as follows:

- a. The final mission fuel burn in this case is found to be 9558 kg, which was 0.6% higher than the previously found result. This may be attributed to the stochastic behaviour of the optimiser and discretisation of data within the aircraft model.
- b. The climb segment for both trajectories was found to be very similar (as seen in the figure 4.26). This is attributed to the fact that the optimisation being multi objective and the contrail formation occurs only at high altitudes, the variables at lower altitudes are selected with a bias towards fuel optimisation.
- c. For the minimum fuel burn trajectory, the speeds at cruise were observed to continuously reduce through the segment. As discussed in the previous case for minimum fuel consumption at cruise and hence for the condition of maximum specific air range, the ratio  $\frac{c\beta}{V}$  has to be minimum. Through the cruise phase, the weight  $W$  of the aircraft is continuously reducing. If  $V_e^*$  is the

equivalent airspeed of the aircraft for minimum  $\beta$  in straight and level flight, then as  $V_e^* \propto W^{1/2}$  as the weight reduces,  $V_e$  will have to reduce and hence the Mach speed of the aircraft, if allowed to (as in this case), reduces.

- d. The fuel burn for trajectory for contrail avoidance and that found for minimum fuel burn was observed to be marginal with the trajectory for contrail avoidance being 0.8 % higher.

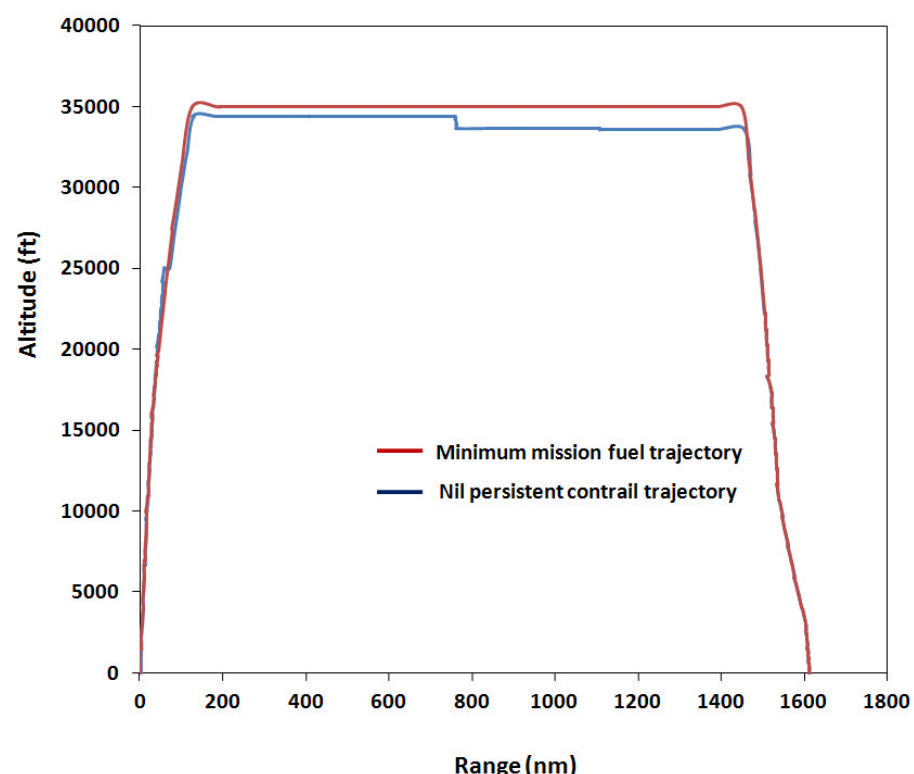


Fig 4.22 Mission profiles of minimum mission fuel burn and persistent contrail trajectories

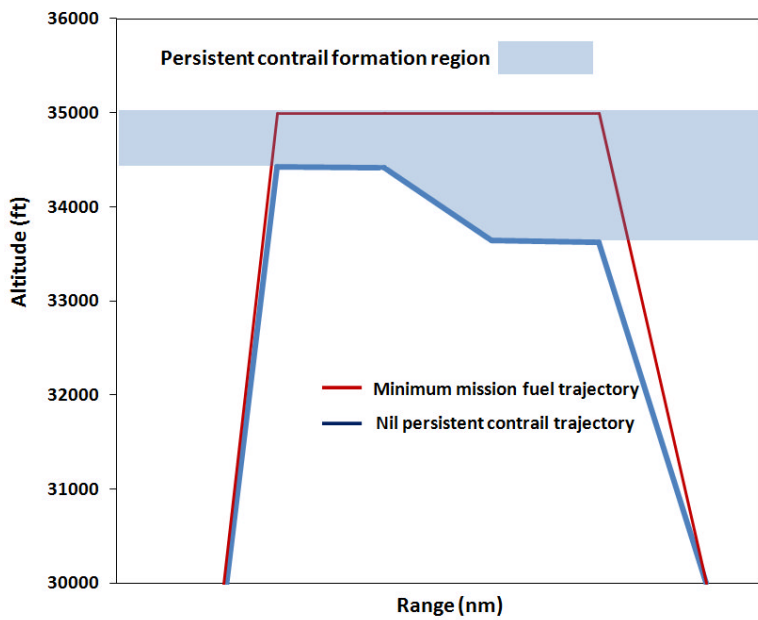


Fig 4.23 Cruise flight profiles of minimum mission fuel burn and persistent contrail trajectories

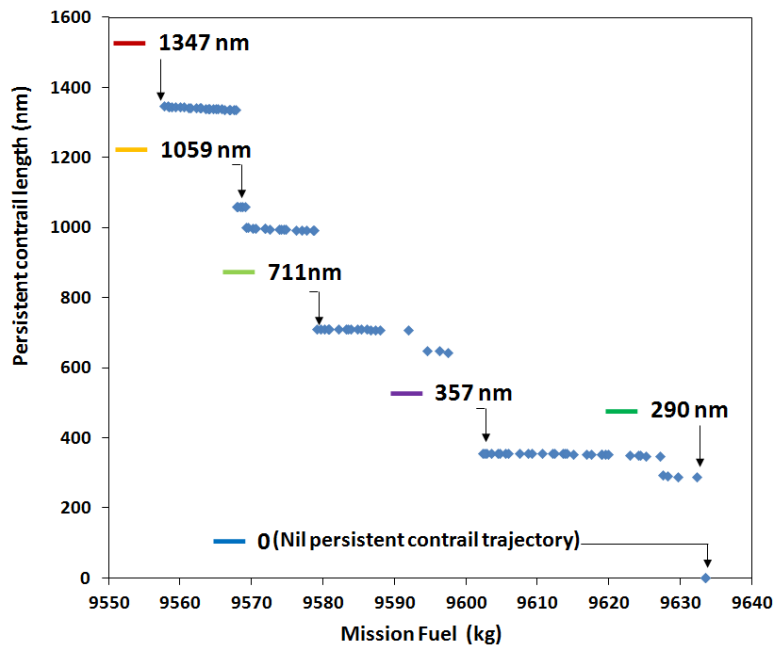


Fig 4.24 Mission fuel burn/range of persistent contrail Pareto optimal front –selected missions for discussions

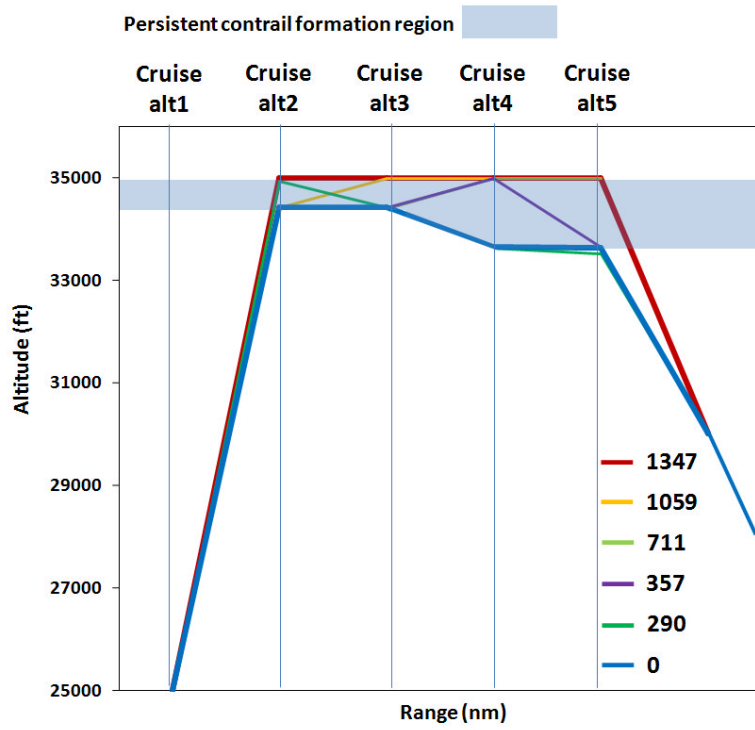


Fig 4.25 Cruise flight profiles of selected missions

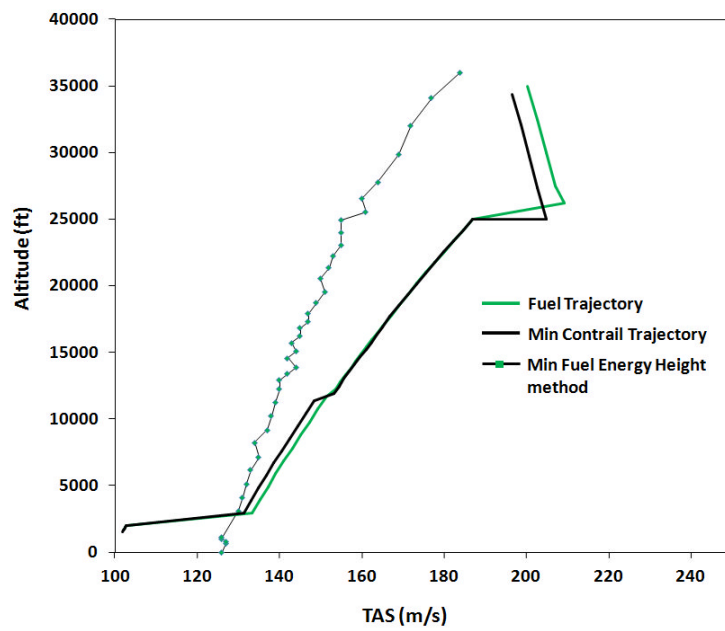


Fig 4.26 Speed profile of optimised trajectories compared with energy height optimised climb

#### 4.4.3 CASE 3: SHORT RANGE (227 NM)

The final case considered is for a short range route of 227 nm (Paris to Geneva). The route was selected, as in the previous case, to enable a comparison of the optimised trajectories with the previously discussed cases for the conventional objectives -mission fuel, mission time, mission operating cost and mission NO<sub>x</sub>.

##### 4.4.3.1 ROUTE OPTIMISATION

Table 4.7 provides the values of the optimised objectives with a list of the selected mission parameters/ variables used by the optimiser, to arrive at the optimised solutions. Figures 4.23 and 4.24 indicate the Pareto optimal fronts for the objectives investigated.

The key observation from the variables selected and the Pareto-optimal fronts are the following:

- a. Mission Fuel optimised trajectory: Figure 4.22 shows the mission profiles of the optimised trajectories. The fuel optimised trajectory was interestingly a cruise climb- trajectory in the climb phase, with no constant altitude cruise segment, which then followed by a long descent. Similar to the previous cases though, the speed schedule in climb at lower altitudes is close to the lower limits and hence as would be required by a fuel optimal energy height climb. The power settings are also predominantly high except in the last phase where the aircraft keeps to lower speeds and lower thrust setting (Mach speed 0.65 and 94% thrust). However, the main strategy used in this solution is that the aircraft tries to maximise the time in descent, making it the longest of the flight phase (57% of the total time) thereby ensuring the aircraft remains in lowest power setting(flight idle condition) and hence minimise the total fuel burn. It may also be noted that the aircraft does not reach the maximum altitude limit, but instead adjusts the climb phase adequately to achieve a significant (and optimal) height 30575 ft, to immediately begin descent. The selection of the height is attributed to the global objective of minimising the fuel for the complete mission.
- b. Mission time optimised trajectory: The lower altitude bound for this case was set at 18000 ft. The time optimised trajectory as in the previous cases is dependent mainly on maximising the time benefit in the cruise segment. The aircraft is therefore observed to initially use high speeds in climb (265-275 kt CAS), at high power settings followed by a typical low altitude high speed cruise phase (18000 ft at Mach speed 0.82).

One key observation from the fuel time optimisation routine is the shape of the Pareto optimal front (figure 4.23). It does not have the typical kink, as

observed for longer range missions. This is primarily attributed to the absence of a constant altitude cruise segment. As discussed in an earlier section the in order, the best fuel benefit is obtained at a high altitude and at this altitude the fuel consumption significantly improves as the speed reduces and approaches the optimal speed for maximum specific range. For minimising time however, the lower the altitude, the greater the benefit in achieving a high true air speed (TAS) for the same Mach speed. In this case as the cruise phase is practically absent so the effect of seeing the improvement of fuel consumption with a lowering of speed at the highest altitude is not present

- c. Mission NO<sub>x</sub> optimised trajectory: The mission NO<sub>x</sub> optimised trajectory is focussed on optimising the NO<sub>x</sub> over the whole mission. Evidently the climb is observed to execute at lower speed and predominantly lower power settings. Similar to the fuel optimisation, the aircraft climbs to 28124 ft and then commences descent at lower power settings (flight idle condition). When the mission is analysed it is found that the aircraft spends 54% of the flight in descent but produces only 26% of the NO<sub>x</sub> in this phase. The trajectory expends just 0.8% more in terms of fuel burn and takes 1.7% longer for the mission fuel, to save up to 2.1% in terms of mission NO<sub>x</sub>. The values even though small may have a significant impact on selection of trajectories in terms of operating cost.
- d. Mission operating cost optimised trajectory: The time optimised trajectory was found to be the minimum operating cost trajectory and hence is not shown separately. For this short range case the maintenance cost, based on the assumptions as previously discussed in section 4.6.1, was recalculated utilising the correlation. Therefore based on an average flight time of the baseline mission of 47 minutes, the maintenance cost per flying hour for the case was set at US\$ 439.2 and US\$ 1219 for the engine(per unit) and airframe respectively. Hence, assuming an absence of any carbon taxation and a fuel price of US\$ 1098/mt as in the previous cases resulted in the time dependant variables in the operating cost to have a stronger influence, thereby resulting in the time optimised solution to be the least in terms of operating cost.

Mission parameter	Baseline mission	Mission fuel burn optimised trajectory	Mission time optimised trajectory	Mission NO <sub>x</sub> optimised trajectory
<b>Optimised variables</b>				
Altitude2(climb) (ft)	3000	2000	2000	2000
Altitude3(climb) (ft)	1000 0	8058	9120	8116
Altitude4 (climb) (ft)	1700 0	17000	13000	16992
Climb speed CAS 2-3(kt)	250	244	275	224
Climb speed CAS 3-4(kt)	300	235	272	217
Climb speed CAS 4-Trns(kt)	300	300	264	300
Climb speed Mach Trns-5	0.65	0.65	0.77	0.65
Throttle setting (climb) 1-2 (%)	100	100	100	90
Throttle setting (climb) 2-3 (%)	100	100	100	90
Throttle setting (climb) 3-4 (%)	100	100	100	90
Throttle setting (climb) 4-Trns (%)	100	100	100	100
Throttle setting (climb) Trns-5 (%)	100	94	97	90
Cruise altitude(ft)	2800 0	30575	18000	28124
Cruise speed Mach	0.65	0.65	0.82	0.65
<b>*Optimised objectives</b>				
Mission fuel burn (kg)	2045	*2020	2321	2037
Mission time (min)	47.10	47.21	*42.5	48.02
Mission operating cost(\$)	8867	8855	8522	8988
Mission NO <sub>x</sub> emission (kg)	29.7	28.9	38.8	*28.3

Table 4.7 Optimised variable climb and cruise segment parameters (227 nm)

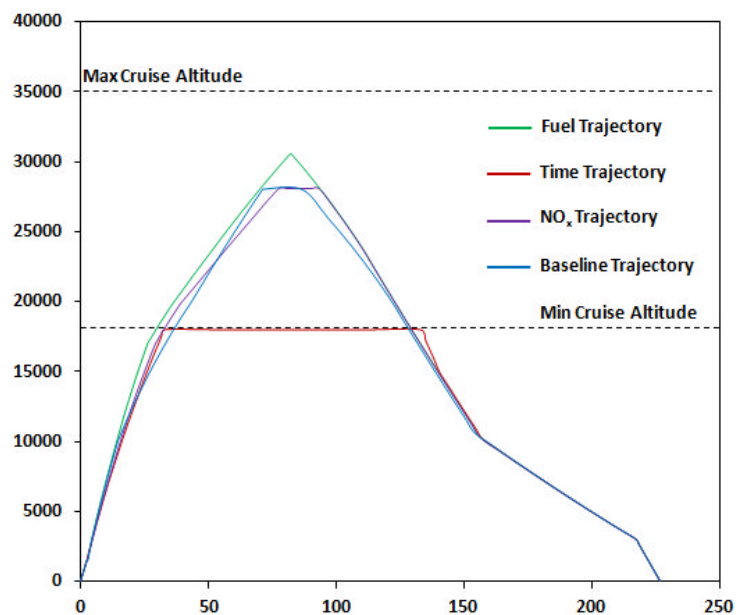


Fig 4.22 Mission profiles of optimised trajectories

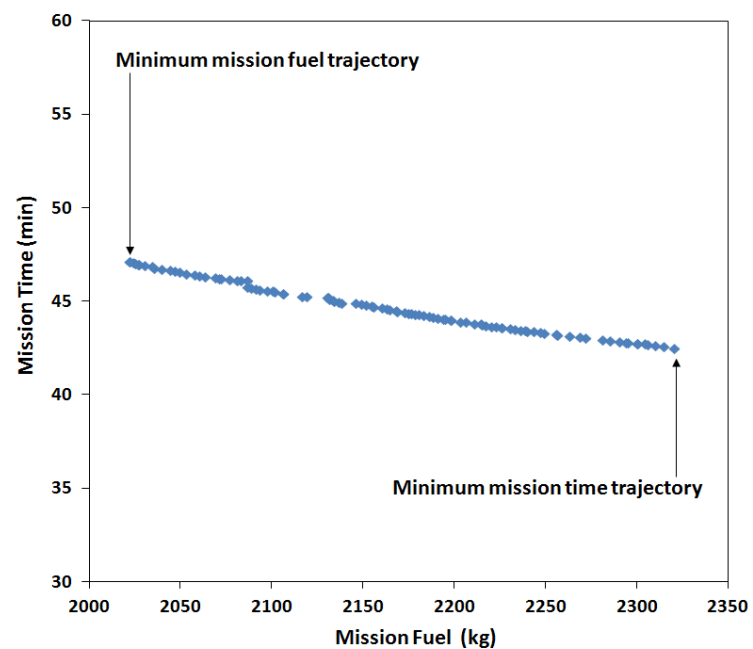


Fig 4.23 Objectives-mission fuel burn/mission time Pareto optimal front (227 nm)

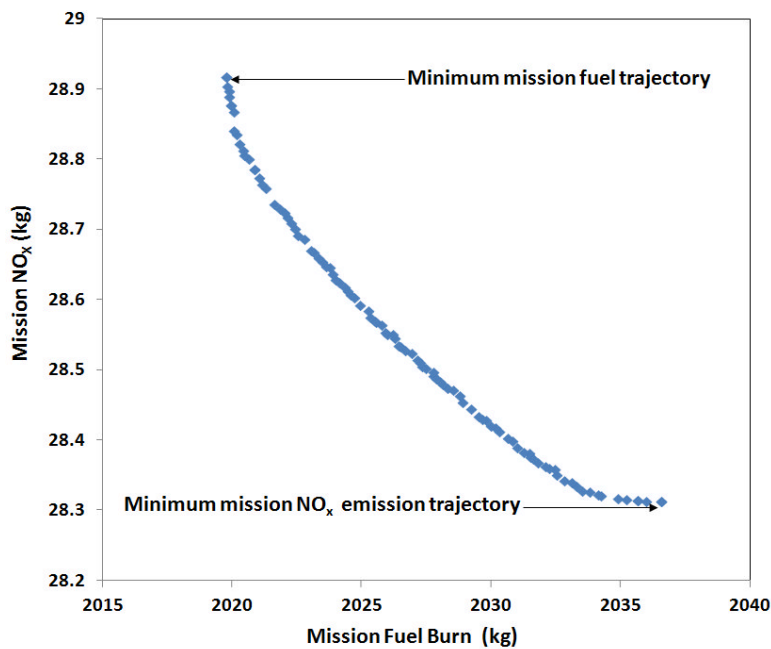


Fig 4.24 Objectives-mission fuel burn/mission NO<sub>x</sub> Pareto optimal front (227 nm)

#### 4.5 CONCLUSIONS

This chapter dealt with the multi objective optimisation of flight trajectories of a civil aircraft to minimise various objectives which included- mission time, mission fuel, mission emissions which included CO<sub>2</sub>, NO<sub>x</sub> and Contrails (medium range flight) and mission operating cost. It began with the description of the flight phases, with a brief look at the specificities and the constraints in currently flown flight trajectories. This was followed by aircraft trajectory definition as set for the optimisation cases.

In the previous chapter, the modelling of a short to medium range single aisle narrow body aircraft equipped with two turbofan engines was discussed. Based on the application of this aircraft, and typical of the aircraft type, three missions were selected as illustrative case studies. The missions were short range (227 nm), short-medium range (815 nm) and medium range (1614 nm), each simulated at 100% load factor (maximum passenger capacity) and hence a specific payload. For each of the case studies, based on the payload and range selected, and information available on the payload-range chart of the aircraft, missions were simulated to establish a baseline for each of the objectives.

Based on the values achieved for each of the objectives, trajectory optimisation was then used to improve the values of each of the objectives. The key observations from the case studies are as follows:

- a. The baseline trajectories are found to be a compromise between the optimised fuel and time trajectories and close to the minimum operating cost

trajectories, for the short-medium range and medium range trajectories. For the short range trajectory it was found to lie closer to the minimum fuel burn trajectory.

- b. In each of the missions the objectives were minimised over the whole mission and hence resulted in some of the segments being flown suboptimal in order to achieve a global (minimisation) objective. This was proved by the implementation of the Energy Height Method of optimisation, which demonstrated that to achieve the minimisation of the objective (fuel and time) in climb, the aircraft was required to execute the climb at slower speeds. However in order to achieve a global minimisation of the objective and to achieve a faster climb to cruise (where the maximum benefit could be achieved), a part of the climb segment was executed at higher speeds.
- c. Fuel optimised trajectories: For the short-medium and medium range missions, the fuel optimised trajectories are all primarily 'high altitude, optimal cruise mach speed (MRC)' trajectories. The cruise altitude selected was the highest with the cruise speed selected to achieve the maximum range, and hence with a fixed range, minimum fuel burn. However when the speed at cruise is allowed to vary, optimisation for fuel burn requires a reduction of speed to maintain optimality, to compensate for reduction in weight (due to consumption of fuel). For the short range mission, the optimal trajectory was a cruise-climb followed by a long descent (and hence 57% of the mission at low/descent idle power settings).
- d. Time optimised trajectories: All time optimised missions were typically 'low cruise altitude, high mach speed' trajectories. As expected due to sub optimal performance conditions and high TETs through the mission, each of the trajectories was found to consume 10% to 17% more fuel and produce 34 to 72% higher NO<sub>x</sub> emissions than the optimised fuel burn trajectories. Hence the time optimised trajectories may be deemed to be environmentally detrimental.
- e. NO<sub>x</sub> emission optimised trajectories: The NO<sub>x</sub> emission optimised trajectories are similar to the fuel burn trajectories, but primarily flown at the lowest power setting and slower speeds. This caused mission times to be longer and hence demonstrated marginally higher fuel burn (0.5% to 0.82%) than the trajectories optimised for fuel burn. However in terms of cost, these trajectories were found to be 5.4 to 10.6% more expensive in terms of operating cost than the optimal operating cost trajectories.

f. Optimal operating cost trajectory: The operating cost for all the cases was calculated for a 'Business As Usual' scenario, wherein the fuel price was set at US\$ 1098/ mt and absence of any carbon tax. For the short-medium and medium missions, the optimal operating cost trajectories were found to be a trade-off between fuel burn and mission time. They were found to be typically 'high cruise altitude, high mach speed' trajectories, which essentially achieves the fuel efficiency of high altitudes and benefit of lesser mission time by virtue of the high speed at cruise. For the short range mission, higher hourly maintenance costs result in the time dependant variables having an overall higher influence and hence the time optimised trajectory is observed to be the least in terms of operating cost.

Consequently, the trajectories for minimum operating cost were found to be far from optimal environmentally. When compared to mission optimised for minimum fuel burn, the fuel burn (and consequently CO<sub>2</sub> emissions) and NO<sub>x</sub> emissions for the mission were found to be 4% to 14% and 11% to 34.5% higher respectively.

g. Trajectory optimised for minimum persistent contrail prediction: A preliminary attempt was made in optimising a trajectory so that the aircraft flies the mission producing minimum persistent contrail by enabling the range of produced persistent contrails as the objective. The optimisation exercise successfully found a trajectory of producing nil contrails by essentially flying a stepped trajectory. It however consumed 0.8% fuel owing to a marginal decrease in altitude at cruise when compared with the fuel optimal trajectory.

A few decades ago aircraft were able commence en-route climb and reach the cruising altitude in a simple and efficient continuous climb, and further were able to fly at an efficient altitudes and speeds. Currently, however, it is known and as brought out in the introduction to this chapter, aircraft are not able to fly environmentally optimal trajectories owing primarily to air traffic and operational constraints. Reference [2.26] has indicated that, just improvements in efficiency of air traffic management can help aviation reduce its environmental foot print and further goes on to state that by doing so civil aviation can reduce its CO<sub>2</sub> emissions by approximately 50 million tons, between the period of 2008 and 2020.

The analysis of the baseline trajectories demonstrate that trajectories when executed with continuous climb/ descent segments and cruise segment at optimal altitudes are 1.3% to 4% higher in fuel burn than the trajectories optimised specifically for fuel burn. Hence, it is opined, that if these trajectories were to be adhered to, will result in reduction of the aviation industry's current environmental impact and therefore any further optimisation of parameters will enable aircraft fly even more optimally.

The study also however demonstrates that in order to achieve these efficiencies, aircraft will require a significantly higher flexibility in terms of continuous speed and altitude evolution at various phases in flight and hence an enhanced air traffic management system can indeed help improve the environmental impact of civil aviation.

## 5. POLICY ASSESSMENTS - OPTIMISED OPERATIONS

### 5.1 INTRODUCTION

As discussed in the literature review, from 1<sup>st</sup> January 2012 The European Commission has fully included aviation in the EU's emissions trading system (EU ETS). This will therefore impose a cap on CO<sub>2</sub> emissions from flights operating to and from EU airports. Like any other industrial unit airlines will receive tradable allowances to allow for CO<sub>2</sub> emissions from their flights per year.

Taxation policy and policy tools (emission trading, emission related charges/taxes) are aimed at specific environmental goals and hence optimal solutions with respect to certain objectives will need to be compared in a consistent manner to ascertain their suitability as a viable solution to reduce emissions. As profitability is one of the important factors necessary for sustainability in the aviation industry, the effect of taxation policies on profitability will also need to be considered.

Airline operators currently operate the aircraft as per the Cost Index methodology wherein, based on the cost of fuel and the cost of time (of operation), and given an allowed flexibility of the prevailing air traffic management, the airline selects the most optimal flight plan in terms of cost.

The previous section has demonstrated that optimisation of trajectories with respect to specific environmental objectives can result in environmental gain and reduction of fuel burn. However it was also observed that, the solution which cost least in terms of operating cost had resulted in higher fuel burn (and consequently CO<sub>2</sub> emissions), NO<sub>x</sub> emissions and contrails.

The operating cost when calculated for the previous cases included only the cost of fuel. However with environmental taxation legislations actively debated, the question then arises, that if the optimised trajectories were implementable, at what level of taxation will an airline shift its operations towards more environmental friendly trajectories and what implications will this have on the operating cost of the airline operator.

The policy module introduced in this chapter may then be effectively used to apply a varying taxation policy to better understand the effect on operating costs for the optimal set of trajectories found and analytically deduce the taxation rate at which an airline may be driven towards a more environmental friendly solution. Alternatively in terms of planning it also allows a decision maker to assess the suitability of an environmentally optimised solution, in terms of cost viability under a particular fuel price and CO<sub>2</sub> taxation policy.

The next part of this study therefore looks at the profitability of these trajectories under various CO<sub>2</sub> taxation policies that may be applied. By application of the a policy assessment

module, the study aims to demonstrate a methodology that will enable a policy maker to assess these solutions in terms of operating cost, in comparison with the reference trajectory and against all the optimal solutions in a consistent manner.

## 5.2 THE POLICY MODULE

The framework used for this study is as indicated in figure 5.1. An input module enables specifying a range of policy scenarios in terms of emission taxes and fuel prices and the policy model creates a set of graphical plots(contour and line plots), which display the inter-relationship between three objectives. In this case study the three objectives that are considered are time, fuel (correspondingly the CO<sub>2</sub> emissions) and the operating cost.

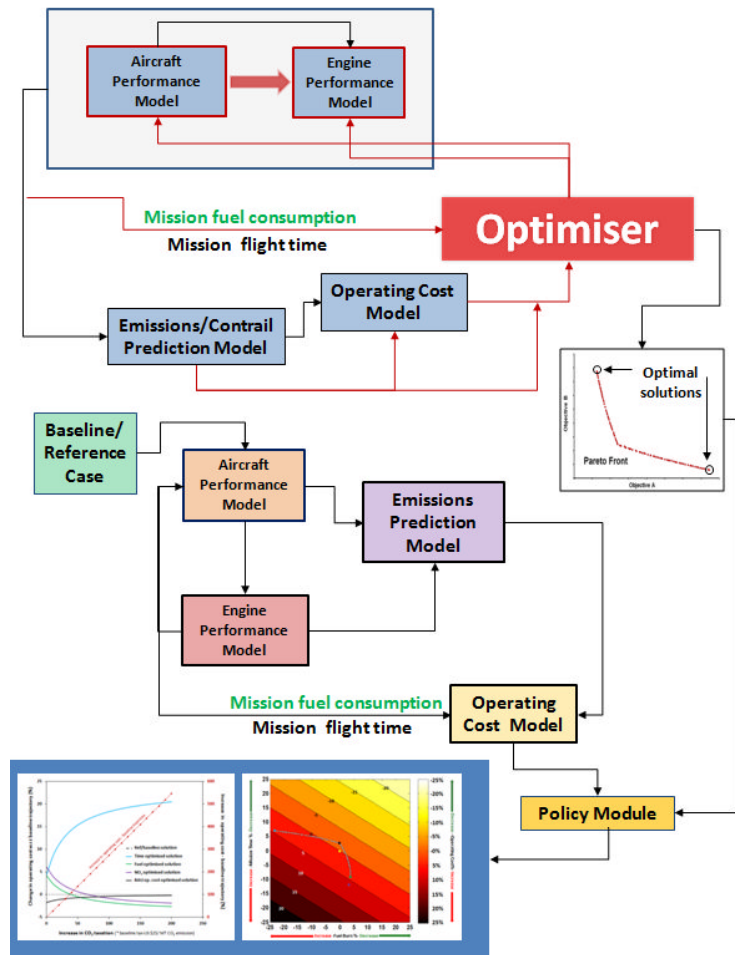


Fig 5.1 Framework for environmental policy analysis on optimised operations

### 5.2.1 THE CONTOUR PLOT

The contour plot generated (as may illustratively be seen in figure 5.2), is a 2-D plot which shows the 1-D curves on which a plotted quantity Z is a constant. These curves are defined by

$$Z(X, Y) = Z_j \text{ where } j = 1, 2, \dots N_c, \text{ where } N_c \text{ is the number of contours that are plotted}$$

Each point on a contour plot will signify a trajectory/solution with its position as function of X, Y and Z

$X = \% \text{ change in } \mathbf{Fuel} \text{ from reference trajectory}$

$Y = \% \text{ change in } \mathbf{Time} \text{ from reference trajectory}$

$Z = \% \text{ change in } \mathbf{Operating Cost} \text{ from reference trajectory}$

where  $\text{Operating cost} = f\{\text{Time}, \text{Fuel}, \text{Emission Tax}\}$

Therefore as emission taxation and/or an increase in fuel price is applied, the contour effectively captures the effect of change in influence of fuel/ emission dependant cost on the overall mission cost. The relative change in operating cost, with respect to the baseline solution is then reflected by the point on the contour at which the plotted solutions lie. The plot is useful in identifying, for any particular scenario of fuel price and CO<sub>2</sub> tax, the set of optimal solutions that have relatively higher economic viability in comparison to the baseline solution.

### 5.2.2 THE LINE PLOT

The line plot enables analysing the relative (percentage) increase in operating cost, in reference to the baseline trajectory, for a particular fuel price and varying CO<sub>2</sub> taxation rates. This plot is therefore useful in identifying the 'break even' taxation rate for any particular optimal solution, while indicating the magnitude of increase in overall operating cost.

## 5.3 CASE STUDIES

As illustrative examples, the three cases for which trajectories were optimised previously will now be considered under various fuel price and carbon taxation scenarios.

### 5.3.1 CASE STUDY: SHORT-MEDIUM RANGE (815 NM)

The optimised trajectories for this case were discussed in detail in section 4.4.1. Table 5.1 provides summarised data (and previously established in table 4.3) for relative difference in mission time and mission fuel burn, with reference to the baseline trajectory for this case.

#### 5.3.1.1 The contour plot

Based on the relative difference of fuel burn and mission time, in comparison to baseline trajectory (as tabulated), figure 5.2A is a scatter plot which graphically represents the relative performance of all the solutions in the fuel- time Pareto set and the optimised solutions found for this case. This plot is then used to create the cost contour for the Business as usual scenario (fuel price of US\$ 1098 per metric ton and no CO<sub>2</sub> tax – figure 5.2B). The key observations from the plot are as follows:

- a. Evidently from prior analysis, the trajectory optimised for operating cost is seen to be the best trajectory on the contour plot. All the solutions above the 0 line on the contour plot will have higher economic viability than the baseline solution. The plot is also able to indicate the set of these solutions from the Pareto optimal set.
- b. The mission fuel burn optimal solution and mission time optimal solution, in reference to baseline solution, lie on iso-cost contour lines very close to each other (4.2% and 4.4% respectively)
- c. The NO<sub>x</sub> optimised solution owing to higher fuel burn and mission time it is the least cost effective solution.

			$\Delta \%$ ( baseline mission as ref)		
	Mission fuel burn (kg)	Mission time (min)	Mission fuel burn %	Mission time%	Mission cost%
Baseline mission	5319	127	0.0	0.0	0.0
Fuel optimised mission	5114	138	3.9% decrease	9.0% increase	4.2% increase
Time optimised mission	6565	118	23.4% increase	7.2% decrease	4.4% increase
Operating cost optimised mission	5322	123	0.1% increase	2.8% decrease	-1.7% decrease
NO <sub>x</sub> optimised mission	5141	142	3.3% decrease	11.8% increase	6.1% increase

Table 5.1 Performance data of optimised trajectories in reference to baseline mission (815 nm)

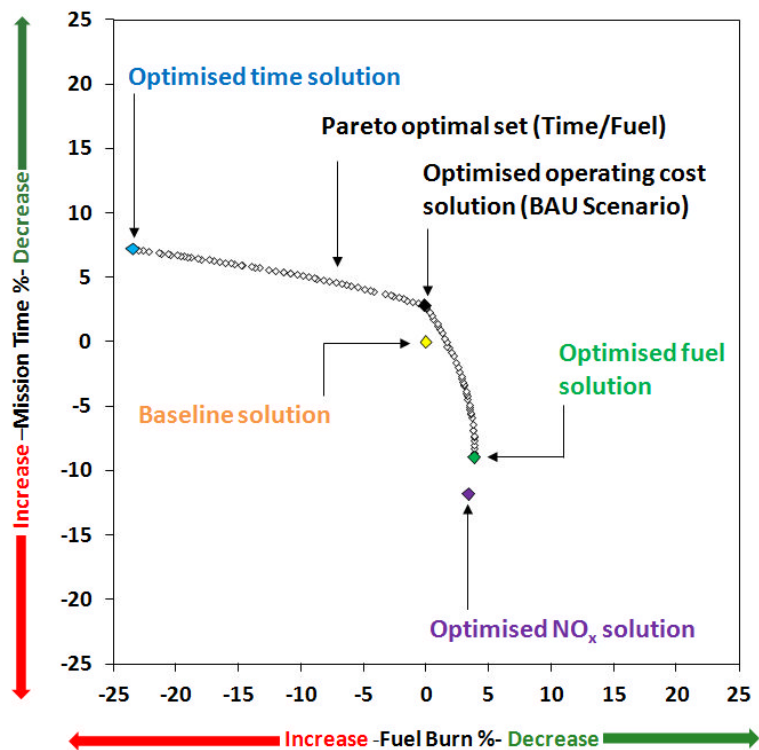


Fig 5.2A Plotted performance data of optimised trajectories in reference to baseline mission (815 nm)

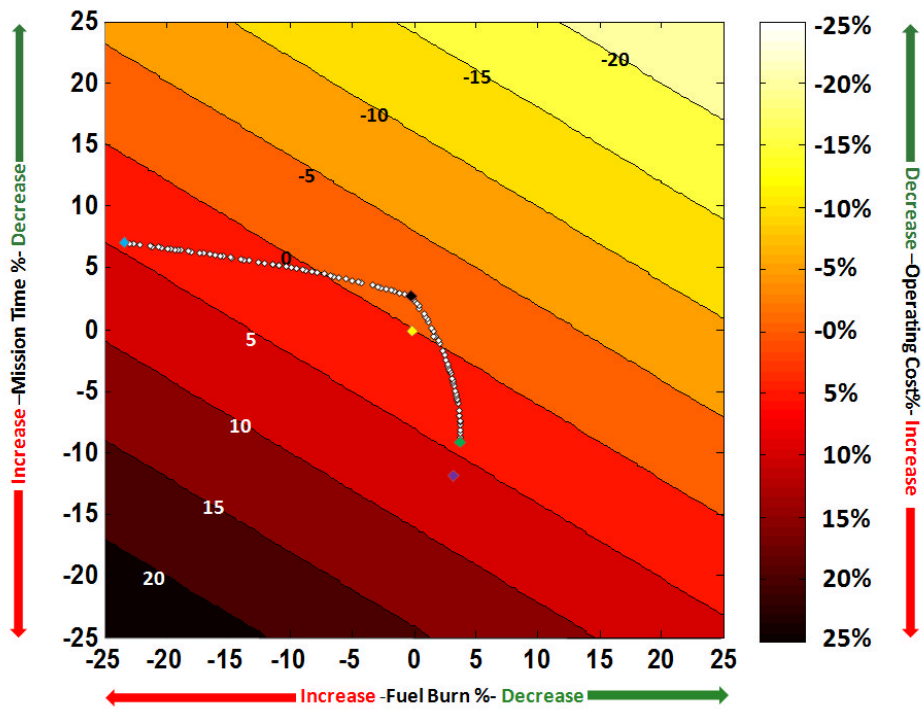


Fig 5.2B Cost contour plot (815 nm); scenario- fuel price US\$ 1098/mt and nil CO<sub>2</sub> taxation

### 5.3.1.2 The line plot

The line plot shown in figure 5.3, assumes the fuel price scenario of US \$ 1098 and a baseline environmental tax of US \$ 25/metric ton CO<sub>2</sub> emissions\*. The primary y axis (in percentage and on left) reflects the change in operating cost of an optimised trajectory with reference to the baseline trajectory, for a changing taxation scenario. The taxation scenario, as applied on the x axis, ranges from nil taxation (at 0) to 200 times the baseline environmental tax. The secondary y axis (in percentage and on right) indicates the overall increase in operating cost due to the taxation, in comparison to the BAU scenario (indicated by the linearly increasing red line).

As the taxation increases, in each of the curves it may be noted that the influence of the time dependant variables in the overall cost, reduces. This causes a decay in the curve thus causing it to become nearly parallel to the x axis.

The line plot is then useful in understanding the various effects of applying the baseline environmental tax (US \$ 25/ mt of CO<sub>2</sub> emissions), and then increasing it.

Utilising the line plot, the effect of applying the baseline environmental tax is first examined. The relevant segment of the line plot (figure 5.3) when magnified (figure 5.4) shows that in terms of cost and in comparison to the baseline trajectory, the optimal fuel solution (marked as A) and improves from 4.2% to 4%), the optimal time solution (marked as B) is more

\*It may be noted that for any assumed fuel price, an application of US \$ 25/metric ton CO<sub>2</sub> emissions will effectively increase the price of a ton of consumed fuel by US \$ 79.5

expensive and shifts from 4.4% to 4.9%), while the baseline solution increases overall by approximately 2.8% (marked as C) from the no emission taxation scenario.

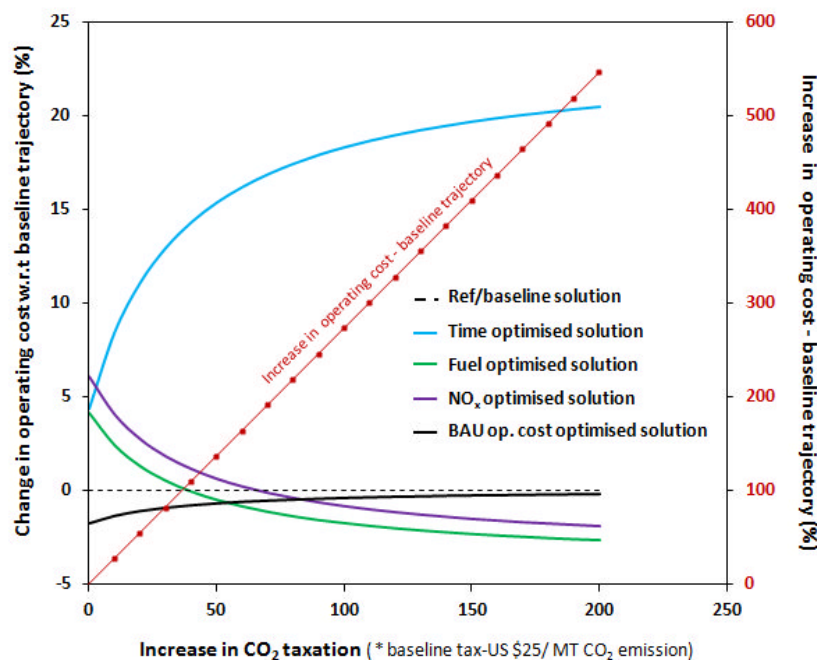


Fig 5.3 Line plot (815 nm); scenario- fuel price US\$ 1098/mt

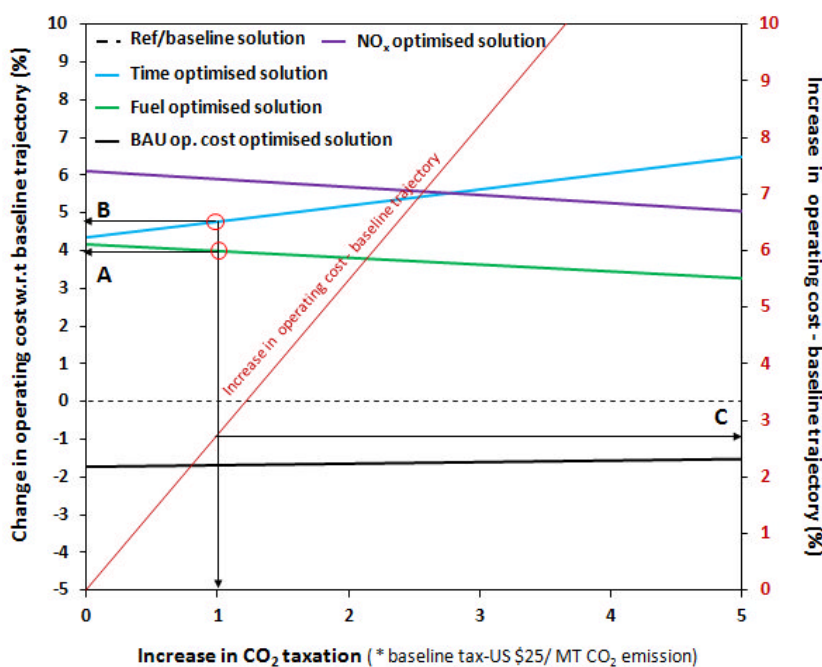


Fig 5.4 Line plot (815 nm); scenario- fuel price US\$ 1098/mt (magnified for illustration)

### 5.3.1.3 Establishing the cross-over taxation rate

From table 5.1, it is observed that the optimal solution reducing mission fuel burn, when compared with the baseline solution, enables a saving of 205 kg of fuel per mission, which is effectively 0.65 tons of CO<sub>2</sub> emission and hence environmentally beneficial. However when no emission tax is applied, it will not be the preferred operational solution as it is 4.2% more expensive than the baseline solution. If we were to then consider the optimal fuel burn solution against the optimal operating cost solution in the nil taxation scenario, it can be seen that flying the optimal operating cost trajectory will result in a higher fuel burn (209 kg resulting in 0.66 tons of CO<sub>2</sub>), but cost 6% lesser.

The pertinent question that then arises is- what would be the tax rate required to effectively render a trajectory optimised for lower CO<sub>2</sub> emissions (and hence the fuel optimised solution) more preferred, in terms of cost? The line plot may then be used to establish the taxation rates at which the cost of flying the fuel optimised solution will be equal to the operating cost of the baseline solution and the minimum operating cost solution in the nil taxation scenarios.

Figure 5.5 shows the section of the line plot (un-shaded region), which is further magnified in figure 5.6 to essentially focus on the region of the plot where the optimal fuel trajectory cost curve may be observed to cross-over the curves of baseline solution (indicated with arrows marked A) and the minimum operating cost solution(indicated with arrows marked B).

It may be seen in figure 5.6, in order for the minimum fuel burn solution cost to be equal to the cost of the baseline solution , the CO<sub>2</sub> tax will require to be 40 times the reference environmental tax (of US \$ 25/metric ton CO<sub>2</sub>emissions), thus increasing to \$1000 /metric ton CO<sub>2</sub> emissions. This would in turn result in the increase of the overall operating cost of the baseline solution, in comparison to current cost in a BAU scenario by 109%, thereby effectively doubling the cost of operation.

When further compared with the minimum operating cost solution, it is found that in order for the minimum fuel burn solution to be equal in cost, the emission tax will have to be increased by 55 times the reference environment tax, thereby increasing it to \$1375/ metric ton CO<sub>2</sub> emission. This would then result in the increase of the overall operating cost, in comparison to current cost in a BAU scenario, by 150%.

Figure 5.7 and 5.8, show the contour plots generated after applying a \$1000 and \$1375/ mt emission. They evidently demonstrate the fuel optimal solution lying on the same iso-cost contour as those of the baseline solution and minimal operating cost solution respectively, thus validating the inference made from the line plot.

The baseline solution, as discussed earlier has been established from analysis of the payload range chart and is used as pivotal point for the analysis. This reference point is however susceptible to change based on the preference of the user of this methodology. But the

optimal trajectory for minimum operating cost on the other hand, will be a unique point for a particular fuel price and emission tax. Therefore as may be seen in this study, depending on the influence of the time variables and fuel/ emission dependant variables, the operating cost solution will be observed to shift along the time vs. fuel Pareto optimal set. An illustration of this shift is seen the contour plots in figures 5.7 and 5.8

As minimising operating cost is always the priority of an airline operator, the taxation rate at which the minimum fuel burn solution cost line crosses the initially established minimum operating cost solution will essentially be the least taxation required for the impetus of operations to shift to environmentally beneficial fuel optimised trajectory. This taxation rate will be referred to as the High Environmental Awareness (HEA) taxation rate, as only in an extreme scenario, critical environmental requirements will take precedence and such a high taxation rate may require to be enforced. As identified in this study the HEA taxation rate will be US\$ 1325 \$/ mt of CO<sub>2</sub> emissions (or 55 times the baseline emission tax of 25\$/ mt of CO<sub>2</sub> emissions)

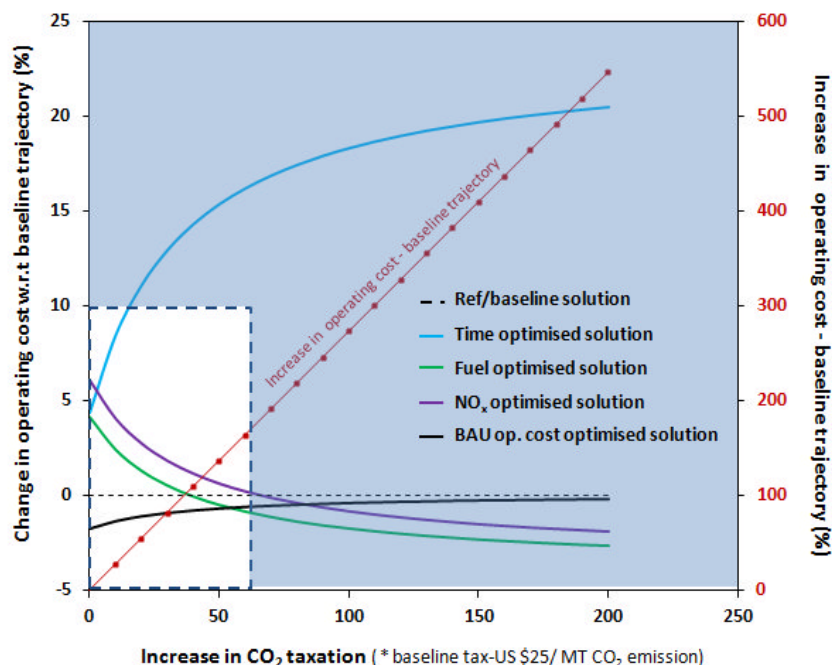


Fig 5.5 Line plot (815 nm); scenario- fuel price US\$ 1098/mt  
(un-shaded area indicated for illustration of cross-over point)

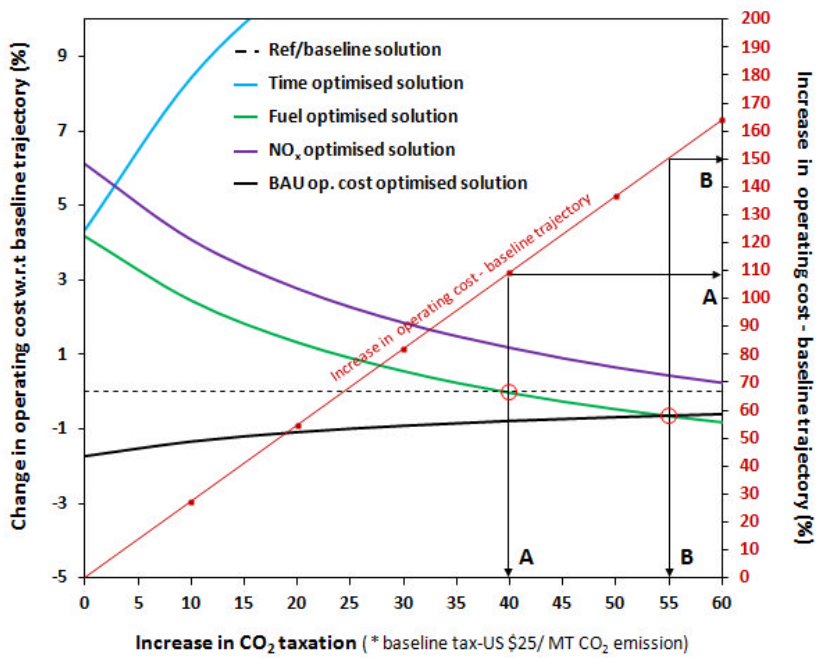


Fig 5.6 Line plot (815 nm); scenario- fuel price US\$ 1098/mt (un-shaded area magnified for illustration of cross-over point)

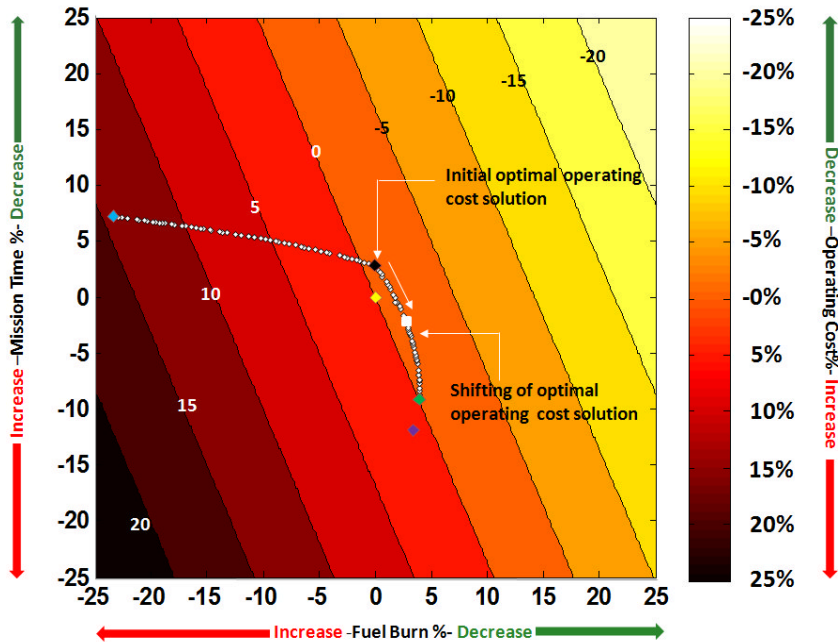


Fig 5.7 Cost contour plot (815 nm); scenario- fuel price US\$ 1098/mt and CO<sub>2</sub> taxation (US\$ 1000/ton CO<sub>2</sub> emission)

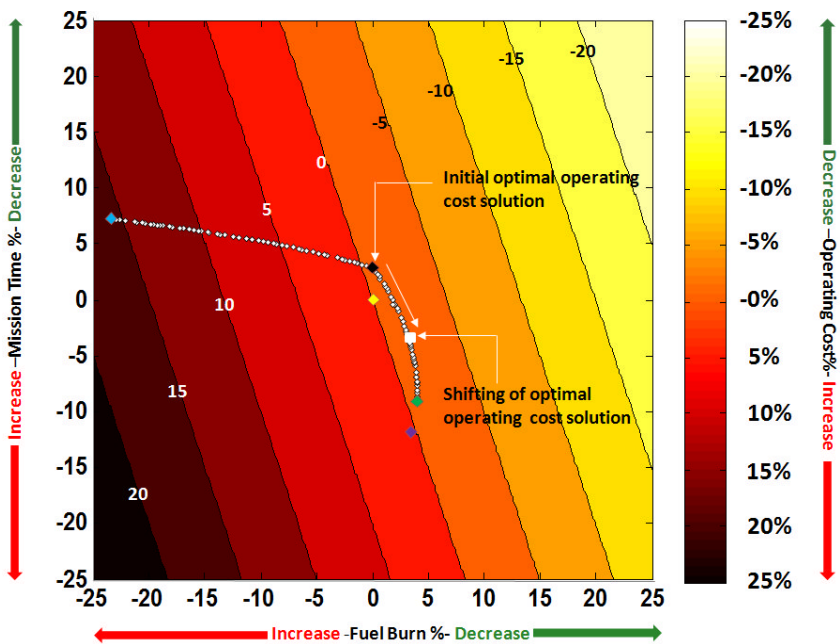


Fig 5.8 Cost contour plot (815 nm); scenario- fuel price US\$ 1098/mt and CO<sub>2</sub> taxation (US\$ 1375/mt CO<sub>2</sub> emission)

#### 5.3.1.4 Increase in fuel price

The previous case assumed a fuel price of US \$ 1098/ mt. However using the method described, a further analysis can be made to analyse the effect an increase of fuel price will have on the High Environmental Awareness (HEA) taxation rate, to enable the shifting of preference from the optimal operating cost solution to a fuel burn optimised solution. Line plots in figures 5.9, 5.10 and 5.11, show the reconfigured curves for an increase in fuel price by 10%, 25% and 50% respectively. The analysis shows that for the increase in fuel price considered, the High Environmental Awareness (HEA) taxation rate will still require to be significantly high (54, 52 and 48 times the baseline emission tax respectively).

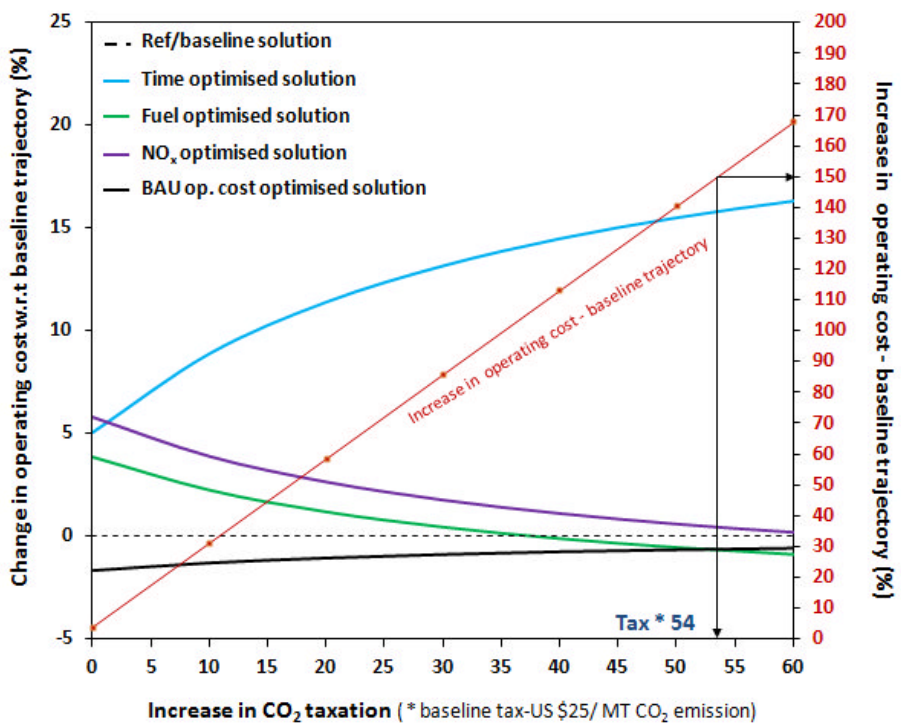


Fig 5.9 Line plot (815 nm); scenario- 10% increase in fuel price (US\$ 1207/mt)

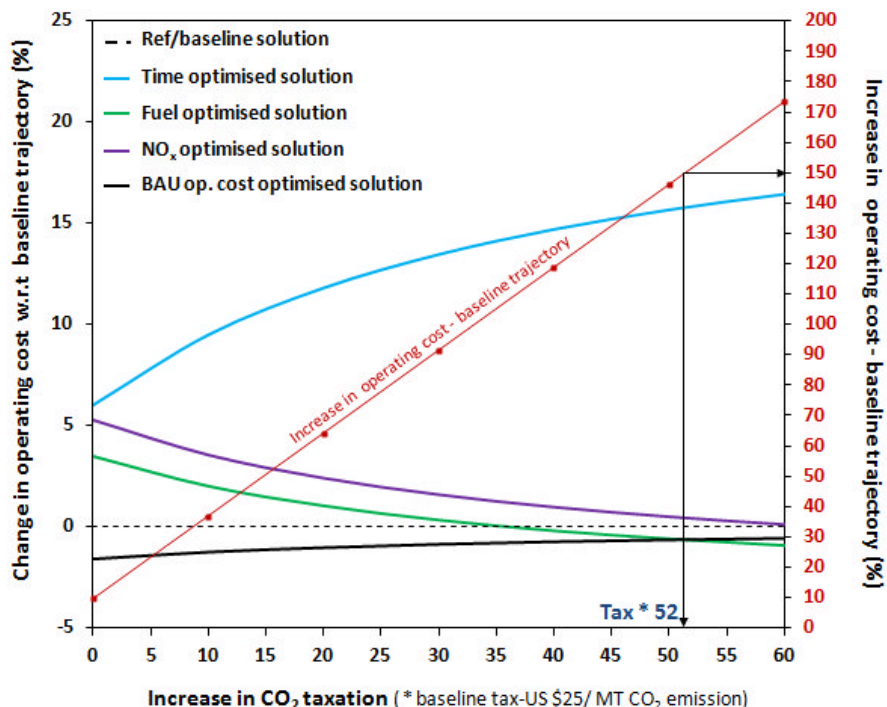


Fig 5.10 Line plot (815 nm); scenario- 25% increase in fuel price (US\$ 1372.5/mt)

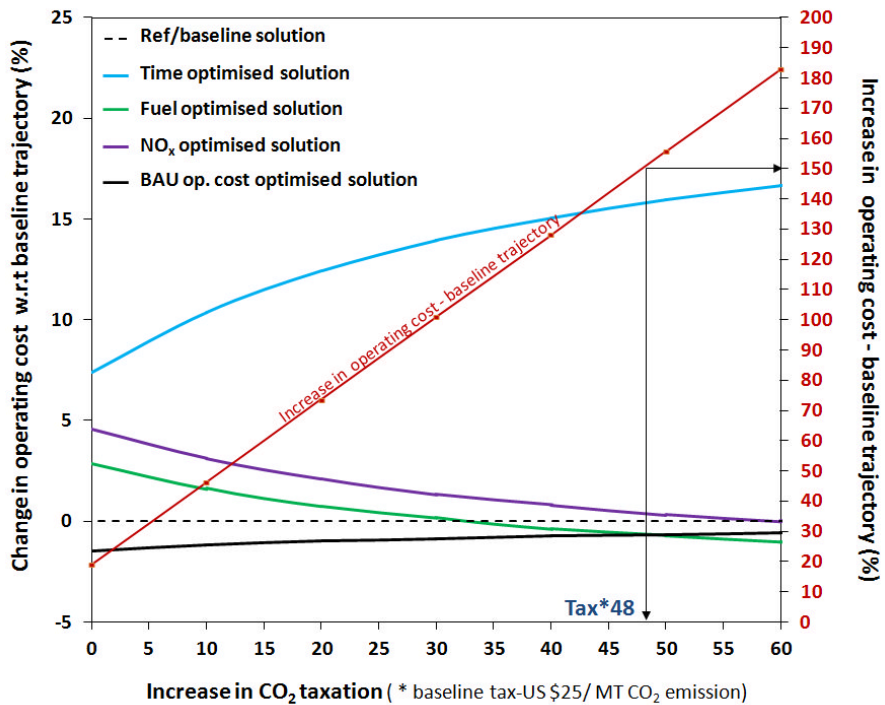


Fig 5.11 Line plot (815 nm); scenario- 50% increase in fuel price (US\$ 1647/mt)

### 5.3.2 CASE STUDY: SHORT RANGE (227 NM)

The next case to be assessed is the short range. The optimised trajectories for this case were discussed in detail in section 4.4.3. Table 5.2 provides summarised data (and previously established in table 4.3) for relative difference in mission time and mission fuel burn, with reference to the baseline trajectory for this case.

Based on the relative difference of fuel burn and mission time, in comparison to baseline trajectory (as tabulated), figure 5.12 is a scatter plot which graphically represents the relative performance of all the solutions in the fuel- time Pareto set and the optimised solutions found for this case. This plot is then used to create the cost contour for the Business as usual scenario (fuel price of US\$ 1098 per metric ton and no CO<sub>2</sub> tax-figure 5.13).

A key observation in the plot is that the time optimised solution is the least operating cost solution for the prevailing fuel price and CO<sub>2</sub> taxation scenario. As discussed in previous sections (section 4.4.3.1 and section 3.6) and covered in reference[3.12], it is observed that in short haul flights the direct maintenance costs are significantly higher owing to higher number of cycles and comparatively longer periods of flight at sub optimal conditions(climb and descent) . Based on this assumption and the relation setup to calculate the maintenance cost and the fact that the operating cost model calculates the maintenance cost on an hourly basis,

the mission time will have a strong influence on the time related cost. Therefore a shorter mission time lowers the time dependant operating cost and hence the time optimised solution is reflected as the optimal cost solution.

			<b><math>\Delta \%</math>( baseline mission as ref)</b>		
	Mission fuel burn (kg)	Mission time (min)	Mission fuel burn %	Mission time%	Mission cost%
Baseline mission	2045	47.1	0.0	0.0	0.0
Fuel optimised mission	2019	47.2	1.24 % decrease	0.23% increase	0.14% decrease
Time optimised mission (optimal cost solution)	2321	42.5	13.47 % increase	9.78 % decrease	3.89% decrease
$\text{NO}_x$ optimised mission	2037	48.0	0.41 % decrease	1.97 % increase	1.36% increase

Table 5.2 Performance data of optimised trajectories in reference to baseline mission (227 nm)

The line plot for the case, assuming a fuel price of US \$1098/mt and varying CO<sub>2</sub> taxation (with a baseline environmental tax at US \$ 25/ ton CO<sub>2</sub> emissions) is as seen in figure 5.14. The time optimised solution is evidently seen to be the most cost effective, but in comparison to the fuel optimised trajectory consumes 15 % higher fuel (302 kg of fuel, resulting in 0.96 tons of CO<sub>2</sub>). The method described can be used to identify the HEA taxation rate; the rate, as in the previous case is the cross-over point, and hence is the minimum taxation required for fuel optimised solution to be competitive in terms of cost when compared with the time optimised (minimum operating cost) solution. Figure 5.14 and the magnified section (in figure 5.15) indicate for this to occur, at the assumed fuel price, the carbon taxation will have to be increased by a factor of 14 (to US \$ 350/ mt CO<sub>2</sub> emissions). This will result in the overall cost increasing by 26 % (indicated by A in figure 5.15). However if the fuel optimal solution were to be driven towards becoming the optimal cost solution amongst the Pareto optimal set of solutions, the taxation rate will then have to be increased by a factor of 35 (to US \$ 875/ mt CO<sub>2</sub> emissions), thus increasing the overall cost by 65%(indicated by B in figure 5.15). The cost contours for the cases (A and B) are as seen in figures 5.16 and 5.17.

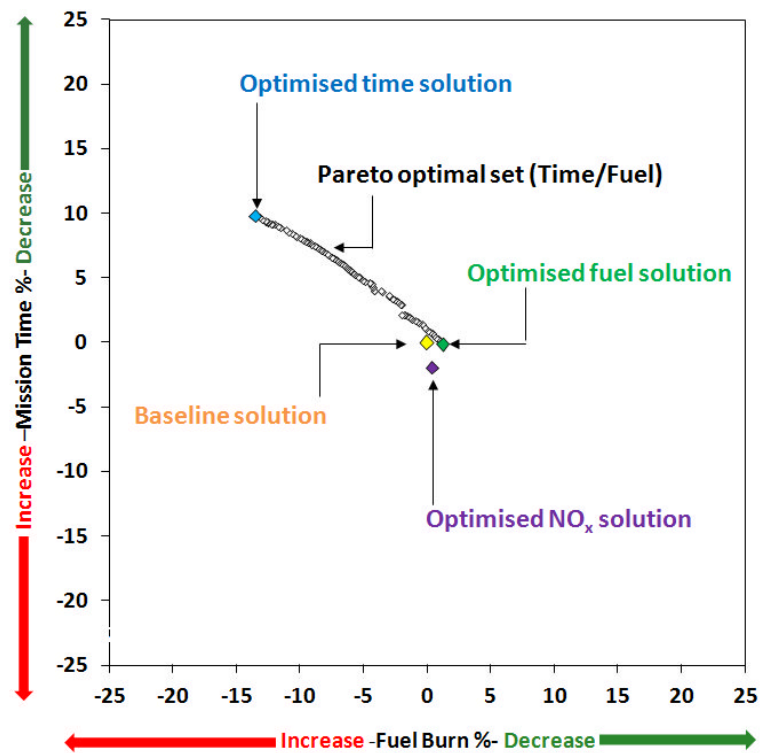


Fig 5.12 Plotted performance data of optimised trajectories in reference to baseline mission (227 nm)

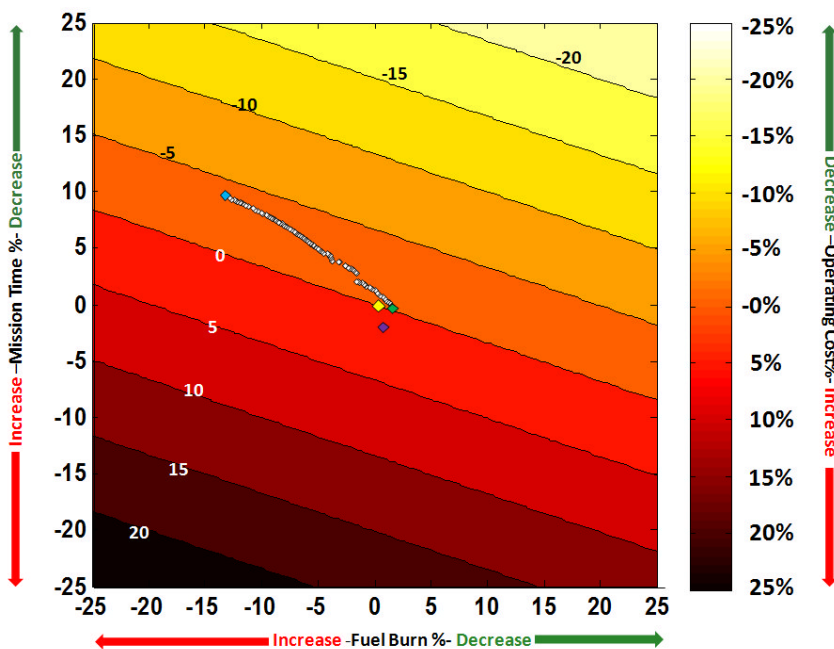


Fig 5.13 Cost contour plot (227 nm); scenario- fuel price US\$ 1098/mt and nil CO<sub>2</sub> taxation

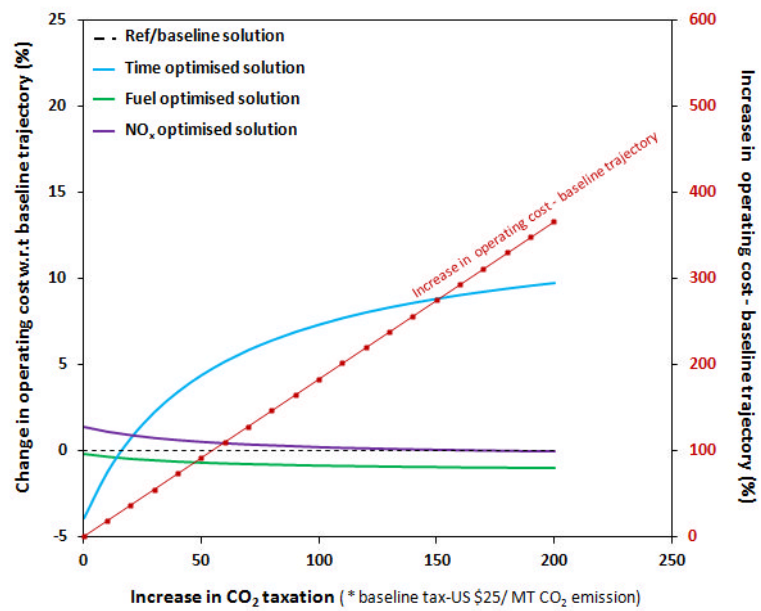


Fig 5.14 Line plot (227 nm); scenario- fuel price US\$ 1098/mt

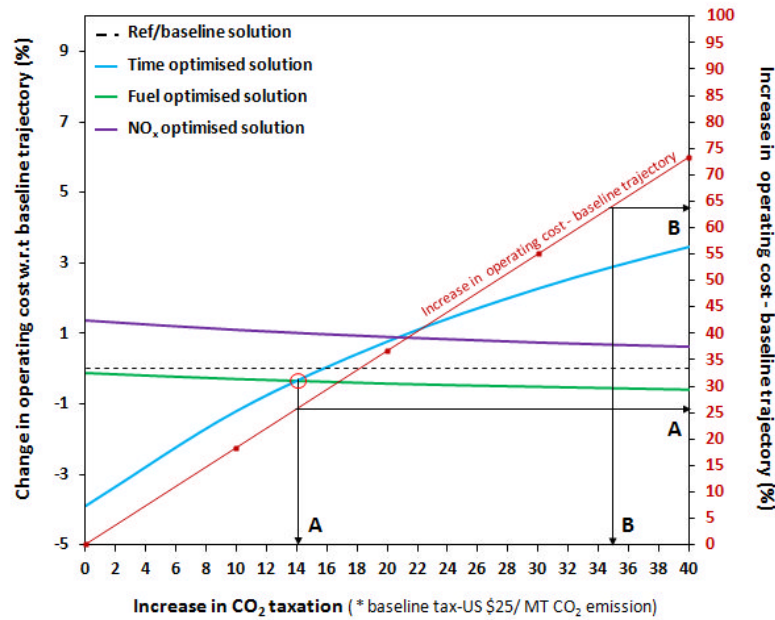


Fig 5.15 Line plot (227 nm); scenario- fuel price US\$ 1098/mt (magnified to illustrate the cross-over point)

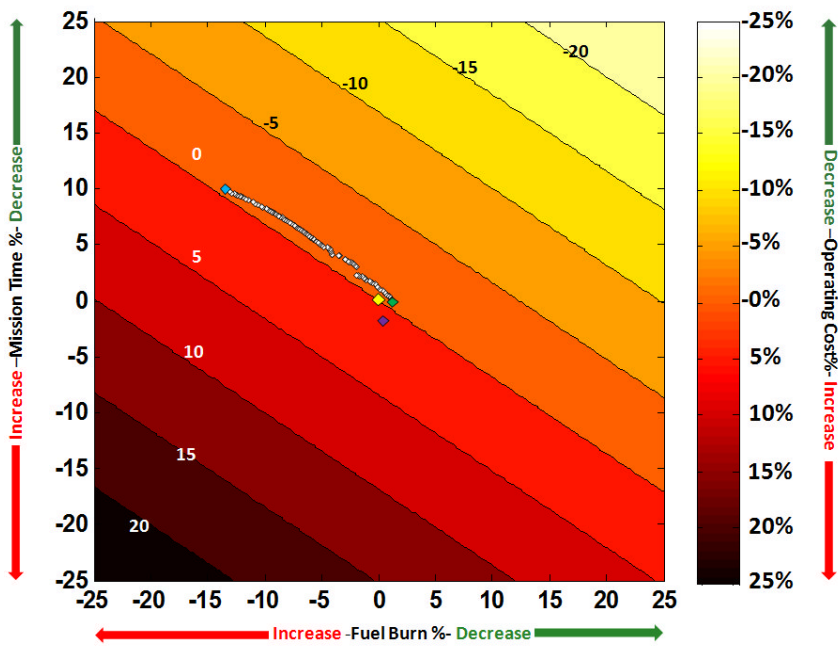


Fig 5.16 Case A- Cost contour plot (227 nm); scenario- fuel price US\$ 1098/mt and CO<sub>2</sub> tax of US\$ 350/mt CO<sub>2</sub> emission

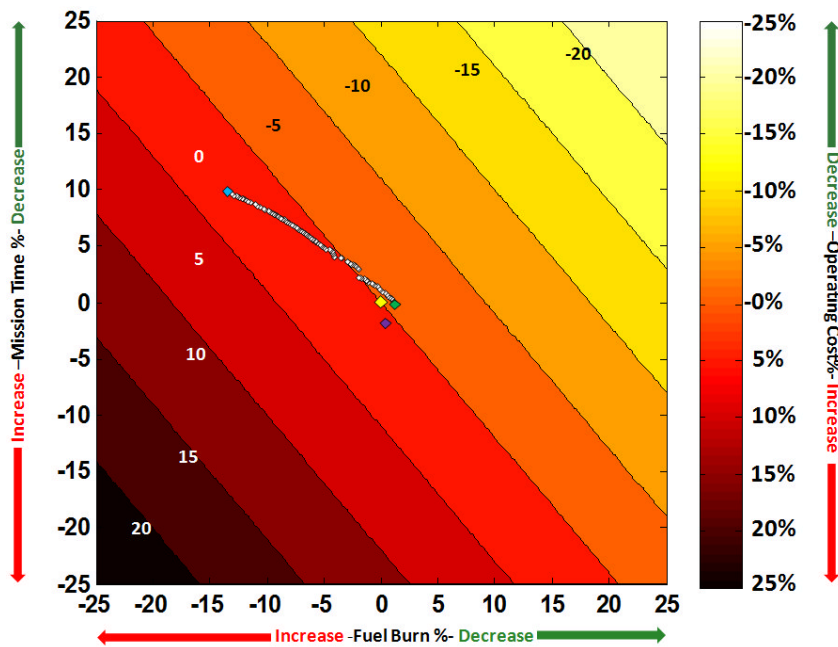


Fig 5.17 Case B- Cost contour plot (227 nm); scenario- fuel price US\$ 1098/mt and CO<sub>2</sub> tax of US\$ 875/mt CO<sub>2</sub> emission

### 5.3.3 CASE STUDY: MEDIUM RANGE (1614 NM)

The case discussed in the following section is for the medium range trajectory. The optimised trajectories for this case have been described in detail in section 4.4.2. Table 5.3 summarises the performance data for various missions optimised for the specific objectives, in terms of change in mission time and fuel burn. Figure 5.19 shows the cost contour plot for the BAU scenario (fuel price of US \$ 1098/ mt and nil CO<sub>2</sub> tax), while figure 5.20 shows the line plot for varying CO<sub>2</sub> taxation scenarios.

Similar to the previous cases the plots can be used to analyse the HEA taxation rate. Figure 5.20 illustrates the crossover point. It indicates that for the BAU scenario fuel price of US\$ 1098/ mt, a minimum taxation of US\$ 1512.5/ mt of CO<sub>2</sub> emissions (60.5 times the baseline emission tax) is required for the optimised fuel solution to be equal to the previously established optimal operating cost solution. This will drive the operating cost up by 167% when compared with the BAU scenario operating. Figure 5.21 shows the cost contour for the case and further validates this analysis. The figure also demonstrates the shifting of the optimal operating cost solution essentially being the point of tangency between the frontier of time and fuel needed and the iso-cost contour.

If the fuel price were to increase by 10% or 25 % then the taxation levels would still remain significantly high and vary between 58 to 60 times the baseline emission tax rates. Figures 5.22 and 5.23, effectively demonstrate this trend.

			<b>Δ % (baseline mission as ref)</b>		
	Mission fuel burn (kg)	Mission time (min)	Mission fuel burn %	Mission time%	Mission cost%
Baseline mission	9808	234	0.0	0.0	0.0
Fuel optimised mission	9499	259	3.2% decrease	10.5% increase	5.3% increase
Time optimised mission	12586	215	28.3% increase	8.0% decrease	5.7% increase
Operating cost optimised mission	9919	225	1.1% increase	3.7% decrease	8.6% increase
NO <sub>x</sub> optimised mission	9559	270	2.5% decrease	15.4% increase	1.86% decrease
Contrail optimised mission	9634	262	1.8% decrease	11.8% increase	6.7% increase

Table 5.3 Performance data of optimised trajectories in reference to baseline mission (1615 nm)

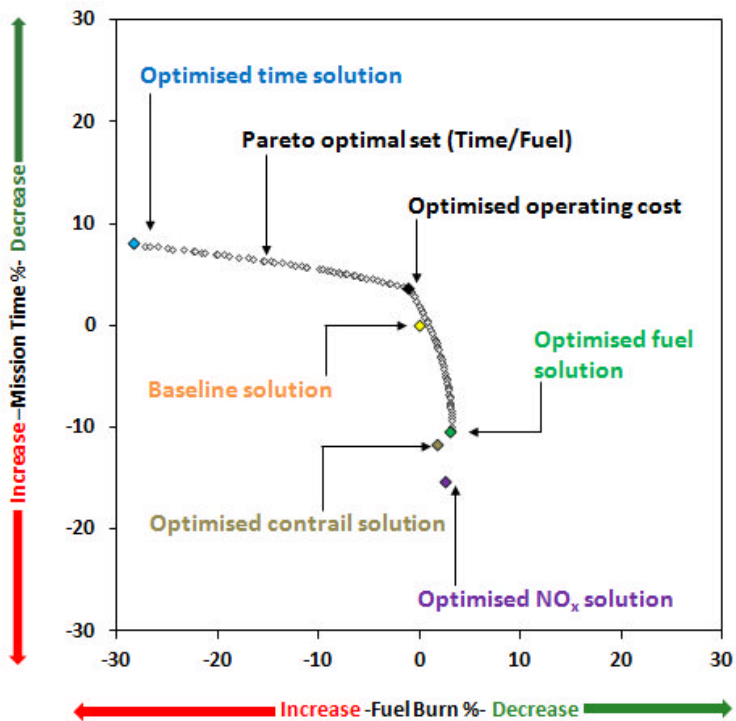


Fig 5.18 Plotted performance data of optimised trajectories in reference to baseline mission (1614 nm)

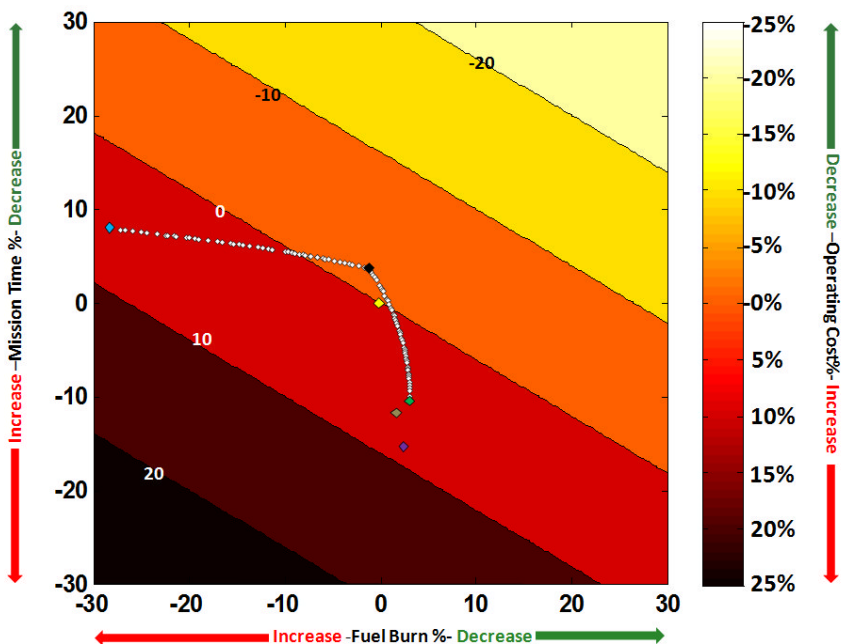


Fig 5.19 Cost contour plot (1614 nm); scenario- fuel price US\$ 1098/mt and nil CO<sub>2</sub> taxation

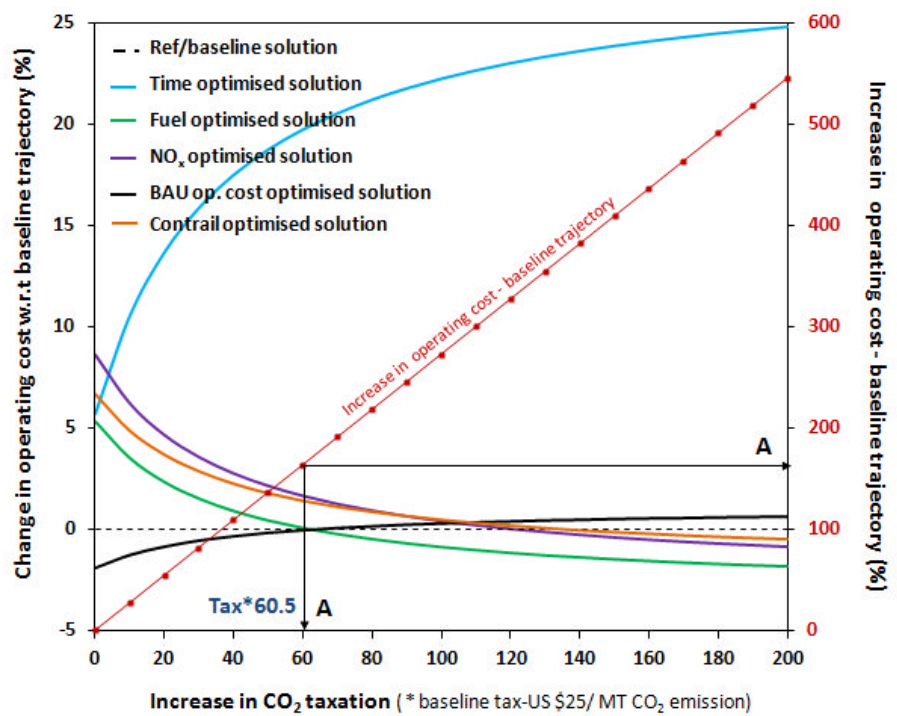


Fig 5.20 Line plot (1614 nm); scenario- fuel price US\$ 1098/mt (cross-over point illustrated)

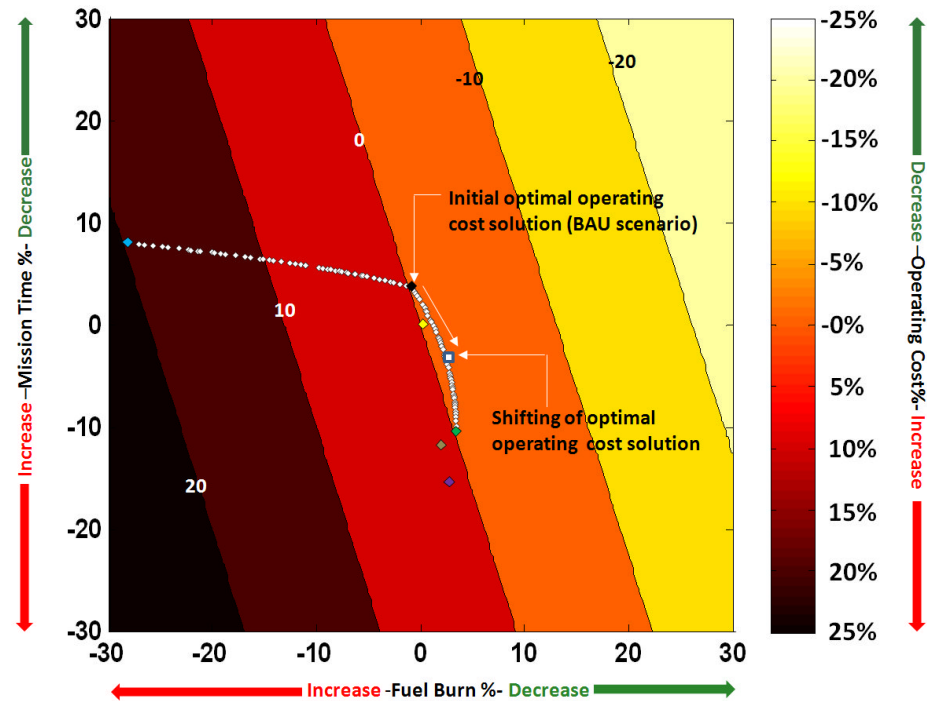


Fig 5.21 Cost contour plot (1614 nm); scenario- fuel price US\$ 1098/mt and CO<sub>2</sub> tax of US\$ 1512.5 /mt CO<sub>2</sub> emission

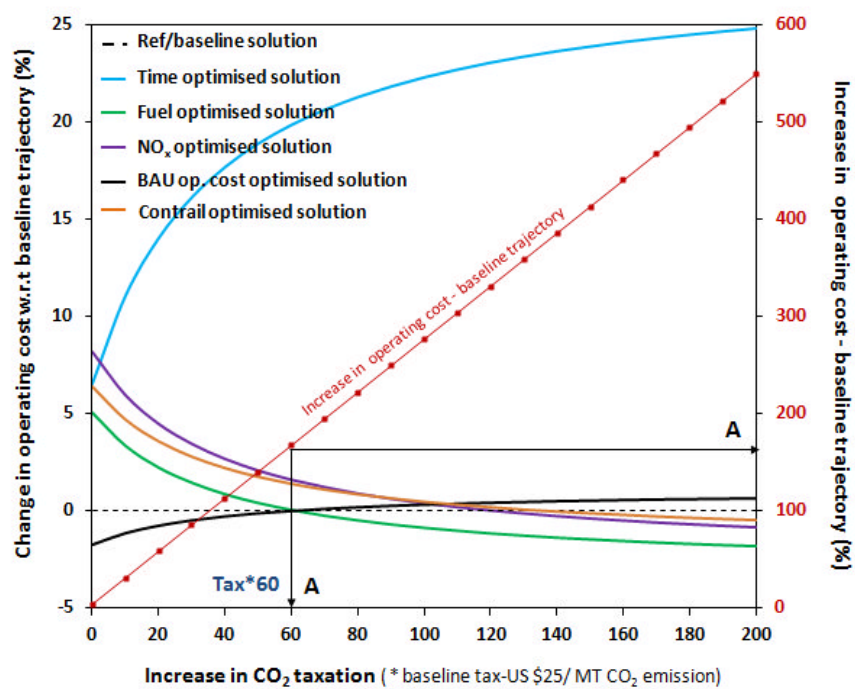


Fig 5.22 Line plot (1614 nm); scenario- 10% increase in fuel price (US\$ 1207/mt)

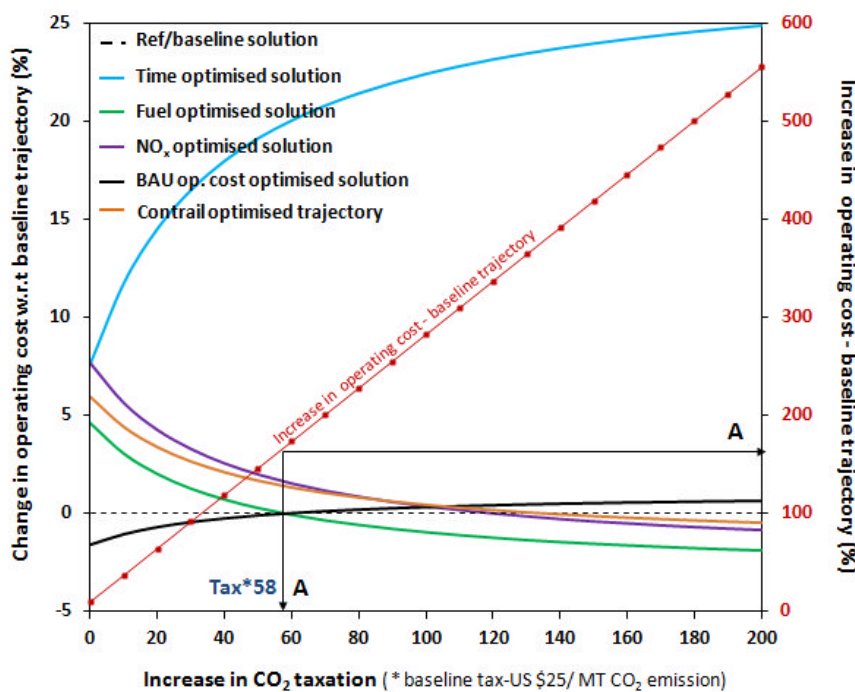


Fig 5.23 Line plot (1614 nm); scenario- 25% increase in fuel price (US\$ 1372.5/mt)

## 5.4 CONCLUSION

Chapter 5 demonstrated that an improved air traffic management system, if available, will allow current aircraft with conventional technology to fly more flexible trajectories that will in turn have significantly lower environmental impact in terms of emissions and lower fuel burn. It however also demonstrated that in a current fuel price scenario (and with no emission taxation) these trajectories were not economically viable.

The methodology introduced in this chapter then allows an assessor, to reconsider the optimised trajectories found earlier and apply various environmental taxation policies (in the form of varying CO<sub>2</sub> taxation and fuel prices) to establish the level of taxation and fuel price at which the environmentally greener trajectories become economically competitive.

Created specifically within the scope of this PhD, the methodology essentially uses a policy module in the TERA framework. The framework along with the module produces a set of line and contour plots which essential capture the effect changing taxation and fuel price scenarios will have on the cost effectiveness of the set of optimised trajectories.

For the previously discussed missions (short range (227 nm), short-medium range (815 nm) and medium range (1614 nm), the framework and the policy module were further used to analyse the optimal set, in a scenario wherein the fuel price of US \$ 1098/Mt and baseline tax of US \$25/ton of CO<sub>2</sub> emission are assumed. The study establishes the following:

- By using a cost contour plot and, when given a particular (CO<sub>2</sub> emission taxation and fuel price) scenario which of the optimised solutions from either a Pareto optimal set or individually is most economically profitable (alternatively, least in operating cost)
- By using a line plot, when give a particular fuel price scenario, what level of taxation on CO<sub>2</sub> emission will render the optimal fuel burn solution most economically viable, hence encouraging an operator to 'crossover'.

The key observations included the following:

- a. Effect of baseline tax US \$25/ton of CO<sub>2</sub> emission: For the three cases of varying ranges (227,815 and 1614 nm), when the best fuel solution was compared against the optimal cost solution under a nil CO<sub>2</sub> taxation scenario, it was found that the difference in cost was 3.76, 5.65 and 6.83% respectively, thus making the optimal cost trajectory more economically attractive. The line plots (figure 5.14, 5.6 and 5.20 respectively) further indicate that when the baseline tax of US\$ 25/ ton CO<sub>2</sub> is applied, the difference reduces marginally to 3.4, 5.4 and 6.55% respectively. However this would result in the operating cost of the baseline solution going up by 1.85 to 2.75% as the range increases.
- b. Establishing the 'cross-over' taxation rate: This is effectively defined as the taxation rate at which cost of operating the initially found optimal operating

cost trajectory will be equal to cost of operating the fuel optimal trajectory. The line plots (figure 5.14, 5.6 and 5.20 respectively) indicate that as the range increases the level of taxation will have to be considerably increased and hence will range from 14 times to 60.5 times the baseline taxation level, thus driving up the taxes to range from US\$ 350/ton to US\$ 1512/ton CO<sub>2</sub> emissions. This in turn will result in the increase of the operating cost of the baseline trajectory to increase by 25% to 160% over today's nil taxation scenarios.

- c. Effect of increase in fuel price on the taxation rate: The analysis shows that an increase in fuel prices would result in these taxes being reduced. An illustrative example may be seen in the 815 nm case (figures 5.6 and 5.11). When the fuel price was assumed to be US\$ 1098/mt, the taxation level at the cross over point is found to be US\$ 1375/ ton CO<sub>2</sub> emissions (55 times the baseline tax), however when the fuel price was increased by 50% (US\$ 1647/mt) the cross-over taxation level dropped to US\$ 1200/ ton CO<sub>2</sub> emissions (48 times the baseline tax).
- d. Diminishing influence of time variable on operating cost: A significant observation from the plots is that, as higher rates of taxation are applied the influence of the time variables continually decreases and hence results in the cost curves becoming increasingly parallel to the x axis (figure 5.14, 5.6 and 5.20). This indicates a finite effect of the level of taxation and hence considering taxation levels up to the cross over point may then only be prudent.

The methodology thus introduced in this chapter, aims to provide an assessor with adequate information on the effect, proposed taxes, probable fuel prices or a combination of both may have on the economic competitiveness of environmentally optimised operational solutions. It further aims to, additionally, also provide a perspective on the actual economic viability of such an emission tax (in terms of operational cost and its effect on ticket pricing) and hence adequately assess the suitability of the a future environmental policy or the effect of probable future policies / fuel prices.

## 6 POLICY ASSESSMENTS -TECHNOLOGY

### 6.1 INTRODUCTION

The technical work described in this far in this thesis introduced a methodology, based on an operational cost analysis approach, to examine the actual economic feasibility of the optimised trajectories in today's fuel price scenario. It then goes onto examine the effect of future CO<sub>2</sub> taxation policies will have on the acceptance of trajectories and in turn established the taxation rate that may be required to encourage an operator to switch from a conventional (baseline) trajectory to more environmentally friendly trajectories.

However, as discussed earlier in chapter 2, in order to achieve the steep environmental goals set by various regulatory authorities and governing bodies such as ICAO and ACARE, a combination of initiatives will be required. These initiatives include incremental improvements in current technology and introduction of novel technology. However, similar to operational improvements, any introduction of new technology will also depend upon its economic viability. Hence this chapter introduces a similar methodology, as discussed for assessing operational improvements, to assess future technology.

Over the years, the industry has consistently invested in improving technology and infusing it into commercial application, with an aim to always remain profitable. With fuel expenses being a significant part of an airlines operating cost, the core focus of technology development has been to constantly improve fuel economy, whilst maintaining Landing and Takeoff (LTO) cycle noise and NO<sub>x</sub> within certification limits and improving safety and reliability. However, with aviation emissions now becoming a cause for growing global concern and various emission mitigation policies coming into focus, the industry is actively pursuing even greener and quieter solutions for the future.

Sustainability of the aviation industry, as any other industry, depends on the elasticity of demand for the product and profitability through minimising operating costs. Apart from other factors, this profitability is directly affected by any technology infusion, be it aimed towards any of the global objectives which include reducing fuel burn, environmental emissions or noise. Therefore assessing and understanding the interdependency and effects of future technology and emission mitigation policies is paramount.

As previously covered in chapter 3, some of the key insights in this area have been provided by Kirby [2.37], Dray et al. [2.34, 2.35], Henderson and Kroo [2.36, 2.38].

To recap, all these methods use elaborate model integration frameworks and tools to provide interesting perspectives into the interdependencies of technology solutions and emission mitigation initiatives in unique ways. While Dray's work assessed the effect mitigation policies and technology options may have on the potential of reducing emissions on a regional and

global scale, Kirby proposed a methodology to forecast and select future technologies to select an ideal combination amongst a set of emerging technologies, so as to provide after induction, the maximum economic profitability and hence the maximum return on research and development investments. [2.37]

Another aspect of this field of study was seen in research, which dealt with aircraft conceptual design optimised for environmental performance. The work utilised numerical optimisation techniques in aircraft design on multiple aircraft to investigate the tradeoffs between the various environmental performance metrics and direct operating costs. [3.36]

The approach presented in this work differs from those listed above in the insight it provides. It aims to introduce a unique methodology that may be used in selection of a novel technology, whilst examining the effects of acquisition and maintenance cost in assessing economic viability.

The methodology is applied through a Techno-economic Environmental Risk Assessment (TERA) framework to produce a set of assessments [2.28, 2.29]. These assessments compare a novel technology with competing conventional solutions and establish its benefits in terms of performance and energy efficiency. These studies are undertaken for various emission taxation and fuel price scenarios to further establish if the observed efficiency may be translated to improvements in operating cost. The focus of the work is to then utilise these assessments and concepts of Net Present Value (NPV) and Internal Rate of Return (IRR) in an investment cost analysis approach. The aim is to answer questions from a policymaker's or airline operator's perspective, on the issue of whether the technology can translate efficiency to operating profits, sufficient to supersede what's already on the market and thus offset a higher acquisition price and complexity of aircraft. Alternatively, what taxation or fuel price scenario will establish its viability and actually justify a technology shift from a conventional solution, given a particular acquisition and maintenance cost?

In the last decade with the price of fuel rapidly rising and CO<sub>2</sub> emissions from aviation being driven into focus, a renewed interest has been shown by the industry in rejuvenating fuel saving concepts like the Counter Rotating Open Rotor (CROR) technology. The proof of concept of the approach is demonstrated, by assessing the CROR concept as a competitive technology solution, against the conventional high bypass turbofan.

## 6.2 TECHNICAL APPROACH

The TERA framework utilised for the methodology is as depicted in figure 6.1, to produce a set of performance and policy assessments in terms of payload range performance, energy efficiency, relative operating cost benefits and acquisition and maintenance cost analysis.

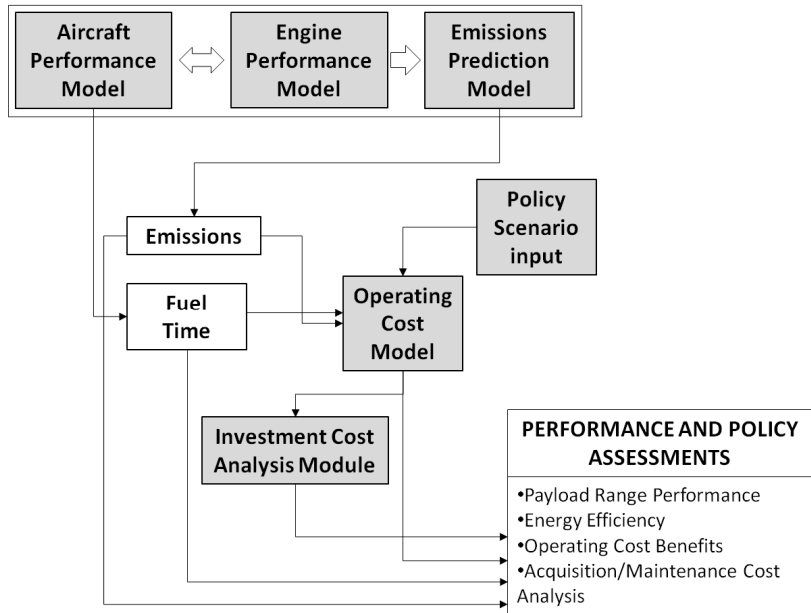


Fig 6.1 Schematic of TERA framework for technology assessments

This study utilises TERA in a framework as depicted in figure 6.1, to produce a set of performance and policy assessments in terms of payload range performance, energy efficiency, relative operating cost benefits and acquisition and maintenance cost analysis.

The analysis of a novel technology begins by utilising the aircraft and engine performance models to establish its payload-range performance. This provides the assessor at the design stage with a performance summary giving an estimation of its overall performance characteristics. The performance and payload range capability is then compared with a single or a set of competing conventional technologies.

For a transportation to be profitable it requires to be energy efficient and hence the optimal utilisation of available energy is of prime importance. Various efficiency metrics have been used to assess energy efficiency of transportation modes. Hileman[6.9] in his work has summarised some of the relevant metrics and introduces a metric based on the concept of Payload Fuel Energy Efficiency (PFEE) to examine fleet wide aviation fuel efficiency. The metric analyses the amount of productivity in terms of payload transferred across a distance per unit cost of energy consumed. Another significant work in this area is by Poll, in which he identifies the ratio of the energy liberated during a flight to the revenue work done or Energy to Revenue Work (ETRW), as a key indicator in the assessment of energy efficiency, and may also be used to measure the environmental impact of CO<sub>2</sub> emissions [6.10]. Amongst the other metrics, ETRW was found to be particularly useful as it can be used to assess a technology purely from an energy efficiency perspective, whilst taking into account the useful work done in terms of its revenue earning potential. The minimum value of this metric is considered as the optimal value in terms of energy efficiency.

$$ETRW = \frac{M_f \cdot LCV}{M_{pl} \cdot g \cdot R} \quad 6.1$$

ETRW = Energy to revenue work

$M_f$ = Mass of the mission fuel actually burned on trip (kg)

$M_{pl}$ =Maximum payload mass of the aircraft (passenger+ cargo) (kg)

$g$  = Acceleration due to gravity (9.81 m/s<sup>2</sup>)

R = Great circle distance for a mission (m)

LCV= Lower calorific value of fuel ( $\approx$  43 MJ/kg for kerosene)

Therefore, the next stage of the assessment utilises the ETRW metric to map the energy efficiency of a technology. This is done in comparison with the competing technologies, across its range of payload-range operations. This analysis whilst providing a broader perspective on the operational capability of aircraft in comparison to various other solutions also enables identifying the solution against which the economic viability of the combination of aircraft and route may be assessed.

The framework then forwards the performance and energy efficiency results to the operating cost model to assess the operating cost benefits of the novel technology as opposed to the selected conventional solution. This is undertaken for a set of missions that best represent the aircraft in terms of payload and range.

The benefit in operating cost is established in terms of the relative changes and the overall increase in operating costs between the two technologies, for a series of emission tax and fuel price scenarios.

The final phase of the approach uses the investment cost analysis module to produce the DOC and IRR contour plots. These plots illustrate the effect of the relative changes in acquisition and maintenance costs, on operating cost using concepts of IRR and NPV, for a selected set of missions.

The assessments produced using this approach aim to provide an assessor with a clearer visibility of the operational and economic viability of utilising a novel technology, through a performance and cost benefit analysis.

### 6.3 CASE STUDY

The transition from turbojets to turbofans in the late 1960s was specifically aimed at reducing fuel burn and LTO cycle NO<sub>x</sub> and noise, whilst improving safety and reliability. The oil embargo

in the 1960s and the instability in Middle East in the 1970s drove the oil prices to new heights [6.1]. This resulted in airlines around the world paying the penalty through staggering losses. Within the aviation industry, these events primarily led to the focused research and development that was aimed at revolutionary reductions in fuel burn, in comparison to the high bypass turbofan. In the late 1970s, this research led to the genesis of the revolutionary concept of CROR.

Owing to its ultra high bypass ratio and hence a very high propulsive efficiency, the CROR concept implemented as the Un-Ducted Fan (UDF), was stated to provide an SFC of 25-27% lower than that of the best turbofan engine going into service at the time [3.3]. However, due to low fuel prices prevailing in the late 1980s, complexity in design and strong competition from conventional and technically settled high bypass ratio engines, the concept never reached commercial application [6.2].

With fuel prices on the rise in the last decade, now averaging at 125 \$/barrel and aviation a part of the European Union's Emission Trading Scheme from 2012, the CROR technology is being actively pursued by the industry as a possible future solution.

The approach described in this paper is demonstrated through a proof of concept study to assess the potential of the CROR technology, as a technology solution to compete with the conventional high bypass ratio turbofan technology. This case study aims to illustrate the wealth of useful insights provided by the proposed approach, rather than to assess comprehensively the CROR concept.

Following the methodology discussed earlier, the analysis begins with the payload - range and energy efficiency assessments of the novel technology. These performance assessments are compared with those of conventionally used short-medium range aircraft. These include a single aisle narrow body aircraft with twin high bypass ratio turbofan engines, as modelled in chapter 4 and based on the design and operational characteristics of a Boeing 737-800 equipped with CFM56-7B high bypass ratio engines), a conventional short range turbo prop aircraft (ATR 72).

Based on a comparison of payload range and energy efficiency of these solutions, a conventional solution is then selected as a baseline to analyse the relative operating cost and investment cost benefits of the novel technology.

All discussed in chapter 4, all the aircraft missions simulated in this study for the novel and conventional aircraft, were done so for ideal performance and assumed to follow International Flight Rules, which include standard assumptions on fuel reserves, diversion fuel and contingency fuel. The aircraft and engine performance models are validated against public domain data and achieve accuracies in payload-range capability of within 4-5%, as demonstrated earlier.

## 6.4 CROR AIRCRAFT/ENGINE MODELLING

Limited design information is available in the public domain on the actual implementation of the CROR concept on a commercial aircraft. McDonnell Douglas in the 1980s used a derivative approach and designed a new variant of the existing MD80 aircraft, by replacing the JT8D engines with the UDF (as seen in figures 6.1 and 6.2)[6.6]. In this work the technology was modelled in a similar approach; i.e. the aircraft and engine performance model were based on the aerodynamic and performance characteristics of the MD-80 aircraft and NASA's Un-Ducted Fan (UDF) engine respectively.



Fig 6.1 MD 80 equipped with a single UDF engine in 1980s [6.5]



Fig 6.2 GE's UDF engine based on the Open Rotor Concept [6.5]

The aircraft and engine model are developed using the aircraft and engine performance (Turbomatch) tools discussed in chapter 4. The engine simulation performance trends and design parameters were validated and verified against public domain data for the UDF and were found to agree within an accuracy of 7-8% with the optimal/true design values [6.3]. The performance of the aircraft is verified against the actual payload-range chart of the MD80 to

establish the payload range capability of the modelled aircraft (figure 6.12) [6.4]. All missions simulated for the aircraft follow typical take-off, initial climb, approach configurations and speed-schedules for climb, cruise and descent. Each trajectory was set to complete the cruise segment of the mission at a fixed altitude of 35000 ft and at a design cruise speed of 0.72 Mach. All missions simulated to include standard reserve fuel onboard, which included diversion of 200 nm, hold at 5000 ft for 20 minutes and 5% of block fuel.

#### 6.4.1 ENGINE MODELLING

The engine performance of the open rotor engine, essential to the demonstration and application of this technology, was simulated using Cranfield University's in house engine simulation tool, Turbomatch. The work has been developed in collaboration with and adapted from research on advanced turboprop modelling at Cranfield University by Giannakakis. It utilises advanced propeller maps which are integrated with the engine simulation software [6.7]. Figures 6.3 and 6.4 show the schematic and modelled component view of the open rotor engine while figure 6.5 shows the flow of data required to simulate the design and off design performance of the engine using Turbomatch. Reference [6.3] was used in designing the engine model for simulation and the design parameters used are as indicated in table 6.1

The design point for the engine was chosen at top of climb (10668 ft, 0.72 Mach), based on data available in reference 6.3. Several iterations were performed at design point and off-design conditions to match the performance of the model with the limited data available for the engine on the public domain. The mass flow rate at the engine intake was estimated on the measured intake area and assuming inlet Mach number of 0.50-0.60. The turbine entry temperature (TET) were based on the net thrust at the top of climb [6.3]. Additionally propeller diameter, component pressure ratios, efficiencies and compressor bleeds for turbine cooling were guessed and iterated to match required thrust requirements at take off and cruise.

Parameter	
Flight altitude m/ft	10668/35000
Flight Mach. number	0.72
Deviation from standard temperature	0.0 (ISA)
Overall pressure ratio	25
Turbine entry temperature(K)	1357
Air mass flow Kg/s	19.54
Intake total pressure recovery	1.0
LP compressor pressure ratio	4.0
LP compressor isentropic efficiency	0.85
Total pressure loss between LPC and HPC	1%
HP compressor pressure ratio	6.25
HP compressor isentropic efficiency	0.85
Cooling air at HPC outlet	10%
Combustor total pressure loss	5%
Combustion efficiency	0.999
Power takeoff from HP turbine	0.0
HP Turbine isentropic efficiency	0.88
Power takeoff from LP turbine	0.0
LP Turbine isentropic efficiency	0.88
Power turbine isentropic efficiency	0.90
Propeller efficiency	0.85
Propeller blades-number	8
Propeller diameter m	3.56
Nozzle characteristic	Fixed Convergent

Table6.1 Design point assumptions for the CROR engine model

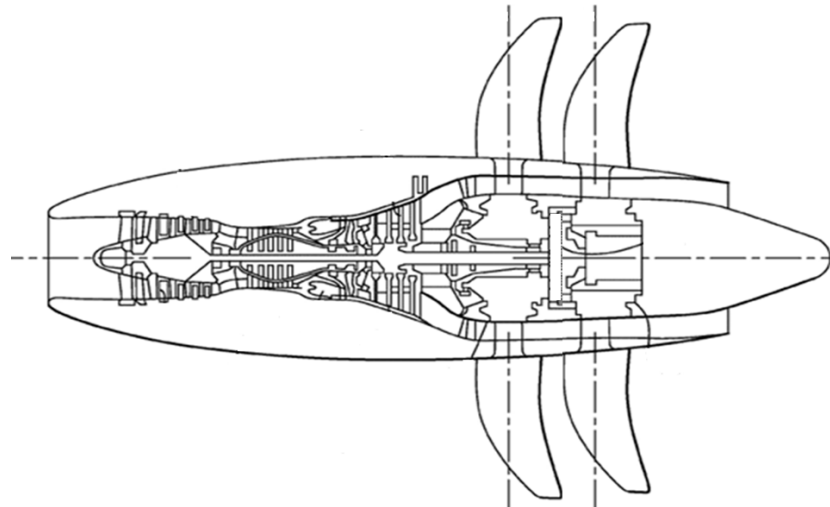


Fig 6.3 Outline of the CROR engine

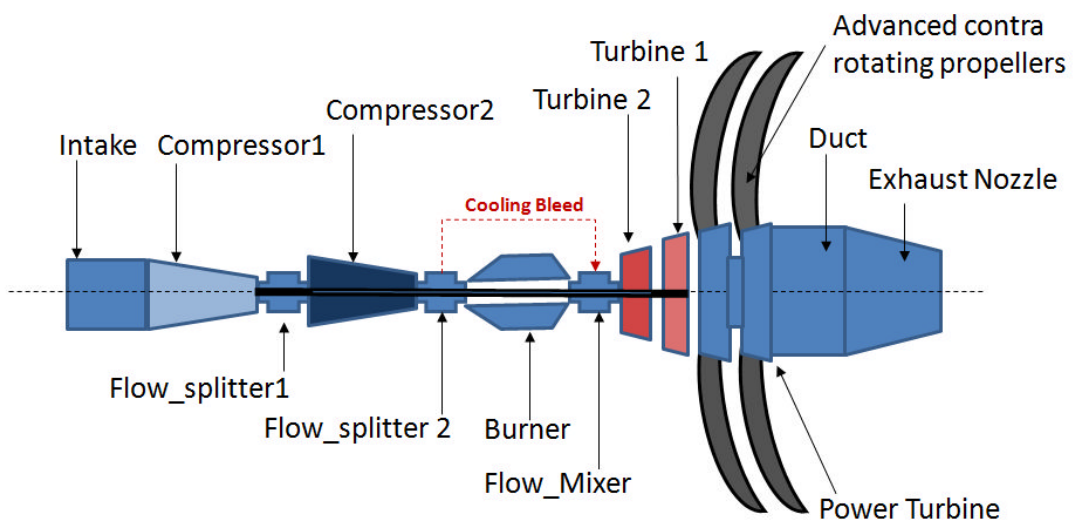


Fig 6.4 Components of CROR engine used in modelling engine performance

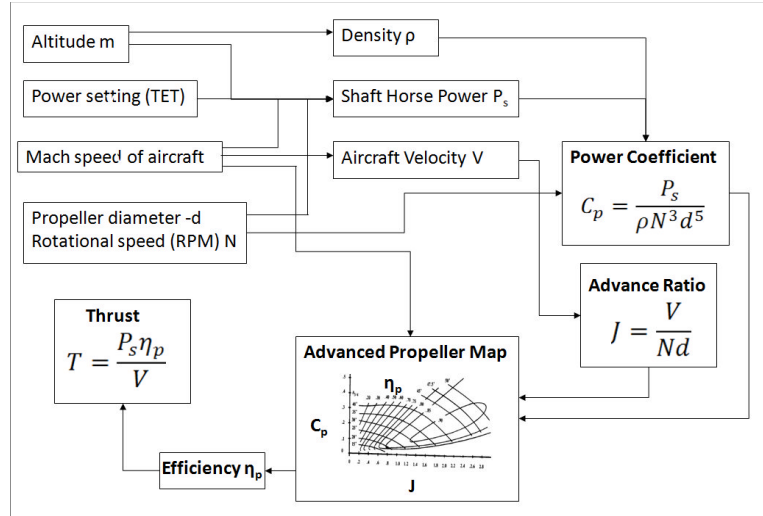


Fig 6.5 Representation of data flow to calculate thrusts, given mission specific data

#### 6.4.1.1 Engine performance validation and verification

In order to validate and verify the performance of the simulated engine, it was compared with the actual design data of the Un-Ducted Fan (UDF). Even though very little data is currently available in the public domain, an attempt was made to match as many design parameters for which the information was available. Table 6.2 indicates the error that was achieved in matching some of the design parameters from reference [6.3]

Parameter	Required	Achieved	Error%
LPT design point efficiency. pc	87.76	88	0.27
Propeller diameter. ft	11.67	11.67	0.00
Altitude at design point. ft	35000	35000	0.00
Speed at design point. mach	0.72	0.72	0.00
RPM at design point	1000	1000	0.00
Takeoff thrust @SLS isa conditions .N	111205	110000	-1.08
Core nozzle area. m <sup>2</sup>	0.47419	0.4735	-0.15
No rotor blades on each stage	8	8	0.00
Net thrust at design point .N	22645.9	23813	5.16
Takeoff pressure ratio	17.5	15.2	-13.14
Propeller RPM	1000	1000	0.00
Advance ratio at design Point	-	3.38	-
Power coefficient C <sub>p</sub> at design point	-	1.794	-

Table6.2 Validation of simulated engine against public domain design data on the UDF

In order to establish the mathematical model of the open rotor engine is able to simulate the actual performance, a series of off-design performance simulation calculations were performed. Reference [3.3] discusses in a fair detail the concept of open rotors and high bypass engines as aircraft propulsion systems, its expected performance and correspondingly various characteristic performances. The data from the off design simulations was used to reproduce off-design performance characteristics of open rotor engines (as against that of high bypass engines) whilst highlighting the effects of altitude, flight Mach number and turbine entry temperature on the net thrust and specific fuel consumption.

The plot, as shown in figure 6.6 indicates the variation of SFC ratio ( $C/C_{cr}$ ) with varying throttle setting, and hence thrust ratio ( $F/F_m$ ), at a constant altitude for a high bypass turbofan and an open rotor engine, where  $C_{cr}$  and  $F_m$  are the rated SFC and thrust values at cruise respectively. Figure 6.7 additionally shows the typical effect of flight speed.

For a high bypass turbofan, when the thrust is reduced by lowering the TET, the minimum SFC at typical cruise condition of mach 0.8 and cruise altitude of 35000 ft will lie between 75% and 80% of the rated value, which will effectively give 2-3% reduction of SFC, and hence turbofans will have an optimal SFC at the bottom of the loop for a particular flight condition. However for an open rotor engine the lowering of the throttle setting will result only in the increase of the SFC similar in characteristic to that of a turboprop engine. Throttling up of the engine will result in an increase of thermal efficiency and a decrease in propulsive efficiency for both the propulsion system. However the rate of decrease of propulsive efficiency for an open rotor engine is lower in comparison to that of a high bypass turbofan engine. The net thermo-propulsive efficiency will first increase for a turbofan and then decrease whereas for the open rotor engine will only decrease. The rate of change of specific fuel consumption is inversely proportional to that of thermo-propulsive efficiency and hence will demonstrate the characteristic behaviour as shown.

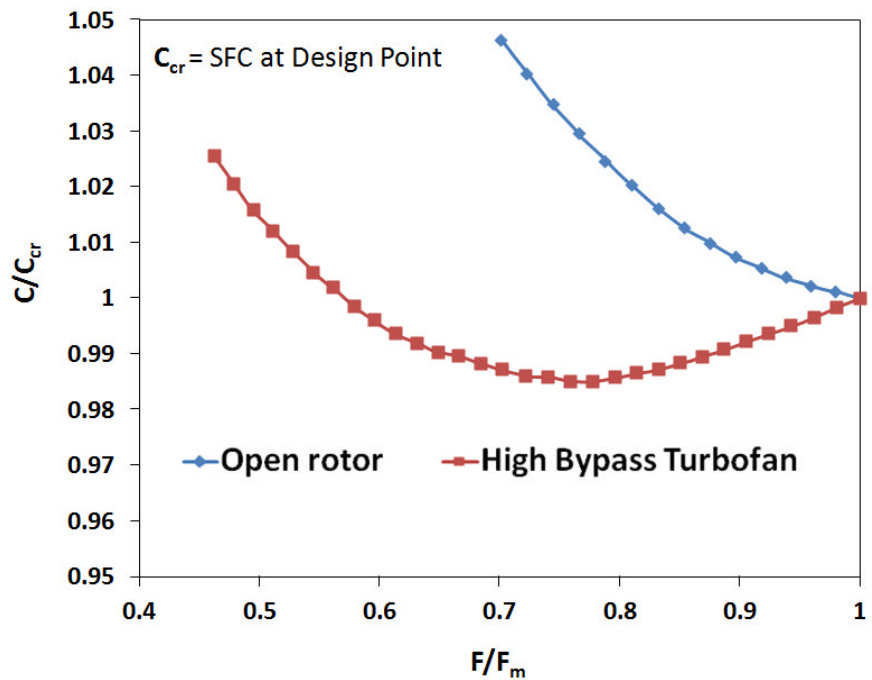


Fig 6.6 Variation of SFC with varying thrust at constant altitude (Non dimensionalised)

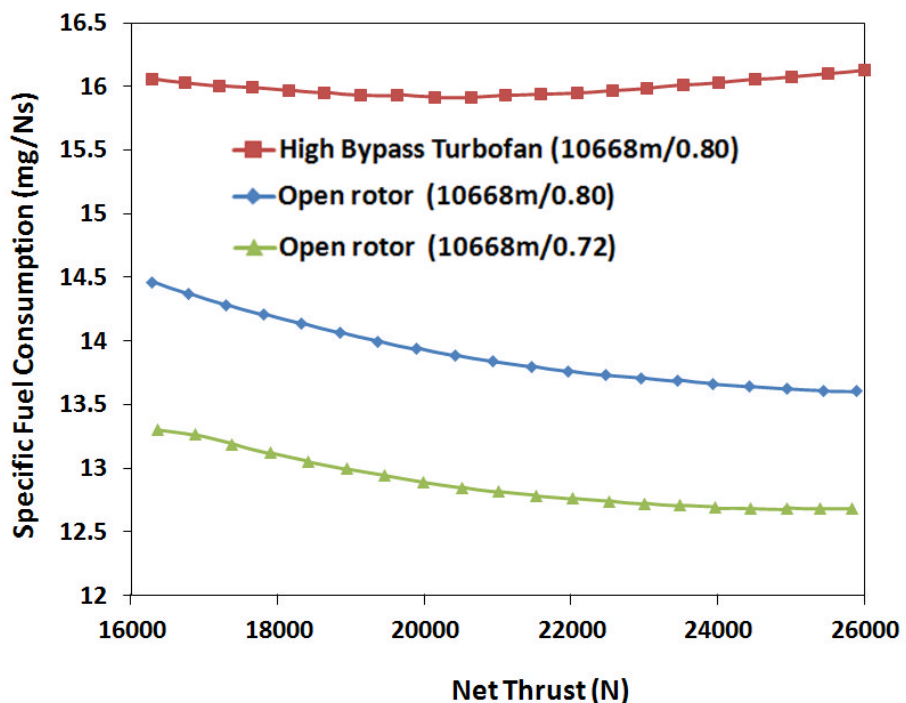


Fig 6.7 Variation of SFC with varying thrust at constant altitude

The figures 6.8 and 6.9 show the typical behaviour observed for the open rotor and high bypass engine , with regard to the variation of maximum thrust with forward speed at a constant altitude (sea level and at cruise respectively) , where  $F_0$  is the rated maximum rated thrust at the altitude.

At sea level (figure 6.8), at a constant height for both the engines the rotational speed for maximum thrust is fixed by rating and thrust is primarily a function of Mach number or TAS. As the Mach number or TAS increases from a low value at a fixed height with constant rotational speed, there will be two main effects on thrust  $F$ . First there will be a decrease of  $F$  due to increase in momentum drag, which is a dominant effect at ground level during takeoff. As the velocity increases, there is an increase in ram pressure at entry to the fan or compressor, which in turn increases the effective overall pressure ratio and this, gives an increase in thrust. As the flight Mach number increases above mach 0.4 (135 m/s) the effect of increase in ram pressure at the fan and compressor entry becomes more pronounced and the rate of decrease of thrust with increasing mach becomes smaller. This effect as may be seen in the open rotor engine is less pronounced as the nacelle is much smaller in size and hence the ram pressure effect is not dominant. It may be noted that the curve for the open rotor shows a slight dip as the speed increases from zero, this is attributed to an anomaly in the modelling due to non availability of propeller maps at very low speeds.

Figure 6.9 shows the same parameters represented at cruise altitude (10668m) and due to the dominant effect of the ram pressure effect in the turbofan the, thrust at a particular altitude and power setting will remain almost constant, whereas for an open rotor engine there will be a decrease.

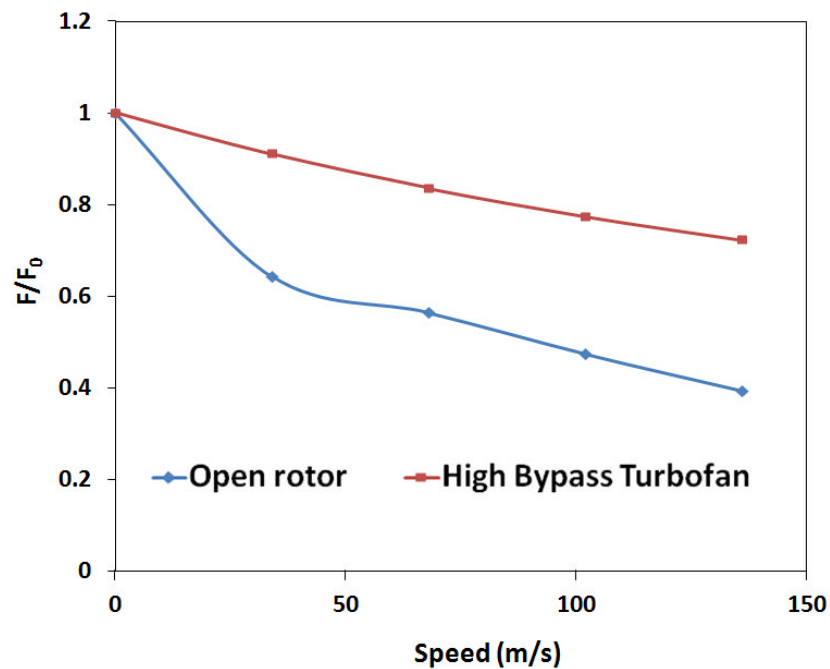


Fig 6.8 Variation of maximum takeoff thrust with forward speed at sea level

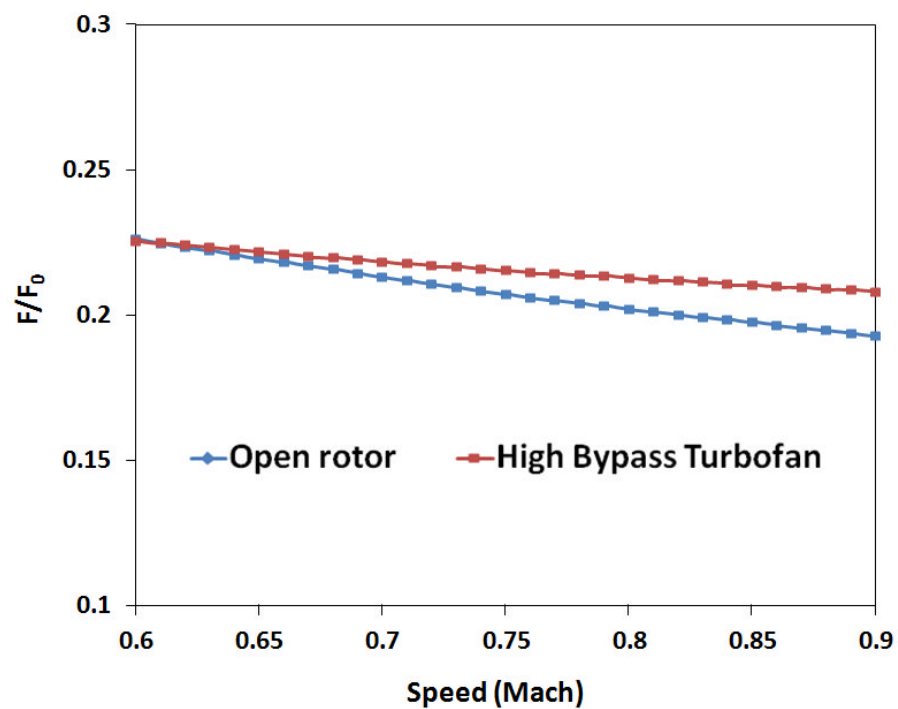


Fig 6.9 Variation of maximum thrust with forward speed at cruise altitude (35000 ft)

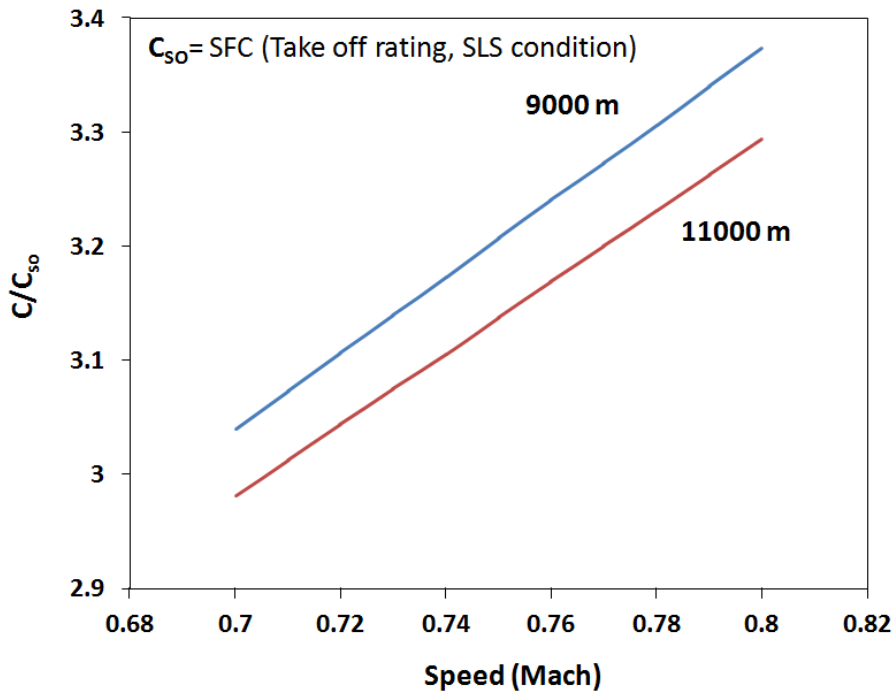


Fig 6.10 Variation of SFC with speed at fixed altitude (cruise rating)

#### 6.4.2 AIRCRAFT MODELLING

The study currently does not consider any optimisation of the airframe and propulsion system design and hence assumes the basic characteristics, dimensions and aircraft/ propulsion system limitation parameters remain unchanged. These include the aircraft mass and balance (comprising maximum take-off weight (MTOW), maximum landing weight (MLW), maximum zero fuel weight (MZFW), operating empty weight (OEW), fuel capacity, max payload), number of passengers, mean centre of gravity position, maximum operational altitude, environmental envelope and aircraft dimensions (wing span, overall length, tail height, wing span, reference wing surface area).

##### Operating point of the aircraft

The design point of the simulated open rotor engine, as discussed, was set at an altitude of 35000 ft and at a speed of mach 0.72 based on public data information [6.3]. Figure 6.11 shows the specific air range calculated for various cruise altitudes and speeds. The trends observed using the model have been verified against trends expected from a turboprop aircraft from references [6.8, 3.3] and are in agreement. The key observation from the plot is that the maximum specific air range increases with altitude and there exists an optimal speed for each altitude, which will decrease as the altitude decreases. Therefore based on figure 6.11 and data available from reference [6.3], a cruise speed and altitude of Mach 0.72 and 35000

ft was selected to establish the payload range performance of the propfan aircraft, to further simulate various missions in the study.

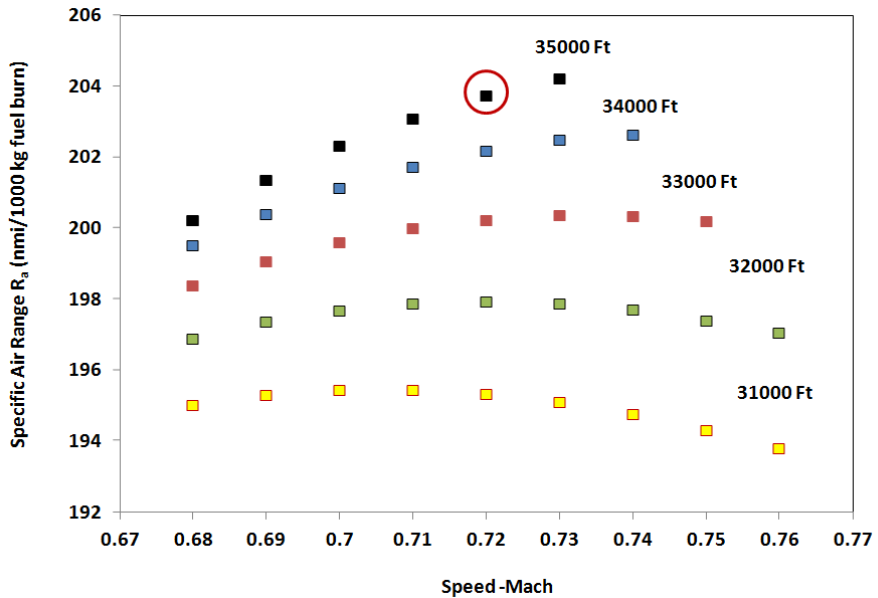


Fig 6.11 Variation of specific air range with speed at different cruise altitudes

#### Payload range

In order to establish the performance benefit of a propulsion system with higher propulsive efficiency, the payload range performance of the simulated propfan aircraft was compared against that of the original MD 83 aircraft, with conventional turbofan engines. As previously discussed in chapter 4, the payload range performance was gauged by simulating missions at three key points of the payload range chart. For each of the points simulated on the payload chart, except for the cruise and the final climb speed of (0.72 and 0.65 respectively), the mission flight profile is based on assumptions described in section 3.2.3.

As expected due to the higher propulsive efficiency, the payload range chart in figure 4 illustrates that with the use of the CROR concept the aircraft's range capability improves(illustrated by three key points on the payload range chart, figure 6.12):

- The range with maximum payload (point B) has increased by 67% (point B').
- The range flown with maximum fuel and associated payload to maintain maximum takeoff weight (point C) has increased by 57%(point C').
- The ferry range (point D) has increased by 43 %( point D').

As the payload range analysis of modelled aircraft indicated that the calculated performance is typical of an aircraft similar to the MD-80, equipped with CROR engines similar to the UDF, the model was used within the proposed framework to conduct the techno-economic assessments.

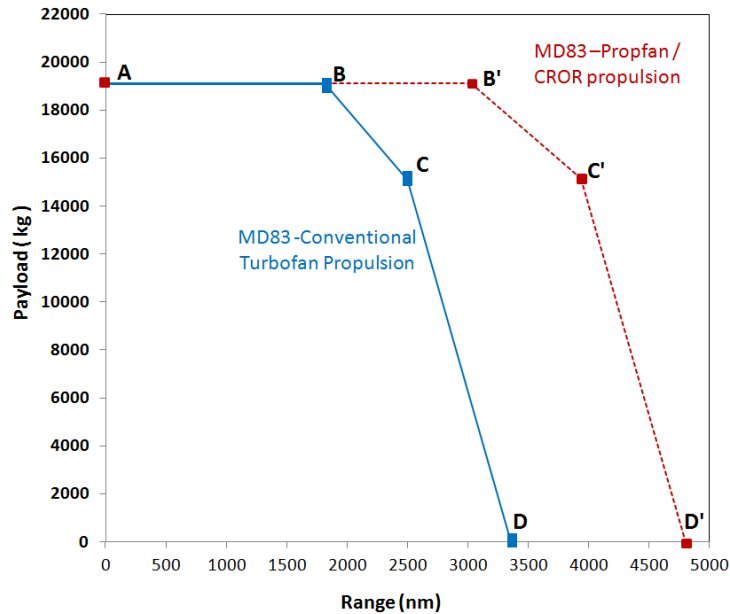


Fig 6.12 Plotted payload range performance of MD80 aircraft with conventional turbofan propulsion and CROR propulsion

## 6.5 PAYLOAD RANGE PERFORMANCE AND ENERGY EFFICIENCY

In terms of payload range performance and energy efficiency, the aircraft considered for comparison with the CROR aircraft are typical aircraft used by the industry for short/ medium range routes. These therefore include a conventional single aisle narrow body short/ medium range turbofan (TF) aircraft (Boeing 737-800 with high bypass turbofan engines (CFM 56- 7B27) and a short range turbo prop aircraft (ATR 72-200).

**Boeing 737-800-** The aircraft is a part of the New Generation series of Boeing aircraft and entered service in 1998. Designed as a replacement for the MD-80/90 and the 737-400, the aircraft is able to carry up to 189 passengers in a one class layout (162-166 passengers in a two class layout) and a maximum designed payload of 19108 kg. For analysis the model used to simulate the performance of this aircraft is the same as described in chapter 4, with the assumptions for the mission profile described in section 3.2.3.

**ATR-72-210** is one of the most widely used turbo props by the industry for regional routes. Equipped with two PW 120 turbo-prop engine, it is capable of covering a range of up to 900 NMI with a full passenger capacity of up to 72 passengers. For the purpose of this study a

detailed modelling of the performance of the aircraft has not been undertaken as it is compared for its payload range and energy efficiency only on typical routes. For these routes, information is available in referenced literature. The routes considered are for ranges of 100 and 200 nm and for maximum design payload and passenger loads.

The plots in figure 6.13 and 6.14 demonstrate the payload-range performance and energy efficiency (in terms of previously defined ETRW) of the novel and different conventional technology solutions, respectively. The plots enable the identification of the set of competing technologies in terms of comparable payload range capability and energy efficiency. The assessments from the plots are summarised as follows:

- The conventional turboprop aircraft was observed to be less energy efficient amongst the selected solutions, in terms of ETRW. This is attributed to the fact that even though the aircraft may exhibit lower fuel burn in terms of absolute quantities, the aircraft are designed to fly with lower passenger capacity / payloads and significantly shorter ranges, which results in overall lower values of energy efficiency.
- The CROR and TF(Turbofan) aircraft are observed to be less energy efficient at very short ranges, this is attributed to the fact that significant part of the weight carried on aircraft over short distances includes the weight of the reserve fuel, which reduces the overall energy efficiency.
- The CROR aircraft is able to achieve longer ranges at equivalent payloads than the aircraft under comparison.
- For the particular payload-range requirements associated for a short to medium range aircraft, the CROR aircraft is found to have a lower energy to revenue work ratio, of up to 15-22% in comparison to the single aisle narrow body aircraft across its representative range (500-2500 nm) capability, and hence is considered to be a more energy efficient solution than the conventional aircraft.
- The assessments indicate that the CROR aircraft has comparable payload range capabilities and improved energy efficiency, in comparison to the conventional TF aircraft and is therefore considered for operating and investment cost analysis.

## 6.6 OPERATING COST ANALYSIS

The economic performance for both the novel and conventional aircraft/engine combinations is assessed based on a set of trajectories representing similar missions in terms of ranges and payloads typical of this aircraft (figure 6.15).

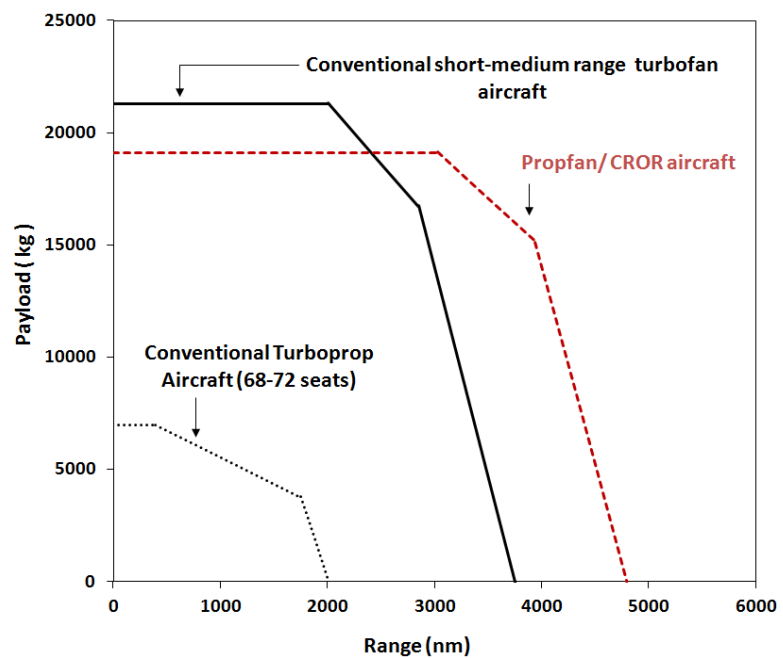


Fig 6.13 Payload range capability of aircraft with conventional propulsion and CROR propulsion

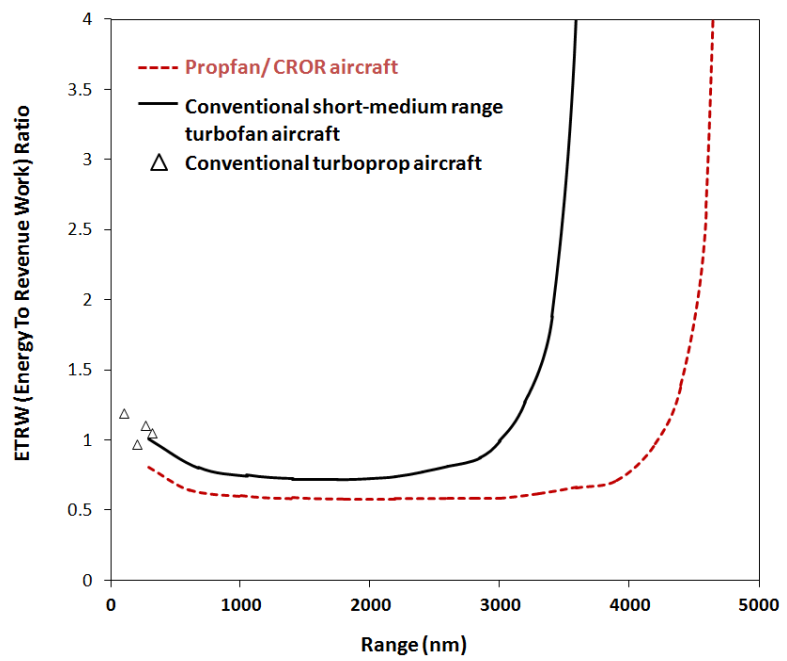


Fig 6.14 Energy efficiency curves of aircraft with conventional propulsion and CROR propulsion

The analysis begins by first calculating the mission fuel burn and time for the set of missions selected for both the aircraft. On each mission both aircraft are assumed to be carrying a payload of 19108 kg. This payload has been selected as it is the maximum common payload at which the capability of both aircraft can be compared. A summary of the fuel burn and time for the different missions of the conventional aircraft and relative change when the CROR aircraft is used is as illustrated in table 6.3.

Based on the mission fuel burn for both the technologies the operating cost model as described in section 4.6 is used to calculate the operating cost for the mission. At this stage apart from the fuel burn and mission time, all the other inputs for the operating cost model (which include the acquisition price and maintenance costs for both aircraft), are assumed the same for both technologies.

The operating cost is calculated for five different fuel price and emission ( $\text{CO}_2$ ) taxation scenarios as indicated in table 6.4. The first scenario is the BAU (Business As Usual) scenario reflecting the current fuel price and no taxation on  $\text{CO}_2$  emissions. The next three scenarios (BET, PEA and HEA) reflect the current levels of fuel pricing and an increasing level of  $\text{CO}_2$  taxation, while the HEA\_HFP scenario reflects a fuel price that has doubled, along with a high  $\text{CO}_2$  taxation level. It may be noted that the carbon taxation levels and fuel prices used in the scenarios have been selected in order to examine the progressive effects of increasing taxation and fuel prices to very high levels for the case under consideration.

The fuel burn and block time are then used to calculate the operating cost for the missions for both the technologies and a relative change in operating cost is estimated.

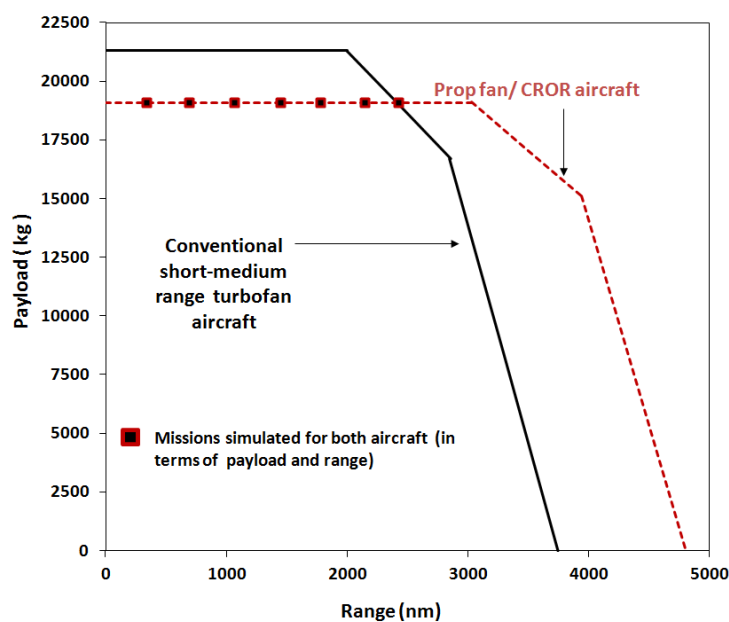


Fig 6.15 Representative missions selected for performance comparison of conventional TF aircraft and CROR aircraft

		Conventional TF aircraft	CROR/ Propfan aircraft				
	Range nm	Fuel burn (kg)	Flight_time (min)	Fuel burn (kg)	Flight_time (min)	%Improvement in fuel consumption	%Increase in flight time
1	344	2902	64	2060	65	29.0	1.9
2	697	4982	111	3559	115	28.6	3.6
3	1068	7130	160	5175	169	27.4	5.0
4	1450	9385	212	6884	224	26.6	5.6
5	1783	11390	257	8416	273	26.1	6.2
6	2148	13633	306	10140	326	25.6	6.5
7	2433	15420	345	11525	367	25.3	6.5

Table 6.3 Block fuel burn and time for representative missions

	Scenario	Fuel Price (\$/MT)	CO <sub>2</sub> (Tax \$/MT)
△	Business As Usual(BAU)	1062	0
○	Baseline Environmental Taxation (BET)	1062	25
✖	Progressive Environmental Awareness(PEA)	1062	250
✗	High Environmental Awareness(HEA)	1062	500
▲	High Fuel Price and Environmental Awareness (HFP_HEA)	2124	500

Table 6.4 Environmental taxation and fuel price scenarios considered

Fig. 6.16 demonstrates the relative benefits in fuel burn and operational costs, from using the CROR concept, for the five scenarios and the set of representative missions discussed earlier. The fuel burn reduction ranges from 21.8% to 29%, with the best fuel efficiency improvement being achieved for the shorter ranges. This is attributed to the lower equivalent cruise speed for the CROR aircraft (Mach 0.72) in comparison with that for the conventional TF aircraft (Mach 0.78). More specifically, as the trip range increases the time penalty of the lowered cruise speed is manifested by lowered reductions in trip fuel consumption. The predicted fuel savings and trends are similar to the ones presented in several studies sponsored by NASA in the 70s and 80s [6.11, 6.12].

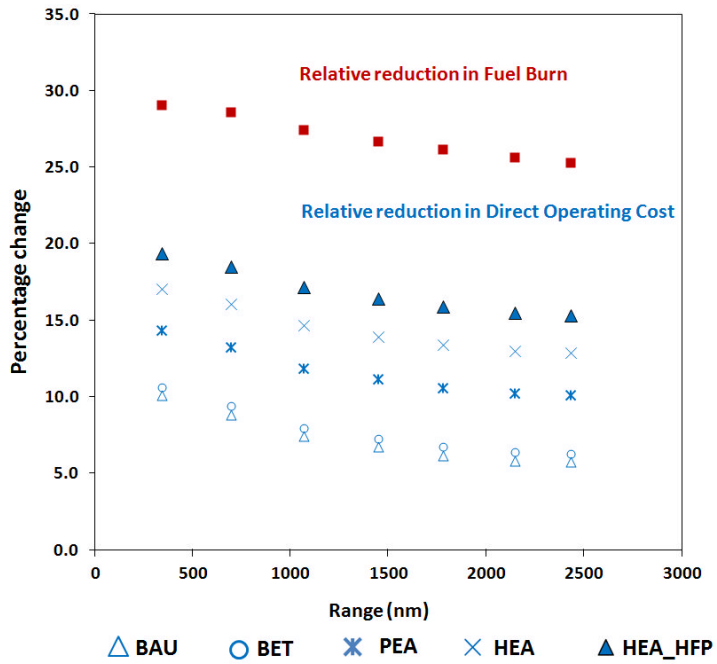


Fig 6.16 Relative fuel burn and operating costs for representative missions under various emission taxation and fuel price scenarios.

The improvement in operating cost for the BAU scenario is lower than the fuel consumption improvement, and varies from 10.1% to 5.8% for increasing range. This difference is attributed to the influence of time, fuel and emissions in the calculation of cost. In the BAU scenario the increased weight of the time dependent costs, coupled with the slight increase in block time for the CROR aircraft result in a lower impact of the fuel benefits on the operating cost. As the emission taxation and fuel price increase, the effect of fuel dependant costs increase and consequently the cost benefit improves. For example, as shown in figure 6.16, in a HEA\_HFP scenario the operating cost benefit has increased relative to the BAU scenario and now ranges from 19.4% to 14.1%. It has to be noted here that the DOC savings predicted for the BAU scenario are again in agreement with the figures reported in the literature [6.13], a fact that strengthens the confidence in the conducted modelling.

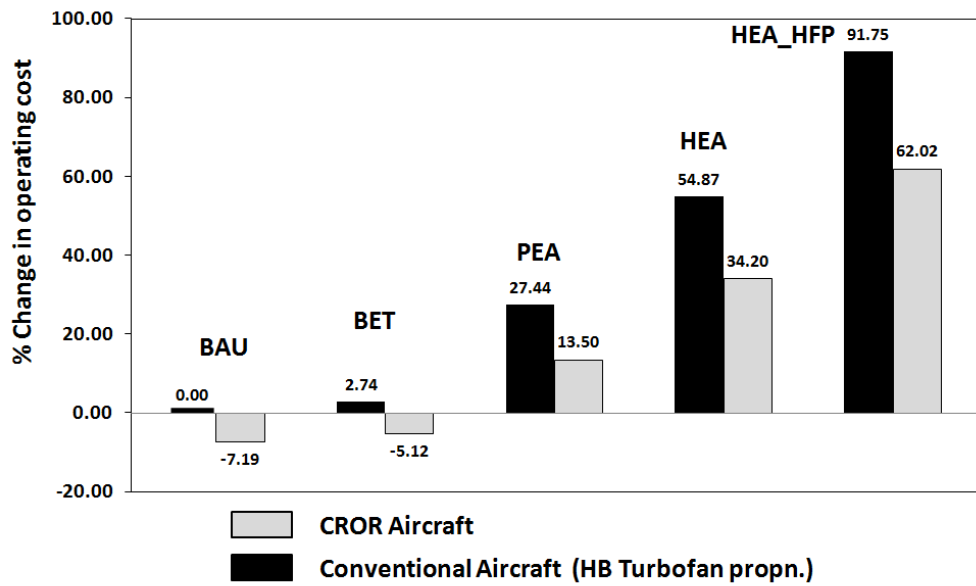


Fig 6.17 Variation in operating cost for scenarios, relative to the operating cost of the conventional TF aircraft in the BAU scenario, for a 697nm mission.

The benefits of the technology are further highlighted if the revenue potential of the technology is considered under higher taxation scenarios. As an illustrative example, the 697nm mission is considered.

Figure 6.17 shows the increase in operating cost of both the technologies for the scenarios considered, relative to the operating cost of the conventional TF aircraft in the BAU scenario. This comparison demonstrates the effect taxation and fuel price scenarios will have on the operating cost of both technologies when compared with the BAU scenario. It is observed that in a scenario of higher environmental awareness or fuel shortage, the operating cost of the conventional TF aircraft might increase up to 92% relative to the BAU baseline scenario. This would have an immediate impact on ticket prices, which would probably increase considerably. Although the CROR aircraft operating cost increases too, it is still 7% to 30% cheaper to operate. Hence such a scenario would render the CROR aircraft an attractive and economical option, which helps keep the air transport in a sustainable path.

## 6.7 INVESTMENT COST ANALYSIS APPROACH

### 6.7.1 INTRODUCTION TO THE APPROACH

The investment cost analysis module examines the effect of increased acquisition and maintenance costs on the relative change in operating cost, which is then plotted on an iso-cost contour plot. Figure 6.18 shows a typical contour plot.

The contour plots are essentially two dimensional plots that show one dimensional curves, on which a plotted quantity Z is a constant.

Each point on a contour plot signifies a solution's operating cost Z, with its position as a function of X, Y.

$X = \text{\% increase in Maintenance Cost}$

$Y = \text{\% increase in Acquisition Cost}$

$Z = \text{\% change in Direct Operating Cost}$

Where Direct Operating cost is a function of the flight block time, flight fuel burn, emissions ( $\text{CO}_2$ ), acquisition cost and maintenance costs, as discussed in the chapter 4.

At the datum (bottom left corner), the relative benefit in operating cost is calculated with the assumption that the novel technology has the same acquisition and maintenance costs with the baseline one, and the change in operating cost is primarily due to the difference in block fuel burn, block time and environmental emissions. However as the relative acquisition and maintenance costs increase, there is a corresponding decrease in relative improvement in operating cost which eventually diminishes to zero (as indicated by the black line in figure 6.18).

The investment analysis cost module is then used to analyse if the increase in acquisition cost or/and maintenance cost, and consequently the diminishing operating cost benefit is still viable economically. This is achieved by using the widely used economic assessment concepts of Net Present Value (NPV) and Internal Rate of Return (IRR).

Net Present Value (NPV) as defined by Raymer is the total of the net present values of all of the yearly operating profits during the life of the aircraft (usually taken to be the depreciation period)[6.14].

This concept is used in this module and hence, for a combination of increase in acquisition and maintenance cost, assuming a discount rate, the yearly profit from the difference in operating costs for the two competing technologies (considered as operating profits) is converted to the NPV. The NPV of each year, over the operational life of the aircraft, assumed as the payback

period is then summed up. For the investment to be profitable the sum of the NPV values over the life of the aircraft must be greater than the difference in acquisition cost incurred in procuring the new technology.

The IRR of a project is the discount rate at which the NPV is equal to zero and is a measure to evaluate if a project is economically viable. In investment terms, if a minimum required rate of return, essentially the Weighted Average Cost of Capital (WACC) is specified for the assessment then an IRR higher than the WACC will indicate towards a profitable investment. However if the IRR is lower than the WACC, the project is then deemed unprofitable and the investment may be considered infeasible.

The module, using a Newton-Raphson method, calculates the IRR of the investment by solving for the discount factor at which the NPV equals the difference in acquisition cost. Figure 6.19 indicates the methodology used to calculate the IRR.

If a minimum required rate of return – Weighted Average Cost of Capital (WACC) is specified for the assessment, the module calculates the area of the contour plot for which the IRR falls below the WACC. The shaded region in figure 6.18 is effectively where the IRR is lower than the WACC, and therefore the investment is not justified despite the lower DOC of the novel technology.

For any particular point on the contour, the NPV/IRR is calculated based on the following assumptions:

- Profit generated per year is calculated on a relative basis, from the difference in operating costs, derived from the percentage change in direct operating costs for the two competing technologies. This profit is then assumed constant through the lifespan of the aircraft.
- The discount rate or interest rates used to calculate the NPV is constant throughout the lifetime of the annuity.
- The competing solutions have the same economic life in terms of years.

Therefore for a mission of a particular range, and for a given fuel price and emission taxation scenario, each contour plot created provides information on the datum operating cost benefit and then illustrates the effect of increased acquisition and maintenance costs on the economic viability of the technology.

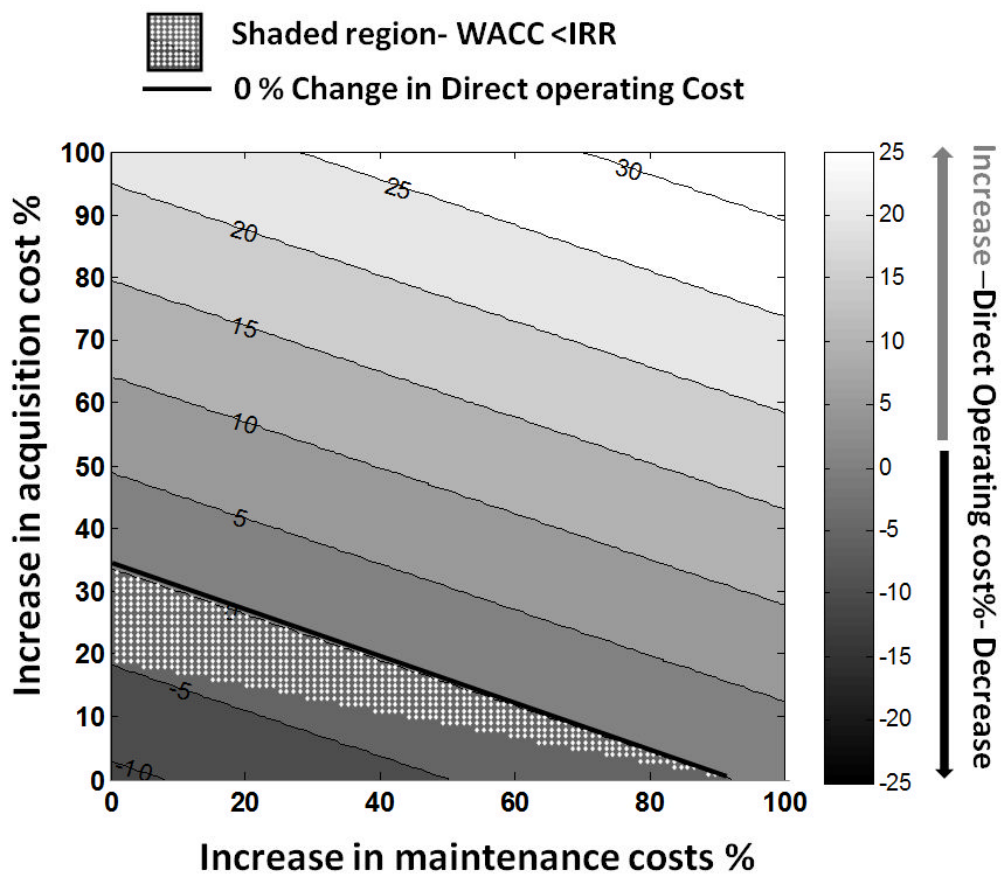


Fig 6.18 Illustrative example of investment cost analysis contour

**Initial cash outlay(ICO) =**  
Technology acquisition price difference

**Residual value(RV) =**  
End of life NPV of ~10% technology  
acquisition price difference

**$V_n$**  = Profit generated per year

**n** = Years in service

**x** = Discount factor

**$V_0$**  = Sum of Discounted Operating  
Profits

**NPV (Net Present Value) =  $f(x_z)$ =**  
 $V_0$  – Initial cash outlay+ Residual value

**IRR (Internal Rate of Return ) =**  
Discount factor at which value of NPV  
equals 0

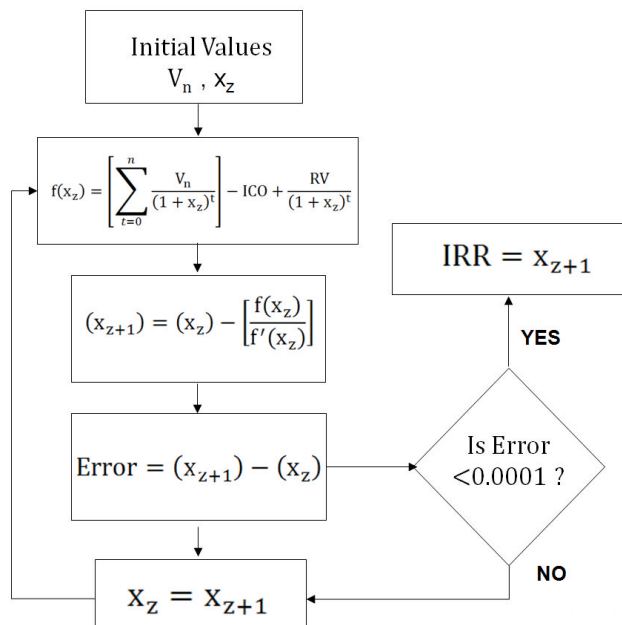


Fig 6.19 Methodology used to calculate Internal Rate of Return (IRR)

## 6.7.2 APPLICATION OF THE APPROACH

The promising potential of reducing the fuel burn and operating cost by using the CROR concept has been demonstrated.

However, as the reader may recollect, the operating cost calculated, was made under the assumption that the acquisition and maintenance cost for both technologies under consideration are equal. This section, through illustrated cases, examines the effect of increasing these costs on the operating cost benefit demonstrated earlier in section 6.6

Two cases are considered to examine the sensitivity of the operating cost reduction. The first analyses the effect of relative changes in acquisition and maintenance cost, for a set of missions of varying ranges, under a HEA\_HFP scenario. The second analyses the effect of a relative increase in acquisition cost (by 10%) for a short-range mission, under varying emission taxation and fuel price scenarios.

Case 1: Effect of mission range on the operating cost benefit for the HEA\_HFP scenario.

▪ The first case considers the effect of the mission range on the operating cost benefit for an extreme environmental scenario (HEA\_HFP- Fuel price and carbon tax assumed at US\$ 2124/ mt and US\$ 500/ton CO<sub>2</sub> emission respectively). Three missions of ranges 1450, 2433 and 697 nm have been considered for this case and for ease of reference, have been illustrated again in figure 6.20. The investment cost analysis module produced the operating cost contours for the three missions (as shown in figures 6.21, 6.23 and 6.24 respectively). Based on reference [2.35], the Weighted Average Cost of Capital (WACC) for all cases considered is assumed to be 7%. The shaded area on each plot indicates the non-feasible investment region, in which the IRR was found to be less than or equal to 7%. In order to illustrate the effect of increase in acquisition cost and maintenance cost, for each of three missions, three sub-cases are considered and are as follows :

- Sub-case A: Assumes 20% increase in acquisition and maintenance cost.
- Sub-case B: 35% and 40% increase in acquisition and maintenance cost respectively.
- Sub-case C: 45% and 10% increase in acquisition and maintenance cost respectively.

First considering the 1450 nm mission, figure 6.21 illustrates the effect of increasing acquisition and maintenance cost on the operating cost, for the HEA\_HFP scenario. The operating cost advantage at the datum (refers to 0-0 in figure 6.21) is 16.4%, as calculated previously by the operating cost module.

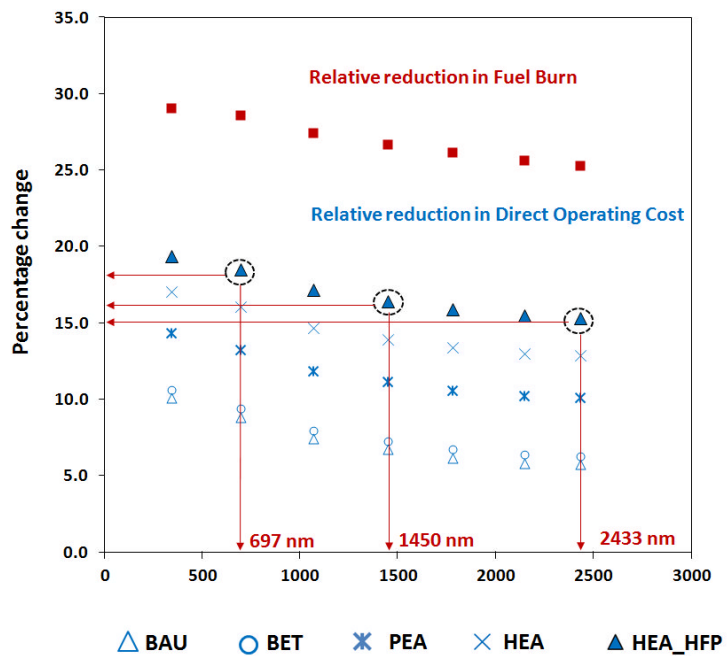


Fig 6.20 Case 1 missions illustrated (Reproduction of fig 6.16)

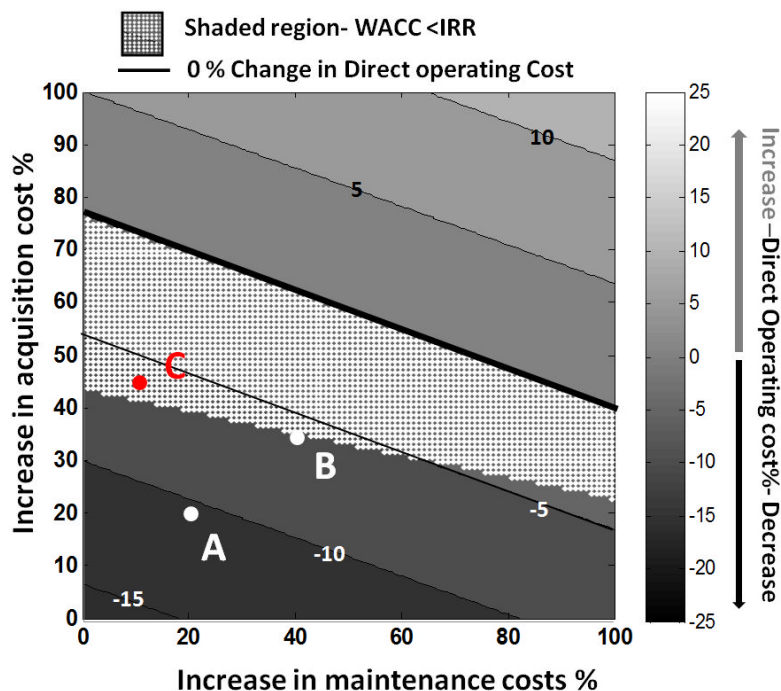


Fig.6.21 Investment cost analysis contour (mission range- 1450 nm, Scenario- HFP\_HEA, DOC% benefit at datum 16.4%)

When for the three sub cases of this mission, the NPV is plotted against the discount rate (figure 6.22) using the procedure discussed earlier, the IRR values calculated for

each of the three sub-cases are 30.9%, 7.4% and 4.72% respectively. Based on these values and on figure 6.21, the following observations can be made:

- The direct operating cost benefit of sub-case A (20% increase in acquisition and maintenance cost) has been reduced to 10.6% from the datum value of 16.4% due to the increased maintenance and acquisition costs. However, the technology is still profitable as the IRR is 30.9%, which is greater than the assumed WACC of 7% which leads to the point A lying outside the shaded non-feasible area in figure 6.21.
- In sub-case B (35% and 40% increase in acquisition and maintenance cost respectively) the direct operating cost improvement has dropped to 5.8% but the technology is still just profitable (lying outside the border of shaded non-feasible area) with an IRR of 7.4%.
- In the high acquisition and low maintenance cost sub-case C (figure 6.21) the DOC benefit (6.0%) is actually 0.2% higher than sub-case B. However the IRR is lower than required (4.72%) and the point falls inside the shaded region of (marked as red dot in figure 6.21). This happens because the increased acquisition cost is a current cost incurred when the aircraft is purchased, contrary to the direct operating cost benefits, which come as annual cash flows throughout the lifespan of the aircraft and thus have a lower present value.

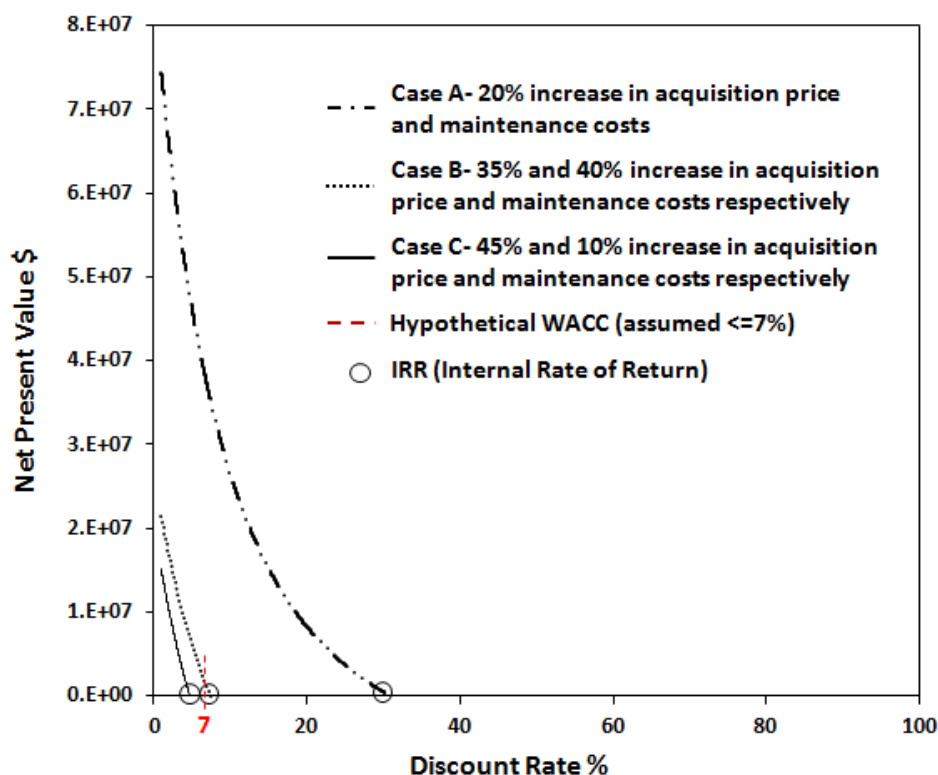


Fig.6.22 Verification of IRR calculation- NPV vs Discount rate curves

The case study shows that in order to translate the reduction in fuel burn to a benefit in operating cost and most importantly to an adequate IRR, the relative change in acquisition price and maintenance costs should be low. The acquisition cost seems to have a greater impact, mainly because it is a cost incurred today.

For the three sub-cases, when considered for a longer range of 2433 nm (contour plot in figure 6.23) and under the same environmental taxation scenario(HEA\_HFP), it is observed that for sub-case B and C, even though profitable in terms of operating cost, are in the non-feasible investment region (marked as red dots figure 6.23). However for the three sub-cases, when considered for a shorter range of 697 nm case under the same scenario, it is observed that for sub-case A, B and C, are all profitable in terms of operating cost, and are all within the feasible investment region (figure 6.24). This observation is further illustrated when the IRR for the sub-cases are plotted against the mission range (figure 6.25), where it is clearly seen that an increase in range decreases the achieved IRR.

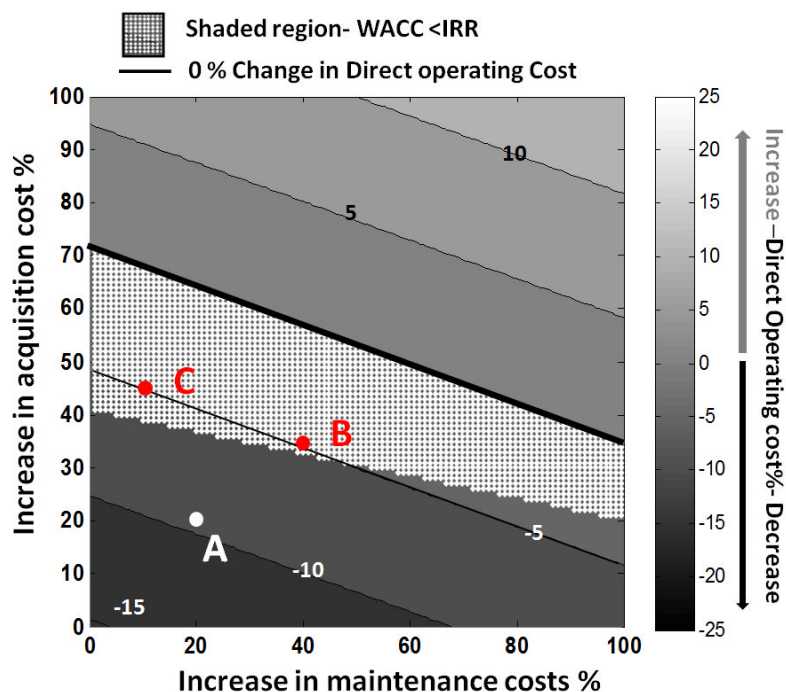


Fig.6.23 Investment cost analysis contour (mission range- 2433 nm, Scenario- HFP\_HEA, DOC% benefit at datum 15.3%)

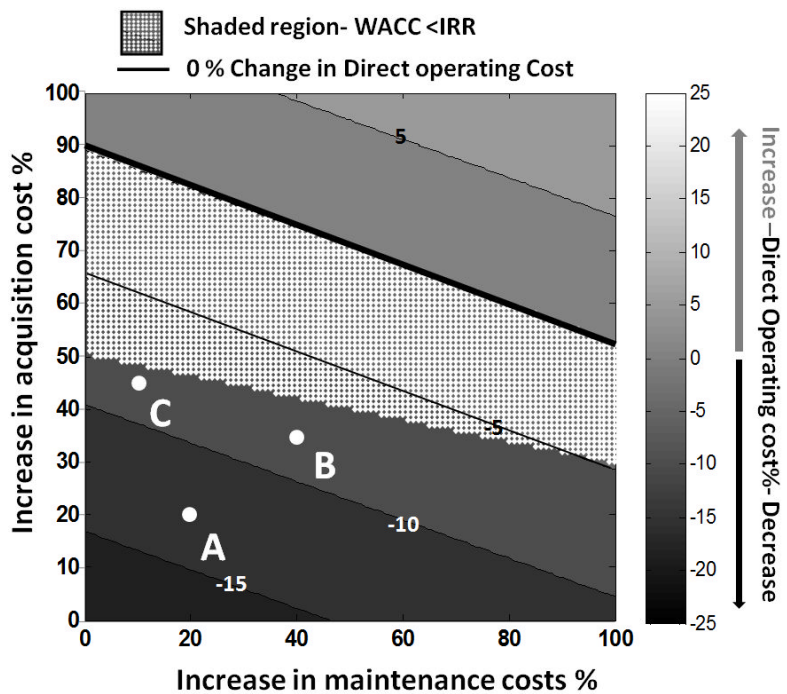


Fig 6.24 Investment cost analysis contour (mission range- 697 nm, Scenario- HFP\_HEA, DOC% benefit at datum 18.5%)

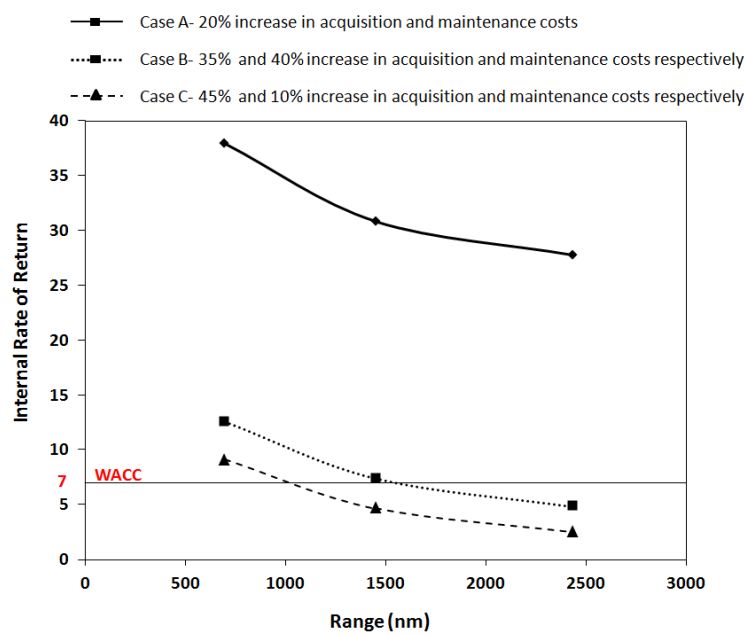


Fig 6.25 IRR analysis for various mission ranges

This phenomenon can be explained by referring back to figure 6.20. The technology is best suited for shorter ranges as the relative reduction in fuel burn is higher and time penalty is

lower and hence produces a relatively higher improvement in operating cost. With an increase in relative acquisition price and maintenance costs (as demonstrated in Case B and C) longer range missions become unprofitable (figure 6.25).

Case 2: Effect of an increase in acquisition cost for a 697nm mission, under varying emission taxation and fuel price scenarios.

Having established the higher benefit of the technology when applied to shorter ranges the next case examines the effect of an increase in acquisition cost for a 697nm mission, under varying emission taxation and fuel price scenarios. For illustrative purposes the study assumes an increase of 12.5%\*.

The fuel benefit accrued from using the CROR aircraft for the 697nm mission is shown to be 28.6% with an increase in time of 3.6% (Table 6.3). The DOC/IRR contour plots are created for the five scenarios as seen in table 6.4(figure 6.26.a to 6.26.e). For the selected increase in acquisition cost (12.5%), figure 6.27 separately shows the effect an increase in maintenance cost will have on the IRR.

In a BAU scenario with no increase in acquisition and maintenance cost, the cost contour shows a benefit of 8.81% in operating cost at the datum (figure 6.26a). If the acquisition cost were to increase by 12.5%, with no increase in maintenance cost, the benefit in operating cost will drop to 3.72%. Furthermore, as seen in figure 6.26a the point now lies in the non-feasible investment region as the IRR (6.42%) is lesser than WACC (may also be further seen in figure 6.27)

If this case were now to be considered under the BET taxation scenario, the cost contour (figure 6.26.b) shows an improvement of 9.4% in operating cost at the datum. With an increase in acquisition cost of 12.5%, the operating cost benefit would decrease to 4.41%, which is slightly higher than the BAU scenario for the same condition. On the other hand, the impact of the BET scenario on the IRR will be much higher, which is now equal to 9.1%. The solution therefore lies outside the shaded region and hence makes it a feasible investment option.

If according to the PEA, HEA and HEA\_HFP scenarios, the taxation and fuel price were to further increase, the benefits in operating cost would go up to 9.6%, 12.8% and 15.9% respectively, for the 12.5% increased acquisition cost case (figure 6.26.c, 6.26.d and 6.26.e).

This case study indicates that with the current fuel price and with no emission taxation (BAU scenario), a higher relative acquisition price (of 12.5%) will negate the fuel burn advantage of the CROR aircraft. This effect becomes more pronounced with a relative increase in maintenance costs. Therefore, an increase in acquisition price and maintenance cost will then necessitate a high level of taxation and/or fuel price (PEA, HEA and HEA\_HFP scenarios) to

\*An increase in acquisition cost by 12.5% is specifically chosen for illustrative purposes , as it happens to be the least relative increase in acquisition price of the CROR ,in the BAU scenario, to lie inside the shaded non-feasible area for the case see figure 6.26A

translate the benefits of reduced fuel burn to operating costs and thus render the CROR technology economically viable.

If the focus now turns to the maintenance cost effect, the following comments can be made. As the acquisition cost increases, the maximum maintenance cost that still gives a solution in the feasible region falls. This means that engines with lower acquisition cost are allowed to have a much higher maintenance cost before they become unprofitable. Furthermore, figure 6.27 indicates that as the emission taxation and fuel price increase, the effect of maintenance cost on the operating cost reduces. From the PEA, HEA and HEA\_HFP scenario contours (figure 6.26 c, d and e) it is observed that if the acquisition cost increase is below 3%, 12.2% and 30% for the three scenarios respectively, then even with a 100% increase in the relative maintenance costs, the operating cost benefit decreases, but still remains profitable (IRR remains greater than WACC). This may have important implication on the engine design. Under these scenarios engine designs could be optimised for very high fuel efficiency and low emission, by sacrificing the engine life and increasing by choice the maintenance costs.

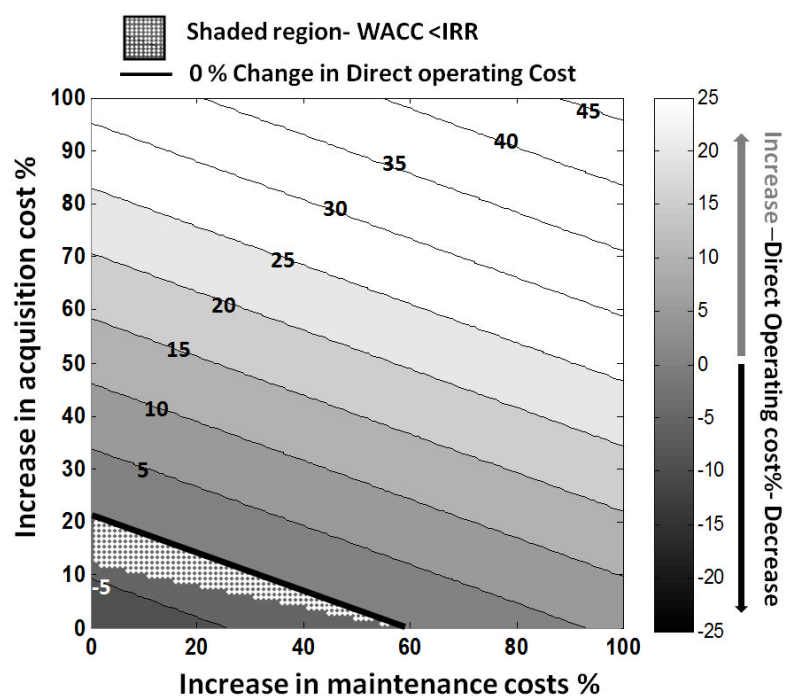


Fig 6.26.a Investment cost analysis contour (mission range- 697 nm, scenario- BAU, DOC% benefit at datum 8.8%)

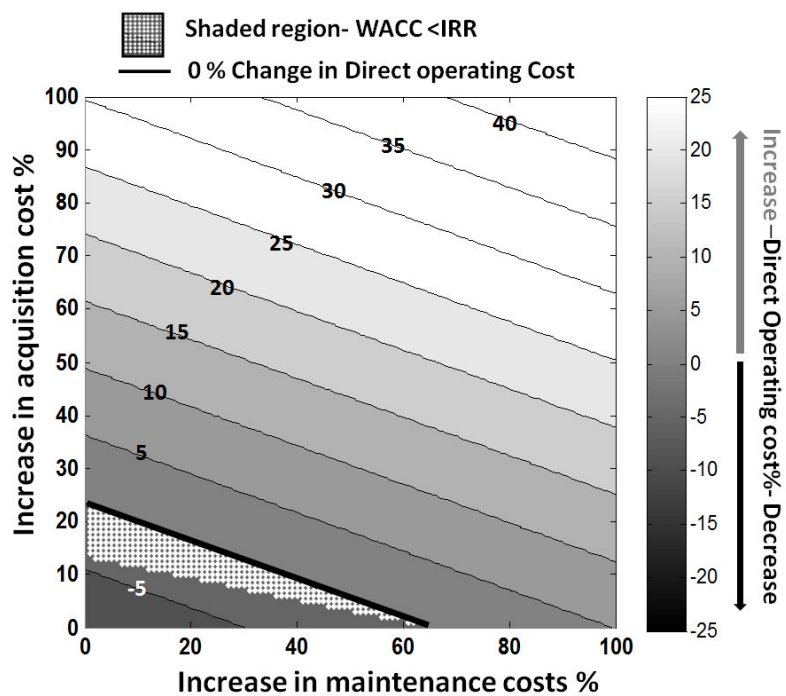


Fig 6.26.b Investment cost analysis contour (mission range- 697 nm, scenario- BET, DOC% benefit at datum 9.4%)

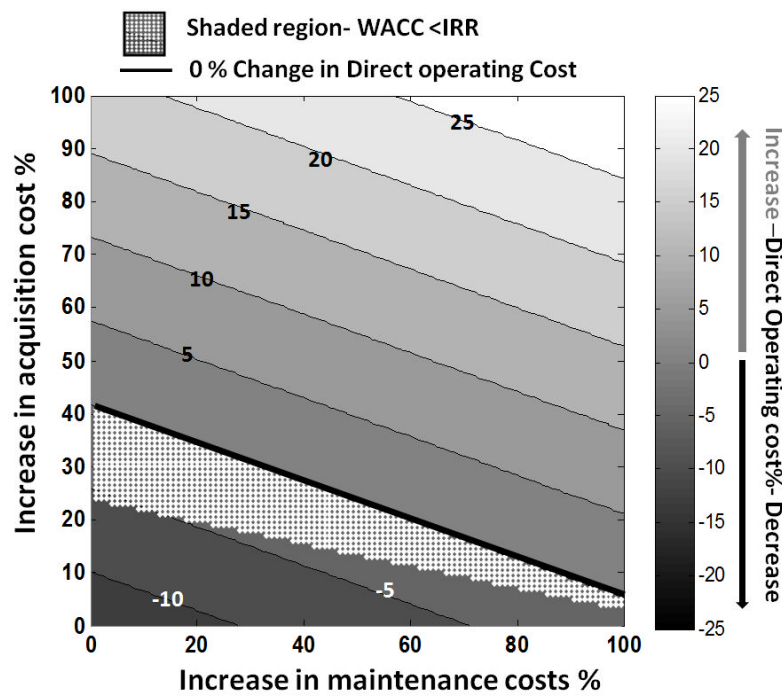


Fig 6.26.c Investment cost analysis contour (mission range- 697 nm, scenario- PEA, DOC% benefit at datum 13.2%)

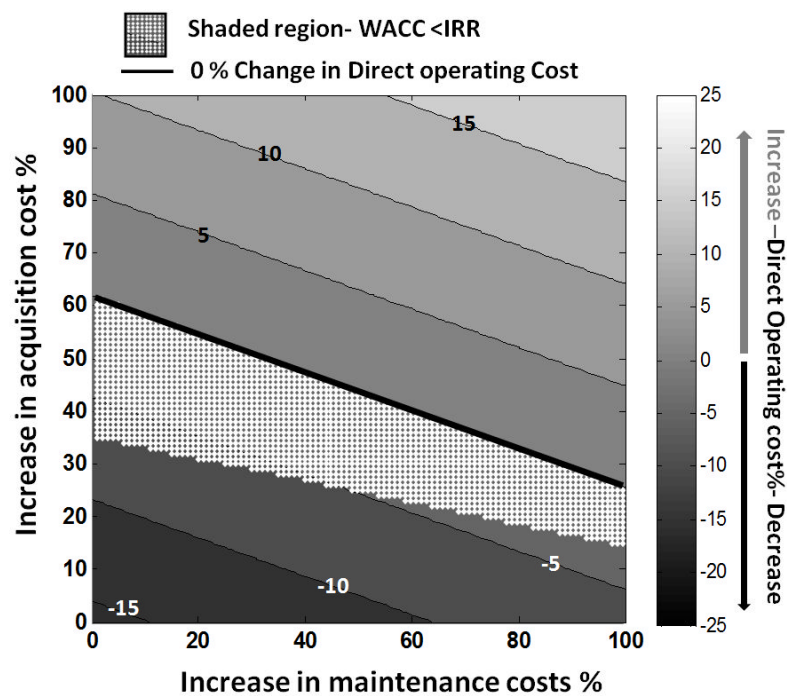


Fig 6.26.d Investment cost analysis contour (mission range- 697 nm, scenario - HEA, DOC% benefit at datum 16%)

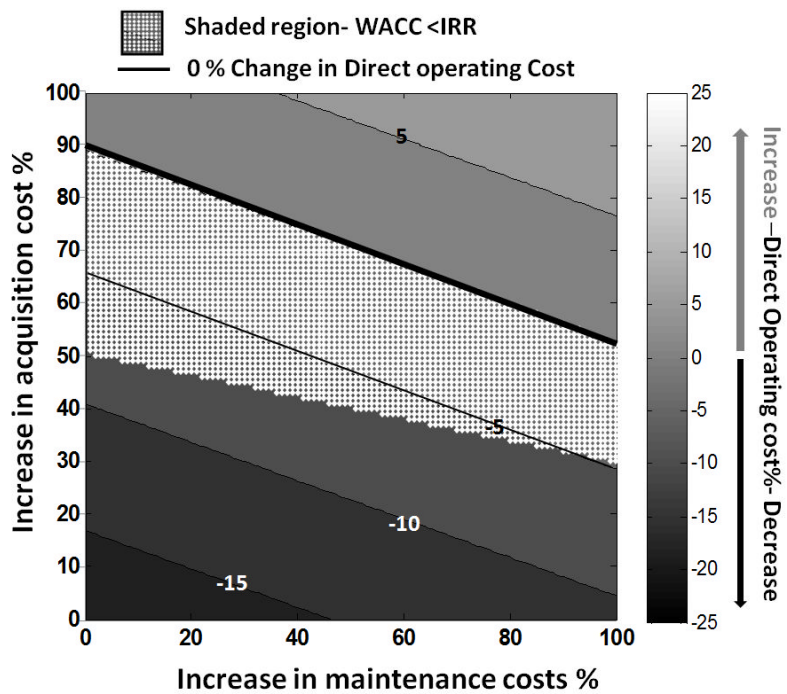


Fig 6.26.e Investment cost analysis contour (mission range- 697 nm, scenario- HEA\_HFP, DOC% benefit at datum 18.5%)

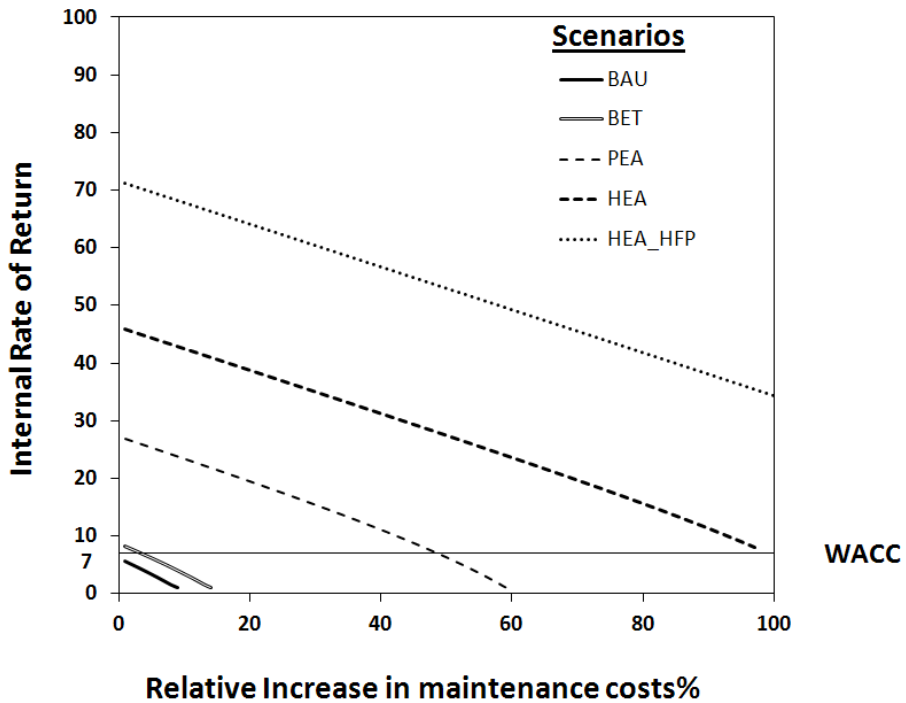


Fig 6.27 Effect of maintenance cost on IRR for different scenarios and a case of 12.5% increase in acquisition price (mission range: 697nm)

## 6.8 CONCLUSIONS

A methodology was presented to assess the viability of a new technology relative to a conventional technology in civil aviation. Using a TERA framework, the methodology first establishes the benefit in terms of performance and energy efficiency. It then examines, for various emission taxation and fuel price scenarios, the effects of relative increase in acquisition price and maintenance costs on economic viability.

A proof of concept of this methodology was demonstrated by assessing the viability of the CROR aircraft as a competitor to a short to medium range conventional TF aircraft. The payload-range performance and energy efficiency assessments initially establish the suitability of CROR aircraft. The study then simulates the performance of the aircraft for a set of typical short to medium range missions.

The CROR concept, by virtue of high propulsive efficiency, has been proven to reduce fuel burn in comparison to a conventional TF aircraft. This effect is demonstrated over the set of missions chosen, by the relative reduction in fuel burn which ranged from 25.3% to 29%. The highest fuel burn reduction is observed for the shortest missions, with a reduction in the

benefit over longer missions. This was attributed to a time penalty due to slower cruising speeds in comparison to the conventional TF aircraft, and hence longer flight time.

When the fuel burn was translated to operating costs for the simulated missions, it resulted in a much lower relative benefit in terms of cost, ranging from 5.7% to 10.1%, for a current fuel price (1062 \$/mt) in the absence of environmental tax environmental tax scenario (BAU scenario).

For a mission, the direct operating cost is essentially a function of the cost of time, fuel and emission dependant variables. Therefore in the absence of emission taxation and at the current fuel price, as assumed in the BAU scenario, the time variable has a more influential effect and hence the time penalty of slower cruising speeds results in a low operating cost benefit.

As the emission taxation and fuel price increases, the influence of fuel and emission dependant variables on the operating cost consequentially increase. The lower fuel burn then results in the improvement of the relative benefit in terms of operating cost. It is therefore observed that in the high fuel price and emission taxation scenario (HEA\_HFP scenario), the operating cost benefit reaches highs of 15.3% to 19.3%, thus making the technology more economically viable.

The direct operating cost of the conventional baseline aircraft could increase by more than 90% in the HEA\_HFP (high environmental awareness and high fuel price) scenario as compared to the BAU (business as usual) scenario. The CROR concept could then be seen as an economically attractive solution, which offers cost reductions up to 30% and hence help to retain reasonable ticket prices.

The operating cost benefit was established based on the assumption that the acquisition price and the maintenance costs of both conventional and novel technologies were equal. However, the investment analysis module further assesses the sustainability of the economic benefit demonstrated, under the effect of relative increases in acquisition and maintenance costs. Some of the key observations are as follows:

- In order to translate the reduction in fuel burn to a benefit in operating cost the relative change in acquisition price and maintenance costs should be low for all scenarios.
- In short-range missions the profitability of the CROR concept is more resistant to increases in acquisition price and maintenance cost, as the fuel benefits are higher in that case.
- Based on the modelling assumptions, at the current fuel price and with no emission taxation (BAU scenario), a higher relative acquisition price (of 12.5%) will negate the fuel burn advantage of the CROR aircraft. This effect becomes more pronounced with a parallel increase in the maintenance cost.
- For the high emission taxation and fuel price scenarios (HEA and HEA\_HFP) there is limited influence of maintenance costs. This has important implications on engine design.

Engines could be designed for high efficiency by sacrificing the engine life and accepting an increase in maintenance costs.

- In the BAU (business as usual scenario) an increase in relative acquisition price and maintenance cost could make the CROR technology unprofitable, despite its fuel benefits. If the policy makers wanted to direct the industry towards the greener CROR solution, they could increase the emission taxation thereby making the operation of CROR technology economically beneficial and hence a preferred option.

Finally, it has to be noted once more that this case study aims to demonstrate the wealth of interesting insights offered by the proposed method, and not to analyse thoroughly the CROR concept. This would require a more detailed investigation of aircraft design, engine performance, noise, life and integration.

## 7 DISCUSSION AND CONCLUSION

### 7.1 BACKGROUND

ICAO identifies global economic growth, reducing ticket prices and market liberalisation within the aviation industry as the key drivers of growth in the aviation industry. Reducing cost of fares is primarily attributed to improved aerospace technology, which has enabled airline operators to operate and manage their assets more economically and efficiently, hence resulting in air passengers being the end beneficiaries, through lower and more affordable ticket prices. Additionally, market liberalisation introduced, increased airline competition and hence again the customers benefited from the lowest and competitive ticket pricing. The net result of the combination of these factors, have resulted in enabling people from all incomes to travel more. As reference [2.4] claims, these factors have caused a growth significantly larger, than that which may have been created by economic growth alone.

Over the years, the industry has consistently invested in improving aerospace technology and infusing it into commercial application, with an aim to always remain profitable. With fuel expenses being a significant part of an airlines operating cost, the core focus of technology development has been to constantly improve fuel economy, whilst maintaining Landing and Takeoff (LTO) cycle noise and NO<sub>x</sub> within certification limits and improving safety and reliability. Consequently today's aircraft are known to utilise 80% lower fuel, create 75% less noise than fifty years ago, yet carry twice as many passengers with increased safety and at much lower Direct Operating Costs (DOC) [2.2]. Such an improvement in performance and efficiency in an industry is truly remarkable in terms of progress.

There exist various futuristic predictions of further growth within the aviation industry and most estimates average around 4.8% and 5.5% per year through the year 2036 [2.1, 2.4]. Irrespective of an absolute number in terms of percentage, and given the past trends observed of the industry being resilient against calamities, disasters and economic downturns, a constant growth of the industry is an indisputable fact.

The current level and future predicted increase in air traffic has therefore brought into focus amongst others, two important aspects that will be critical in the future- The fuel consumption by the aircraft needed to cater for the increased number of passengers and the environmental impact of aviation related emissions. This therefore leads to the fact that for a sustainable future, significant and continued improvements will need to be introduced to balance the underlying growth within the aviation industry.

Consequent to these environmental concerns, organisations like the ICAO have set up ambitious environmental goals to enable the industry to achieve a carbon neutral status by 2020 and further achieve a 50% reduction in CO<sub>2</sub> emissions by 2050 (compared to the year 2005). In line with these goals various research programs have been launched around the

world, which aim to achieve these environmental targets by implementing improvements through every aspect of civil aviation and through the lifecycle of the civil aircraft. Broadly, these initiatives include improvements of current technology, operations and infrastructure, application of bio-fuels as a substitute to fossil fuels and introduction of economic measures (through emission trading schemes and environmental taxation). However, introduction of any of these environmental initiatives, will inadvertently affect the operating cost and hence the profitability.

Economic survival of an airline operator (and sustainability of civil aviation as an industry), as any other industry, depends on the elasticity of demand for the product, a good safety record and profitability (through minimising operating costs). Therefore in a fragile and highly sensitive financial environment, assessing and understanding the economic implications of the introduction of any of the initiatives currently being focussed upon, is paramount.

The focus of this PhD. was to create a Techno-economic Environmental Risk Assessment (TERA) framework to enable assessments of three of these initiatives from a fleet planning and operations perspective– improvement of operations through optimisation of flight trajectories with respect to specific operational and environmental objectives, implementation of a novel technology and introduction of economic measures.

## 7.2 SUMMARY OF WORK AND DISCUSSION ON FINDINGS

### 7.2.1 POLICY ASSESSMENTS – OPTIMISED OPERATIONS

Reference [2.26] indicates one of the most effective methods of reducing civil aviation's environmental impact is through enhanced and effective flight management. The reference further suggests that this will result in the reduction of the total CO<sub>2</sub> emissions (in tons) produced by civil aviation between the period of 2008 and 2020 by approximately 50 million tons, than if no initiative is taken at all.

The first part of work therefore, approaches the subject from an operations perspective wherein it initially establishes an environmental gain through application of concepts of optimised flight trajectories. It then introduces a methodology based on an operational cost analysis approach to examine the actual economic feasibility of the optimised trajectories in today's fuel price scenario. It further goes on to examine the effect that future CO<sub>2</sub> taxation policies will have on the acceptance of trajectories and in turn establish the taxation rate that may be required to force an operator to switch from a conventional trajectory to more environmentally friendly trajectories.

A set of short-medium range missions (227nm, 815nm and 1614 nm) and suitable aircraft (and engine) were first selected for the study. To establish a frame of reference, the baselines trajectories for the selected missions were simulated, and verified against the performance of

the original aircraft on the payload range chart. The analysis of the baseline trajectories indicate, trajectories when executed are 1.3% to 4% higher in fuel burn than the trajectories optimised specifically for fuel burn.

Currently flown mission trajectories by civil aircraft, in controlled airspace, are limited primarily by the operational and technical procedures /regulations of air traffic management and by airline policy and hence are not able to achieve the design efficiency in terms of fuel burn. Air traffic management systems are aimed at ensuring traffic separation, whilst providing protection with respect to terrain and a structured and predictable framework for traffic control. This therefore results in aircraft having to revert to highly constrained routes, usually following speeds and altitudes that are sub optimal and hence requiring the aircraft to climb and descend in a series of steps which are not environmentally friendly (or energy efficient). Airline policy, on the other hand, due to overall network considerations, such as connections in a hub and spoke network or crew duty limits , may revert to a suboptimal trajectory even though they may still be able to achieve reduced environmental footprint in a mission.

From the baseline trajectory analysis, It is therefore opined that if even with currently maintained standard speed restrictions, as set in the baseline trajectory, the aircraft will still be able to achieve reasonable efficiencies (as demonstrated in the baseline cases), if allowed to climb/ descend continuously and cruise at optimal (or close to optimal) altitudes).The study also further demonstrates that in order to achieve the optimal fuel burn as demonstrated through the trajectory optimisation runs, the aircraft will necessarily require a significantly higher flexibility in terms of continuous speed and altitude evolution at various phases in flight. This will entail a reconfiguration of the control configuration of the aircraft and accompanied with a highly enhanced air traffic management system. Such air traffic management systems are currently being extensively researched by programs such as SESAR and Clean Sky [4.1].

However, as indicated earlier one of the most critical factors for sustainability in commercial aviation is cost effective operations. The time of the mission therefore is an important factor when it comes to cost and hence airlines apart from adhering to non flexible and sub optimal (w.r.t fuel burn) trajectories, necessarily trade-off fuel economy for mission time by flying at further sub optimal (w.r.t fuel burn) conditions. This was further proven from analysing optimised trajectories, which effectively showed the gain in time is found at an expense of fuel.

Most airframers recommend the cost index method of flying. The Cost Index (CI) as discussed earlier, in the operational sense is effectively the ratio of the cost of time dependant variables of a mission and the cost of fuel, hence reflecting the relative effects of cost of fuel as compared to time in the operating costs. Reference [3.14] indicates that for a similar aircraft type as modelled (Boeing 737-800) the ideal cost index ranges from 0-500, with 0 being selected when fuel costs are high in comparison to other costs. A study in the same reference indicates that when a similar aircraft type (all Boeing 737 models) was evaluated in an airline fleet, it indicated that the fuel optimal CI was determined to be 12, the current cost index used

was observed to be 45. A shift to the lower CI would have resulted in a +3 minutes impact on time of the mission.

Similar observations are made from the optimisation study for the short range. The optimisation indicated that the least expensive trajectory is the time optimised trajectory as the cost of time dependant variables are high. When compared with the fuel optimised trajectory, this resulted in a 15% higher fuel burn (300 kg), a 10% improvement in time (4.7 minutes) and consequently improves the operating cost of the mission by 3.7%.

If one were to then consider cases of the short to medium (884 nm) and medium ranges (1614 nm) the cost of time optimised missions were almost the same as the fuel optimised missions (in terms of operating cost the time optimised mission was 0.2% and 0.37% higher, respectively). This indicates that with constraints such as premium time slots at a destination, the operator may prefer to fly a time optimised trajectory, which will have a limited impact on operating cost as seen but will have a significant environmental impact due to a higher fuel burn (28.3% and 32.5% respectively) and correspondingly produce higher carbon emissions.

If one were to now compare the optimal operating cost trajectory with the optimal fuel burn trajectory, for the assumed fuel price scenario (US\$ 1098/ mt), the trajectory was found to be a trade-off between fuel and time. Analysis of the trajectories indicated that the operating cost improved by 5.65% and 6.8% relative to the optimal fuel burn trajectory, primarily by an improvement of mission time (a gain of 15 and 34 minutes respectively) and at the expense of 4 and 4.4% higher fuel burn. If we were to convert this excess fuel burnt to CO<sub>2</sub> emissions, it ranges for the two trajectories from 1124 and 2269 tons of excess CO<sub>2</sub> per year.

To illustrate the effect of this one can consider Ryanair currently operate a fleet of 272 aircraft of the type modelled [3.19]. Hence if calculated over an entire fleet, assuming that these are the typically representative missions of the fleet, it would then result in an excessive CO<sub>2</sub> emission of between 305,728 tons to 617,168 tons per year.

The optimisation studies further revealed that NO<sub>x</sub> optimised trajectories were also found to be environmentally efficient in terms of CO<sub>2</sub>. NO<sub>x</sub> optimised trajectories when analysed and compared with the optimal fuel burn trajectories, were found to be typically high altitude, low power setting trajectories in climb and cruise (attributable to lower speeds at cruise) and hence varied in fuel consumption by just 0.5% and 0.8% (when compared with the optimal fuel burn trajectory). However for the three ranges, these trajectories were found to be more expensive in terms of operating cost (varying between 5% and 10%) than the optimal operating cost trajectory.

As it may be seen the revamping of the air traffic management system will definitely be beneficial in reducing emissions by effectively allowing aircraft to fly more flexible and environmentally friendly, in terms of CO<sub>2</sub> and NO<sub>x</sub> emissions. However, as discussed when compared with the current optimal operating cost trajectory, these fuel burn optimal

trajectories are observed to be 3.7% to 6.8% more expensive trajectories to fly at today's fuel price (assumed at US\$ 1098/ mt) and no prevailing CO<sub>2</sub> taxation scenarios. If the percentages were converted to economic values they result in an increase in operating cost, and depending on the mission range considered, ranges from US\$ 0.56 million to US\$ 3.5 million per aircraft. The pertinent question then is- What policy will actually cause the operational shift to greener solutions? The intuitive answer is taxation!

The next phase of the study was the development of a tool to analyse and assess the economic viability of the optimised set of solutions for environmental and operational objectives, under various taxation policies and scenarios. The tool, with the help of two graphical plots, provides an assessor with key information. Firstly, for any particular fuel price and taxation scenario and in comparison to a prior established baseline solution, it enables identifying amongst a set of optimised solutions (as seen in the previous section), the most economically viable. Secondly, when certain key solutions are picked from an optimised set, it enables identifying the effect a changing taxation scenario will have on the economic viability of each of these solutions. It therefore enables the assessor to identify a 'cross-over' taxation rate that may be necessarily required to enforce a switch from currently flown cost effective trajectories to environmentally greener trajectories. At such a taxation rate, it further enables the assessor to gauge the overall increase in operating cost of the baseline trajectory, thus providing an indication on the practicality of such a tax.

For the previously discussed missions (short range (227 nm), short-medium range (815 nm) and medium range (1614 nm), the framework and the policy module were further used to analyse the optimal set, in a scenario wherein the fuel price of US \$ 1098/Mt and baseline tax of US \$25/ton of CO<sub>2</sub> emission are assumed. The key observations included the following:

- a. Effect of a baseline CO<sub>2</sub> emission tax (US \$25/ton): For the three ranges considered (227nm, 815nm and 1614 nm), when the best fuel solution was compared against the optimal cost solution under no prevailing CO<sub>2</sub> tax, it was found that the differences in cost were 3.76%, 5.65% and 6.83% respectively, thus making the optimal cost trajectory more economically attractive. The line plots (figure 5.14, 5.6 and 5.20 respectively) further indicate that when the baseline CO<sub>2</sub> emission tax of US\$ 25/ ton is applied, the difference reduces marginally to 3.4, 5.4 and 6.55% respectively. However this would result in the operating cost of the baseline solution increasing as (ranging from 1.85 to 2.75%) as the mission range increases.
- b. Establishing the 'cross-over' taxation rate: This is effectively defined as the taxation rate at which cost of operating the initially found optimal operating cost trajectory will be equal to cost of operating the fuel optimal trajectory. The line plots (figure 5.14, 5.6 and 5.20 respectively) indicate that as the mission range increases, the level of taxation will have to be considerably increased (from 14 times to 60.5 times the baseline taxation level), thus driving

up the taxes, to vary from US\$ 350/ton to US\$ 1512/ton of CO<sub>2</sub> emissions. This in turn will result in the increase of the operating cost of the baseline trajectory to increase by 25% to 160% over today's no taxation scenario.

- c. Effect of increase in fuel price on the taxation rate for the same cross over point: The analysis shows that an increase in fuel prices would result in 'cross-over' taxation rate being reduced. An illustrative example may be seen in the 815 nm case (figures 5.6 and 5.11). When the fuel price was assumed to be US\$ 1098/mt, the taxation level at the cross over point is found to be US\$ 1375/ ton CO<sub>2</sub> emissions (55 times the baseline tax), however when the fuel price was increased by 50% (US\$ 1647/mt) the cross-over taxation rate dropped to US\$ 1200/ ton CO<sub>2</sub> emissions (48 times the baseline tax).
- d. Diminishing influence of time variable on operating cost: A significant observation from the plots is that, as higher rates of taxation are applied the influence of the time variables continually decreases and hence results in the cost curves becoming increasingly parallel to the x axis (figure 5.14, 5.6 and 5.20). This indicates a finite effect of the level of taxation and hence considering taxation levels up to the cross over point may then only be prudent.

#### 7.2.2 POLICY ASSESSMENTS – TECHNOLOGY

The second part of the study looks at the subject from the perspective of induction of novel technologies. It again introduces another methodology. Based on set of specific assessments, the methodology compares a novel technology with a competing conventional solution, and establishes its benefits in terms of performance and energy efficiency. These studies are undertaken for various emission taxation and fuel price scenarios to further establish if the observed efficiency may be translated to improvements in operating cost. The focus of the work is to then utilise these assessments and concepts of Net Present Value (NPV) and Internal Rate of Return (IRR) in an investment cost analysis approach. The aim is to answer questions from a policymaker's or airline operator's perspective, on the issue of whether the technology can translate efficiency to operating profits, sufficient to supersede what's already on the market and thus offset a higher acquisition price and complexity of aircraft. Alternatively, what taxation or fuel price scenario will establish its viability and actually justify a technology shift from a conventional solution, given a particular acquisition and maintenance cost?

A proof of concept of this methodology was demonstrated by assessing the viability of the CROR aircraft as a competitor to a short to medium range conventional TF aircraft. The payload-range performance and energy efficiency assessments initially establish the suitability of CROR aircraft. The study then simulates the performance of the aircraft for a set of typical short to medium range missions.

The CROR concept, by virtue of high propulsive efficiency, has been proven to reduce fuel burn in comparison to a conventional TF aircraft. This effect is demonstrated over the set of missions chosen, by the relative reduction in fuel burn which ranged from 25.3% to 29%. The highest fuel burn reduction is observed for the shortest missions, with a reduction in the benefit over longer missions. This was attributed to a time penalty due to slower cruising speeds in comparison to the conventional TF aircraft, and hence longer flight time.

For the study, five scenarios were selected and include

- BAU scenario (Business As Usual) – Fuel Price assumed at US\$ 1062/mt and no taxation
- BET scenario (Baseline Environmental Tax) – Fuel Price assumed at US\$ 1062/mt and CO<sub>2</sub> emission taxation at US\$ 25/ ton
- PEA scenario (Progressive Environmental Tax) – Fuel Price assumed at US\$ 1062/mt and CO<sub>2</sub> emission taxation at US\$ 250/ ton
- HEA scenario (High Environmental Tax) – Fuel Price assumed at US\$ 1062/mt and CO<sub>2</sub> emission taxation at US\$ 500/ ton
- HEA\_HFP scenario (High Environmental Tax and High Fuel Price) – Fuel Price assumed at US\$ 2124/mt and CO<sub>2</sub> emission taxation at US\$ 500/ton

When the fuel burn was translated to operating costs for the simulated missions, it resulted in a much lower relative benefit in terms of cost, ranging from 5.7% to 10.1%, for a current fuel price (1062 \$/mt) in the absence of environmental tax environmental tax scenario (BAU scenario).

For a mission, the direct operating cost as seen earlier is essentially a function of the cost of time, fuel and emission dependant variables. Therefore in the absence of emission taxation and at the current fuel price, as assumed in the BAU scenario, the time variable has a more influential effect and hence the time penalty of slower cruising speeds results in a low operating cost benefit.

As the emission taxation and fuel price increases, the influence of fuel and emission dependant variables on the operating cost consequently increase. The lower fuel burn then results in the improvement of the relative benefit in terms of operating cost. It is therefore observed that in the high fuel price and emission taxation scenario (HEA\_HFP scenario), the operating cost benefit reaches highs of 15.3% to 19.3%, thus making the technology more economically viable.

The direct operating cost of the conventional baseline aircraft could increase by more than 90% in the HEA\_HFP (high environmental awareness and high fuel price) scenario as compared to the BAU (business as usual) scenario. The CROR concept could then be seen as an economically attractive solution, which based on the modelling assumptions offers potential cost reductions up to 30% and hence help to retain reasonable ticket prices.

The operating cost benefit was established based on the assumption that the acquisition price and the maintenance costs of both conventional and novel technologies were equal. However, the investment analysis module further assesses the sustainability of the economic benefit demonstrated, under the effect of relative increases in acquisition and maintenance costs. Some of the key observations are as follows:

- In order to translate the reduction in fuel burn to a benefit in operating cost, and hence make the technology a viable option, the relative change in acquisition price and maintenance costs should be low for all scenarios.
- In short-range missions the profitability of the CROR concept is more resistant to increases in acquisition price and maintenance cost, as the fuel benefits are higher in that case.
- Based on the modelling assumptions, at the current fuel price and with no emission taxation (BAU scenario), a higher relative acquisition price (of 10%) will negate the fuel burn advantage of the CROR aircraft. This effect becomes more pronounced with a parallel increase in the maintenance cost.
- For the high emission taxation and fuel price scenarios (HEA and HEA\_HFP) there is limited influence of maintenance costs. This has important implications on engine design. Engines could be designed for high efficiency by sacrificing the engine life and accepting an increase in maintenance costs. This however may have additional implications and a possible increase in capital costs due to the requirement of replacing engines before the airframe is retired.
- In the BAU (business as usual scenario) an increase in relative acquisition price and maintenance cost could make the CROR technology unprofitable, despite its fuel benefits. If the policy makers wanted to direct the industry towards the greener CROR solution, they could increase the emission taxation thereby making the operation of CROR technology economically beneficial and hence a preferred option.

This case study aimed to demonstrate the wealth of interesting insights offered by the proposed method, and not to analyse thoroughly the CROR concept. This would require a more detailed investigation of aircraft design, engine performance, noise, life and integration.

### 7.3 CONCLUSION

The key contribution to knowledge from this PhD was to develop, implement and demonstrate methodologies to better understand the effect that environmental taxation in the future may have on the adaptation of optimised operation methods and novel technologies, which will be aimed specifically at reducing the aviation industry's impact on the environment.

With regard to optimised operations, a methodology introduced for assessments, demonstrated that carbon taxation has limited effect if applied in isolation. Increasing it to extreme levels as demonstrated, apart from resulting in an increase in operational costs and

raising governmental revenues, may not necessarily result in influencing an airline operator's operational strategy to move to greener solutions. Instead an application of a taxation level, commensurate to global standards, coupled with an improved air traffic management system which would allow aircraft to fly closer to their design efficiency (as demonstrated in the baseline trajectory cases), will help reduce the environmental impact of the aviation industry to significant levels.

The Stern review report [7.1] quotes the following statement "Policy to reduce emissions should be based on three essential elements: carbon pricing, technology policy, and removal of barriers to behavioural change." The report further goes onto state- "Putting an appropriate price on carbon – explicitly through tax or trading, or implicitly through regulation – means that people are faced with the full social cost of their actions. This will lead individuals and businesses to switch away from high-carbon goods and services, and to invest in low-carbon alternatives. Economic efficiency points to the advantages of a common global carbon price: emissions reductions will then take place wherever they are cheapest." The statement rightly states that an appropriately priced carbon taxation is necessary, as it will enable building necessary awareness, however to be effective in any way it will need to be administered along with other mitigation measures which include- introduction of improved technology, improved ground operations and introduction of biofuels.[7.1,2.4]

The second aim of the PhD was to introduce a methodology to assess the economic viability of a new technology in comparison to a conventional technology, when considered in terms of relative increase in acquisition price and maintenance costs, for various emission taxation and fuel price scenarios. The proof of concept of the method was provided by assessing a CROR/propfan aircraft in comparison with a conventional short range aircraft. The study indicated that at current levels of fuel price and in the absence of environmental taxation, despite being highly fuel efficient technology, an increase in relative acquisition price and maintenance cost than the conventional aircraft , could render the CROR technology unprofitable. Hence as suggested by the study in the analysis of optimised operations and the Stern report, a simultaneous increase in the emission taxation may make the operation of CROR technology economically beneficial, and hence a preferred option.

The study shows that in order to achieve lower environmental impact, the implementation of taxation with the introduction of greener technologies will evidently drive the price of aviation up. A train of thought stems from some of the observations made and conclusions drawn in the course of this research, and hence the following questions, more of a 'political and socio-economic nature' become pertinent:

- If taxes above the global industry standards are introduced for the aviation industry, and they are higher than in comparison to that applied on some other carbon intensive sectors, will it raise questions on equity of treatment?
- If taxation is introduced, airline operators and the ticket price paying passengers being amongst the key stakeholders in the aviation industry, will such high pricing as demonstrated be practical for long term sustenance?

- Will policies be driven by the fact that they will be aimed as a trade-off between achieving global sustenance of the industry and achieving environmental gain?
- Will high taxation have global acceptance or will it have to be compromised upon, based on growth potential or GDP of a country/ region?

#### 7.4 RECOMMENDATIONS FOR FUTURE WORK

The objective of this research was to develop a policy assessment tool utilising a TERA framework for civil aviation, with an aim to capture interactions and hence analyse the operational, environment and economic interactions between its modules.

The key requirements set for the framework at the conceptual stage of this project required it to be modular, integrated and built for continuity. Even though it is opined that these have been achieved, there however exists scope for further development of the framework and consequently the research.

Further application and development of existing models:

- a. Aircraft and engine performance model: The current aircraft performance model is a simple model based on the implementation of aerodynamic model of BADA, which is coupled with Cranfield University's in-house engine performance simulation code. Currently the integrated model created, has been validated for ideal performance of conventional aircraft and is able to effectively simulate simple trajectories two dimensional trajectories (in the vertical and horizontal plane). However in order to simulate more complicated and realistic trajectories to more accurately assess the penalty of diverting from an optimal path the model will require to be further developed.  
Another area of development that may be considered is the incorporation of a new aerodynamic model so as to allow the investigation and optimisation of future conceptual aircraft and propulsion systems.
- b. NO<sub>x</sub> emission model: The current model incorporated within the framework uses the prevalently used P3T3 (correlation based) model to predict NO<sub>x</sub>. Even though this method has been validated [3.10], it can be used only for conventional aircraft and combustor technology, where the EINO<sub>x</sub> is established. If the framework has to be used to investigate novel technology, incorporation of a more sophisticated model will be required (such as the physics based stirred reactor model)
- c. Contrail prediction model: A contrail model was used in this study for preliminary analysis of optimised trajectories to avoid formation of persistent contrails. The study provided promising results, but there exists scope for more in-depth analysis of the subject, utilising the current framework and incorporation of a more advanced weather systems model.

- d. Operating cost model: The currently implemented operating cost model has been effectively used to establish the operational, environmental and economic interactions for conventional aircraft, with a methodology of extending it to a novel technology. Currently the maintenance costs for the conventional aircraft are based on public domain information for a particular utilisation. Hence the model currently uses a correlation based method to enable maintenance cost calculations for utilisation of an aircraft, other than for which data is available. There is therefore scope to improve the analysis through incorporation of a more elaborate maintenance cost model.

As demonstrated, the integrated framework described in this work and the methodologies introduced may enable a fleet operator to answer certain specific questions as posed at the beginning of the report. Using this framework as a foundation and with the incorporation and integration of specific models, the analysis may be further extended to effectively enable the assessor to understand the specific dynamics and environmental impact of an entire fleet, within an airline, on a local (e.g. a country) or global scale. Some of these models could include:

- a. Air transport demand model: This model based on geographic location of a region, GDP and population should enable prediction of future passenger traffic on a set of routes or within a geographical area. This will then be able to further establish the drawbacks of a current air traffic management systems, and possible requirements of future systems.
- b. Air traffic management and delay model: Based on predicted demands, this model will enable simulation of actual delays due to inefficiencies in future air traffic systems and hence establish an environmental impact due to these delays.
- c. Global weather /climate model: Aircraft are sometime required to necessarily avoid weather patterns and hence fly sub optimal trajectories. Therefore in order to bring in further degrees of realism the framework may also incorporate a global weather /climate module. This will enable identifying the effect weather patterns may have as constraints in achieving environmentally optimal trajectories and hence establish in terms of excess fuel burn (or emissions) the environmental impact.
- d. Noise prediction model: The frame work currently does not incorporate an aircraft noise model. This is considered critical in order to assess aircraft impact in the vicinity of airport during the LTO cycle. This can be used to then analyse any trade-offs that may be pertinent in terms of future aircraft and engine design.
- e. Socio- economic modelling: ACARE in its report describing its vision for 2050 has categorised socio economic effects as an important factor on decision making in aviation in the future. Even though commoditisation has set into the industry, the perception of passengers is critical in a highly price sensitive environment. As air transport is exposed to socio-economic fluctuations and hence ACARE states—"In future, airlines will seek to further develop business models with reactivity and flexibility (evolution of LCCs and major carriers,

alliances, market segmentation, and so on) in response to volatile market conditions." These factors may have a significant impact on the acceptance and application of environmentally sound initiatives and hence it is considered important to develop such a model to assess and establish any conflicting interests that may develop [2.23].

## REFERENCES

- 1.1 Pilidis, P., Sethi,V.,Singh,R.,DiLorenzo,G., Nalianda, D., Pervier,H., Marzal,R.E(2011) Powerplant selection, deployment and asset management: The TERA(Techno-economic Environmental Risk analysis) COMADEM 2011- Proceedings of the 24th International Congress on Condition Monitoring and Diagnostics Engineering Management, 30th May to 1st June 2011, Norway
- 1.2 Pervier,H., Nalianda, D., Marzal,R.E, Sethi,V., Pilidis, P., Zammit-Mangion,D( Cranfield University) Rogero,J.M and Entz, R. (Airbus France)(2011) Application of genetic algorithm for preliminary trajectory optimization, SAE 2011 AeroTech Congress & Exhibition, October 18-21, 2011,Toulouse, France
- 2.1 Airbus (2011), Global Market Forecast 2011-2030, available at: <http://www.airbus.com/en/corporate/gmf2011/> (accessed 26 April 2012).
- 2.2 European Commission (2010), Aeronautics and Air transport Report by the Advisory Council for Aeronautics Research in Europe, Directorate-General for Research, Communication Unit, Brussels.
- 2.3 Historical Crude Oil Prices (2012), Oil prices 1946-present, available at: [http://inflationdata.com/inflation/inflation\\_rate/historical\\_oil\\_prices\\_table.asp](http://inflationdata.com/inflation/inflation_rate/historical_oil_prices_table.asp)
- 2.4 ICAO Environmental Report (2010) Environmental Branch, International Commercial Aviation Organisation, Montreal, Canada.
- 2.5 Easy Jet annual report and accounts (2011), available at: <http://corporate.easyjet.com/investors/reports-and-accounts.aspx> (accessed 18 Mar 2012).
- 2.6 ICAO (2012),available at [http://www.icao.int/icao/en/m\\_about.html](http://www.icao.int/icao/en/m_about.html) (accessed April 2012)
- 2.7 Strategic Objectives of the ICAO (2012) International Commercial Aviation Organisation, available at [www.icao.int/Pages/Strategic-Objectives.aspx](http://www.icao.int/Pages/Strategic-Objectives.aspx). (accessed April 2012)
- 2.8 Lee, D.S., et al., (2009) Aviation and global climate change in the 21st century, Atmospheric Environment, Volume 43, Issues 22-23, July 2009, Pages 3520-3537
- 2.9 Penner, J.E., Lister, D.H., Griggs, D.J., Dokken, D.J., McFarland, M. (1999) Aviation and the Global Atmosphere, IPCC special report, Intergovernmental Panel on Climate Change, Cambridge University Press, Cambridge, England
- 2.10 ICAO(2009), Group on International aviation and Climate Information Report -GIACC/4-IP/9- Aviation and Climate Change, ICAO, Montreal Canada, Available at: [http://www.icao.int/env/meetings/2009/GIACC\\_4/GIACC\\_4.html](http://www.icao.int/env/meetings/2009/GIACC_4/GIACC_4.html) ,accessed on 20 July 2010
- 2.11 Khun, M. (2010), ICAO to examine timeline for aircraft CO2 standard, Available at <http://www.flightglobal.com/articles/2010/02/22/338681/icao-to-examine-timeline-for-aircraft-co2-standard.html> (accessed 01 August 2010).

- 2.12 ICAO (2009), ICAO News Release -PIO 14/09.- ICAO, Uniting International Aviation on Climate Change, ICAO, Montreal, Canada Available at - [www.bangkok.icao.int/news/2010/pio-14-09-final.pdf](http://www.bangkok.icao.int/news/2010/pio-14-09-final.pdf) (accessed on 01 August 2010)
- 2.13 Environmental Protection Agency (2000), Report for the USEPA, Air and Radiation, Report EPA430-F-00-005- Aircraft Contrails Factsheet, United States Environmental Protection Agency Washington DC, United States of America
- 2.14 ICAO (2010), Presentation by the ICAO Environment Branch at ICAO Colloquium on Aviation and Climate Change (12 May 2010)- ICAO technology goals process for Aviation Environmental Protection, ICAO , Montreal, Canada . Available at [www.icao.int/ CLO10/Docs/3\\_Jahangir\\_Icao.pdf](http://www.icao.int/ CLO10/Docs/3_Jahangir_Icao.pdf), accessed on 20 July 2010
- 2.15 *Thrasher, T. (2010)*, Presentation by the ICAO Environment Branch at Eco - Aerovision UC symposium (02 March 2010), Current Status of the ICAO CAEP Process. Available at - [airquality.ucdavis.edu/pages/events/2010/ aerovision/ THRASHER.pdf](http://airquality.ucdavis.edu/pages/events/2010/ aerovision/ THRASHER.pdf) (accessed on 01 August 2010)
- 2.16 Archer, B. K., et al., (2007), Insights into the role of soot aerosols in cirrus cloud formation, Atmospheric Chemistry and Physics, volume7, part 15, page numbers 4203-4227
- 2.17 Parliamentary Office of Science and Technology (2003) POST Note June 2003 No.197 – Aircraft Noise, The Parliamentary Office of Science and Technology, London United Kingdom
- 2.18 Air Travel - Greener by Design, Design Steering Group(2001)Report by Technology Sub Group- Greener By Design, Society of British Aerospace Companies Limited, London
- 2.19 Aircraft Commerce (2009) The implication of the EU's ETS, Aircraft Commerce , Issue no 66-Oct/Nov 2009, Page Numbers 33-39
- 2.20 Ranson, L. (2010), Global Puzzle- Emissions Trading, Flight International , 8-14 June 2010, Page numbers-41-42
- 2.21 Air France (2010), Sustainable Development- Air France, [http://developpement-durable.airfrance.com /FR/en/local/environnement/N4\\_gaz\\_qualitair\\_en.htm](http://developpement-durable.airfrance.com /FR/en/local/environnement/N4_gaz_qualitair_en.htm), (accessed on 05 August 2010)
- 2.22 Girvin, R. (2009), Aircraft Noise Mitigation and Mitigation Strategies, Journal of Air Transport Management, Issue 15(2009) page numbers- 14-22
- 2.23 Aeronautics and Air Transport: Beyond vision 2020 (Towards 2050)(2010), Report by Advisory Council for Aeronautics Research in Europe (ACARE)
- 2.24 European Commission (2010), Aeronautics and Air Transport Research, 7<sup>th</sup> Framework Programme 2007-2013,Project Synopses, Volume 1 Office, Directorate –General for Research, Communication Unit, Brussels
- 2.25 Clean Sky (2010), About Clean Sky, [http://www.cleansky.eu/index.php?arbo\\_id=35](http://www.cleansky.eu/index.php?arbo_id=35) (accessed on 05 August 2010)
- 2.26 Inderwildi, O., et al.., (2010), Future of Mobility Roadmap, final report of the Future of Mobility horizon-scanning project, The Smith School of Enterprise and the Environment, Oxford University, Oxford, England
- 2.27 Sethi, V. (2011), Presentation on the concept and application of Techno-Economic and Environment Risk Assessments, Cranfield University, Cranfield, England

- 2.28 Pascovici, D.S, Colmenares, F, Ogaji, S.O.T, Pilidis, P.(2007), An Economic and Risk Analysis Model for Aircrafts and Engines, Proceedings of Gt2007 ASME Turbo Expo 2007: Power for Land, Sea and Air May 14-17 2007, Montreal, Canada. GT2007-27236, 2007.
- 2.29 Goulos, I., Pachidis, V., Celis, C, D'Ippolito, R., Stevens, J.(2010), Simulation Framework Development for Aircraft Mission Analysis, GT2010-23379, Proceedings of GT2010, ASME Turbo Expo 2010, Power for Land, Sea and Air, Glasgow, UK, 2010.
- 2.30 Gabbrielli, P. and Singh, R. (2005), Economic and Scenario Analyses of New Gas Turbine Combined Cycles with No emissions of CO<sub>2</sub>, Journal of Engineering for Gas Turbines and Power, Volume no 27, issue no 3 (Jul 2005) , Page numbers 531-538
- 2.31 Maritato, T. (2008), Climate energy prices and their likely impact on Civil Aero propulsion and stationary power generation, Published MSc. Thesis, Cranfield University, Cranfield
- 2.32 Pascovici, D. (2008), Climate Thermo Economic and Risk Analysis for advanced Long Range Aero Engines, Published PhD Thesis, Cranfield University, Cranfield
- 2.33 Techer, R. (2009), Assessment of civil aviation's medium and long term impacts on Global warming and Climate challenge, Published MSc. Thesis, Cranfield University, Cranfield
- 2.34 Dray, L., Antony, E., Reynolds, T.G. & Schäfer, A. (2009), A Comparison of Aviation Greenhouse Gas Emission Policies for Europe, 9th AIAA Aviation technology, Integrations and Operations Conference, Hilton Head, South Carolina, 21-23 September 2009.
- 2.35 Dray, L., Morrell, P. (2009), Environmental aspects of fleet turnover, retirement and life cycle, Final report March 2009, Omega, Cranfield University, UK
- 2.36 Henderson et al. (2012), Aircraft conceptual design for optimal environmental performance, January 2012, volume 116 no. 1175, The Aeronautical Journal, pg 1-22
- 2.37 Michelle, R. K., Dimitri, M. N. (2001), A Technique for Selecting Emerging Technologies for a Fleet of Commercial Aircraft to Maximize R&D Investment, SAE Aerospace Congress and Exhibition, Seattle, WA, September 10-13, 2001
- 2.38 Kroo, I.M., et al., (1994). Multidisciplinary optimization methods for aircraft preliminary design, AIAA 5th Symposium on Multidisciplinary Analysis and Optimization, September 1994, Panama City Beach, FL, AIAA 1994-4325.
- 2.39 Image reference: GE(2011) website: <http://www.geaviation.com/aboutgeae/history.html>, accessed on 12 Jan 2010
- 3.1 Eurocontrol (2010) User manual for the base of aircraft data, EEC Technical/Scientific Report No. 2010-003, Eurocontrol, France
- 3.2 Jenkinson, L. R., Simpkin, P., Rhodes, D. (1999), Civil jet aircraft design, 1st edition, Butterworth Heinmann, MA, USA
- 3.3 Mair, A. W., Birdsall, D. L. (1996), Aircraft Performance, Cambridge University Press, Cambridge, United Kingdom
- 3.4 CFM (2011) CFM Technical specification engine database, available at: <http://www.cfm56.com/products/cfm-technical-data>, sourced on 26 April 2011

- 3.5 CFM56 7B emissions datasheet(2011) sourced from ICAO emissions databank, available at <http://www.caa.co.uk/default.aspx?catid=702>, sourced on 12 June 2011
- 3.6 Gunston, B. (1996), Janes Aero Engines, Janes Information Group, London England
- 3.7 Aircraft performance data-737, Boeing, available at - <http://www.boeing.com/commercial/airports/acaps/737sec3.pdf>, sourced on 13 March 2011
- 3.8 European Commission (2005), Report for the European Commission, DG Environment No. ENV.C.2/ETU/2004/0074r –Giving Wings to emission Trading, CE Solutions for Environment Economy and Technology, Delft
- 3.9 Celis, C. (2009), Gaseous emission formation model, WP3.1 report D3.1.2\_1 (SGOITD, Clean Sky), Cranfield University, Cranfield
- 3.10 Norman, P. D., et al. (2003), Development of the technical basis for a New Emissions Parameter covering the whole AIRcraft operation: NEPAIR, Final Technical Report, NEPAIR/WP4/WPR/01, European Community under the 'Competitive and Sustainable Growth' Programme (1998-2002), United Kingdom.
- 3.11 Pervier, H., et al. (2012), Specifications of contrails, WP3.1 report O\_3.1\_25-a / SGO-WP3.1-C-U-OUT-0248-A (SGOITD, Clean Sky), Cranfield University, Cranfield.
- 3.12 Clark, P. (2007), Buying the big jets-Fleet planning for airlines, 2<sup>nd</sup> edition, Ashgate publishing Ltd, Hampshire, England
- 3.13 Vasigh, B., Fleming, K. and Thomas, T. (2008), Introduction to airline economics, Ashgate publishing Ltd, Hampshire, England.
- 3.14 Roberson, B. (2007), Fuel conservation strategies: cost index explained, Aero Magazine, Article 5-Qtr\_02\_7, available at: [http://www.boeing.com/commercial/Aero\\_magazine/articles/qtr\\_2\\_07/AERO\\_Q207\\_article5.pdf](http://www.boeing.com/commercial/Aero_magazine/articles/qtr_2_07/AERO_Q207_article5.pdf) (accessed 12 Nov 2010).
- 3.15 Airbus (1998) Getting to grips with cost index, Flight operations support and line assistance, Airbus report STL 945.2369/98, Issue 2, May 1998, Toulouse, France
- 3.16 Operator's & Owner's Guide: 737NG family(2010) Aircraft Commerce, Issue 70 June/July 2010, Nimrod Publications Limited, United Kingdom
- 3.17 Source: Aircraft list prices and lease rates (2012), Airline fleet Management, issue 78, May-June 2012, UBM Aviation Publications, London, United Kingdom
- 3.18 Pilot hourly pay rates (2011) available at: <http://www.airlinepilotcentral.com/airlines/legacy/american.html>, accessed on 12 July 2011
- 3.19 Source : Ryan Air Annual reports and financial holdings (2011) Ryan Air holdings plc
- 3.20 Deb, K., Pratap, A., Agarwal, S. and Meyarivan, T. (2002), A Fast and Elitist Multiobjective Genetic Algorithm: NSGA-II, IEEE Transactions on Evolutionary Computations, Volume. 6, Number 2., Pg 182-197
- 3.21 Deb, K. (2002), Multi Objective Optimisation using Evolutionary Algorithms, John Wiley and Sons, New York , USA
- 3.22 Clean Sky (2010), Description of Work, WP3 Mission and Trajectory Management, Systems for Green Operation ITD, Clean Sky Project, Framework Programme 7
- 3.23 Pervier,H., Nalianda, D., Marzal,R.E, Sethi,V., Pilidis, P., Zammit-Mangion,D( Cranfield University) Rogero,J.M and Entz, R. (Airbus France)(2011) Application of Genetic

- Algorithm for Preliminary Trajectory Optimisation, SAE International Journal of Aerospace, November 2011, 4:973-987, doi:10.4271/2011-01-2594.
- 3.24 Zitzler, E., et al. (2001), 'SPEA2: Improving the Strength Pareto Evolutionary Algorithm'. Tech. Rep. 103, Gloriastrasse 35, CH-8092 Zurich, Switzerland
- 3.25 Holland, J. H. (1975), Adaptation in Natural and Artificial Systems, 1 Edition, University of Michigan Press, Michigan USA
- 3.26 Fletcher, R., Practical Methods of Optimisation. 2nd. Chichester : John Wiley, 1987.
- 3.27 Rao, S.S. (1996), Engineering Optimisation: Theory and Practice. 3rd. New York: John Wiley, 1996.
- 3.28 Schwefel, H.P. (1981), Numerical Optimisation of Computer Models. Chichester : John Wiley, 1981.
- 3.29 Norvig, P. and Russell, S. (2003), Artificial Intelligence: A Modern Approach. 2nd. New Jersey: Prentice Hall, 2003.
- 3.30 Quagliarella, D. (1998), Genetic Algorithms and Evolution Strategy in Engineering and Computer Science, Recent Advances and Industrial Applications. Chichester : John Wiley, 1998.
- 3.31 Betts, J.T. (1998) Survey of Numerical Methods for Trajectory Optimisation. 2, s.l. :, Vol. 21.- 1998, AIAA - Journal of Guidance, Control and Dynamics
- 3.32 Bramlette, M.F. and Bouchard, E.E. (1991), Genetic Algorithms in Parametric Design of Aircraft, Lawrence Davis (ed.). Handbook of Genetic Algorithms. 1991, pp. 109-123.
- 3.33 Al-Garni, A. and Kassem, A.H. (2007) On the Optimisation of Aerospace Plane Ascent Trajectory., No.168, Transaction of the Japan Society of Aeronautical and Space Sciences, Vol. 50, p. 113.
- 3.34 Qing, L., Wei, G., Yuping, L., and Chunlin, S., (1997), Aircraft Route Optimisation using Genetic Algorithms, Genetic Algorithms in Engineering Systems: Innovations and Applications, 2 -4 September 1997, Glasgow, UK
- 3.35 Miki, S., Takano, H., Baba, Y. (2002), Trajectory Optimisation for an Aircraft with Genetic Algorithm. Proceedings of Aircraft Symposium. Vol. 40, pp. 119-122.
- 3.36 Gulati, A. (2001), An Optimisation Tool for Gas Turbine Engine Diagnostics, PhD Thesis, Cranfield University, Cranfield
- 3.37 Rogero, J.M. (2002), Genetic Algorithms Based Optimisation Tool for the Preliminary Design of Gas Turbine Combustor, PhD Thesis, Cranfield University, Cranfield
- 3.38 Sampath, S. (2003), Fault Diagnostics for Advanced Cycle Marine Gas Turbine Using Genetic Algorithms, PhD Thesis, Cranfield University, Cranfield
- 3.39 Whellens, M.W. (2003), Multidisciplinary Optimisation of Aero-Engines Using Genetic Algorithms and Preliminary Design Tools, School of Engineering - Cranfield University, 2003. PhD Thesis.
- 3.40 Hartjes, S., Quaglia, D., Madani, I., Nalianda, D., Sammut, M. (2011), Performance analysis of optimised trajectories, Report number SGO-WP 3.2.2-C-U-DEL-0039-B1 , Project Clean Sky SGO ITD, TU Delft, Cranfield University, University of Malta.
- 3.41 Nuic, A., Poles, D. and Mouillet, V. (2010), BADA: An advanced aircraft performance model for present and future ATM systems, International journal of adaptive control and signal processing 2010, Volume 24, pg 850–866

- 3.42 Mattingly, J.D (1996)Elements of gas turbine propulsion, McGraw-Hill series in aeronautical and aerospace engineering, McGraw-Hill book co., Singapore
- 3.43 CFM56\_7B27 emissions datasheet(2012) ICAO Aircraft engine emissions databank, accessed from website at [http://easa.europa.eu/environment/edb/datasheets/docs/easa/CFM%20International/4CM043%20-%20CFM56-7B27\\_2%20\(27.01.2012\).pdf](http://easa.europa.eu/environment/edb/datasheets/docs/easa/CFM%20International/4CM043%20-%20CFM56-7B27_2%20(27.01.2012).pdf), accessed on 14 Feb 2012
- 4.1 D'silva, C., Laso-leon, E. (2009),Deployment of SESAR Concept of Operations on Clean Sky, Clean Sky Report no: Output\_3.2.3\_1, Thales, Toulouse
- 4.2 Hartjes, S., Quaglia, D., Madani, I. (2011), Optimal trajectory concepts, Clean Sky report O\_3.2.2\_3/ SGO-WP 3.2-C-U-OUT-0143, Cranfield University, Cranfield
- 4.3 Mcenteggart, Q., Zammit-Mangion, D., Madani, I., Quaglia, D. (2010), Trajectory mathematical definition ATM constraint rules V1, Clean Sky report 0\_3.2.3\_2/ SGO-WP 3.2-C-U-SPEC-0087, Cranfield University, Cranfield.
- 4.4 Rutowski, E.S. (1953), Energy approach to the general aircraft performance problem, Report number: SM-14875, McDonnell Douglas Research, Santa Monica, USA
- 4.5 ESDU 90012 (1990)Energy height method for flight path optimisation,ESDU Report number 90012, Engineering Sciences Data Unit
- 4.6 ESDU 91016 (1991)Energy height method for flight path optimisation-Addendum A-Numerical methods,ESDU Report number 91016, Engineering Sciences Data Unit
- 4.7 Stanbrook, A. and Mitchell, D.J. (1993), Flight path optimisation using a multi variate gradient search method,ESDU Report number 93021, Engineering Sciences Data Unit
- 4.8 Jet fuel price monitor (2012) International Air Transport Association (IATA) website. Accessed at : <http://www.iata.org/about/Pages/index.aspx>
- 4.9 Schoeffmann, E., Platteau, E. (2010), SESAR and the environment, Report: 10.2829/10029, SESAR joint undertaking, Brussels
- 6.1 Bowles, M. D. and Dawson, V. P. (1998), The advanced turboprop project: Radical innovation in a conservative environment- Chapter 14, From engineering science to big science, National Aeronautics and Space Administration, Washington, D.C., USA
- 6.2 Flight International (2007) Whatever happened to the propfans, Flight Global, <http://www.flightglobal.com/news/articles/whatever-happened-to-propfans-214520/> (accessed on 15 May 2012)
- 6.3 Hager, R.D. (1987), Full scale technology demonstration of a modern counter rotating unducted fan engine concept, report number:NASA-CR\_180867, National Aeronautics and space administration(NASA) and GE Aircraft Engines , Cincinnati, Ohio, USA
- 6.4 Boeing (1990), MD 80 Series- Airplane characteristics for airport planning, Boeing Commercial airplanes, Seattle Washington
- 6.5 Image reference: [http://www.airliners.net/photo/McDonnell-Douglas/McDonnell-Douglas-MD-81\(UHB\)/0405754/L/](http://www.airliners.net/photo/McDonnell-Douglas/McDonnell-Douglas-MD-81(UHB)/0405754/L/)
- 6.6 Warwick, G. And Moxon, J. (1987) (Propfan) The power of persuasion, Flight International archives,Flight international, 23 May 1987, accesed at: <http://www.flightglobal.com/pdfarchive/view/1987/>, on 11 Nov 2011
- 6.7 Giannakakis, P.,(2012) Advanced engine concepts (TBF) , (unpublished PhD thesis), School of Engineering, Cranfield University, Cranfield.

- 6.8 ESDU 75018 (1975) estimation of cruise range-propeller driven aircraft-ESDU Report number 91016, Engineering Sciences Data Unit
- 6.9 Hileman, J.I., Katz, J.B., Mantilla, J.G. and Fleming, G. (2008), Payload fuel energy efficiency as a metric for aviation environmental performance, September 2008, 26th International Congress of the Aeronautical Sciences, Anchorage, Alaska, USA.
- 6.10 Poll, D.I.A. (2009), The optimum aeroplane and beyond, March 2009, volume 113 no. 1140, The Aeronautical Journal, pg 151-164
- 6.11 Jeracki, R. J., Mikkelsen, D. C. and Blaha, B. J. (1979), Wind Tunnel Performance of four energy efficient propellers designed for Mach 0.8 cruise, report Number TM-79124, NASA
- 6.12 Stefko, G. L., Bober, L. J and Neumann, H. E. (1983), New Test Techniques and Analytical Procedures for Understanding the Behaviour of Advanced Propellers, Report number TM-83360, NASA
- 6.13 Rohrbach, C. (1976), A report on aerodynamic design and wind tunnel test of a propfan model,AIAA paper no: 76-667, AIAA/SAE 12<sup>th</sup> Propulsion conference, July 26-29,1976, Palo Alto, California, USA
- 6.14 Raymer, D.P. (2006),Aircraft design- a conceptual approach, 4<sup>th</sup> edition,AIAA education series,American Institute of Aeronautics and Astronautics, Inc., Reston,Virginia, USA
- 7.1 Stern, N. (2006). "Stern review on the economics of climate change" (executive summary) HM Treasury, London. Accessed on 12 march 2012 websit accessed at [http://webarchive.nationalarchives.gov.uk/+/http://www.hmtreasury.gov.uk/independent\\_reviews/stern\\_review\\_economics\\_climate\\_change/stern\\_review\\_report.cfm](http://webarchive.nationalarchives.gov.uk/+/http://www.hmtreasury.gov.uk/independent_reviews/stern_review_economics_climate_change/stern_review_report.cfm)



## APPENDIX A: BENCHMARKING AND TESTING OF THE OPTIMISER

### A1 INTRODUCTION

This chapter aims to provide the reader with information on the validation and verification process carried out on the optimisation algorithm, primarily conducted to ensure the correctness in development and secondly to benchmark and test its performance against other available optimisers.

The chapter briefly touches upon the structure of the algorithm used and then goes onto describe the metrics used to test the algorithm. This is followed by a detailed discussion on the three phases of testing which include- testing using mathematical function, testing for constraint handling and finally, handling of multi modal problems such as trajectory optimisation

### A2 GENETIC ALGORITHMS

The basic idea of using Evolutionary Concepts in creating a problem solving algorithm was first conceptualised by John Holland and his colleagues of the University of Michigan [1, 2]. It basically uses the principle of 'survival of the fittest and extinction of the weaker species through Natural Selection'. The salient points of the theory suggest that strong individuals in a population have a greater chance of passing their genes to future generations via reproduction (cross over) and therefore over a period of time (after many generations) species carrying the correct combination of genes become the dominant population. During the lengthy process of evolution random changes may occur in genes (mutation) thus changing characteristics of an individual chromosome and its future generation. However, if these processes provide an additional benefit/ advantage in terms of survival or fitness, new species evolve or they are duly eliminated through the process of Natural Selection.

At this point the reader may note that the study undertaken uses the real parameter Genetic Algorithm and not a Binary Coded Genetic Algorithm, the essential difference being the variables are all treated as real numbers and not *Binary Bits*. The difference is very significant and hence the reader is referred to literature for more elaborate explanations. [1]

The Genetic Algorithm however replicates approximately the same basic process in finding solutions. The variables used are termed as *Genes*. A set of Genes used at any instance form a *Chromosome*. The set of chromosomes defines the *population*. The solutions thus calculated using the variables or *Genes* form the *Raw Fitness* of each Chromosome in the population. The Genetic Algorithm sorts the Chromosomes out based on their fitness and based on a preset population count, the algorithm eliminates the least fit individuals. Finally the fit individuals selected form a *New Generation*.

Amongst the fit individuals (or Chromosomes) selected, a further set is randomly selected to form a mating pool and Genetic Operators are utilised to *Cross-Over*(essentially reproduction where two chromosomes are used to create *Offspring*) and *Mutate* (the operator introduces a random 'genetic change') the selected chromosome. The crossed over and Mutated Offspring are again merged into the population and fitness value of each Chromosome is calculated. The process then continues iteratively to form new generations till prefixed criteria, such as maximum fitness possible or maximum generations are reached.

### A3 MULTI OBJECTIVE GENETIC ALGORITHM (MOGA)

As discussed in the previous section, the concept of Genetic Algorithm being a population based approach is ideal to solve multi objective optimisation problems as they effectively search the whole feasible objective space or design space. As the algorithm progresses it will try and find a set of *Non Dominated solutions* that is each solution dominates another solution in at least one objective. The final Non Dominated set will meet the following two conditions:

- Any two solutions of the Non Dominated set must be non-dominated with respect to each other.
- Any solution not in this set, but in the feasible objective space, must be dominated by at least one member of the Non Dominated set

This Non Dominated set then forms the Pareto Optimal set as seen in figure A1.

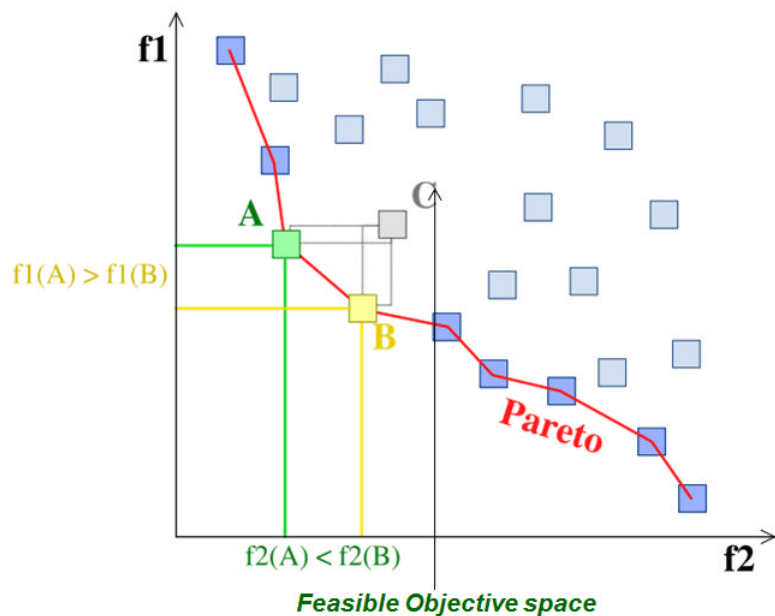


Fig A1 Pareto Optimal (Non Dominated) front

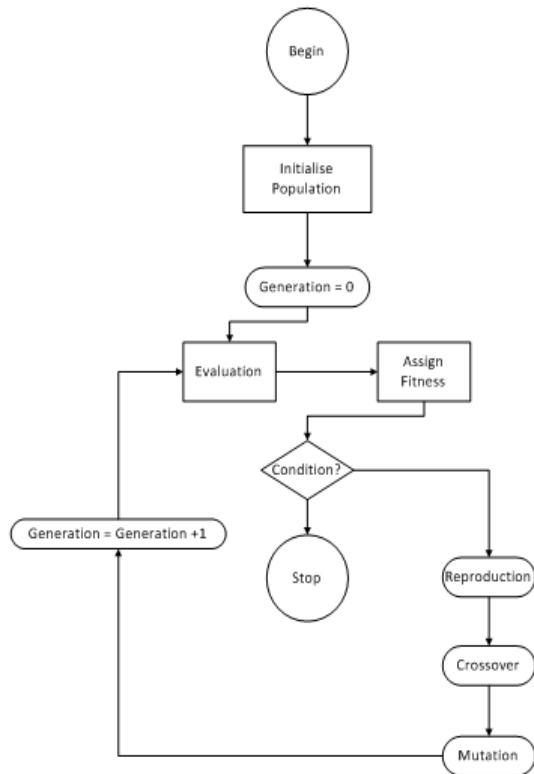


Fig A2 Schematic describing the working principle of the GA

#### A4 OBJECTIVES OF MULTI OBJECTIVE OPTIMISATION

The ‘objectives’ of multi objective problems may be *Non Conflicting* or *Conflicting*. The result of the former will be that the cardinality of the Pareto optimal set may be one. However if the objectives are conflicting, which they invariably are, then the Non Dominated set (or Pareto optimal set) will form a defined Pareto front with a cardinality higher than one. Therefore the main objective of a multi objective optimisation algorithm is to ensure:

- It finds solutions as close as possible to (or preferably on) the true Pareto optimal Front, which will be used as an indicator of its accuracy.
- It finds solutions as close and as diverse as possible along the true Pareto Optimal Front, which provide the user with a good range of ‘Trade off’ solutions for its objectives (its diversity).

#### A5 PERFORMANCE METRICS

To test the performance of a Multi Objective Genetic Algorithm, literature on the subject has suggested two key metrics based on the objectives as discussed in the previous section [1].

- a.  **$\gamma$ -Convergence (Distance) Metric:** This metric is an indicator of the measure of the extent of convergence an algorithm achieves, to a known set of Pareto-optimal solutions. It is primarily used when testing an algorithm using *testing functions* (such as ZDT functions) and the set of Pareto-optimal solutions are known. To calculate this metric a set of uniformly spaced solutions are selected from the true Pareto-optimal front in the objective function space (as indicated with open circles in Figure A3). Then for each solution obtained, with the algorithm being tested (as indicated with dark circles), the minimum Euclidean distance of it from chosen solutions on the Pareto-optimal front is computed. The average of these distances is used as the convergence metric. The smaller the value of this metric the better the convergence to the Pareto front

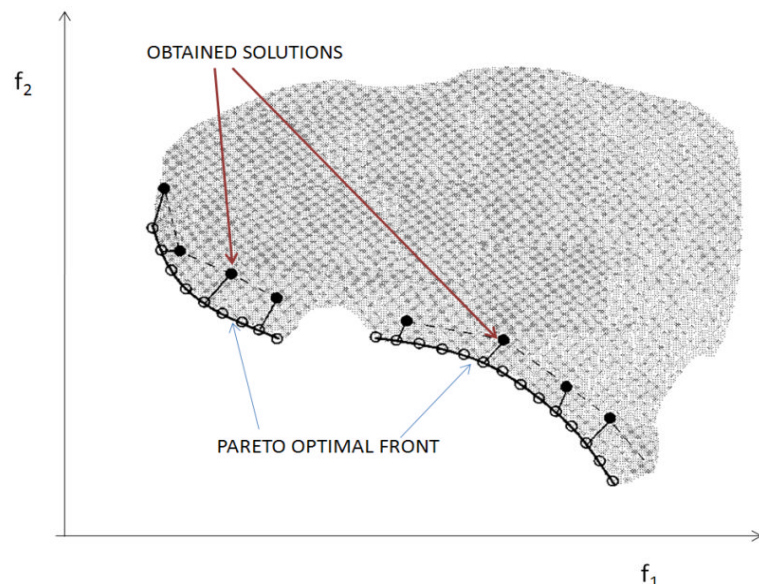


Fig A3 Methodology to calculate the Convergence Metric [1, 3]

- b.  **$\Delta$  – Diversity Metric:** These metric measures the extent of spread achieved among the obtained solutions and is indicative of the extent to which a set of solutions spans the entire Pareto-optimal front. This metric is calculated using the Euclidean distance between consecutive solutions in the obtained non-dominated set of solutions. Non-uniformity in the distribution is calculated by (Eq 1) :

$$\Delta = \frac{d_f + d_l + \sum_{i=1}^{N-1} |d_i - \bar{d}|}{d_f + d_l + (N-1)\bar{d}} \quad A1$$

$d_f$  and  $d_l$  = Euclidian distance between the extreme solution and boundary solutions of the obtained non dominated set

$\bar{d}$  = Average of all distances  $d_i$  ( $i = 1, 2..n-1$ )

$N$  = Number of solutions in the Non-dominated front

For most widely and uniformly spread-out set of non-dominated solutions the numerator of  $\Delta$  would be ideally zero and hence the value of the metric as close to zero is always considered to be the optimal performance.

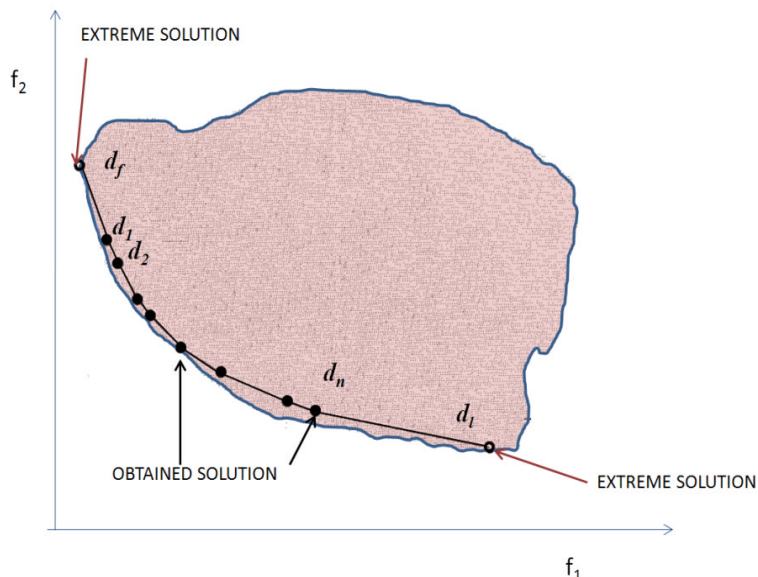


Fig A4 Methodology to calculate the Diversity Metric [1, 3]

#### A6 NON-DOMINATED SORTING GENETIC ALGORITHM II (NSGA II)

The optimiser is based on the concept of "Non dominated Sorting Genetic algorithm"(NSGAII) created by Deb [1,3]. It is considered the 'state of the art' genetic algorithm for multi objective optimisation as it has been designed for lower computational complexity of Non Dominated sorting and has introduced *Elitism*, by which apart from improving its ability to retain good solutions, once found it also speeds up the performance of genetic algorithms.

The basic sequence of the algorithm is as follows (see figure A5):

- The algorithm begins with an Initial population of  $N$  Individuals and multiplies it with an initialisation ratio for the 1<sup>st</sup> Generation

- This population is sorted based on the principle of Constraint Non Dominated sort to form the initial generation  $P_t$  [4.20]
- If after sorting, individuals exceeds  $N$ , then  $N$  individuals are selected based on Crowding Distance from the Final Front
- Using Constrained Crowded Tournament Selection, a mating pool is created from  $P_t$
- The Genetic operators(Mutation and Crossover) are then used to form Offspring Population  $Q_t$
- On the merged set  $R_t (=Q_t + P_t)$  steps II-III are performed to form the next Generation

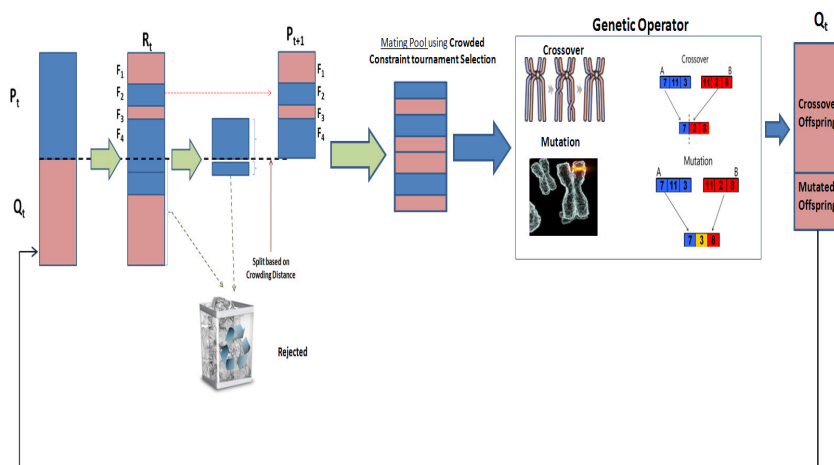


Fig A5 NSGAII- Basic principle

#### A7 STRENGTH PARETO EVOLUTIONARY ALGORITHM II (SPEA II)

This is another type of algorithm based on evolutionary techniques. It basically uses an initial population and an archive (or an external set). A brief description of the algorithm is as follows, however for a more detailed description of the fitness assignment and environmental selection procedure, the reader is referred to the reference [4]:

- The Initial population  $P_t$  consists of  $N$  Individuals with an empty archive  $P_t'$  of size  $N'$  individuals.
- The population is merged ( $P_t + P_t'$ )and then qualified using fitness assignment (based on strength and density information in addition to non dominated front sorting )
- Environmental selection- In this process all non dominated solutions are copied into an archive  $P_{t+1}'$ . This results in the following two possible cases:

- If number of non dominated elements are less than archive size  $N'$  - The remaining slots are then filled with dominated elements using crowded distance information.
  - If number of dominated elements is larger than the number in the archive, then individuals are removed using Truncation Operator.
- The mating pool is then created using Constrained Crowded Tournament operator,
- The mating Pool is shuffled and Genetic Operators (crossover and mutation) are used on the chromosomes to form the new generation.

#### A8 ADAPTATION OF NSGAII FOR THE GATAC OPTIMISER- NSGA MO2

The optimiser that was built was essentially based on the NSGAII and created using the Object Oriented Language JAVA. The Algorithm termed as NSGA MO2, essentially used the same basic process of Non-dominated Sorting as in NSGA II but differed in two respects:

- It used a different selection processes to form the mating pool
- It used an entirely different sequence of genetic operators (Dynamic Vector Mutate method for mutation[5] and double crossover methods for Cross over/ reproduction- Tri Linear Crossover and SBX crossover)

A brief description of the algorithm is as follows:

- The algorithm begins with an Initial population of  $N$  Individuals and multiplies it with an Initialisation Ratio for the 1<sup>st</sup> generation
- This population is sorted based on Constraint Non Dominated sort to form the Initial generation  $P_t$
- If after sorting individuals exceeds  $N$ , then  $N$  individuals are selected based on crowding distance from the Final Front
- The Offspring Population  $Q_t$  formed from  $P_t$
- Using Stochastic Universal Sampling Selection individuals are selected for Crossover Using Random Selection individuals are selected for Mutation
- On  $R_t (=Q_t + P_t)$  perform steps II-II to form the next generation

#### Further Improvement of NSGA MO2- NSGA MO3

After benchmarking and testing against other available algorithms, minor modifications were made to MO3. These included alternative selection methods and genetic operators. The basic framework being the same, the mating pool was created using a Random Selection Process for both Genetic operators. The Genetic Operators used were Polynomial Mutation and SBX Crossover. The modifications improved the performance to a certain extent as is evident in the benchmarking and testing results discussed in the next section.

## A9 BENCHMARKING AND TESTING OF MULTI OBJECTIVE ALGORITHM

During the initial phase of the project, the optimiser used the genetic algorithm NSGA MO2 to first perform single objective optimisation. Therefore the benchmarking was initially done to compare the performance of the optimiser against the commercially available optimiser in MATLAB. The tests were conducted using standard mathematical test functions (for e.g. Hedgehog function and Ackley function). The performance criteria examined, included number of evaluations required for convergence, time required for evaluations and the criteria on which convergence was reached (for e.g. Maximum Fitness or stall). The results observed after testing indicated that the NSGA MO2 had a superior performance in comparison to the MATLAB optimiser.

The next phase of the project involved the use of NSGA MO2 for multi objective optimisation, and hence the benchmarking and testing was undertaken against other optimisation algorithms such as NSGA II, SPEA II and NSGA MO3 (as discussed earlier, an improved version of NSGA MO2) algorithms. It may be noted at this point that all algorithms were tested using the same parameter settings for all three phases of testing.

To validate the performance of the optimiser algorithms three phases of systematic benchmarking and testing activities were undertaken. The phases were as follows:

### Phase 1: Performance testing using ZDT Functions

- Evaluations to reach the Pareto optimal front
- Convergence Metric
- Diversity Metric

### Phase 2: Constraint Handling Performance

### Phase 3: Trajectory optimisation using aircraft performance software Hermes

#### A9.1 PHASE 1: PERFORMANCE TESTING USING ZDT TEST PROBLEMS

These test problems were conceptualised by Zitzler et al. to gauge the performance of a multi objective optimiser algorithm for the following criteria: [1,3]

- Minimum number of evaluations required by the algorithm to converge to the Pareto optimal front
- Ability of the algorithm to handle complexities lateral to the Pareto optimal front and hence converge as close as possible to it. The convergence metric, as described earlier, is used to assess this ability.

- Ability of the algorithm to handle complexities along the Pareto Optimal Front and hence produce a diverse set of trade off solutions. The diversity metric, as described earlier, is used to assess this ability.
- Ability to handle different shapes of Pareto optimal front (convex non, convex and/or discontinuous)

A description of the mathematical functions (ZDT) used are as follows:

#### A9.1.1 ZDT1

This problem tests the ability of the multi objective GA to tackle a large number of variables (30) and a Convex Pareto-Optimal Set. All Variables of the function lie in the range [0, 1]. The optimal solutions are  $x_1 \in [0, 1]$ ,  $x_i = 0$  where  $i = 2, \dots, n$ . The objective functions are as follows:

$$f_1(x) = x_1 \quad A2$$

$$f_2(x) = g(x) \left[ 1 - \sqrt{x_1/g(x)} \right] \quad A3$$

$$g(x) = 1 + \frac{9(\sum_{i=2}^n x_i)}{(n-1)} \quad A4$$

#### A9.1.2 ZDT3

This problem is considered to be of a higher level of complexity. It tests the ability of the multi objective GA to tackle a large number of variables (30) and a number of convex and disconnected Pareto optimal fronts. All variables of the function lie in the range [0, 1]. The optimal solutions are  $x_1 \in [0, 1]$ ,  $x_i = 0$  where  $i = 2, \dots, n$ . The objective functions are as follows:

$$f_1(x) = x_1 \quad A5$$

$$f_2(x) = g(x) \left[ 1 - \sqrt{x_1/g(x)} - \frac{x_1}{g(x)} \sin(10\pi x_1) \right] \quad A6$$

$$g(x) = 1 + \frac{9(\sum_{i=2}^n x_i)}{(n-1)}$$

#### A9.1.3 ZDT6

This is considered to be a very complex problem as it tests the ability of the multi objective GA to reach a non-convex Pareto optimal front. The additional complexity that the GA encounters is that the density across and towards the Pareto optimal region is considered to non uniform and thin respectively. Most Genetic Algorithms are known to face problems converging towards the Pareto optimal front with this function. This problem uses 10 variables with

variable bounds in the range [0, 1]. The optimal solutions are  $x_1 \in [0, 1]$ ,  $x_i = 0$  where  $i = 2, \dots, n$ . The objective functions are as follows:

$$f_1(x) = 1 - \exp(-4x_1) \sin^6(6\pi x_1) \quad A8$$

$$f_2(x) = g(x)[1 - (f_1(x)/g(x))^2] \quad A9$$

$$g(x) = 1 + 9 \left[ \frac{(\sum_{i=2}^n x_i)}{(n-1)} \right]^{0.25} \quad A10$$

#### A9.1.4 Discussion of Results

The tests were conducted using ZDT functions as discussed. The algorithms were tested against the three criteria - number of evaluations required by the algorithm to reach the Pareto Optimal front, convergence and diversity characteristics. The progress of each algorithm was evaluated after 4600, 13000 and 22000 evaluations

*Evaluations required reaching the Pareto Optimal front:* The progress of each algorithm is graphically represented in figure A6, A7 and A8. It may be observed that ZDT1 and ZDT 3 being relatively less complex functions enabled most algorithms to reach the Pareto Optimal Front by 13000 evaluations. However by 22000 evaluations all the algorithms had converged on the Pareto optimal front. For the ZDT6, being more a complex function due to the Non Convex front, it is observed that all algorithms were unable to reach the actual Pareto front and only achieved near optimal set of solutions.

*Convergence towards the Pareto Optimal front:* The convergence metric calculated for each algorithm after the prefixed set of evaluations are as graphically represented in figure A9. The algorithms displayed similar performance trends as discussed earlier. ZDT 1 and ZDT3 indicated good convergence overall with all algorithms, except NSGA MO2, reaching near complete convergence within 13000 evaluations.

*Diversity along the Pareto Optimal front:* The Diversity metric calculated for each algorithm after the prefixed set of evaluations are as graphically represented in Figure A10. It may be observed that a good and close to the final diversity in solutions is reached by all algorithms within 13000 evaluations for ZDT1 and ZDT 3 functions. However ZDT 6 needed significantly larger number of evaluations to reach an improved diversity and that again may be attributed to the complexity of the test function.

In conclusion of discussion for this phase the following were the key observations

- A significantly lower number of evaluations are required for NSGA MO3 and SPEA2

- For the complexity of ZDT6 even though the algorithms did not converge onto the true Pareto front, a set of 'near optimal' solutions were found, however the diversity achieved was very good.
- The diversity and convergence is comparable for all algorithms after Pareto Optimal Front is reached
- SPEA 2 provides overall better diversity but was found to be computationally more expensive. This is attributable to its fine grained fitness assignment strategy which incorporates density information and the selection procedure (Environmental Selection)

It must also be noted that all algorithms have been used with the same basic setting (i.e. Genetic Operator ratios, Mutation and Cross Over methods, Population sizes etc.). The algorithms may improve in performance if optimal settings for each individual algorithm are identified for a particular case and incorporated. This however may be achieved either through extensive trial and error methods of testing or application of another Genetic Algorithm (or alternate control methodology) to actually monitor the settings and based on the performance, change the settings as the optimisation progresses.

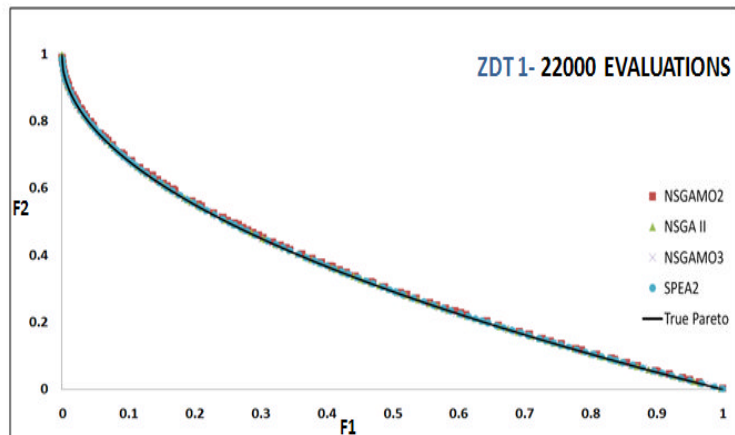
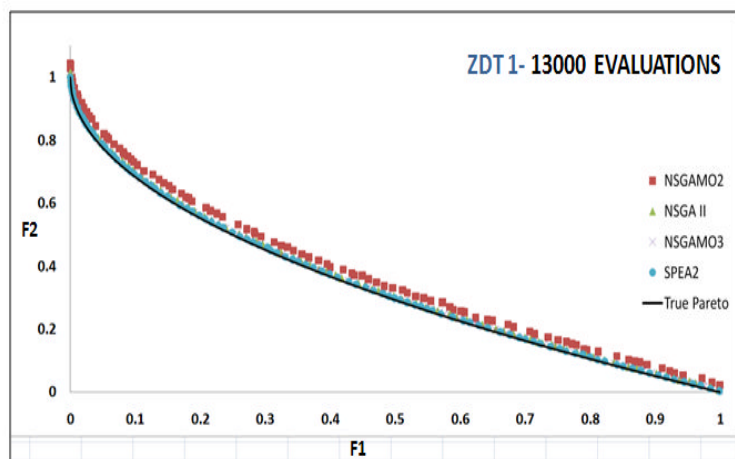
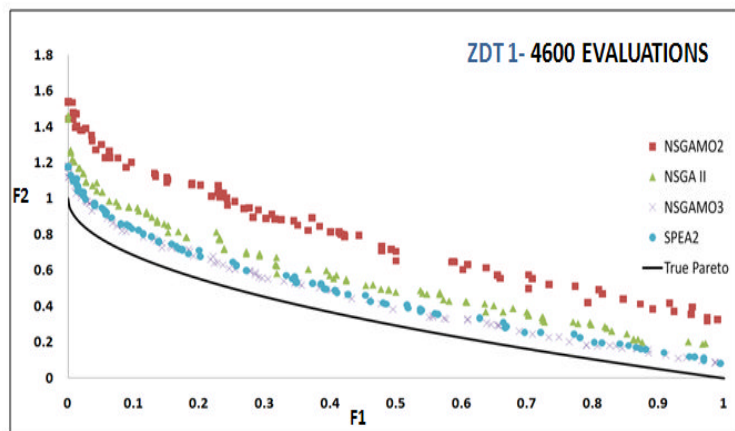


Fig A6 Progress of algorithms towards Pareto-optimal front- ZDT1

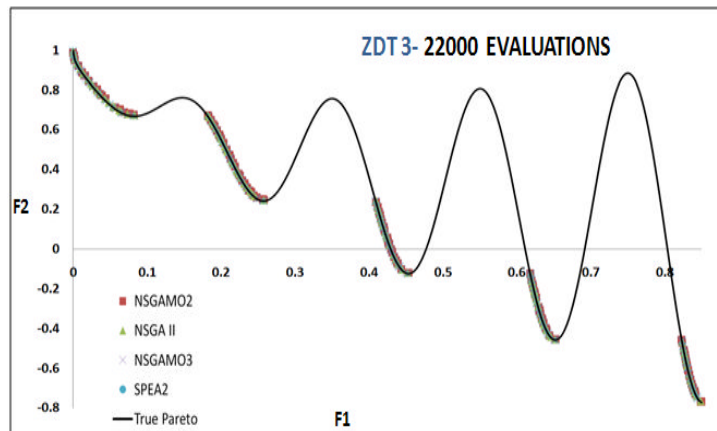
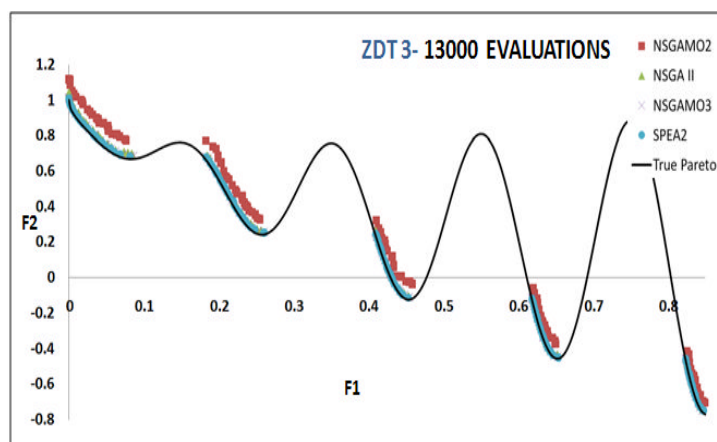
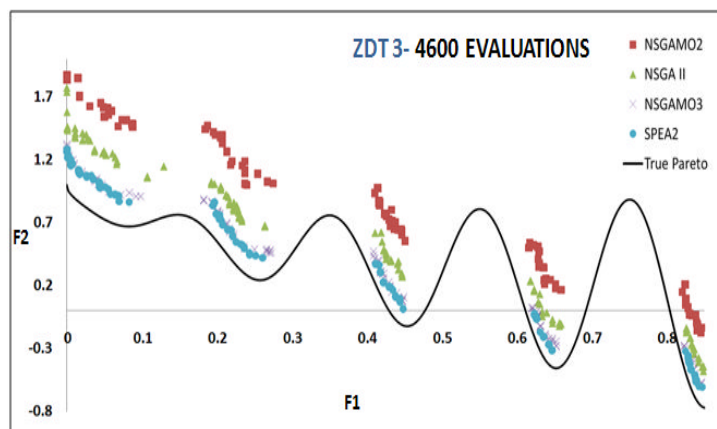


Fig A7 Progress of algorithms towards Pareto-optimal front- ZDT3

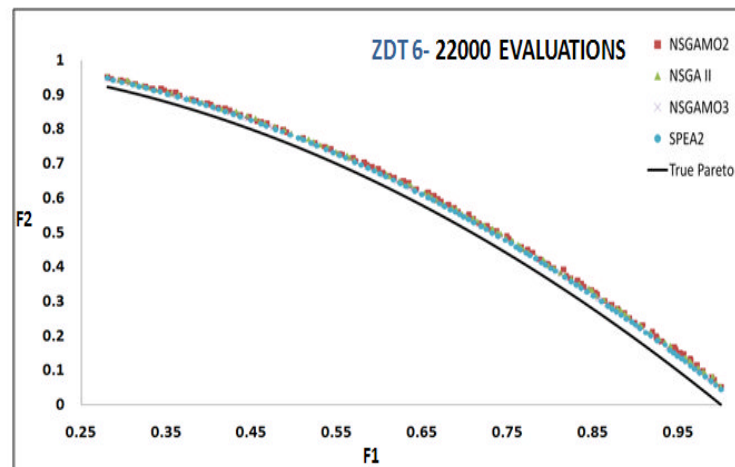
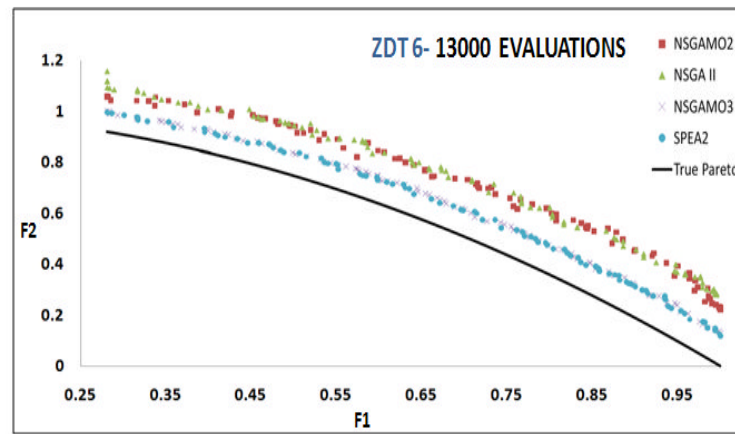
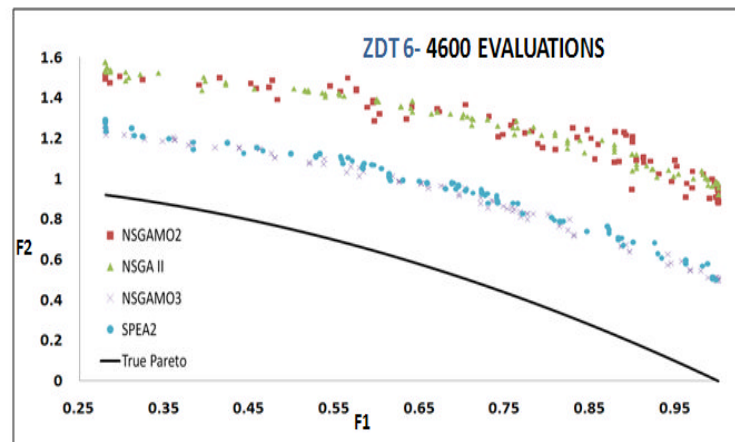


Fig A8 Progress of algorithms towards Pareto-optimal front- ZDT6

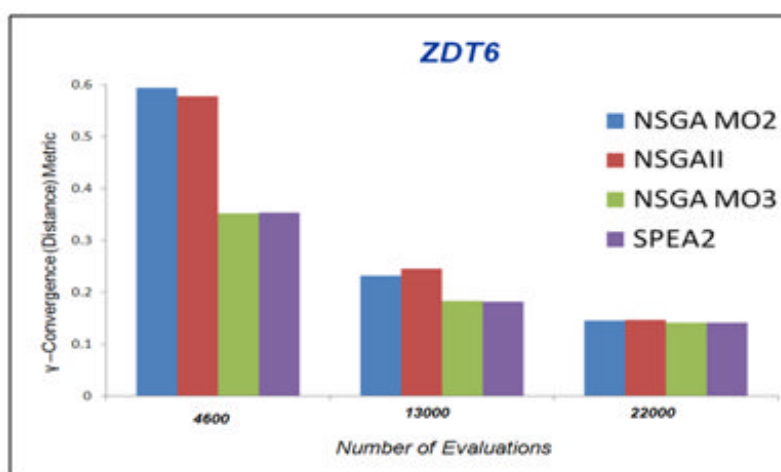
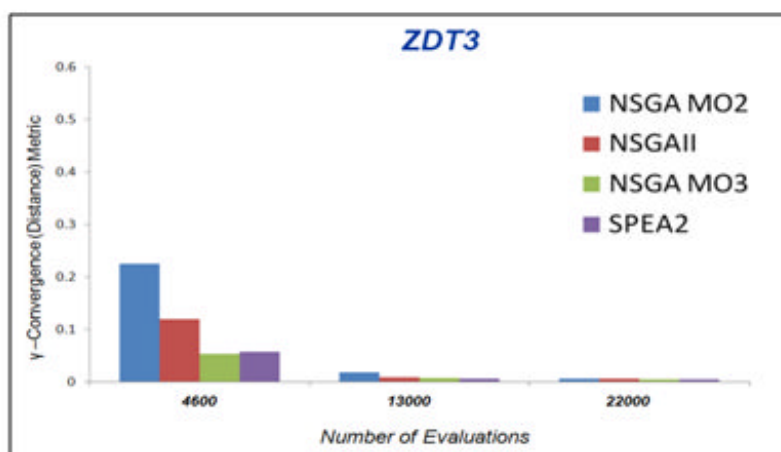
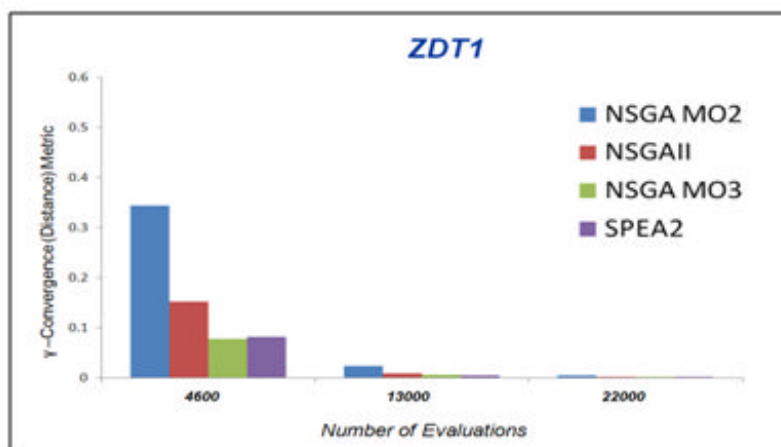


Fig A9 Convergence metric results- ZDT1, ZDT3 & ZDT6

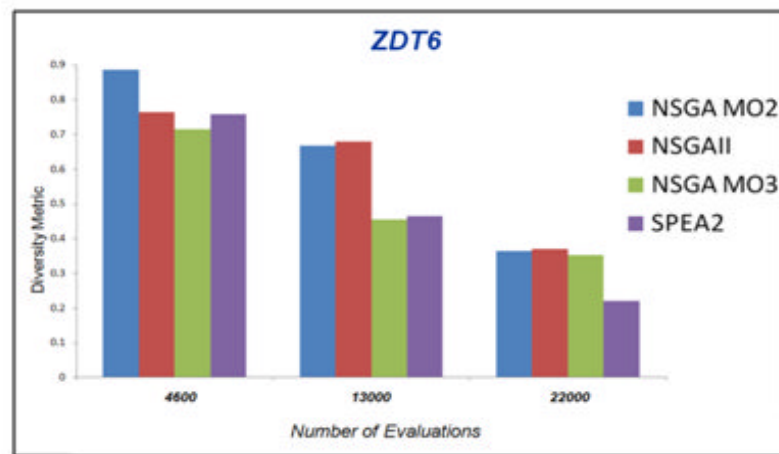
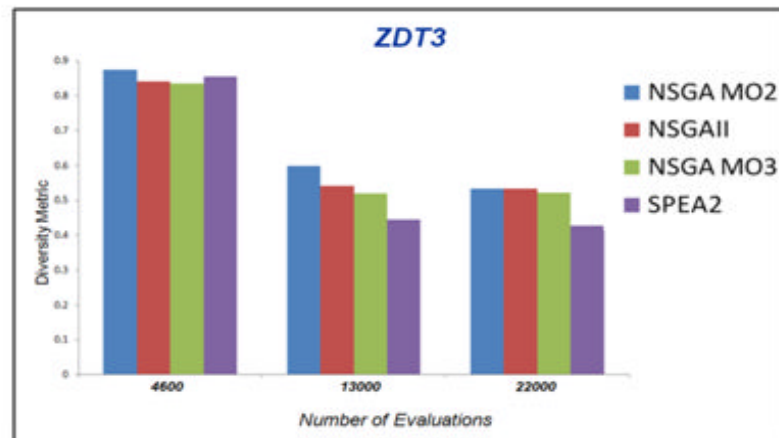
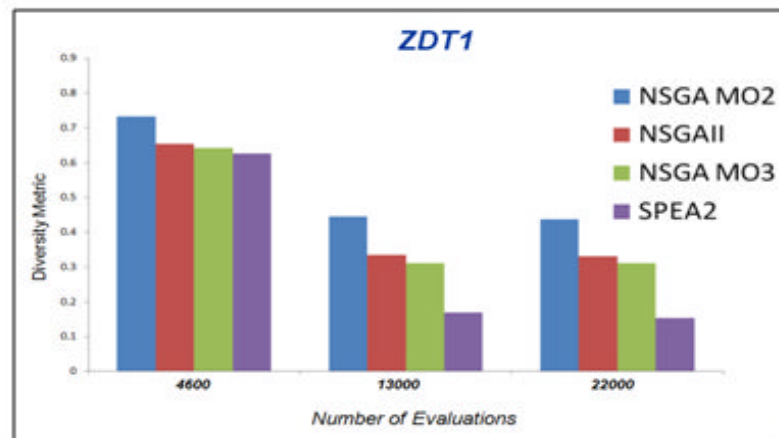


Fig A10 Diversity metric results- ZDT1, ZDT3 & ZDT6

## A9.2 PHASE 2: PERFORMANCE TESTING FOR CONSTRAINT HANDLING

These test problems were suggested by the authors of NSGAII to gauge the constraint handling performance of a multi objective genetic algorithm. The functions used are as follows [1, 3]:

### A9.2.1 CONSTR

This problem tests the ability of the Multi objective genetic algorithm to reach the Pareto Optimal front when a part of the unconstrained Pareto Optimal region is not feasible. A graphical representation of the problem is as shown in figure A11

This is a two variable problem. The variables are  $x_1 \in [0.1, 1.0]$  and  $x_2 \in [0, 5]$ . The objective functions and constraints are as follows:

$$f_1(x) = x_1 \quad A11$$

$$f_2(x) = (1+x_2)/x_1 \quad A12$$

$$g_1(x) = x_2 + 9x_1 \geq 6 \quad A13$$

$$g_2(x) = -x_2 + 9x_1 \geq 1 \quad A14$$

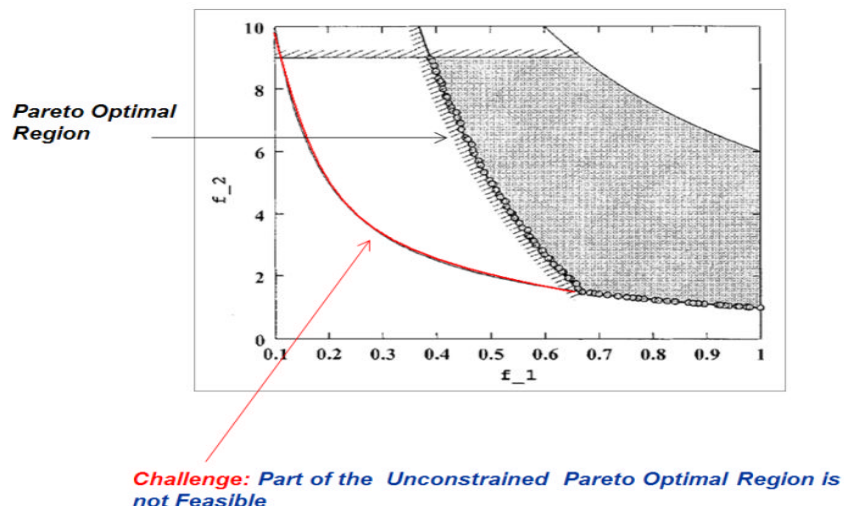


Fig A11 Schematic of CONSTR function indicating constraint altered Pareto optimal front

### A9.2.2 TNK

This problem suggested by Tanaka et al. [3] is aimed at testing the ability of the Multi Objective Genetic Algorithm to reach the Pareto Optimal front that is discontinuous and on application of constraints the constrained Pareto Optimal region falls entirely on the first constraint boundary. A graphical representation of the problem is as shown in Figure A12.

This is a two variable problem. All variables of the function lie in the range  $[0, \pi]$ . The objective and constraint functions are as follows:

$$f_1(x) = x_1 \quad A15$$

$$f_2(x) = x_2 \quad A16$$

$$g_1(x) = -x_{12} - x_{22} + 1 + 0.1 \cos(16 \arctan(x_1/x_2)) \leq 0 \quad A17$$

$$g_2(x) = (x_1 - 0.5)^2 + (x_2 - 0.5)^2 \leq 0.5 \quad A18$$

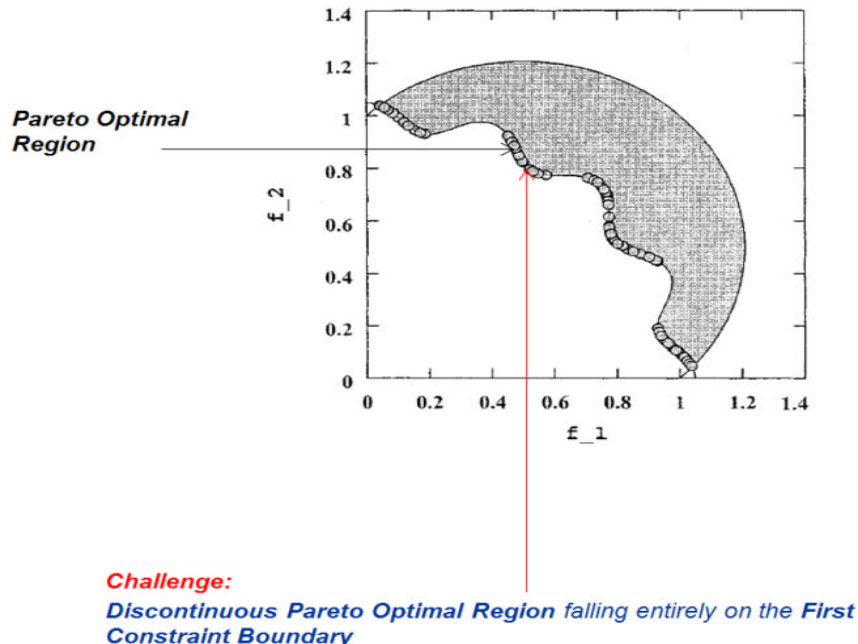


Fig A12 Schematic of TNK Function indicating constraint altered Pareto Optimal Front

### A9.2.3 Discussion of Results

The tests were conducted using CONSTR and TNK functions as discussed. The algorithms were tested for their ability to reach the Pareto optimal front with the application of constraints. All the optimisers were used with same settings as before. Figures A13 and A14 indicate plots of the converged runs for all Optimisers. All algorithms successfully reached the Pareto optimal front within 10000 evaluations and hence displayed good constraint handling ability.

#### **Problem: CONSTR**

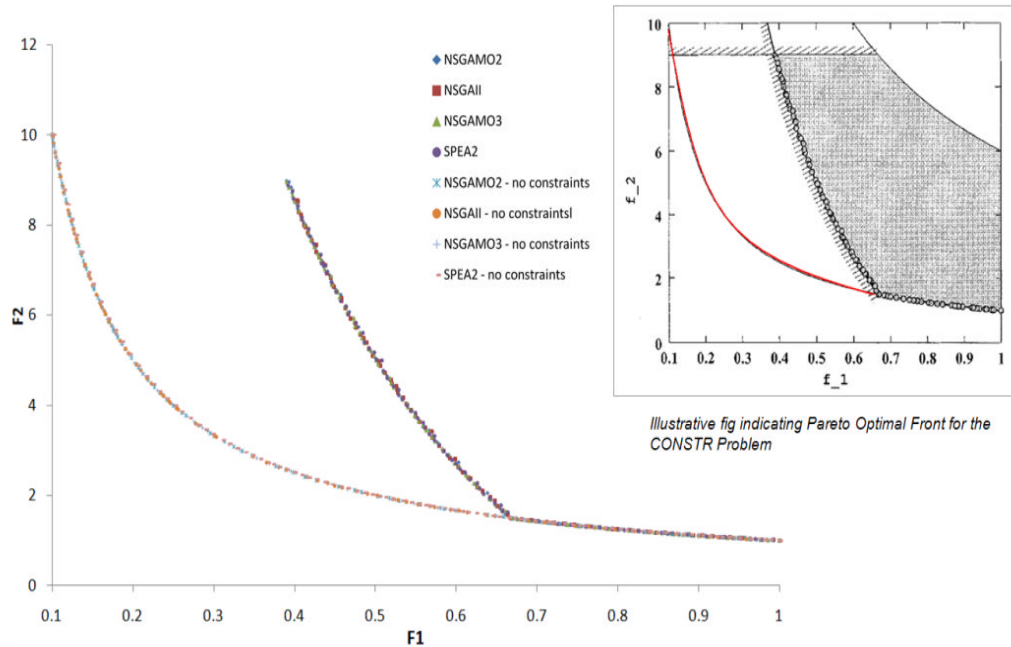


Fig A13 Pareto optimal front formed by algorithms for CONSTR function

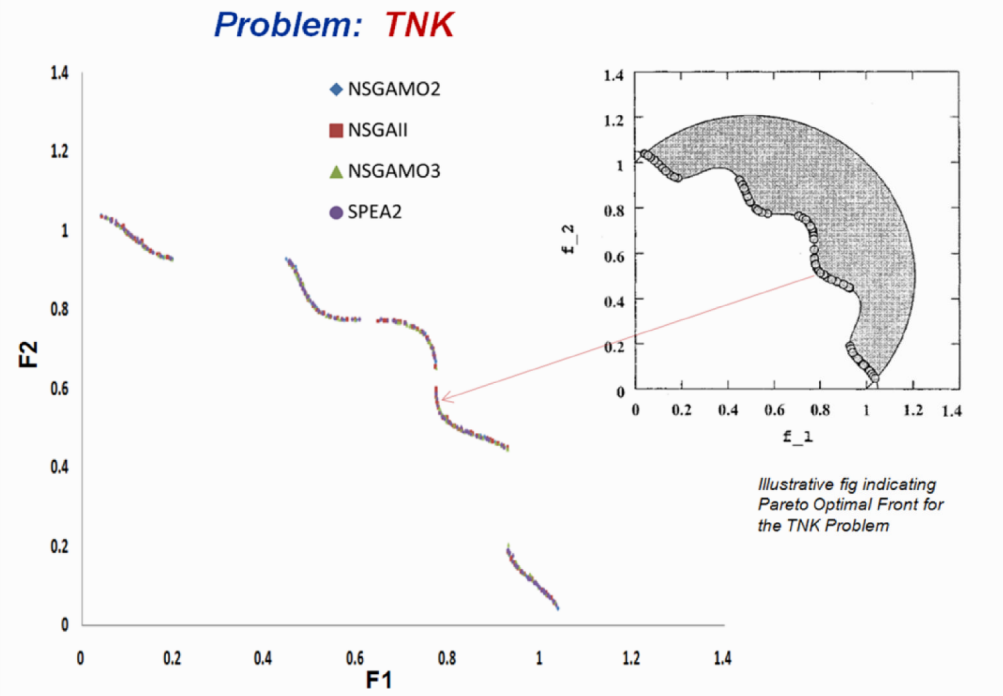


Fig A14 Pareto optimal front formed by algorithms for TNK function

### A9.3 PHASE 3: AIRCRAFT TRAJECTORY OPTIMISATION

As part of the third phase of preliminary testing of the Optimiser, multi objective optimisation of trajectories were undertaken with the aim of creating trajectories optimised for minimum fuel and least possible time for the full flight.

#### A9.3.1 Aircraft and Engine model

In order to simulate aircraft and engine performance during trajectory simulation the aircraft performance software HERMES and gas turbine performance simulation and diagnostics software TURBOMATCH both being in-house software of Cranfield University, were utilised[6,7].

The Aircraft model created in HERMES was based on the specification of a Boeing 737-700, a commonly used narrow body, single aisle aircraft used primarily for short and medium haul flights. The engine model created for the aircraft is based on the characteristics of a typical twin spool, high bypass turbofan aero engine with separate exhausts, similar to the CFM56-5B engine.

### A9.3.2 Specifications of the trajectory for optimisation

The total range flown for all the trajectories was 3000 Km (1619 nm). The takeoff, initial climb (up to 475 m), Descent and Landing Phases (from 475 m) was the same for all trajectories. The optimisation was primarily done on the Climb and Cruise segments. A schematic of the same is as shown in figure A15

The optimiser was given the flexibility of changing the following variables in the range as indicated:

Climb Altitude 1:	1000 to 3500 m
Climb Altitude 2:	3000 to 5500 m
Climb Altitude 3:	5000 to 7500 m
Climb Altitude 4:	7000 to 10668 m
Climb Altitude 5:	9500 to 11000 m
Cruise Altitude 5:	Same as climb altitude 5
Cruise Mach No:	0.75 to 0.85

### A9.3.4 Algorithms used

All 4 Algorithms (NSGA II, SPEA II, NSGA MO2 and NSGA MO3) were used with the same parameter settings. The Pareto optimal front generated is as plotted in figure A16. The trajectories generated are as plotted in figures A17/18/19

### Optimisation of The Climb and Cruise Segment

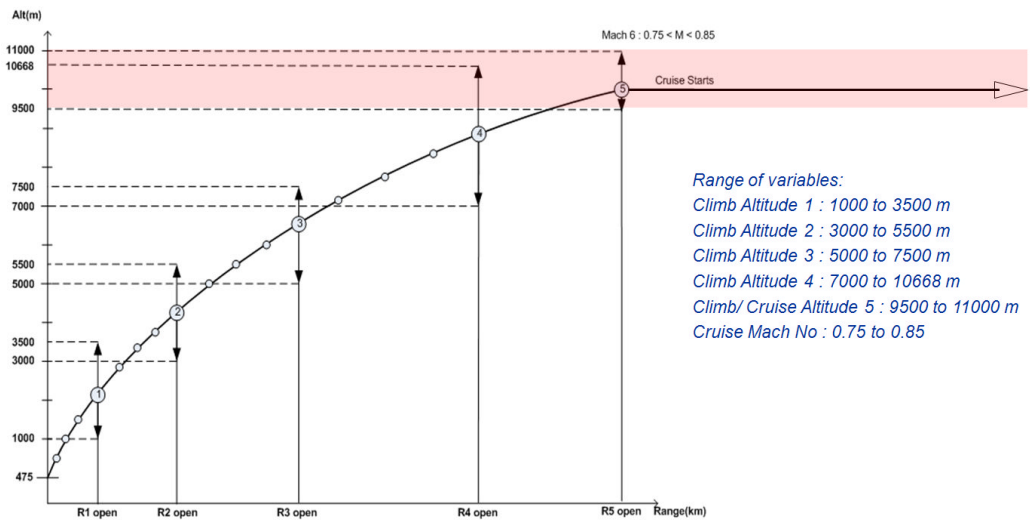


Fig A15 Trajectory setup

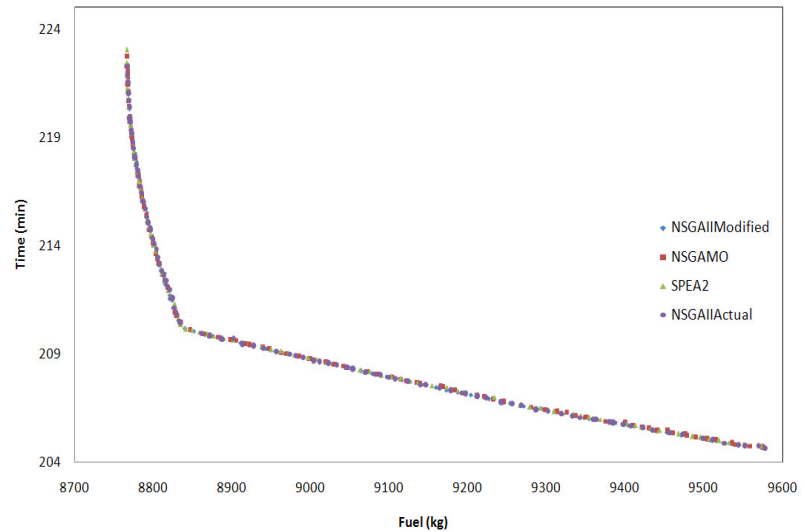


Fig A16 Pareto optimal front formed by algorithms for trajectory optimisation

### Optimised Trajectories for Time and Fuel

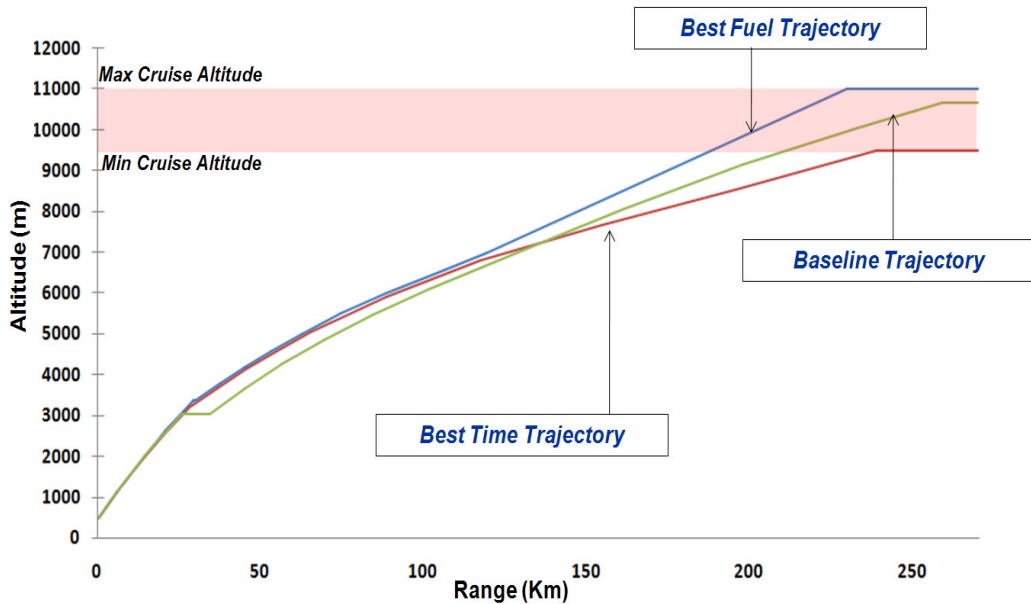


Fig A17 Climb segments for optimised trajectories

### Optimised Trajectory for Fuel

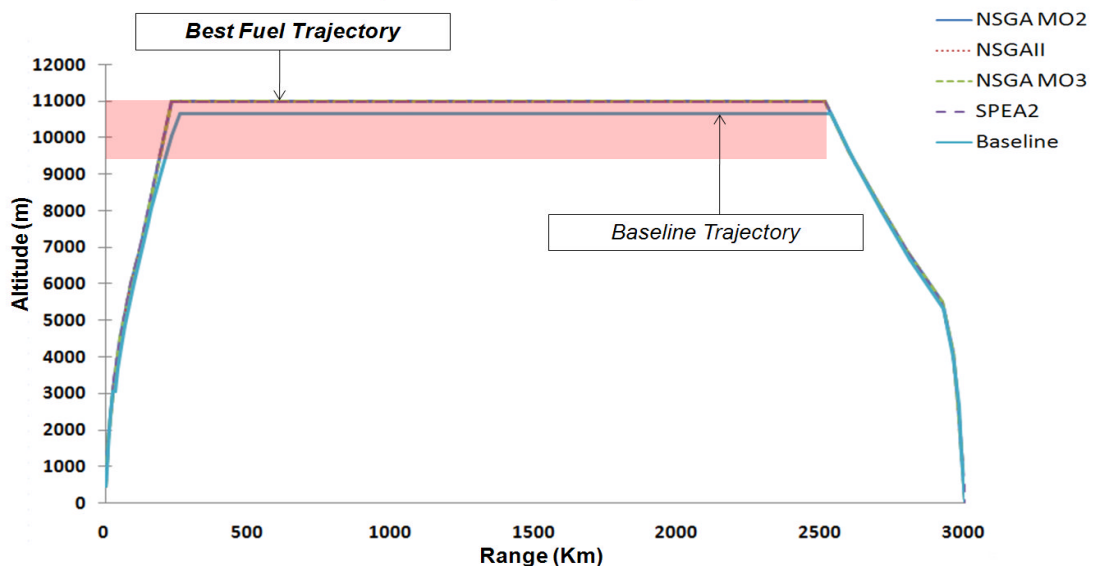


Fig A18 Optimised trajectory for minimum fuel

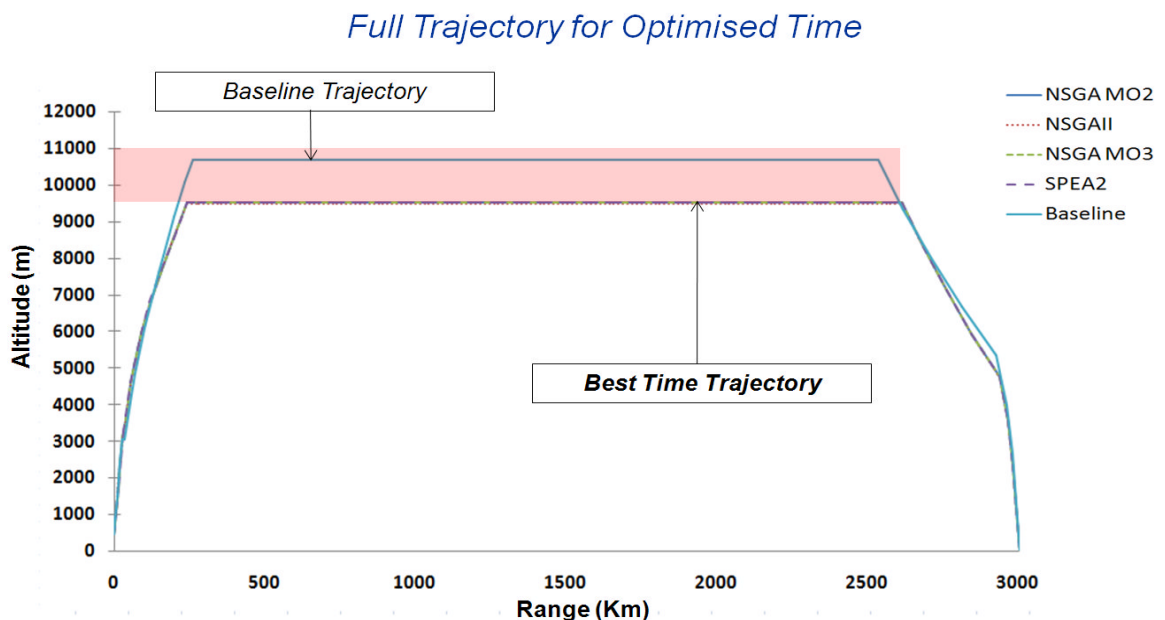


Fig A19 Optimised Trajectory for minimum time

#### A9.3.5 Discussion of results

Trends observed: Given the flexibility of altering only climb altitudes in the climb segment and single speed and altitude for the cruise segment, the optimised trajectories displayed the following trends

Trajectories for minimum fuel burn: The optimiser created trajectories for minimum fuel burn by flying the aircraft at the highest possible cruise altitude and at the slowest speed permissible (11000m and 0.75 Mach). (Figure A18)

Trajectories for optimised time: The optimiser created trajectories for minimum time by flying the aircraft at the lowest possible cruise altitude and at the fastest speed permissible (9500m and 0.85 Mach). (Figure A19)

Pareto Optimal Front: All the algorithms were run for 8500 evaluations and in terms of the shape and trend of the Pareto optimal front generated, indicated very similar results.

In conclusion of discussion for this phase, the following were the key observations

- All algorithms displayed the similar trends
- In comparison to a baseline trajectory it was found that in selecting an optimal trajectory for fuel economy, the optimiser by increasing the total duration of flight by 0.54% reduced the fuel consumption by 2% and when selecting an optimal trajectory for minimum time, the total time was reduced by 7.7 % and

fuel consumption increased by 7%. This therefore verified the optimiser's performance for simple trajectories and preliminary analysis.

#### A10 Conclusion

The genetic algorithm optimiser developed was tested under various conditions for a multitude of test cases as described in the chapter. Each algorithm was tested for its convergence characteristics and its ability to produce diverse trade off solutions. Due to the limitation of time and requirements of the Clean Sky project, for the phases testing the constraint handling and trajectory optimisation, the level of testing was limited to ensuring that all optimisers produced coherent realistic and comparable results. All these objectives were successfully achieved as described and analysed in results.

#### A11 References

1. Deb, K.(2002), Multi Objective Optimisation using Evolutionary Algorithms, John Wiley and Sons, New York , USA
2. Holland, J. H. (1975) Adaptation in Natural and Artificial Systems, 1<sup>st</sup> Edition, University of Michigan Press, Michigan USA
3. Kalyanmoy Deb, Amrit Pratap, Sameer Agarwal, and T. Meyarivan(2002), A Fast and Elitist Multiobjective Genetic Algorithm: NSGA-II, IEEE Transactions on Evolutionary Computations, Volume. 6, Number 2., Pg 182-197
4. Zitzler, E., et al. (2001). SPEA2: Improving the Strength Pareto Evolutionary Algorithm, Tech. Rep. 103, Gloriastrasse 35, CH-8092 Zurich, Switzerland
5. Rogero.J.M (2002), A Genetic Algorithm based Optimisation tool for preliminary design of Gas Turbine Combustors (published PhD Thesis), Cranfield University, Cranfield
6. Gianakakis, G.,(2009) Hermes V5 & TmatchCalls V3 User Manual, Cranfield University, Cranfield
7. Pachidis, V., (2008) Gas Turbine Performance Simulation, Simulation and Diagnostics Course Notes: School of Engineering – Cranfield University.

## APPENDIX B: CONTRAIL MODEL: SPECIFICATION AND DESCRIPTION

### B1 Model Description

The contrails formation process is fairly well established and can be described as follows. An aircraft engine produces hot air at the engine exhaust with high water content due to the reaction of complete combustion in the combustor. This hot and moist air mixes with the colder and drier ambient atmospheric air. If the water partial pressure exceeds the saturation pressure with respect to water then according to the Appleman [1] methodology condensation will occur and a contrails is predicted to form. Depending on the final local atmospheric conditions, two cases can arise. If the mixing between the plume and the ambient air do not lead to saturation with respect to ice, then the water will quickly evaporate and the contrails disappear after a short period. On the other hand if saturation with respect to ice is attained, then contrails will persist. In this case they are called persistent contrails and can last for hours as long as atmospheric conditions remain ice saturated.

The contrails model that will be developed is based on the methodology of Appleman [1] with a modification brought by Schumann [2].

The model will be able to predict the formation of persistent contrails so that based on segment length; it will be possible to derive the number of kilometres of persistent contrails generated by an aircraft flying a given trajectory with known atmospheric conditions (pressure, temperature and relative humidity). This value will subsequently be used as an objective for an aircraft trajectory multidisciplinary optimisation framework.

The contrails prediction will be done through the use of the water phase diagram (see Figure B1). This diagram contains two curves. The first curve corresponds to the vapour partial pressure saturation with respect to water (green curve) and the second is the saturation curve with respect to ice (red dashed curve).

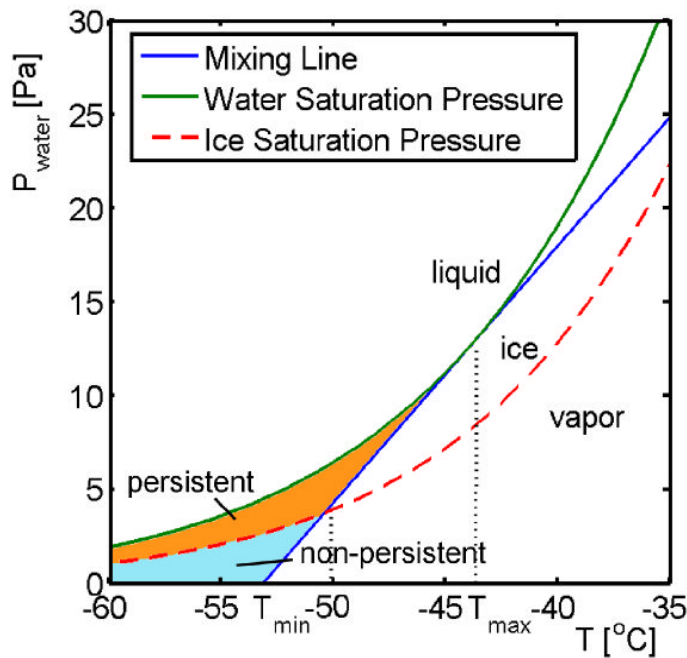


Figure B1 - Water phase diagram with critical mixing line (blue line) from Noppel [3]

By assuming that the mixing between the exhaust plume and ambient air is adiabatic and isobaric and considering an equal mixing rate of heat and water, it is possible to represent the mixing process as a line on the water phase diagram (blue line in Figure B1) [3]. If the mixing line crosses the water saturation curve, contrails will form. The critical mixing line is used to find the critical temperature. The critical temperature is the maximum temperature at which contrails will form (for a given slope and final ambient conditions). The critical mixing line is defined by the slope calculated from equation (1) (critical slope) given by [2] and is tangent with the water saturation curve.

$$G = \frac{EI_{H_2O} \cdot P \cdot c_p}{\varepsilon \cdot LHV \cdot (1 - \eta)} \quad B1$$

$G$  is the critical slope in  $\text{Pa.K}^{-1}$ ;  $EI_{H_2O}$  is the emissions index of water in  $\text{kg/kg}$  of fuel.  $EI_{H_2O}$  can be considered constant in a first approximation with a value of  $1.223 \text{ kg/kg}$  of fuel.  $P$  is the ambient pressure in  $\text{Pa}$ ,  $c_p$  is the specific heat capacity of air in  $\text{J.kg}^{-1}.\text{K}^{-1}$ ,  $\varepsilon$  is the molar mass ratio of water and air ( $=0.622$ ),  $Q$  is the combustion heat in  $\text{J.kg}^{-1}$  and  $\eta$  is the overall engine efficiency.

Overall engine efficiency can be calculated using the following expression (this value will need to be calculated beforehand using an aircraft and an engine model).

$$\eta = \frac{F_n * V_{TAS}}{W_{ff} * LHV * 10^6}$$

B2

Where,  $F_n$  is the engine net thrust in N,  $V_{TAS}$  is the aircraft true air speed in m/s and  $W_{ff}$  is the engine fuel flow in kg/s.

## B2 General Algorithm

This section describes the steps to be implemented in the program in order to predict if contrails are formed and whether they are persistent.

The first step is to calculate the critical slope using equation (1). Based on the critical slope value, the critical temperature is retrieved. To calculate the critical temperature, it is necessary to find the temperature at which the critical mixing line is tangent to the water saturation curve.

The formula for water saturation, taken from Goff and Gratch [6] (2), will be replaced with a simplified equation (3) in order to calculate the critical temperature in a quicker way.

Goff and Gratch formulation for water saturation:

$$\log_{10}(e_w) = -7.90298 \times \left( \frac{373.16}{T} - 1 \right) + 5.02808 \times \log_{10}\left(\frac{373.16}{T}\right) - 1.3816 \times 10^{-7} \\ \times \left( 10^{\left(11.344 \times \left(1 - \frac{T}{373.16}\right)\right)} - 1 \right) + 0.0081328 \times \left( 10^{-3.49149 \times \left(\frac{373.16}{T} - 1\right)} - 1 \right) \\ + \log_{10}(1013.246)$$

B3

Where, T is the temperature in K and  $e_w$  is the saturation pressure with respect to water in Pa.

Simplified formulation for water saturation:

$$e_w = 19.55769739 \times \exp^{(0.114555811 \times T)} - 0.00069542$$

B4

Where, T is the temperature in °C and  $e_w$  is the saturation pressure with respect to water in Pa. The three constants were found using a least square method to approach Goff curve as closely as possible.

Fig B shows the results using the two formulations and shows a very good agreement for the temperature range of -85°C to -45°C.

## Water saturation curve for Goff and Gratch and simplified formulation

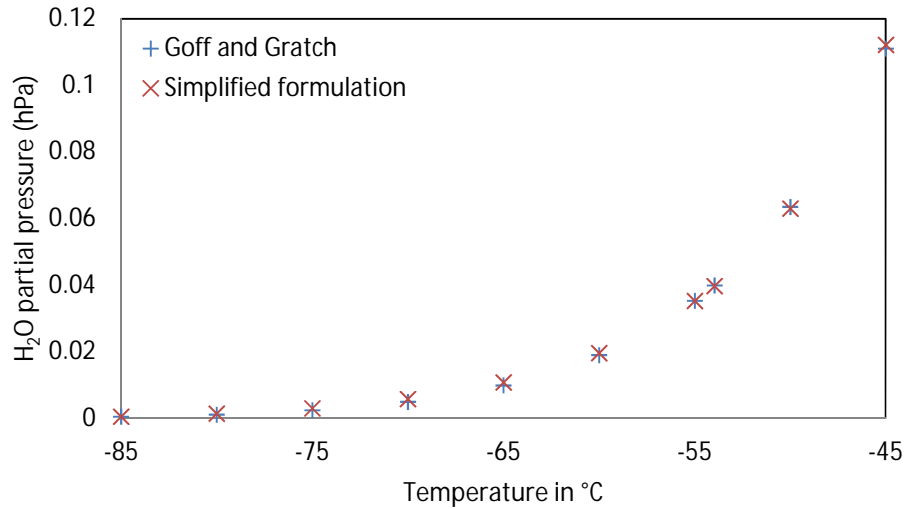


Fig B2 - Comparison of Goff and Gratch water saturation formulation against simplified equation

This simplified formula is useful because it is simpler to obtain its first order derivative. Thus having access to the derivative which allows for a direct calculation of the critical temperature as opposed to using a search method to find the critical temperature using the Goff formula. This is an advantage in terms of computational speed.

It is then possible to calculate the saturation pressure with respect to water and ice at the critical temperature (this time using the Goff formula).

The next step is to obtain the air conditions at which the exhaust exits the engine. The exhaust vapour pressure will be calculated using (4).

$$P_v = esw_0 + (G \times (EGT - T_c)) \quad B5$$

Where  $esw_0$  is the water saturation pressure at critical temperature,  $G$  is the critical slope,  $EGT$  is the exhaust gas temperature and  $T_c$  is the critical temperature.

The ambient vapour pressure  $p_a$  (in Pa) will be calculated using (5).

$$\begin{aligned} \log_{10}\left(\frac{P_{amb}}{100 * RH_f}\right) &= -7.90298 \times \left(\frac{373.16}{T_{amb}} - 1\right) + 5.02808 \times \log_{10}\left(\frac{373.16}{T_{amb}}\right) - 1.3816 \times 10^{-7} \\ &\times \left(10^{\left(11.344 \times \left(\frac{1-T_{amb}}{373.16}\right)\right)} - 1\right) + 0.0081328 \times \left(10^{-3.49149 \times \left(\frac{373.16}{T_{amb}}\right)} - 1\right) \\ &+ \log_{10}(1013.246) \end{aligned} \quad B6$$

Where  $RH_f$  is the relative humidity relative to ice saturation and  $T_a$  is the ambient temperature. It will subsequently be possible to recalculate the actual mixing slope by using (6).

$$G_{actual} = \frac{P_v - P_{amb}}{EGT - T_{amb}}$$

B7

Contrails will form if the difference between  $G_{actual}$  and  $G$  is negative; it basically means that the mixing line crosses the water saturation curve. In addition if the ambient vapour pressure ( $P_{amb}$ ) is greater than the ice saturation pressure at the ambient temperature ( $T_{amb}$ ) then the contrail is considered persistent.

### B3 Validation methodology and model limitation

The validation methodology that will be used for this model is based on the state-of-art validation method for contrails prediction available in the public domain [4] and is therefore expected to be satisfactory for model validation for GATAC. Shull [4] provides ground based contrails observation data taken at Wright Patterson Air Force Base during the month of September and October of 1997. Each day, sounding balloons were sent to obtain atmospheric conditions at aircraft flying level. Each aircraft was identified by its flight number. The information available is the flight level, the corresponding pressure altitude, the ambient temperature and relative humidity with respect to water. For each observation, it is indicated if a contrail was spotted or not. Two main limitations arise in this database with respect to the contrails model developed in this work. Firstly, it is never indicated if the contrails is persistent or not. This lack of information will limit the validation of the persistent contrails prediction of the model. The second limitation comes from the fact that data is gathered within a relatively short period of time. It can be seen in the data that during the whole period of observation, the relative humidity reported was systematically very low. This limitation could also be a problem for validation purpose as the whole range of atmospheric conditions is not covered by this database.

As mentioned, the flight level, pressure, temperature and relative humidity are known, but no information is given about the engine parameters that are required by the contrails model. In this case, these parameters will need to be considered constant in the validation process.

The model limitation comes from the simplification of the definition of the water saturation curve. The expression is only valid from  $-45^{\circ}\text{C}$  to  $-90^{\circ}\text{C}$ . So the user must ensure that the atmospheric temperatures lie within this boundary. The program will ensure that each time the limit is violated the model will predict no contrails for the segment considered.

B4      References

1. Appleman H., "The formation of exhaust Contrails by jet aircraft", Bull. Amer. Meteor. Soc., pp14-20, 1954.
2. Schumann, U., "On conditions for Contrails formation from aircraft exhausts", Meteorol. Zeitschrift, Vol. 5, February 1996, pp. 4–23.
3. Noppel, F., Singh, R., "An overview on Contrails Cirrus Cloud Avoidance Technology", AIAA, Journal of Aircraft 2007, 0021-8669, vol.44 no.5 (1721-1726), doi: 10.2514/1.28655, 2007.
4. Shull, J., D., "A Validation Study of the Air Force Weather Agency (AFWA) Jetrax Contrails Forecast Algorithm", MSc Thesis, Air Force Institute of Technology, AFIT/GM/ENP/98M-10, 1998.
5. Schrader, M., L., "Calculations of Aircraft Contrails Formation Critical Temperature", Notes and Correspondence, Air Weather Service, Illinois, 1996.
6. <http://cires.colorado.edu/~voemel/vp.html> from Smithsonian Tables, 1984, after Goff and Gratch, 1946, accessed 21-09-2011.
7. Hanson, H., M. And Hanson, D., M., "A Re-examination of the Formationof Exhaust Condensation Trails by Jet Aircraft", J. Appl. Meteor., 34, 2400-2405, 1995.
8. Noppel, F., Singh, R., "Contrail avoidance in the aircraft design process", The aeronautical Journal, Vol.112, No. 1138, pp.733-737, Dec 2008.